Targeting pain and degeneration in osteoarthritis and intervertebral disc disease

A. R. Tellegen

Targeting pain and degeneration in osteoarthritis and intervertebral disc disease
A. R. Tellegen
PhD thesis, Utrecht University, Faculty of Veterinary Medicine, the Netherlands

ISBN: 978-94-6332-411-3

Cover: Lisanne van der Voort, Anna Tellegen
Lay-out: Anna Tellegen
Printing: GVO drukkers & vormgevers B.V.

Copyright © A. R. Tellegen, 2018. All rights reserved. No part of this thesis may be reproduced, stored in a retrieval system of any nature or transmitted in any form or by any means, without prior written consent of the author. The copyright of the articles that have been published has been transferred to the respective journals.

Publication of this thesis was financially supported by Elanco Animal health, Royal Canin, Henry Schein Animal health, De Nederlandse Databank Gezelschapsdieren, the Netherlands Society for Biomaterials and Tissue Engineering, The Netherlands Society for Matrix Biology, Orthopedie Medisch Centrum voor Dieren Amsterdam, Fysio/Manuele Therapie Hofstede, and Orthopedieren.

Targeting pain and degeneration in osteoarthritis and intervertebral disc disease

Op weg naar nieuwe behandelingen voor artrose en lage rugpijn

(met een samenvatting in het Nederlands)

Proefschrift

ter verkrijging van de graad van doctor aan de Universiteit Utrecht op gezag van de rector magnificus, prof. dr. H. R. B. M. Kummeling, ingevolge het besluit van het college voor promoties in het openbaar te verdedigen op
dinsdag 29 januari 2019 des middags te 2.30 uur

door

Anna Reinilda Tellegen

geboren op 8 januari 1988 te Utrecht

Promotoren:
Prof. dr. B. P. Meij
Prof. dr. M. A. Tryfonidou

Copromotoren:
Dr. L. B. Creemers
Dr. J. C. Thies

This research forms part of the ArIADNE project of the Health~Holland, Dutch Life Sciences & Health sector. The financial contribution of the Dutch Arthritis Society is gratefully acknowledged (LLP22).

Contents

Chapter 1

General introduction, aims and outline of this thesis

Degenerative joint disease in man and dog

The musculoskeletal system incorporates bones, cartilage, skeletal muscles and connective tissues. It provides form, stability, strength and protection while it enables movement. During life, the musculoskeletal system can be burdened with lack of exercise and physical overload, making it susceptible to wear-and-tear. Two of the most important musculoskeletal diseases are osteoarthritis (OA) of joints such as the knee and low back pain (LBP) due to intervertebral disc degeneration (IVDD). In the Netherlands alone, 1.25 billion people were affected by OA in 2016 [1]. Over 80% of the population will experience an episode of LBP at least once in their lives, half of which are young to middle-aged people [2]. Globally, LBP ranks highest in terms of disability [3]. Osteoarthritis and IVDD are complex and multifactorial diseases and can be influenced by several factors, such as (epi)-genetic modifications, sex, ethnicity and age, but can also be aggravated by obesity, metabolic syndrome, sedentary lifestyle and injuries [4-6]. For example, the incidence of hand OA is expected to increase due to the use of smart-phones, tablets, keyboards and mice. Musculoskeletal diseases cost the European Union up to 2% of gross domestic product (GDP) annually. These costs are related to both direct health care costs and indirect losses due to reduced performance at work and work absence. Patients with chronic LBP are at higher risk of comorbidities such as depression, anxiety and sleep disorders [7]. The burden of LBP and OA will continue to increase because of the global population growth, improved socio-economic growth and the increase in risk factors such as ageing, obesity and urbanization [1, 3, 5, 8-12].

Osteoarthritis and IVDD show several similarities regarding disease aetiology, pathogenesis and symptoms and are also treated in a similar fashion [10, 13]. Therefore, treatment strategies for these two disease entities could be developed in a joint manner and have been combined in this thesis.

The (osteoarthritic) joint

Joints facilitate smooth movement of articulating bones. Articular joints contain a joint cavity that separates the adjoining bones and is filled with synovial fluid (SF). Synovial fluid acts as a lubricant as the high concentration of hyaluronic acid make it highly viscous, and SF nourishes the joint. The synovial membrane, or synovium, lines the joint and consists of a 1-3 thick cell layer surrounded by loose connective tissue. Two types of cells reside in the synovium: A-cells (macrophage-like cells) and B-cells (fibroblast-like cells that produce the SF components). The synovium is surrounded by a tougher fibrous joint capsule that attaches to the bone and offers structural support and attachment sites for ligaments [14]. The articular surfaces of bone are covered with hyaline cartilage, an avascular and aneural tissue that mainly consist of a sparse population of chondrocytes that is responsible for generating and remodelling the extracellular matrix (ECM), mainly consisting of type II collagen, proteoglycans and water. Proteoglycans are composed of a long, non-polysulphated

glycosaminoglycan backbone (hyaluronan), connected to smaller negatively charged glycosaminoglycan side chains (GAGs). The negatively charged polysaccharide side chains attract cations and therefore water, resulting in a high osmotic swelling pressure. The high water content enables nutrients and oxygen to diffuse through the cartilage and makes the tissue particularly suitable for load bearing and shock absorption. The proteoglycans are interwoven with collagen type II fibres, that give the cartilage its high tensile and resilient strength.

Osteoarthritis is the most common form of arthritis. Symptoms, diagnostic modalities and treatment options for OA are comparable in humans and dogs. Pain, swelling and stiffness of affected joints are the most reported symptoms of OA in humans [15]. Osteoarthritis can occur in multiple synovial joints, the knee- and hip joint being most commonly affected [16, 17]. OA can broadly be divided into primary and secondary OA. Primary OA is associated with risk factors such as increasing age and obesity, without an identifiable initiating cause, while secondary OA results from a pre-existing joint abnormality such as injury or a congenital disorder [5, 18]. There is a strong individual variability in the rate of OA changes, which is dependent on the several risk factors [19].

In canines, naturally occurring OA is highly prevalent as well, with 20% of adult dogs and 80% of geriatric dogs being affected [20]. As in humans, knee- and hip joint are frequently affected. In the canine population, most cases of OA arise secondary to hip dysplasia, elbow dysplasia or cranial cruciate ligament degeneration [21]. Cranial cruciate ligament rupture, with or without secondary meniscal injury, is highly prevalent in certain dog breeds. In most cases, it can be attributed to progressive degeneration, influenced by genetic, inflammatory, anatomic and environmental factors [22, 23]. Spontaneous joint pathology as a result of anterior cruciate ligament damage, meniscal injury, osteochondrosis or trauma is comparable in people and pets. Similar risk factors for the development of OA, such as obesity, nutrition, injuries, age and genetic factors have been identified in the canine species [20, 24-28].

Regardless of the species, OA is a disease of the whole joint, with changes occurring in cartilage, synovium and subchondral bone [20, 29]. Osteoarthritis is characterized by degeneration of articular cartilage through fibrillation, fissures, ulceration and ultimately full-thickness loss of cartilage (Fig 1). Activation of matrix degrading enzymes such as matrix metalloproteases (MMP1, -3, 7, -13) and aggrecanases (ADAMTS4, -5) by pro-inflammatory mediators originating from both cells from the innate immune system and chondrocytes themselves, cause breakdown of the healthy cartilage [19, 30] (Fig. 2). Synovitis can arise after an initial insult to the joint and can also be triggered by inflammatory mediators and degradation products originating from the cartilage in early OA. Breakdown products of the ECM can activate toll-like receptors and the complement system, thereby initiating inflammation [29]. Inferior SF quality and synovial inflammation can further aggravate OA [19]. Initially, there is an increase in bone resorption (as a result of inflammatory cytokine expression), followed by increased bone remodelling, leading to bone marrow lesions,

subchondral bone sclerosis and peri-articular osteophytes [31, 32]. Already in early OA, there is a clear interplay between cartilage, synovium and subchondral bone [32] with inflammation as one of the important mediators.

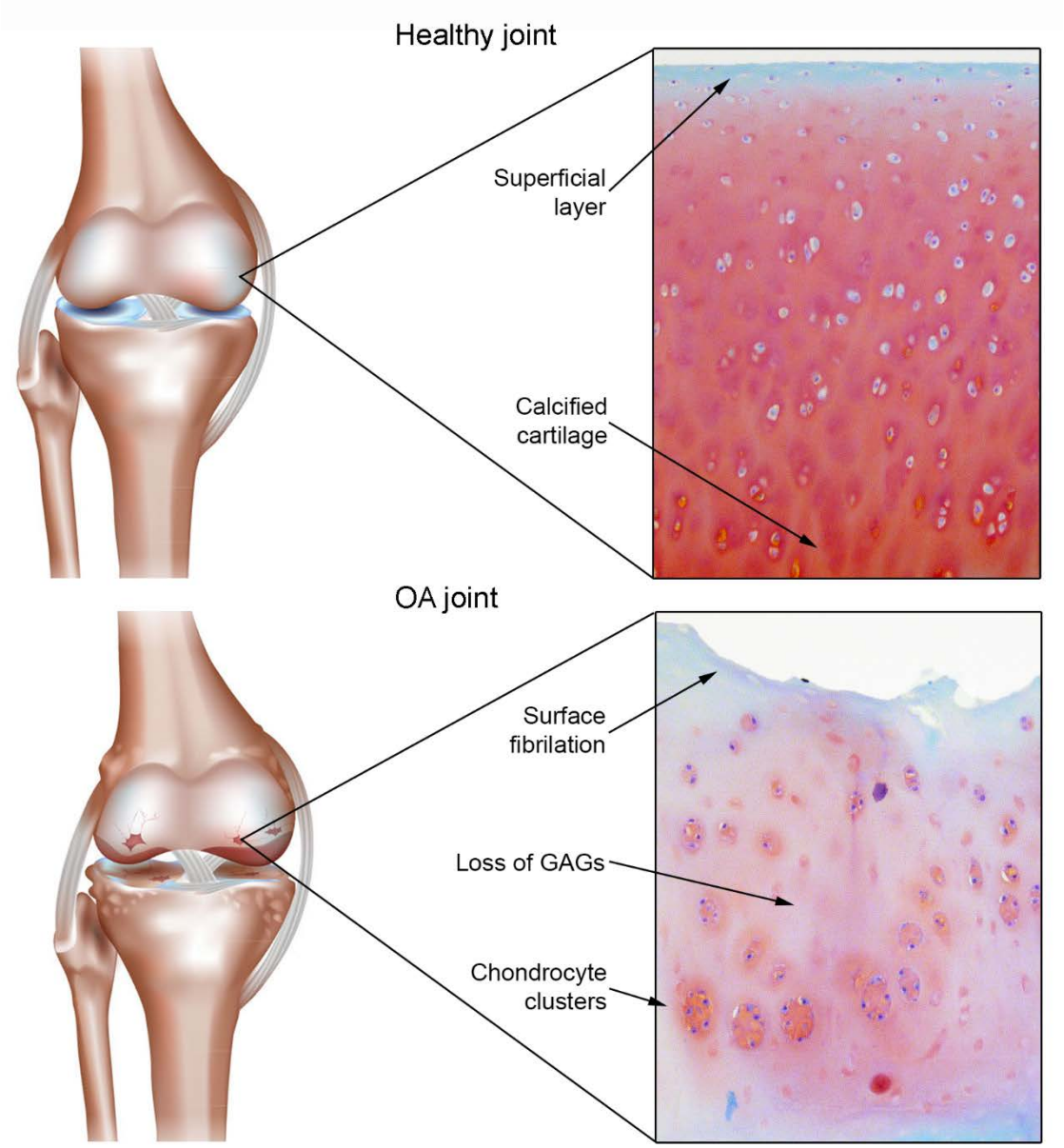

Figure 1. Schematic overview of a healthy and osteoarthritic joint (left) with a histological close-up of the cartilage (right) showing characteristics of healthy (top) and degenerated cartilage (bottom).

Pain in OA

Acute pain can arise by stimulation of mechanoreceptors or can be triggered by inflammation [14]. The major cytokines that are produced in association with tissue damage and OA (tumour necrosis factor α, interleukin 1β; TNF-α, IL-1β) are responsible for inflammatory signs, but can also exert a pain response by influencing Aδ or C-nerve fibers in peripheral nerves and the dorsal root ganglion (DRG). TNF-α and IL-1β can achieve direct

regulation of ion channels that generate nociceptor potentials, and can alter gene expression of DRG neurons, thereby contributing to the mechanisms that underlie chronic pain [33]. They also mediate efferent effects of peripheral nerves to the central nervous system and can stimulate release of neuropeptides such as substance P, that mediate the release of nitric oxide (NO) and prostaglandin E_2 (PGE_2). The cyclooxygenase-2 (COX-2) mediated PGE_2 has been implicated as major pain mediator in OA [34-38]. In addition to sensitization of joint structures to pain, alterations of central nervous system pathways associated with chronic pain have been described in humans, complicating the treatment of chronic pain [14], but explaining the disparity between the degree of pain perception and the severity of OA changes [39]. In addition, pain is a subjective condition that can be influenced by individual factors (age, gender, hormonal status, vitamin D deficiency, activity level, mood disturbances) and environmental factors (weather conditions) [40]. Lastly, joint effusion, subchondral bone changes such as bone cysts and osteophytes (by causing periosteal activation and impingement of surrounding structures) can also contribute to joint pain and stiffness [14, 29, 39, 41].

Current treatments

Treatment for OA broadly consists of conservative management and surgery in amendable cases or patients refractory to conservative management. Surgery can delay OA progression in patients with congenital malformations such as hip dysplasia [19, 42] and anterior cruciate ligament disease [24, 43, 44], and can also be committed for palliation in end-stage OA (i.a. total joint replacement) [45, 46]. For mild or intermittent complaints, an armamentarium of non-surgical therapies is available [47-50]. As pain is the main feature of OA, treatments are focused on pain relief, with a combination of pharmacological and non-pharmacological therapies [19]. Non-steroidal anti-inflammatory drugs (NSAIDs) are the most commonly administered systemic drugs for human and veterinary patients, as they attenuate both pain and inflammation [49]. Recently, an oral PGE_2 receptor (prostaglandin E_2 receptor 4; EP4 receptor) inhibitor was developed for humans and dogs [51, 52]. Other analgesic drugs that are applied in OA, alone or combined with NSAIDs, are opioids or *gamma*-aminobutyric acid (GABA) agonists [53]. Systemic or local corticosteroids (CS) are known to be effective against OA flare ups. Intra-articular CS injections, although effective, have a short duration of action, requiring frequent re-injections [54-56]. There is some evidence that local or systemic use of omega-3 fatty acids, glucosamine and chondroitin sulphate and hyaluronic acid can exert beneficial effects on clinical symptoms and OA progression [48, 57]. Although hyaluronic acid is postulated to lubricate the joint and decrease inflammatory and nociceptive pathways, clinical efficacy remains inconclusive [58]. A healthy body weight, exercise and physical therapy can also positively influence OA symptoms [5, 27]. It should be noted that current treatments are aimed at reduction of clinical symptoms and do not necessarily treat the underlying disease process [14].

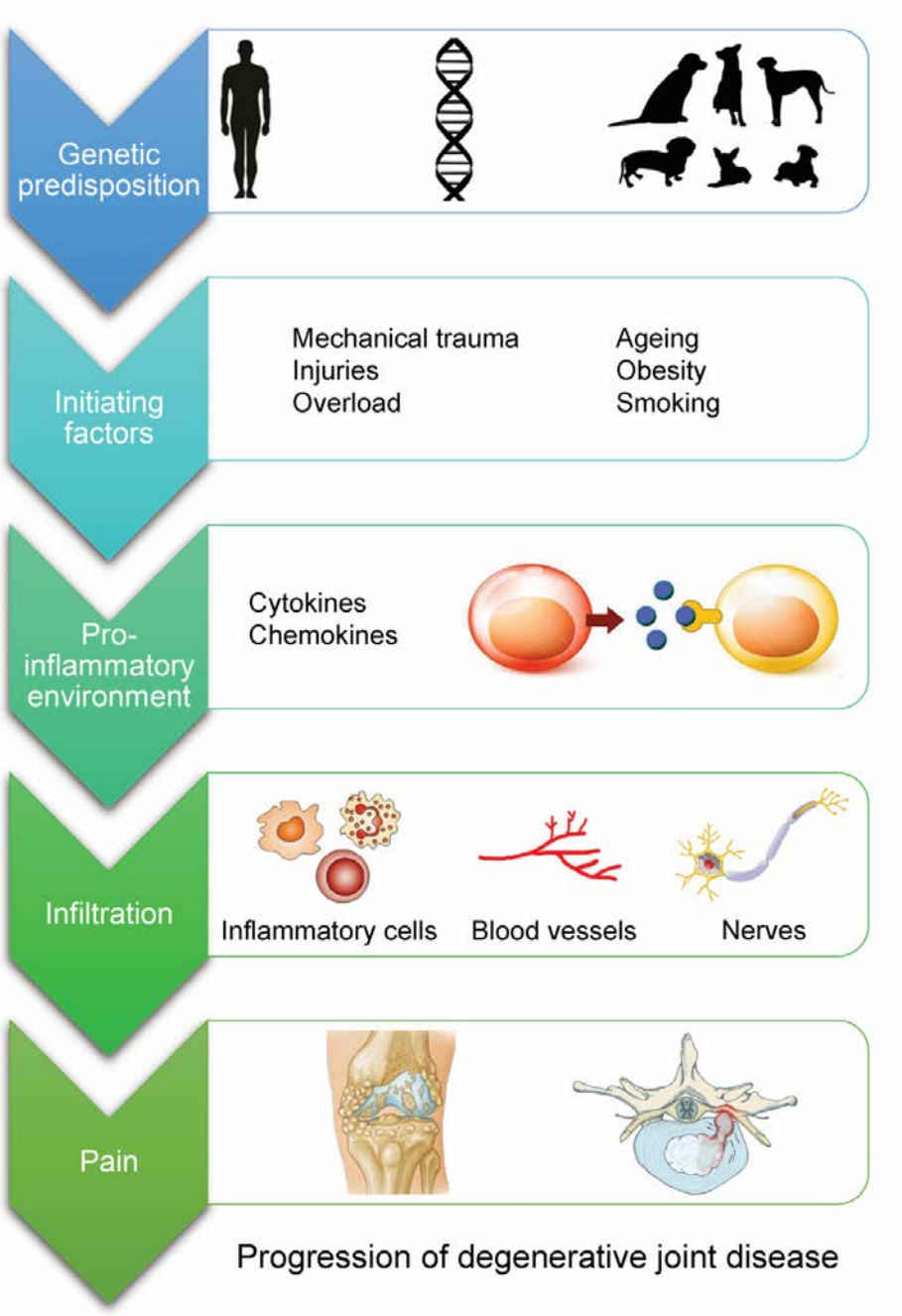

Figure 2. Osteoarthritis and intervertebral disc degeneration are multifactorial diseases, associated with upregulation of pro-inflammatory mediators that lead to catabolic processes and the influx of inflammatory cells, blood vessels and nerve endings, eventually leading to pain.

Intervertebral disc degeneration

Between all adjacent vertebral bodies, except between the first and second vertebrae, there is an intervertebral disc (IVD). The IVD consists of an annulus fibrosus (AF), a nucleus pulposus (NP) and two cartilaginous end plates (EPs). The AF is made up out of concentric fibrous lamellae, running from one end plate to the subsequent endplate, thereby

constraining the NP [59]. The fibres of the AF mainly consist of collagen type I, interconnected by elastic fibres. The transition zone lies between the AF and NP and consists of poorly organised collagen type I and II fibres and aggrecan. Sharpey fibres run from the AF to the vertebral bodies and EPs. Cartilaginous end plates border the vertebrae on both sides and provide the disc cells with oxygen and nutrition by diffusion, as the healthy disc is avascular [60]. Neural innervation is limited to the outermost layers of the AF [61]. Gradually, from the peripheral layers of the AF to the NP, the cellular population and biochemistry changes from a fibroblast-cell like, collagen type I rich tissue to a collagen type II rich tissue populated with chondrocyte-like cells. The healthy NP is a mucoid, gel-like structure and consists of proteoglycans, collagen type II and 80-88% water. When the IVD is loaded, water molecules are pressed out of the NP, to be drawn back to the GAGs when the compressive loading has finished [62]. Several MMPs and aggrecanases are being produced by the discs cells to remodel the IVD, maintaining a healthy disc. Tissue inhibitors of metalloproteases (TIMPs) can inhibit the production of these enzymes [4, 59, 61]. Over time, IVD cells fail to maintain a normal ECM, as the quantity and quality of type II collagen and proteoglycans decline but there is an upregulation of degradative enzymes. This leads to a decreased capacity of the NP to attract water, altering the disc biomechanics. Although ageing is the main factor for degeneration, not all discs become painful. There are several risk factors contributing to the development or aggravation of disc degeneration and disc-related pain. From epidemiologic- and twin studies, it has been estimated that genetic factors account for 70% of susceptibility to lumbar IVDD [61, 63]. Environmental factors such as lack of exercise, smoking, obesity, injuries, heavy weight lifting or occupational exposures such as vibration contribute as well [64].

During IVDD, the water-retaining properties of the NP decline, with a concurrent decrease in shock-absorbing capacity and disc height. Fissures compromise the constraining function of the AF (Fig. 3). End plates are susceptible to damage when they are subjected to high tensile strains. Damaged EPs can lead to reactive bone marrow lesions that include proliferating blood vessels and nerves, which are susceptible to chemical sensitization and mechanical stimulation. Moreover, EP disruption may impede nutrient transport to the NP, thereby evoking inflammatory responses in the IVD and compromising biomechanics of the NP [60]. Bone marrow abnormalities adjacent to painful discs are imperative evidence for the role of EPs in LBP [60, 65] ; they can be imaged on magnetic resonance imaging (MRI) and referred to as Modic changes (MC)[66]. Secondary end plate changes such as sclerosis can compromise nutrition of disc cells, thereby impairing disc health [60].

Degenerative spinal instability, defined as the inability of the spine to maintain its normal patterns of displacement, can be the result of altered disc mechanics and structural changes of the affected spinal unit [67, 68]. In turn, this leads to load transfer to adjacent vertebral bodies and facet joints. During IVDD, the disc space progressively narrows, thereby permitting collapse of the AF and ligaments, leading to subluxation of vertebral bodies. Moreover, disc protrusion or herniation into the spinal canal can take place, resulting in pain or neurologic compromise due to compression of neural structures. Eventually,

restabilization occurs through fibrosis of joint capsules, remodelling of facet joints and vertebrae, and osteophyte formation. This leads to overall reduction of mobility and neuroforaminal and spinal stenosis, LBP and sciatica (radiating pain due to compression of nerve roots that form the sciatic or femoral nerve) [69, 70].

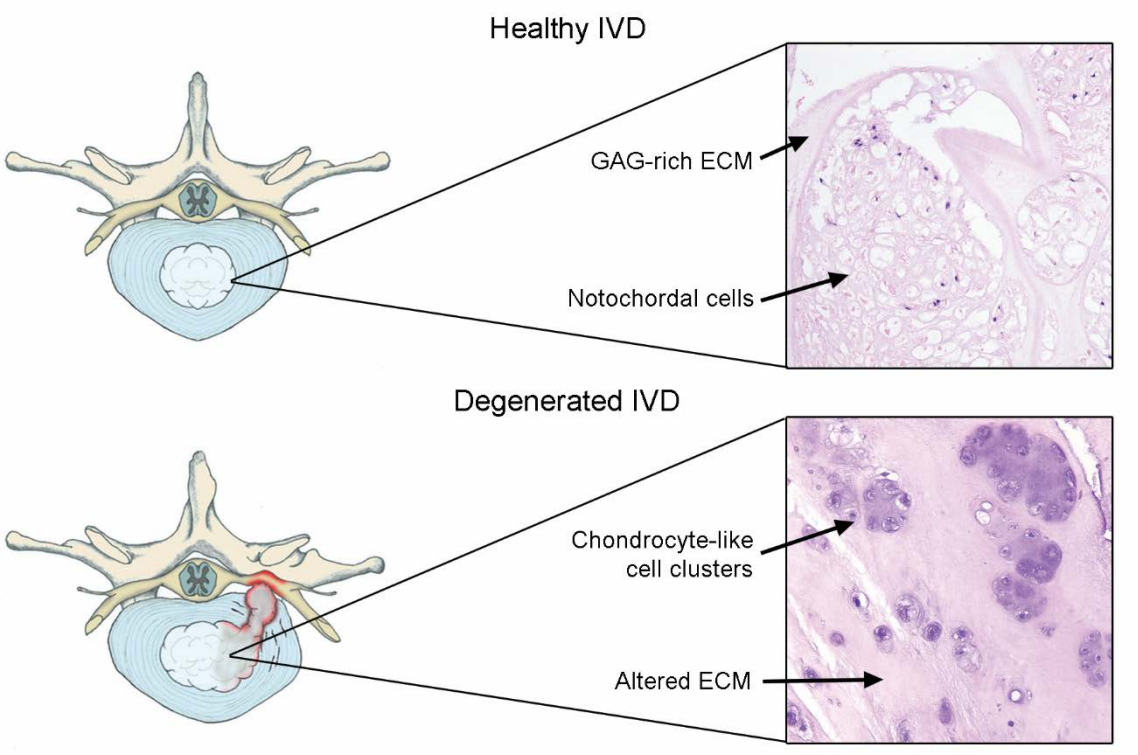

Figure 3. Schematic overview of a healthy and degenerated intervertebral disc (left) with a histological close-up (right) of the nucleus pulposus (NP) showing notochordal cells of a healthy NP (top) and chondrocyte-like-cells in a degenerated extracellular matrix (ECM) (bottom).

As in humans, back pain in dogs is also a common phenomenon [28]. The reported lifetime prevalence of back pain in dogs was estimated to be at least 3% in an investigated population of dogs in Sweden but can be as high as 20% in certain breeds. Clinical IVD disease can be a reason for euthanasia. The mortality rate due to disc disease was calculated to be 34% [71]. In the early 50s, it was as first described by Hansen that chondrodystrophy predisposes dogs to IVDD [72]. Chondrodystrophic dog breeds such as the Dachshund, Basset Hound, Beagle and French Bulldog are characterised by disproportionally short, curved limbs. Acute herniation of NP material into the spinal canal (Hansen type I) occurs typically in these breed types at 3-7 years of age in the cranial cervical or thoracolumbar spine. Non-chondrodystrophic dogs such as the German Shepherd, Dobermann, Labrador Retriever and Rottweiler often show slowly progressing IVD disease, mainly in the caudal cervical and lumbosacral regions. In these dogs, the AF can bulge into the spinal canal and cause chronic

neck or low back pain (Hansen type II) [73]. On a histological level, chondroid metaplasia is present in the NPs of both breed types [74].

Role of inflammation in IVDD

Pro-inflammatory cytokines, produced by cells of the NP and AF, and by infiltrating inflammatory cells, have been associated with IVDD (Fig. 2) [75, 76]. As in OA, IL-1β and TNF-α are the main driving factors [61, 76]. They have been shown to upregulate levels of PGE_2, chemokines and stimulate the expression of degradative enzymes, while suppressing the production of structural ECM components [76]. PGE_2 produced by NP cells from degenerated IVDs has been associated with reduced GAG synthesis and upregulation of catabolic enzymes. It enhances sensitivity to pain-inducing mediators such as bradykinin and is known to interact with macrophages [77].

Low back pain

Low back pain can originate from the disc itself ('discogenic pain') or from pathological changes in surrounding structures. Discogenic pain is accompanied by fissures in the AF, disc collapse and mechanical failure, with no significant modification of disc shape on imaging modalities. Discogenic origin of LBP accounts for approximately 40% of LBP cases, which is supported by the finding that local anaesthetics into the IVD eliminate LBP in these patients [78]. In a healthy IVD, GAGs inhibit neurovascular ingrowth [79], while in a degenerated IVD, de-glycolated aggrecan is no longer capable of inhibiting ingrowth of blood vessels and nerve endings. Intruding free nerve endings originating from the DRG produce nociceptive mediators such as substance P and neuronal growth factor (NGF). Along with vascular ingrowth, influx of immune cells such as neutrophils, macrophages and T cells to the disc occur. Immune cells enhance the production of pro-inflammatory cytokines and nociceptive mediators by cells of the AF and NP. As in OA, these cytokines and nociceptive mediators can directly influence ion channels of nociceptive nerves and neurons in the DRG [61]. It should be noted that even in the absence of immune cells, NP cells are capable of producing pro-inflammatory and nociceptive mediators, contributing to discogenic pain [68, 77, 80].

Degenerative disc disease can also lead to painful disc herniations, spinal canal stenosis, facet joint OA and compression of neural tissues, the latter leading to sciatica [81, 82]. Damaged EPs can lead to bone marrow lesions, which in turn are associated with so-called vertebrogenic LBP. Degenerative spinal instability is considered a major cause of axial and radicular pain and is a frequent indication for surgery [68]. With the rise of dynamic-positional MRI, spinal instability is increasingly recognised as an important factor in IVDD [67]. Interestingly, LBP in younger patients is more likely to originate in the IVD, while in older patients, pain originates more often from pathologic changes in the facet joints or sacroiliac joint [78]. In dogs, much less is known regarding the origination of LBP. Considering the similarities between man and dog, it is plausible that dogs can also suffer from both discogenic pain and pain caused by secondary changes in the lumbosacral region.

Current treatments

Despite a considerable body of research that has already been performed, much is still to be elucidated regarding pathophysiology, diagnostic imaging and treatment of IVDD, which could be one of the reasons that a curative treatment is not yet available in clinical practice. Nowadays, therapy for IVDD is mostly aimed at reducing clinical symptoms and slowing down disease progression. Similar to therapies for OA, current treatments consist mainly of non-pharmacological and pharmacological modalities such as lifestyle modifications, physical therapy and/ or rest supplemented with systemic or epidural analgesics. For patients with advanced IVDD, surgical intervention can be considered. Disc arthroplasty and instrumented spinal fusion are mostly used to address pain and disability caused by IVDD in humans. Drawbacks of these methods are the high costs and invasiveness; they also alter spinal motion that could possibly lead to increased stiffness and adjacent segment pathology [56, 83, 84]. In dogs, standard of care surgical intervention for chronic LBP is dorsal laminectomy, which can be complemented with nuclectomy, foraminotomy and/ or facetectomy [28].

Translational models to study degenerative joint diseases

As the burden of degenerative joint diseases (DJD) will continue to increase, there is an urgent need for regenerative therapies. Both *in vitro* and *in vivo* models have been extensively used to study DJD like OA and IVD-related low back pain. Besides from contributing to the 3R concept to refine, reduce and replace the use of animals in science, *in vitro* assays can be more easily manipulated and used for high-throughput screening [85]. The simplest models used are based on 2D monolayer cultures or 3D pellet cultures, employing one or multiple cell types ("co-culture"). Tissue explant cultures have been developed to more closely study cells in their natural ECM and more advanced models even make use of bioreactors culturing entire spinal units or joints, to not only apply cytokine stimulation, osmotic stress and physical injury, but also alterations in biomechanical loading [85, 86]. These different ways of manipulating tissues allow improved understanding of development and progression of cartilaginous diseases and provide a way to study specific elements of DJD. It is also a manner to discover and evaluate novel treatment options, prior to testing in live animals. *Ex vivo* models lack the complexity present in whole organs or even organisms, and therefore safety studies employing animal models are still dictated by regulatory bodies [87].

Overall, animal models rely on surgical or chemical induction of OA or IVDD, genomic intervention or strains that spontaneously develop OA, and involve both small and large animals [88-90]. Advantages of experimentally induced models are a high uniformity and predictability. Moreover, the process of degeneration can be monitored from the start, which grants researchers the opportunity to investigate disease progression and treatment effect. Since DJD in human and canine patients is mostly diagnosed in an advanced state, this opportunity is often missed. Surgically induced models mostly resemble traumatic DJD, which frequently occurs in active human beings and dogs and could therefore provide a

suitable model. One has to bear in mind that induced tissue degeneration generally progresses much more rapid, due to the traumatic nature of the induction method [91]. Furthermore, specifically in the case of OA, (experimental) animals will generally use the affected limb after trauma better than humans [92]. Chemical models have less clinical relevance [87].

Small (mice, rats, guinea pigs, rabbits) and large (goats, sheep, horses, dogs) animals are commonly used for OA research [88, 90, 92-94]. Although small animal models can be very useful for screening purposes and to answer more fundamental research questions, large animal models are necessary as a translational step towards man in the development of novel treatments. Multiple OA models have been described in the past decades, mostly focusing on the tibiofemoral joint, with the anterior cruciate ligament (ACL) transection and the groove model used most commonly in several species such as the dog [93]. Kuroki *et al* (2011) stated that the instability created by complete ACL transection is quite severe and if untreated it is associated with a degree of biomechanical dysfunction that may overrule the biological effects of treatments [95]. Others show that the model can indeed be very useful when evaluating therapies that are aimed at slowing down the progression of OA [96-99]. The groove model generates slowly progressing joint damage, with highly reproducible results [100, 101]. Since the induction procedure consists of a single event, without joint instability, the groove model might be more sensitive for monitoring the outcome of treatment, as possible beneficial treatment effects are not counteracted by the presence of instability for the first several weeks [102, 103]. Impact loading [93, 104-106], valgus osteotomy [107, 108], and chemical induction have also been described as OA induction method in dogs. The impact loading model is designed to study changes after joint impact trauma and is also suitable for studying the effects of subchondral bone changes on cartilage. An advantage of this model is the fact that the joint cavity is not opened.

There is a wide variety of animal models developed for IVDD research as well [86, 87, 109]. There are, however, some important differences regarding the size and cell population of the disc, and anatomy and biomechanics of the spine between humans and the many animals deployed for the study of IVDD that should be kept in mind when translating results obtained from *in vivo* experiments. There are some mouse strains that develop IVDD as a result of specific knockouts, but the most models rely on a specific method to induce IVDD degeneration. IVDD can be induced by injection of chemical substances (e.g. chondroitinase ABC or chymopapain), direct injury of the disc or end plates through a stab incision or aspiration of the NP, or an alteration of spinal biomechanics (e.g. lumbar arthrodesis, facet joint resection). Results obtained in small animals such as rodents should be extrapolated with caution, as disc size differs markedly. Given the largely avascular nature of the disc and dependence on diffusion of oxygen and nutrient, this is of particular significance [110]. In rodents, IVDs in the tail are often used, because of easy access. However, tail IVDs may have significantly different mechanical loading than the lumbar spine. Porcine, caprine and ovine models have also been described, as their disc and body size are more similar to humans [110].

The chondrodystrophic dog is a valuable spontaneous model for IVDD, as in these dogs the notochordal cells disappear early in life, comparable to the normal ageing process in people, and in contrast to most other experimental animals and comparable to the normal ageing process in people [110, 111]. In addition, dogs are also very amendable to induction of IVDD [110]. The larger disc size in dogs relative to rodents make intradiscal interventions more comparable and less technically challenging. Differences between the canine and human spinal unit exist with regard to thicker EPs in humans and the presence of a vertebral growth plate in growing individuals [111].

The dog as a translational animal model

The use of canines in translational research has several advantages. As a large body of research has been performed in canines, an abundance of data is available. For instance, the whole canine genome is sequenced [112]. Dogs, as humans, undergo similar diagnostic procedures, such as CT and MRI, and treatments as humans, such as oral drug therapy, physical therapy, and surgery for DJD. The gastro-intestinal physiology of dogs is similar to that of humans, making them suitable for studying oral therapies. Moreover, dogs have lived in close proximity to humans for approximately 30.000 years. Dogs have thus been subjected to the same environmental influences and nutrition [113, 114] and also suffer from similar disorders such as obesity [115], endocrine diseases [116], spinal diseases [117] and OA [118]. Even more so, the dog is the only animal model that is also clinically treated for OA and IVDD as a companion animal. As such, progress made within the biomedical field can also benefit the canine patient population. Altogether, this supports the notion that both experimental and client-owned dogs are highly appropriate to function as translational models for cartilaginous diseases.

The study by Garner *et al* (2011) elegantly illustrates the use of both experimental and client-owned dogs in translational OA research [119]. In the search of biomarkers for OA three different induction methods for canine OA were compared with SF samples from client-owned dogs with healthy and OA joints. They found similar results in the induced OA models and the spontaneous OA subjects, which all possessed high sensitivity and specificity of biomarkers for the detection of OA. Cartilage integrity and proteoglycan turnover were found to be comparable in canine experimentally induced and human joint degeneration [120]. Moreover, a canine knee instability model confirmed a similar response of cartilage from post-traumatic canine OA to post-traumatic and late-stage human OA on a mRNA expression level [121]. These findings are challenged by Liu *et al* (2003), reporting striking differences between changes in proteoglycan content in dogs with induced and spontaneous OA. It appeared that none of the degradation products found in spontaneous canine or human OA, were found in knee joints that had undergone ACL transection [122]. Considering that OA entails different phenotypes and clinical representations, determining the right match between modelling and the clinical entities is one of the challenges to be addressed.

The natural occurrence and the slow disease progression of spontaneous DJD, which resembles the course of DJD in humans, combined with comparable anatomy and the ease of application of similar diagnostic and therapeutic interventions make the companion dog a highly suitable model. The use of client-owned dogs with spontaneous disease has several other advantages: questionnaires completed by owners can be used as read out parameters, alongside with several diagnostic procedures and gait analysis. Long-term follow-up is possible in canine patients, which makes them highly appropriate to study OA progression and the effects of novel treatment. A large variety in 'subjects' and increasing costs can be viewed as objections against pet clinical trial for the translations of drugs in humans. This implies that relatively large clinical studies need to be conducted to assess treatment effect, with associated financial implications. [94]. In the last decade, there has been an increase in clinical trials in pets, with the human population as an end goal [123, 124]. Regardless of the success of translation towards humans, a successful clinical trial in pets could aid in novel veterinary therapies. This both benefits the veterinary patients, and their owners.

The use of animals in medical research is receiving increasing attention from the public. Dogs in particular are a sensitive subject, since the role of dogs in households has changed from working dog to a being part of the family. Trials in companion animals lead to a decrease in the use of laboratory animals. This is in line with the field of comparative medicine and the One Medicine Initiative concept in which interdisciplinary collaboration and communication between medical and veterinary health care is promoted to provide synergistic gains for both disciplines [125, 126]. Irrespectively of the study setup and study subjects used, it is of the utmost importance to optimise the study design and perform *a priori* power analysis to carefully minimize the number of animals needed. Furthermore, animals should be checked regularly, and pet owners need to be instructed properly to ensure animal welfare is guaranteed.

Novel therapeutic approaches for chronic degenerative joint diseases

Owing to the increasing knowledge on pathophysiology of degenerative joint diseases and recent advancements in tissue engineering and regenerative medicine, various novel treatment strategies have been proposed. These strategies are based on local injection of drugs, cells, growth factors, nucleic acids, biomaterials or combinations of these techniques (extensively reviewed elsewhere [56, 58, 86, 127, 128]). For end stage disease, biologic substances and tissue engineering can be used to optimise salvage techniques (Fig. 4).

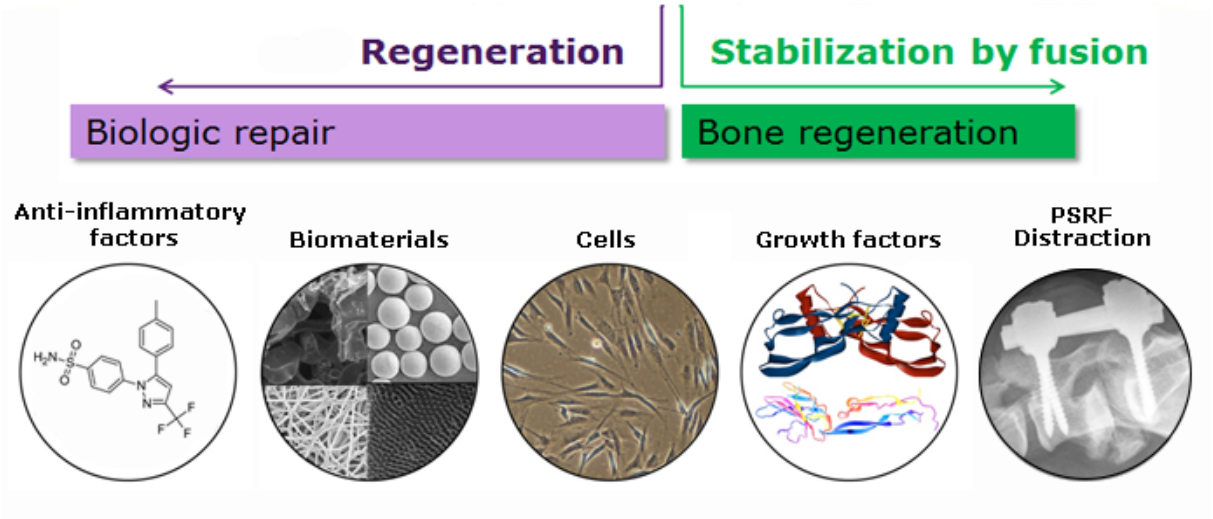

Figure 4. Local delivery of drugs, biomaterials, cells or growth factors seem promising strategies for tissue regeneration and late stage repair of degenerative joint diseases.

Cell-free approaches, such as nucleic-acid based viral or non-viral strategies to alter gene expression of resident cells have shown promising results *in vitro*, but their clinical use is complicated by technical and ethical issues [86, 127, 129]. Therapies that have entered the clinic and are widely applied render inconclusive results. Platelet-rich-plasma (PRP), that contains a myriad or growth factors is applied widely as a treatment for OA even though clinical outcomes remain inconclusive to date [58, 127], possible due to high variations in processing, patient demographics and OA severity [130]. Clinical trials are ongoing to evaluate clinical efficacy for PRP in IVDD [127]. Autologous conditioned serum (ACS), that relies on high levels of anti-inflammatory factors, displays promising results in the treatment of knee OA as well [58, 131]. A pilot study showed promising effects of ACS in patients with single-level NP herniation after local injection, therefore the application of ACS in patients with IVDD should be further optimised [132] .

Another, more straightforward and perhaps cost-effective disease-modifying method, is the local delivery of well-known drugs. Biomaterials could facilitate sustained release of drugs into the diseased tissues, and therefore ensure prolonged treatment effect. Morphine and bupivacaine have been applied intra-articular (IA) in OA joints, but the analgesic effect appeared short-lived [133]. Moreover, bupivacaine showed chondrotoxic properties *in vitro* [134]. Corticosteroids (CS) have been widely applied IA and epidural as analgesic therapy, but their use remains controversial. The main limitation of local CS therapy is the short-duration of action [56]. Especially in older studies, destructive effects on cartilage were reported. From closer examination of these results it can be concluded that most of these chondrotoxic effects were associated with methylprednisolone [135, 136]. On the contrary, for triamcinolone acetonide (TA), beneficial results were obtained [137, 138]. Although systemic NSAIDs are recommended as first choice treatment against OA pain, not much is published on IA NSAID

administration. Intra-articular ketorolac, a NSAID, appeared safe and superior to morphine and bupivacaine in post-operative pain relief [139]. Intra-articular ketorolac was as effective as TA in patients with hip OA during 6 month follow-up and a single IA injection of tenoxicam was superior to placebo and oral tenoxicam [140-142].

In addition to pain relief, it has been suggested that anti-inflammatory drugs might also possess disease-modifying effects. Celecoxib, the first specific COX-2 inhibitor registered for musculoskeletal pain, is one of those. Preclinical studies confirm the inhibition of synovial hyperplasia and bone destruction, suggesting that celecoxib could potentially slow down progression of DJD [143, 144]. The retardation of disease progression by oral celecoxib has to date not been demonstrated in clinical patients. This might in part be due to the fact that orally administered drugs might not be as effective as locally applied drugs. Local delivery not only ensures optimal drug exposure to the target tissue, it also avoids drug binding to plasma components and drug modifications that can influence efficacy [145]. Even more so, local drug delivery facilitates high drug concentrations in the target tissue but decreases systemic side effects [146]. Biomaterial-based drug delivery platforms that facilitate prolonged therapeutic local concentrations are a promising strategy to maximise the potentials of anti-inflammatory drugs.

Outline and aims of this thesis

The main aim of this thesis is to develop novel treatment strategies for osteoarthritis and intervertebral disc degeneration, in order to prevent or delay disease progression. In the event of severe disc degeneration, when both conservative and standard-of-care surgical treatment fail, this thesis explores the feasibility and effectivity of instrumented fusion of the affected spinal unit.

To this end, anti-inflammatory drugs loaded in controlled release platforms are delivered via intra-articular or intradiscal injection directly into the degenerated joint or IVD tissue, in preclinical models as well as in phase I/II studies in veterinary patients. Furthermore, pedicle screw-rod fixation is investigated in twelve client-owned dogs suffering from low back pain due to intervertebral disc degeneration, as a treatment for end-stage IVD disease.

Aim 1. Investigate the differences between CD and NCD dogs on joint level.

Rationale: Chondrodystrophic dogs have disproportionally short limbs and a predisposition for IVD degeneration [73]. Two retrogene insertions of the fibroblast growth factor 4 (FGF4) gene, leading to an over-activation of fibroblast growth factor receptor 3 (FGFR3), have been described that are held responsible for this phenotype [147, 148]. Mutations that enhance FGFR3 activity can also lead to achondroplasia in humans. Together with experimental studies, there are indications that chondrodystrophy may influence OA development.

Approach: Full thickness cartilage chips and synovial tissues from CD and NCD dogs are cultured in the presence of a pro-inflammatory stimulus (TNF-α). In order to determine intrinsic differences and the response to an inflammatory environment, several biochemical and histological analyses of native cartilage tissue or cultured cartilage explants are performed. Moreover, in order to determine whether the detected differences also relate to a differential susceptibility in OA development, samples from CD and NCD cartilage obtained from healthy joints and joints in which OA was induced, are assessed in a meta-analysis. Cartilage degeneration and synovial inflammation on a histological level and GAG incorporation on a biochemical level are investigated (*chapter 2*).

Aim 2. Evaluate the effects and optimal dosage of local application of controlled release of celecoxib in a pre-clinical knee OA model.

Rationale: Osteoarthritis is a common musculoskeletal disease with considerable socio-economic impact [1, 11]. There is evidence that inflammatory components aggravate OA and the clinical symptoms. Local administration of controlled drug release systems loaded with anti-inflammatory drugs may offer a suitable treatment strategy for the long-term OA management [149-151].

Approach: The disease-modifying effects and optimal dose of celecoxib, locally delivered via a controlled release platform comprised of α-amino acid based polyesteramide microspheres (PEAMs), are evaluated. OA is induced in rats, 4 weeks prior to intra-articular (IA) injection of unloaded microspheres or microspheres loaded with celecoxib (*chapter 3*). Static weight bearing, micro-computed tomography, histology and immunohistochemistry are used to assess the effects of local delivery of a wide dose range of celecoxib-loaded PEAMs.

Aim 3. Evaluate the effect of intra-articular celecoxib-loaded microspheres in canine patients suffering from OA.

Rationale: Provided that the developed strategy in chapter 3 is safe, a first step towards translation will be undertaken. The clinical efficacy of celecoxib locally delivered by a controlled release system comprised of PEAMs is evaluated in client-owned dogs suffering from naturally occurring OA and compared to placebo-treatment with unloaded PEAMs.

Approach: First, the release and bioactivity of celecoxib from PEAMs are investigated on canine chondrocytes for four weeks. Thereafter, thirty dogs with OA confirmed on clinical and radiographic evaluation are included in the prospective, randomized, controlled clinical trial. Twenty dogs receive celecoxib-loaded microspheres, ten dogs receive unloaded microspheres (placebo) based on conducted power analysis. Weight-bearing is assessed by visual lameness scoring, kinetic gait analysis, radiographs are scored for OA severity and osteophyte size prior and 2 months after treatment. The administration of analgesics, pain and pain-related behaviour are scored by the owner. Synovial fluid is analysed cytologically and biochemically *(chapter 4).*

Aim 4. Evaluate the effect of local release of TA from microspheres in canine patients suffering from OA.

Rationale: IA corticosteroid therapy is effective against OA flare ups, but available formulations are short-acting [58]. PEAMs loaded with triamcinolone acetonide (TA) were able to attenuate joint inflammation for at least 70 days in a preclinical OA model [152]. The safety and clinical efficacy of locally delivered TA-loaded PEAMs needs to be evaluated in phase I clinical study recruiting client-owned dogs suffering from naturally occurring severe OA.

Approach: Dogs with OA, confirmed clinically and radiologically, are included in this prospective study. Weight-bearing is assessed by visual lameness scoring and kinetic gait analysis, radiographs are scored for OA severity and osteophyte size prior and 2 and 6 months after treatment. The administration of pain and pain-related behaviour are scored by the owner. Synovial fluid is analysed cytologically and biochemically *(chapter 5).*

Aim 5. Investigate inflammatory profiles in canine IVD degeneration.

Rationale: The clinical presentation of IVD disease in veterinary medicine is diverse. Chondrodystrophic and non-chondrodystrophic dogs present with clinical IVD disease with different clinical presentations, at different spinal locations and at different ages [73]. It is known that low-grade inflammation is part of the disease process in IVD degeneration in man [75, 76]. The latter remains to be confirmed in the canine species.

Approach: In order to gain more insight in the natural history of IVD degeneration, and to select canine patients that will benefit most from sustained release of celecoxib, inflammatory mediators and matrix components are determined in IVDs that have been collected during surgical treatment from CD and NCD dogs with and without clinical signs (*chapter 6*).

Aim 6. Assess the intradiscal application of a PCLA-PEG-PCLA hydrogel loaded with celecoxib for the treatment of back pain in canines.

Rationale: Chronic low back pain is a common clinical problem in the human and canine population. Current pharmaceutical treatments often consist of oral anti-inflammatory drugs to alleviate pain [28, 153]. Novel treatments for degenerative disc disease focus on local application of sustained released drug formulations [127]. The aim of this study is to determine safety and feasibility of intradiscal application of a thermoresponsive poly(ε-caprolactone-co-lactide)-b-poly(ethylene glycol)-b-poly(ε-caprolactone-colactide) PCLA-PEG-PCLA hydrogel gradually releasing celecoxib.

Approach: Biocompatibility is evaluated after subcutaneous injection in mice, and safety of intradiscal injection of the hydrogel is evaluated in experimental dogs with early spontaneous IVD degeneration. Ten client-owned dogs with chronic low back pain related to IVD degeneration receive an intradiscal injection with the celecoxib-loaded hydrogel and are evaluated by MRI, force plate analysis and owner questionnaires for three months as a preliminary safety and efficacy study (*chapter 7*).

Aim 7. Evaluate the controlled release of celecoxib from microspheres in a pre-clinical canine IVD degeneration model and translation towards the clinic.

Rationale: Provided that local delivery of the COX-2 inhibitor celecoxib, is effective in inhibiting pain and inflammation, further fine-tuning of the local delivery of celecoxib is indicated in order to provide for a safe treatment and effective long term effects. The PEA platform shown to provide prolonged and sustained drug delivery seems to be suitable for IVD-related back pain which is usually a chronic condition.

Approach: First, the controlled release and biologic potency of celecoxib-loaded PEAMs are investigated *in vitro*. Thereafter, safety and efficacy of injection of celecoxib-loaded microspheres are evaluated *in vivo* in a canine intervertebral disc degeneration model (*chapter 8*). MRI, CT and histology are used to assess IVD integrity. In addition, PGE_2 levels and neuronal growth factor expression are determined to assess the effects on pain and inflammation. Finally, the clinical efficacy of celecoxib-loaded PEAMs is assessed in client-owned dogs suffering from naturally occurring degenerative lumbosacral stenosis, compared to placebo-treatment with unloaded microspheres. Based on power analysis, twenty dogs should receive celecoxib-loaded microspheres, ten dogs should receive unloaded microspheres (placebo) via CT-guided intradiscal injection. Low back pain is assessed by clinical examination and kinetic gait analysis. MRI is repeated after three months, Pfirrmann degeneration score, disc height index and T2 mapping values are assessed before and after treatment. The administration of analgesics, pain and pain-related behaviour are scored by the owner *(chapter 9).*

Aim 8: Assess long-term outcome of dogs with DLSS treated with PSRF.

Rationale: Surgical management is the treatment of choice for dogs with refractory signs of DLSS [28]. Although the safety and efficacy of pedicle screw-rod fixation (PSRF) for the treatment of DLSS in large breed dogs has been established, long-term results and evaluation of spinal fusion were not reported thus far [154].

Approach: In *chapter 10* we assess the long-term outcome of treatment in 12 dogs with severe degenerative lumbosacral stenosis. Indications are failure from a previous decompressive surgery, or as a last resort treatment. In these patients the rigid PSRF construct is used in a permanent way to provide stability and promote spinal fusion, thereby reducing low back pain.

Conclusions, limitations and future perspectives of this thesis are discussed in *chapter 11*.

References

1. RIVM. Artrose. 2018;https://www.volksgezondheidenzorg.info/onderwerp/artrose.
2. Andersson GB. Epidemiological features of chronic low-back pain. Lancet 1999;354:581-5.
3. Hoy D, March L, Brooks P, Blyth F, Woolf A, Bain C*, et al*. The global burden of low back pain: estimates from the Global Burden of Disease 2010 study. Ann.Rheum.Dis. 2014;73:968-74.
4. Adams MA and Roughley PJ. What is intervertebral disc degeneration, and what causes it? Spine (Phila Pa.1976) 2006;31:2151-61.
5. Musumeci G, Aiello FC, Szychlinska MA, Di Rosa M, Castrogiovanni P, Mobasheri A. Osteoarthritis in the XXIst century: risk factors and behaviours that influence disease onset and progression. Int.J.Mol.Sci. 2015;16:6093-112.
6. Sandell LJ. Etiology of osteoarthritis: genetics and synovial joint development. Nat.Rev.Rheumatol. 2012;8:77-89.
7. Gore M, Sadosky A, Stacey BR, Tai KS, Leslie D. The burden of chronic low back pain: clinical comorbidities, treatment patterns, and health care costs in usual care settings. Spine (Phila Pa.1976) 2012;37:E668-77.
8. Holt HL, Katz JN, Reichmann WM, Gerlovin H, Wright EA, Hunter DJ*, et al*. Forecasting the burden of advanced knee osteoarthritis over a 10-year period in a cohort of 60-64 year-old US adults. Osteoarthritis Cartilage 2011;19:44-50.
9. Hootman JM, Helmick CG, Barbour KE, Theis KA, Boring MA. Updated projected prevalence of self-reported doctor-diagnosed arthritis and arthritis-attributable activity limitation among US adults. Arthritis Rheumatol. 2016;68:1582-7.
10. March L, Smith EU, Hoy DG, Cross MJ, Sanchez-Riera L, Blyth F*, et al*. Burden of disability due to musculoskeletal (MSK) disorders. Best Pract.Res.Clin.Rheumatol. 2014;28:353-66.
11. Cross M, Smith E, Hoy D, Nolte S, Ackerman I, Fransen M*, et al*. The global burden of hip and knee osteoarthritis: estimates from the global burden of disease 2010 study. Ann.Rheum.Dis. 2014;73:1323-30.
12. Myers H, Nicholls E, Handy J, Peat G, Thomas E, Duncan R*, et al*. The Clinical Assessment Study of the Hand (CAS-HA): a prospective study of musculoskeletal hand problems in the general population. BMC Musculoskelet.Disord. 2007;8:85,2474-8-85.
13. Puig-Junoy J and Ruiz Zamora A. Socio-economic costs of osteoarthritis: a systematic review of cost-of-illness studies. Semin.Arthritis Rheum. 2015;44:531-41.
14. van Weeren PR and de Grauw JC. Pain in osteoarthritis. Vet.Clin.North Am.Equine Pract. 2010;26:619-42.
15. Felson DT. Developments in the clinical understanding of osteoarthritis. Arthritis Res.Ther. 2009;11:203.
16. Jordan JM, Helmick CG, Renner JB, Luta G, Dragomir AD, Woodard J*, et al*. Prevalence of hip symptoms and radiographic and symptomatic hip osteoarthritis in African Americans and Caucasians: the Johnston County Osteoarthritis Project. J.Rheumatol. 2009;36:809-15.
17. Jordan JM, Helmick CG, Renner JB, Luta G, Dragomir AD, Woodard J*, et al*. Prevalence of knee symptoms and radiographic and symptomatic knee osteoarthritis in African Americans and Caucasians: the Johnston County Osteoarthritis Project. J.Rheumatol. 2007;34:172-80.
18. Sen R and Hurley JA. Osteoarthritis. In: StatPearls. Anonymous Treasure Island (FL): StatPearls Publishing LLC, 2018, .
19. Glyn-Jones S, Palmer AJ, Agricola R, Price AJ, Vincent TL, Weinans H*, et al*. Osteoarthritis. Lancet 2015;386:376-87.
20. Johnston SA. Osteoarthritis. Joint anatomy, physiology, and pathobiology. Vet.Clin.North Am.Small Anim.Pract. 1997;27:699-723.
21. Clements DN, Carter SD, Innes JF, Ollier WE. Genetic basis of secondary osteoarthritis in dogs with joint dysplasia. Am.J.Vet.Res. 2006;67:909-18.
22. Griffon DJ. A review of the pathogenesis of canine cranial cruciate ligament disease as a basis for future preventive strategies. Vet.Surg. 2010;39:399-409.
23. Baird AE, Carter SD, Innes JF, Ollier WE, Short AD. Genetic basis of cranial cruciate ligament rupture (CCLR) in dogs. Connect.Tissue Res. 2014;55:275-81.
24. Cook JL. Cranial cruciate ligament disease in dogs: biology versus biomechanics. Vet.Surg. 2010;39:270-7.
25. Frye CW, Shmalberg JW, Wakshlag JJ. Obesity, exercise and orthopedic disease. Vet.Clin.North Am.Small Anim.Pract. 2016;46:831-41.
26. King MD. Etiopathogenesis of canine hip dysplasia, prevalence, and genetics. Vet.Clin.North Am.Small Anim.Pract. 2017;47:753-67.

27. Marshall W, Bockstahler B, Hulse D, Carmichael S. A review of osteoarthritis and obesity: current understanding of the relationship and benefit of obesity treatment and prevention in the dog. Vet.Comp.Orthop.Traumatol. 2009;22:339-45.
28. Meij BP and Bergknut N. Degenerative lumbosacral stenosis in dogs. Vet.Clin.North Am.Small Anim.Pract. 2010;40:983-1009.
29. Loeser RF, Goldring SR, Scanzello CR, Goldring MB. Osteoarthritis: a disease of the joint as an organ. Arthritis Rheum. 2012;64:1697-707.
30. Xia B, Di C, Zhang J, Hu S, Jin H, Tong P. Osteoarthritis pathogenesis: a review of molecular mechanisms. Calcif.Tissue Int. 2014;95:495-505.
31. Funck-Brentano T and Cohen-Solal M. Subchondral bone and osteoarthritis. Curr.Opin.Rheumatol. 2015;27:420-6.
32. Hugle T and Geurts J. What drives osteoarthritis?-synovial versus subchondral bone pathology. Rheumatology (Oxford) 2017;56:1461-71.
33. Miller RE, Miller RJ, Malfait AM. Osteoarthritis joint pain: The cytokine connection. Cytokine 2014;70:185-93.
34. Heikkila HM, Hielm-Bjorkman AK, Innes JF, Laitinen-Vapaavuori OM. The effect of intra-articular botulinum toxin A on substance P, prostaglandin E2, and tumor necrosis factor alpha in the canine osteoarthritic joint. BMC Vet.Res. 2017;13:74,017-0990-y.
35. Hogberg E, Stalman A, Wredmark T, Tsai JA, Arner P, Fellander-Tsai L. Opioid requirement after arthroscopy is associated with decreasing glucose levels and increasing PGE2 levels in the synovial membrane. Acta Orthop. 2006;77:657-61.
36. Martel-Pelletier J, Pelletier JP, Fahmi H. Cyclooxygenase-2 and prostaglandins in articular tissues. Semin.Arthritis Rheum. 2003;33:155-67.
37. Samad TA, Moore KA, Sapirstein A, Billet S, Allchorne A, Poole S*, et al*. Interleukin-1beta-mediated induction of Cox-2 in the CNS contributes to inflammatory pain hypersensitivity. Nature 2001;410:471-5.
38. Trumble TN, Billinghurst RC, McIlwraith CW. Correlation of prostaglandin E2 concentrations in synovial fluid with ground reaction forces and clinical variables for pain or inflammation in dogs with osteoarthritis induced by transection of the cranial cruciate ligament. Am.J.Vet.Res. 2004;65:1269-75.
39. Sofat N, Ejindu V, Kiely P. What makes osteoarthritis painful? The evidence for local and central pain processing. Rheumatology (Oxford) 2011;50:2157-65.
40. Perrot S. Osteoarthritis pain. Best Pract.Res.Clin.Rheumatol. 2015;29:90-7.
41. Yusuf E, Kortekaas MC, Watt I, Huizinga TW, Kloppenburg M. Do knee abnormalities visualised on MRI explain knee pain in knee osteoarthritis? A systematic review. Ann.Rheum.Dis. 2011;70:60-7.
42. Anderson A. Treatment of hip dysplasia. J.Small Anim.Pract. 2011;52:182-9.
43. Bergh MS, Sullivan C, Ferrell CL, Troy J, Budsberg SC. Systematic review of surgical treatments for cranial cruciate ligament disease in dogs. J.Am.Anim.Hosp.Assoc. 2014;50:315-21.
44. Riccardo C, Fabio C, Pietro R. Knee osteoarthritis after reconstruction of isolated anterior cruciate ligament injuries: a systematic literature review. Joints 2017;5:39-43.
45. Chu CR, Millis MB, Olson SA. Osteoarthritis: From Palliation to Prevention: AOA Critical Issues. J.Bone Joint Surg.Am. 2014;96:e130.
46. Cook JL and Payne JT. Surgical treatment of osteoarthritis. Vet.Clin.North Am.Small Anim.Pract. 1997;27:931-44.
47. Ayhan E, Kesmezacar H, Akgun I. Intraarticular injections (corticosteroid, hyaluronic acid, platelet rich plasma) for the knee osteoarthritis. World J.Orthop. 2014;5:351-61.
48. Gallagher B, Tjoumakaris FP, Harwood MI, Good RP, Ciccotti MG, Freedman KB. Chondroprotection and the prevention of osteoarthritis progression of the knee: a systematic review of treatment agents. Am.J.Sports Med. 2015;43:734-44.
49. Lapane KL, Yang S, Driban JB, Liu SH, Dube CE, McAlindon TE*, et al*. Effects of prescription nonsteroidal antiinflammatory drugs on symptoms and disease progression among patients with knee osteoarthritis. Arthritis Rheumatol. 2015;67:724-32.
50. Sanderson RO, Beata C, Flipo RM, Genevois JP, Macias C, Tacke S*, et al*. Systematic review of the management of canine osteoarthritis. Vet.Rec. 2009;164:418-24.
51. Jin Y, Smith C, Hu L, Coutant DE, Whitehurst K, Phipps K*, et al*. LY3127760, a selective prostaglandin E4 (EP4) receptor antagonist, and celecoxib: a comparison of pharmacological profiles. Clin.Transl.Sci. 2018;11:46-53.
52. Rausch-Derra L, Huebner M, Wofford J, Rhodes L. A prospective, randomized, masked, placebo-controlled multisite clinical study of grapiprant, an EP4 prostaglandin receptor antagonist (PRA), in dogs with osteoarthritis. J.Vet.Intern.Med. 2016;30:756-63.

53. Rychel JK. Diagnosis and treatment of osteoarthritis. Top.Companion Anim.Med. 2010;25:20-5.
54. Gaffney K, Ledingham J, Perry JD. Intra-articular triamcinolone hexacetonide in knee osteoarthritis: factors influencing the clinical response. Ann.Rheum.Dis. 1995;54:379-81.
55. Jones A and Doherty M. Intra-articular corticosteroids are effective in osteoarthritis but there are no clinical predictors of response. Ann.Rheum.Dis. 1996;55:829-32.
56. Basso M, Cavagnaro L, Zanirato A, Divano S, Formica C, Formica M*, et al*. What is the clinical evidence on regenerative medicine in intervertebral disc degeneration? Musculoskelet.Surg. 2017;101:93-104.
57. Altman R, Hackel J, Niazi F, Shaw P, Nicholls M. Efficacy and safety of repeated courses of hyaluronic acid injections for knee osteoarthritis: A systematic review. Semin.Arthritis Rheum. 2018;.
58. Richards MM, Maxwell JS, Weng L, Angelos MG, Golzarian J. Intra-articular treatment of knee osteoarthritis: from anti-inflammatories to products of regenerative medicine. Phys.Sportsmed 2016;44:101-8.
59. Bergknut N, Meij BP, Hagman R, de Nies KS, Rutges JP, Smolders LA*, et al*. Intervertebral disc disease in dogs - Part 1: A new histological grading scheme for classification of intervertebral disc degeneration in dogs. Vet.J. 2013;195:156-63.
60. Lotz JC, Fields AJ, Liebenberg EC. The role of the vertebral end plate in low back pain. Global Spine J. 2013;3:153-64.
61. Kepler CK, Ponnappan RK, Tannoury CA, Risbud MV, Anderson DG. The molecular basis of intervertebral disc degeneration. Spine J. 2013;13:318-30.
62. van Uden S, Silva-Correia J, Oliveira JM, Reis RL. Current strategies for treatment of intervertebral disc degeneration: substitution and regeneration possibilities. Biomater.Res. 2017;21:22.
63. Battie MC, Videman T, Kaprio J, Gibbons LE, Gill K, Manninen H*, et al*. The Twin Spine Study: contributions to a changing view of disc degeneration. Spine J. 2009;9:47-59.
64. Pye SR, Reid DM, Adams JE, Silman AJ, O'Neill TW. Influence of weight, body mass index and lifestyle factors on radiographic features of lumbar disc degeneration. Ann.Rheum.Dis. 2007;66:426-7.
65. Dudli S, Fields AJ, Samartzis D, Karppinen J, Lotz JC. Pathobiology of Modic changes. Eur.Spine J. 2016;25:3723-34.
66. Modic MT and Ross JS. Lumbar degenerative disk disease. Radiology 2007;245:43-61.
67. Izzo R, Guarnieri G, Guglielmi G, Muto M. Biomechanics of the spine. Part II: spinal instability. Eur.J.Radiol. 2013;82:127-38.
68. Ohtori S, Inoue G, Miyagi M, Takahashi K. Pathomechanisms of discogenic low back pain in humans and animal models. Spine J. 2015;15:1347-55.
69. Luoma K, Riihimaki H, Luukkonen R, Raininko R, Viikari-Juntura E, Lamminen A. Low back pain in relation to lumbar disc degeneration. Spine (Phila Pa.1976) 2000;25:487-92.
70. de Schepper EI, Damen J, van Meurs JB, Ginai AZ, Popham M, Hofman A*, et al*. The association between lumbar disc degeneration and low back pain: the influence of age, gender, and individual radiographic features. Spine (Phila Pa.1976) 2010;35:531-6.
71. Bergknut N, Egenvall A, Hagman R, Gustas P, Hazewinkel HA, Meij BP*, et al*. Incidence of intervertebral disk degeneration-related diseases and associated mortality rates in dogs. J.Am.Vet.Med.Assoc. 2012;240:1300-9.
72. Hansen HJ. A pathologic-anatomical study on disc degeneration in dog, with special reference to the so-called enchondrosis intervertebralis. Acta Orthop.Scand.Suppl. 1952;11:1-117.
73. Smolders LA, Bergknut N, Grinwis GC, Hagman R, Lagerstedt AS, Hazewinkel HA*, et al*. Intervertebral disc degeneration in the dog. Part 2: chondrodystrophic and non-chondrodystrophic breeds. Vet.J. 2013;195:292-9.
74. Hansen T, Smolders LA, Tryfonidou MA, Meij BP, Vernooij JCM, Bergknut N*, et al*. The myth of fibroid degeneration in the canine intervertebral disc: a histopathological comparison of intervertebral disc degeneration in chondrodystrophic and nonchondrodystrophic dogs. Vet.Pathol. 2017;54:945-52.
75. Phillips KL, Cullen K, Chiverton N, Michael AL, Cole AA, Breakwell LM*, et al*. Potential roles of cytokines and chemokines in human intervertebral disc degeneration: interleukin-1 is a master regulator of catabolic processes. Osteoarthritis Cartilage 2015;23:1165-77.
76. Risbud MV and Shapiro IM. Role of cytokines in intervertebral disc degeneration: pain and disc content. Nat.Rev.Rheumatol. 2014;10:44-56.
77. Hamamoto H, Miyamoto H, Doita M, Takada T, Nishida K, Kurosaka M. Capability of nondegenerated and degenerated discs in producing inflammatory agents with or without macrophage interaction. Spine (Phila Pa.1976) 2012;37:161-7.
78. DePalma MJ, Ketchum JM, Saullo T. What is the source of chronic low back pain and does age play a role? Pain Med. 2011;12:224-33.

79. Purmessur D, Cornejo MC, Cho SK, Roughley PJ, Linhardt RJ, Hecht AC*, et al*. Intact glycosaminoglycans from intervertebral disc-derived notochordal cell-conditioned media inhibit neurite growth while maintaining neuronal cell viability. Spine J. 2015;15:1060-9.
80. Burke JG, Watson RW, McCormack D, Dowling FE, Walsh MG, Fitzpatrick JM. Intervertebral discs which cause low back pain secrete high levels of proinflammatory mediators. J.Bone Joint Surg.Br. 2002;84:196-201.
81. Borenstein D. Does osteoarthritis of the lumbar spine cause chronic low back pain? Curr.Pain Headache Rep. 2004;8:512-7.
82. Izzo R, Popolizio T, D'Aprile P, Muto M. Spinal pain. Eur.J.Radiol. 2015;84:746-56.
83. Lawrence BD, Wang J, Arnold PM, Hermsmeyer J, Norvell DC, Brodke DS. Predicting the risk of adjacent segment pathology after lumbar fusion: a systematic review. Spine (Phila Pa.1976) 2012;37:S123-32.
84. Wang JC, Arnold PM, Hermsmeyer JT, Norvell DC. Do lumbar motion preserving devices reduce the risk of adjacent segment pathology compared with fusion surgery? A systematic review. Spine (Phila Pa.1976) 2012;37:S133-43.
85. Johnson CI, Argyle DJ, Clements DN. In vitro models for the study of osteoarthritis. Vet.J. 2016;209:40-9.
86. Bach FC, Willems N, Penning LC, Ito K, Meij BP, Tryfonidou MA. Potential regenerative treatment strategies for intervertebral disc degeneration in dogs. BMC Vet.Res. 2014;10:3,6148-10-3.
87. Alini M, Eisenstein SM, Ito K, Little C, Kettler AA, Masuda K*, et al*. Are animal models useful for studying human disc disorders/degeneration? Eur.Spine J. 2008;17:2-19.
88. McCoy AM. Animal models of osteoarthritis: comparisons and key considerations. Vet.Pathol. 2015;52:803-18.
89. Little CB and Zaki S. What constitutes an "animal model of osteoarthritis"--the need for consensus? Osteoarthritis Cartilage 2012;20:261-7.
90. Gregory MH, Capito N, Kuroki K, Stoker AM, Cook JL, Sherman SL. A review of translational animal models for knee osteoarthritis. Arthritis 2012;2012:764621.
91. Bendele AM and White SL. Early histopathologic and ultrastructural alterations in femorotibial joints of partial medial meniscectomized guinea pigs. Vet.Pathol. 1987;24:436-43.
92. Bendele AM. Animal models of osteoarthritis. J.Musculoskelet.Neuronal Interact. 2001;1:363-76.
93. Lampropoulou-Adamidou K, Lelovas P, Karadimas EV, Liakou C, Triantafillopoulos IK, Dontas I*, et al*. Useful animal models for the research of osteoarthritis. Eur.J.Orthop.Surg.Traumatol. 2014;24:263-71.
94. Malfait AM and Little CB. On the predictive utility of animal models of osteoarthritis. Arthritis Res.Ther. 2015;17:225.
95. Kuroki K, Cook CR, Cook JL. Subchondral bone changes in three different canine models of osteoarthritis. Osteoarthritis Cartilage 2011;19:1142-9.
96. Pelletier JP, Kapoor M, Fahmi H, Lajeunesse D, Blesius A, Maillet J*, et al*. Strontium ranelate reduces the progression of experimental dog osteoarthritis by inhibiting the expression of key proteases in cartilage and of IL-1beta in the synovium. Ann.Rheum.Dis. 2013;72:250-7.
97. Yun S, Ku SK, Kwon YS. Adipose-derived mesenchymal stem cells and platelet-rich plasma synergistically ameliorate the surgical-induced osteoarthritis in Beagle dogs. J.Orthop.Surg.Res. 2016;11:9.
98. Caron JP, Fernandes JC, Martel-Pelletier J, Tardif G, Mineau F, Geng C*, et al*. Chondroprotective effect of intraarticular injections of interleukin-1 receptor antagonist in experimental osteoarthritis. Suppression of collagenase-1 expression. Arthritis Rheum. 1996;39:1535-44.
99. Smith GN,Jr, Myers SL, Brandt KD, Mickler EA, Albrecht ME. Diacerhein treatment reduces the severity of osteoarthritis in the canine cruciate-deficiency model of osteoarthritis. Arthritis Rheum. 1999;42:545-54.
100. Mastbergen SC, Marijnissen AC, Vianen ME, van Roermund PM, Bijlsma JW, Lafeber FP. The canine 'groove' model of osteoarthritis is more than simply the expression of surgically applied damage. Osteoarthritis Cartilage 2006;14:39-46.
101. de Visser HM, Weinans H, Coeleveld K, van Rijen MH, Lafeber FP, Mastbergen SC. Groove model of tibia-femoral osteoarthritis in the rat. J.Orthop.Res. 2016;35:496-505.
102. Marijnissen AC, van Roermund PM, TeKoppele JM, Bijlsma JW, Lafeber FP. The canine 'groove' model, compared with the ACLT model of osteoarthritis. Osteoarthritis Cartilage 2002;10:145-55.
103. Sniekers YH, Intema F, Lafeber FP, van Osch GJ, van Leeuwen JP, Weinans H*, et al*. A role for subchondral bone changes in the process of osteoarthritis; a micro-CT study of two canine models. BMC Musculoskelet.Disord. 2008;9:20.
104. Brimmo OA, Pfeiffer F, Bozynski CC, Kuroki K, Cook C, Stoker A*, et al*. Development of a novel canine model for posttraumatic osteoarthritis of the knee. J.Knee Surg. 2016;29:235-41.
105. Lahm A, Uhl M, Edlich M, Erggelet C, Haberstroh J, Kreuz PC. An experimental canine model for subchondral lesions of the knee joint. Knee 2005;12:51-5.

106. Mrosek EH, Lahm A, Erggelet C, Uhl M, Kurz H, Eissner B*, et al*. Subchondral bone trauma causes cartilage matrix degeneration: an immunohistochemical analysis in a canine model. Osteoarthritis Cartilage 2006;14:171-8.
107. Johnson RG and Poole AR. Degenerative changes in dog articular cartilage induced by a unilateral tibial valgus osteotomy. Exp.Pathol. 1988;33:145-64.
108. Panula HE, Helminen HJ, Kiviranta I. Slowly progressive osteoarthritis after tibial valgus osteotomy in young beagle dogs. Clin.Orthop.Relat.Res. 1997;(343):192-202.
109. Lotz JC. Animal models of intervertebral disc degeneration: lessons learned. Spine (Phila Pa.1976) 2004;29:2742-50.
110. Daly C, Ghosh P, Jenkin G, Oehme D, Goldschlager T. A Review of Animal Models of Intervertebral Disc Degeneration: Pathophysiology, Regeneration, and Translation to the Clinic. Biomed.Res.Int. 2016;2016:5952165.
111. Bergknut N, Rutges JP, Kranenburg HJ, Smolders LA, Hagman R, Smidt HJ*, et al*. The dog as an animal model for intervertebral disc degeneration? Spine (Phila Pa.1976) 2012;37:351-8.
112. Lindblad-Toh K, Wade CM, Mikkelsen TS, Karlsson EK, Jaffe DB, Kamal M*, et al*. Genome sequence, comparative analysis and haplotype structure of the domestic dog. Nature 2005;438:803-19.
113. Roza MR and Viegas CA. The dog as a passive smoker: effects of exposure to environmental cigarette smoke on domestic dogs. Nicotine Tob.Res. 2007;9:1171-6.
114. Thalmann O, Shapiro B, Cui P, Schuenemann VJ, Sawyer SK, Greenfield DL*, et al*. Complete mitochondrial genomes of ancient canids suggest a European origin of domestic dogs. Science 2013;342:871-4.
115. Chandler M, Cunningham S, Lund EM, Khanna C, Naramore R, Patel A*, et al*. Obesity and associated comorbidities in people and companion animals: a One Health perspective. J.Comp.Pathol. 2017;156:296-309.
116. Rijnberk A, Kooistra HS, Mol JA. Endocrine diseases in dogs and cats: similarities and differences with endocrine diseases in humans. Growth Horm.IGF Res. 2003;13 Suppl A:S158-64.
117. Kranenburg HC, Hazewinkel HA, Meij BP. Spinal hyperostosis in humans and companion animals. Vet.Q. 2013;33:30-42.
118. Cimino Brown D. What can we learn from osteoarthritis pain in companion animals? Clin.Exp.Rheumatol. 2017;35 Suppl 107:53-8.
119. Garner BC, Stoker AM, Kuroki K, Evans R, Cook CR, Cook JL. Using animal models in osteoarthritis biomarker research. J.Knee Surg. 2011;24:251-64.
120. Intema F, Mastbergen S, van Rinsum C, Castelein R, Marijnissen AK, Bijlsma J*, et al*. Cartilage integrity and proteoglycan turnover are comparable in canine experimentally induced and human joint degeneration. Rheumatol Rep 2010;2:50,-54.
121. Lorenz H, Wenz W, Ivancic M, Steck E, Richter W. Early and stable upregulation of collagen type II, collagen type I and YKL40 expression levels in cartilage during early experimental osteoarthritis occurs independent of joint location and histological grading. Arthritis Res.Ther. 2005;7:R156-65.
122. Liu W, Burton-Wurster N, Glant TT, Tashman S, Sumner DR, Kamath RV*, et al*. Spontaneous and experimental osteoarthritis in dog: similarities and differences in proteoglycan levels. J.Orthop.Res. 2003;21:730-7.
123. Grimm D. From bark to bedside. Science 2016;353:638-40.
124. Hoffman AM and Dow SW. Concise review: stem cell trials using companion animal disease models. Stem Cells 2016;34:1709-29.
125. Mobasheri A. Comparative medicine in the twenty-first century: where are we now and where do we go from here? Front.Vet.Sci. 2015;2:2.
126. Anonymous About the One Health Initiative. 2018:http://www.onehealthinitiative.com/about.php.
127. Henry N, Clouet J, Le Bideau J, Le Visage C, Guicheux J. Innovative strategies for intervertebral disc regenerative medicine: From cell therapies to multiscale delivery systems. Biotechnol.Adv. 2018;36:281-94.
128. Zhang W, Ouyang H, Dass CR, Xu J. Current research on pharmacologic and regenerative therapies for osteoarthritis. Bone Res. 2016;4:15040.
129. Grol MW and Lee BH. Gene therapy for repair and regeneration of bone and cartilage. Curr.Opin.Pharmacol. 2018;40:59-66.
130. Whitney KE, Liebowitz A, Bolia IK, Chahla J, Ravuri S, Evans TA*, et al*. Current perspectives on biological approaches for osteoarthritis. Ann.N.Y.Acad.Sci. 2017;1410:26-43.
131. Fotouhi A, Maleki A, Dolati S, Aghebati-Maleki A, Aghebati-Maleki L. Platelet rich plasma, stromal vascular fraction and autologous conditioned serum in treatment of knee osteoarthritis. Biomed.Pharmacother. 2018;104:652-60.

132. Godek P. Use of Autologous Serum in Treatment of Lumbar Radiculopathy Pain. Pilot Study. Ortop.Traumatol.Rehabil. 2016;18:11-20.
133. Uthman I, Raynauld JP, Haraoui B. Intra-articular therapy in osteoarthritis. Postgrad.Med.J. 2003;79:449-53.
134. Stueber T, Karsten J, Stoetzer C, Leffler A. Differential cytotoxic properties of drugs used for intra-articular injection on human chondrocytes: an experimental in-vitro study. Eur.J.Anaesthesiol. 2014;31:640-5.
135. McIlwraith CW. The use of intra-articular corticosteroids in the horse: what is known on a scientific basis? Equine Vet.J. 2010;42:563-71.
136. Vandeweerd JM, Zhao Y, Nisolle JF, Zhang W, Zhihong L, Clegg P*, et al*. Effect of corticosteroids on articular cartilage: have animal studies said everything? Fundam.Clin.Pharmacol. 2015;29:427-38.
137. Conaghan PG, Hunter DJ, Cohen SB, Kraus VB, Berenbaum F, Lieberman JR*, et al*. Effects of a single intra-articular injection of a microsphere formulation of triamcinolone acetonide on knee osteoarthritis pain: a double-blinded, randomized, placebo-controlled, multinational study. J.Bone Joint Surg.Am. 2018;100:666-77.
138. Wernecke C, Braun HJ, Dragoo JL. The effect of intra-articular corticosteroids on articular cartilage: a systematic review. Orthop.J.Sports Med. 2015;3:2325967115581163.
139. Calmet J, Esteve C, Boada S, Gine J. Analgesic effect of intra-articular ketorolac in knee arthroscopy: comparison of morphine and bupivacaine. Knee Surg.Sports Traumatol.Arthrosc. 2004;12:552-5.
140. Oztuna V, Eskandari M, Bugdayci R, Kuyurtar F. Intra-articular injection of tenoxicam in osteoarthritic knee joints with effusion. Orthopedics 2007;30:1039-42.
141. Papathanassiou NP. Intra-articular use of tenoxicam in degenerative osteoarthritis of the knee joint. J.Int.Med.Res. 1994;22:332-7.
142. Park KD, Kim TK, Bae BW, Ahn J, Lee WY, Park Y. Ultrasound guided intra-articular ketorolac versus corticosteroid injection in osteoarthritis of the hip: a retrospective comparative study. Skeletal Radiol. 2015;44:1333-40.
143. Nakata K, Hanai T, Take Y, Osada T, Tsuchiya T, Shima D*, et al*. Disease-modifying effects of COX-2 selective inhibitors and non-selective NSAIDs in osteoarthritis: a systematic review. Osteoarthritis Cartilage 2018;10.1016/j.joca.2018.05.021:.
144. Zweers MC, de Boer TN, van Roon J, Bijlsma JW, Lafeber FP, Mastbergen SC. Celecoxib: considerations regarding its potential disease-modifying properties in osteoarthritis. Arthritis Res.Ther. 2011;13:239-250.
145. Evans CH, Kraus VB, Setton LA. Progress in intra-articular therapy. Nat.Rev.Rheumatol. 2014;10:11-22.
146. Larsen C, Ostergaard J, Larsen SW, Jensen H, Jacobsen S, Lindegaard C*, et al*. Intra-articular depot formulation principles: role in the management of postoperative pain and arthritic disorders. J.Pharm.Sci. 2008;97:4622-54.
147. Brown EA, Dickinson PJ, Mansour T, Sturges BK, Aguilar M, Young AE*, et al*. FGF4 retrogene on CFA12 is responsible for chondrodystrophy and intervertebral disc disease in dogs. PNAS 2017;114:11476–11481.
148. Parker HG, VonHoldt BM, Quignon P, Margulies EH, Shao S, Mosher DS*, et al*. An expressed fgf4 retrogene is associated with breed-defining chondrodysplasia in domestic dogs. Science 2009;325:995-8.
149. Chuah YJ, Peck Y, Lau JE, Hee HT, Wang DA. Hydrogel based cartilaginous tissue regeneration: recent insights and technologies. Biomater.Sci. 2017;5:613-31.
150. Gerwin N, Bendele AM, Glasson S, Carlson CS. The OARSI histopathology initiative - recommendations for histological assessments of osteoarthritis in the rat. Osteoarthritis Cartilage 2010;18 Suppl 3:S24-34.
151. Rai MF and Pham CT. Intra-articular drug delivery systems for joint diseases. Curr.Opin.Pharmacol. 2018;40:67-73.
152. Rudnik-Jansen I, Colen S, Berard J, Plomp S, Que I, van Rijen M*, et al*. Prolonged inhibition of inflammation in osteoarthritis by triamcinolone acetonide released from a polyester amide microsphere platform. J.Control.Release 2017;253:64-72.
153. Meucci RD, Fassa AG, Faria NM. Prevalence of chronic low back pain: systematic review. Rev.Saude Publica 2015;49:10.1590/S0034,8910.2015049005874. Epub 2015 Oct 20.
154. Smolders LA, Voorhout G, van de Ven R, Bergknut N, Grinwis GC, Hazewinkel HA*, et al*. Pedicle screw-rod fixation of the canine lumbosacral junction. Vet.Surg. 2012;41:720-32.

Part I

Development of novel treatment strategies for osteoarthritis in humans and canines

Chapter 2

The dog as a model for osteoarthritis: chondrodystrophy does matter

A. R. Tellegen [1], A. J. Dessing [1*], K. Houben [1*], F. R. Riemers [1], L.B. Creemers [2], S. C. Mastbergen [3], B. P. Meij [1], A. Miranda-Bedate [1], M. A. Tryfonidou [1]

[1] Department of Clinical Sciences of Companion Animals, Faculty of Veterinary Medicine, Utrecht University, The Netherlands
[2] Department of Orthopaedics, University Medical Centre Utrecht, The Netherlands
[3] Department of Rheumatology & Clinical Immunology, University Medical Centre Utrecht, The Netherlands

[*] Shared second authorship

Submitted to Journal of Orthopaedic Research

Abstract

Osteoarthritis (OA) is a degenerative joint disease associated with chronic pain and disability in humans and companion animals. The canine species can be subdivided into non-chondrodystrophic (NCD) and chondrodystrophic (CD) dogs, the latter having disproportionally short limbs due to disturbance in endochondral ossification of long bones. However, the effect of chondrodystrophy on cartilage is unknown and in experimental studies with dogs, breeds are seemingly employed randomly. The aim of this study was to determine if CD and NCD derived cartilage differs on a structural and biochemical level, and to explore the relation between the chondrodystrophy genotype and the development of OA. Cartilage explants from CD and NCD dogs were cultured for 21 days with and without a pro-inflammatory stimulus (TNF-α). Activation of canonical Wnt signalling was assessed in primary canine chondrocytes. Osteoarthritis and synovitis severity from a canine experimental OA model were compared between healthy and OA samples from CD and NCD dogs. Release of glycosaminoglycans, DNA content and COX-2 expression were higher in NCD cartilage explants. Healthy cartilage from NCD dogs displayed higher cartilage degeneration and synovitis scores, this difference was aggravated by the induction of OA. Dikkopf-3 gene expression was higher in NCD cartilage explants. No differences in other Wnt pathway read outs were found. To conclude, chondrodystrophy seems to render CD dogs less susceptible to the development of OA when compared to NCD dogs. These differences should be considered when choosing a canine model to study pathobiology and new treatment strategies of OA.

Introduction

Osteoarthritis (OA), a degenerative joint disease, is one of the leading causes of chronic pain and disability and is accompanied by economic, social, and psychological burdens [1]. Treatment remains symptomatic and current efforts within the scientific community focus on a better understanding of OA pathobiology in order to develop effective treatment strategies. To investigate OA pathogenesis and to evaluate novel therapies, numerous animal models have been utilized in the last decades. The similarities between human and canine joint anatomy and OA pathogenesis, together with the possibility to undergo diagnostic and therapeutic procedures similar to man, contribute to the fact that the dog has often been employed as a large animal model [2, 3]. The dog not only serves as a model to human medicine but also functions as a model for its own species. Osteoarthritis causes clinical signs in over 20% of dogs older than one year of age and 80% of geriatric dogs [4]. OA can occur in all dog breeds; large breeds are affected more frequently [5]. In experimental studies with dogs, breeds are seemingly employed randomly, the majority being either purpose-bred hound type dogs or Beagles, which have a considerably different body conformation.

In this respect, the domestic dog (*Canis familiaris*) is undoubtedly the most morphologically diverse mammalian species. One aspect of variation is leg length, also known as chondrodystrophy. This is defined by dysplastic, shortened long bones and is characteristic for breeds such as the Dachshund and Beagle. From a histological point of view, chondrodystrophic (CD) dogs show shortening of the long bones primarily by calcification of the growth plates early in development. Moreover, the growth plates of the long bones of CD dogs show disorganization of the proliferative zone and reduction in depth of the maturation zone in comparison to non-chondrodystrophic (NCD) dogs [6]. Expressed fibroblast growth factor 4 (*FGF4*) retrogenes on CFA12 or CFA18 leading to over-activation of fibroblast growth factor receptor 3 (FGFR3), have been agreed on as the cause of chondrodystrophy in dogs [6, 7]. In a similar fashion, several mutations causing enhanced FGFR3 activity can lead to achondroplasia in humans [8, 9]. In mice FGFR3 overexpression led to disruption of growth plate architecture, and enhanced terminal chondrocyte differentiation, whereas inhibition of FGFR3 signalling leads to skeletal overgrowth and disruption of chondrocyte homeostasis [10]. Interestingly, FGFR3 signalling also delayed subchondral bone sclerosis and OA progression in knee joints [11, 12], while deletion of FGFR3 induced OA-like defects in temporomandibular joints in adult mice [13]. These findings indicate that chondrodystrophy is associated with a different cartilage (patho)physiology and that this may even have a protective effect against OA.

FGFR3 signalling was found to activate canonical Wnt signalling in a rat chondrosarcoma cell line and mouse limb bud micromass cultures [14]. Furthermore, studies in human and experimental animals also imply multiple roles for Wnt in OA. An increase in Wnt-related molecules has been found in osteoarthritic cartilage [15, 16], accompanied by an increase in Wnt antagonists such as members of the Dickkopf family [17]. Both gain- and loss-of-function

of β-catenin in cartilage induced osteoarthritic changes in mice [18, 19] and the Wnt antagonist Dikkopf-1 (DKK1) displayed both destructive and protective effects on articular cartilage in experimental OA models [20, 21]. Genetic studies in humans suggest that the canonical Wnt pathway participates in the pathogenesis of OA in at least a subset of patients [22, 23]. It is therefore hypothesized that excessive activation of Wnt/β-catenin signalling enhances articular cartilage destruction. A basal level of Wnt/β-catenin signalling may nevertheless be required to promote regenerative potential of articular cartilage [17].

Wnt signalling was shown to differ between CD and NCD dogs at least at the intervertebral disc level, concurring with a different clinical representation of disc disease [24]. Hence the use of dogs as a model in OA, i.e. Beagles (CD) versus purpose-bred hound type dogs (NCD) may be obscured by an important confounder involved in OA susceptibility and progression. To our knowledge, articular joint pathobiology related to canonical Wnt signalling has not been described for the canine species. Therefore, considering the key role of dogs as an OA model, the aim of this study was to identify possible variations in cartilage and synovium homeostasis, and more specifically in the activation of canonical Wnt signalling pathway, between CD and NCD dogs. This was performed in an *ex vivo* explant culture model under basal conditions or in the presence of a pro-inflammatory stimulus to mimic the OA joint environment. The COX-2 inhibitor celecoxib was added to assess the response of CD and NCD cartilage to an anti-inflammatory drug. To transcribe this towards possible translational implications, historical histological sections of healthy and osteoarthritic cartilage and synovial tissues were compared between CD and NCD experimental dogs generated by standardized experimental protocols.

Materials and methods

Ex vivo explant culture of canine articular cartilage and synovial tissue

Cartilage and synovial tissue from the weight-bearing surfaces of femorotibial joints of healthy NCD (Fig 1A; *n*=11) and CD (Fig 1B; *n*=10) donors were collected *post-mortem* complying with the 3Rs principles: all dogs had been euthanized as part of unrelated studies (approved by the Utrecht University Animal Ethics Committee, approval numbers #2016.II.529.002 and #2014.II.06.048). Of the CD dogs, there were 8 Beagles and two Beagle/Bedlington crosses with a median age of 48.5 months (range: 21-26 months), 4 males and 6 females. NCD donors were purpose-bred hound type dogs (*n*=11, median age 24 months (range: 19-36 months, all female) (supplementary file 1). Within 1 h of death, the joint cavity was opened under aseptic conditions in order to collect the non-calcified cartilage layer and synovial tissue. The obtained tissue was collected in 50 mL tubes with 25 mL hgDMEM+Glutamax (31966, Invitrogen) + 1% v/v Penicillin/Streptomycin (p/s, P11-010, PAA laboratories). After washing with hgDMEM+p/s, an overnight rest at 37 °C in a Petri dish (353803, Corning) with 25 mL hgDMEM+p/s was included.

After an overnight acclimatisation period, cartilage and synovium were cut into pieces with mean ± SD wet weights of 10.4 ± 4.9 mg per cartilage explant and 47.5 ± 28.6 mg per synovial explant. Two cartilage or synovial explants from each donor were cultured per well of a 24-wells plate (662160, Greiner Bio-one). To prevent adhesion the plates were coated with 1% agarose (V3121, Promega). Samples were cultured for 21 days in culture medium alone or in combination with 10 ng/mL of the pro-inflammatory mediator tumour necrosis factor α (TNF-α) to mimic the arthritic environment (210-TA, R&D Systems): hgDMEM, 1% v/v ITS+ premix (354352, Corning), 0.04 mg/mL L-Proline (P5607, Sigma), 1% v/v p/s, 0.05% v/v fungizone (15290-018, Invitrogen), 0.1 mM ascorbic acid 2-phosphate (A8960, Sigma), and 1 ng/mL bovine serum albumin (A9418, Sigma). To assess the response of CD and NCD joint tissue to an anti-inflammatory drug, celecoxib (10^{-6} M) was added. The medium was changed and collected on day 3, 7, 10, 14, 17 and 21 (Fig. 1) and stored at -20 °C until further use. Cartilage and synovial explants were collected at day 0, 7 and day 21 of culturing (*n*=3 per donor per condition). The pooled explants per condition per donor were lyophilized to obtain dry weights of the explants.

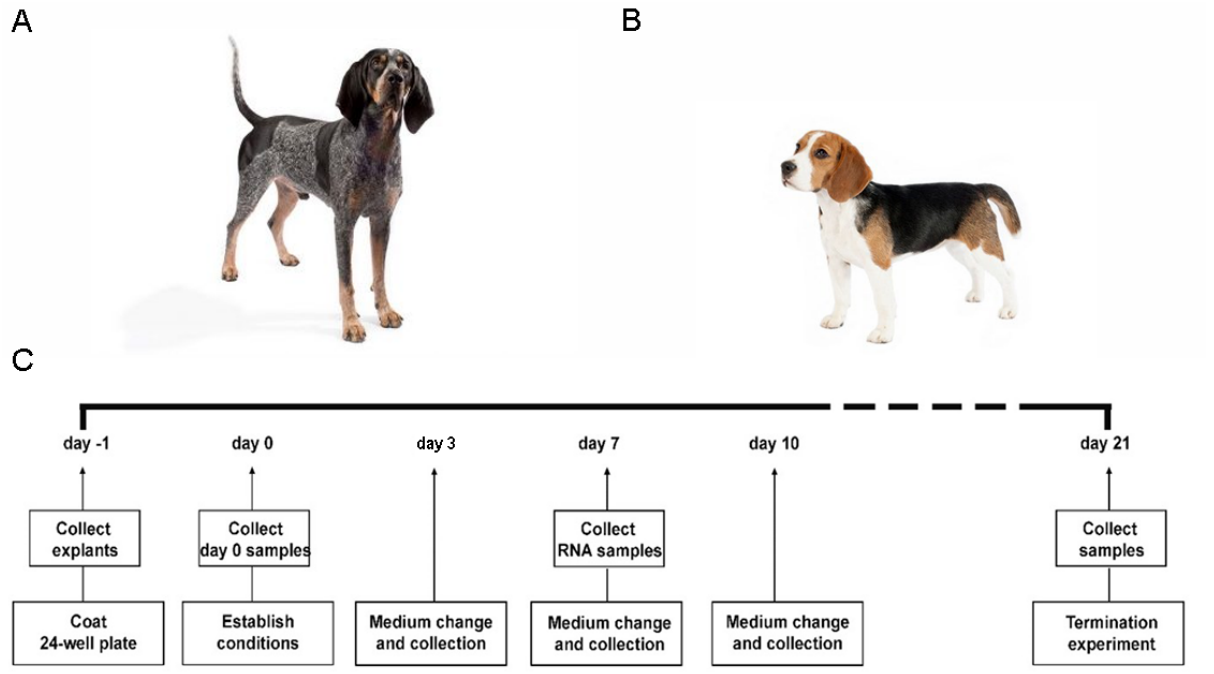

Figure 1. Typical example of an experimental non-chondrodystrophic dog (**A**; Hound-type dog) and a chondrodystrophic dog (**B**; Beagle). **C**. Setup of the cartilage and synovium explant culture. On day 7, samples for RNA isolation were collected. On day 0 and 21, samples for glycosaminoglycan (GAG) and DNA content, and histology were collected. The experiment was terminated after 21 days of culturing. Immunohistochemistry for collagen type I and II, COX-2 and β-catenin was performed on day 0 samples, to evaluate the tissues in their native state. OARSI and Krenn scores were performed on tissue explants on day 0 and after 21 days of culturing, to assess the severity of cartilage degeneration and synovitis, respectively.

Gene expression analysis

Cartilage explants (*n*=2 per donor) were collected, snap frozen and stored at -80 °C after seven days of culturing. To assess cartilage homeostasis, gene expression levels of aggrecan (*ACAN*), collagen1α1 (*COL1A1*), collagen2α1 (*COL2A1*), a disintegrin and metalloproteinase with thrombospondin motifs 5 (*ADAMTS5*) and metalloproteinase 13 (*MMP13*) were measured. Inflammatory mediators (*IL1β, IL6, PTGES1*) and canonical Wnt signalling (*AXIN2, CCND1, DKK3, FZD1, LRP5A* and *WIF1*) were also assessed. A subset of donors were assayed for the *FGF4* retrogene insertion on CFA12 and 18 using a PCR-based assay as described by Brown et al [6], with some minor modifications. Details on *FGF4* genotyping and RT-qPCR methods and primers are provided in Supplementary File 2.

Biochemistry

Cartilage explants were digested overnight in 600 µL of papain digestion solution (papain buffer (200 mM $H_2NaPO_4 \cdot 2\ H_2O$ (21254, Boom BV), pH 6) , 10 mM EDTA (100944, Merck Millipore, pH 6.0), 10 mM Cysteine HCL (C7880, Sigma-Aldrich), and 10 mM papain (P3125, Sigma-Aldrich)). DNA content was measured according to the manufacturer's instructions (Q32851; Invitrogen) and dimethylmethylene blue (DMMB) assay was performed to measure glycosaminoglycan (GAG) levels [25]. Prostaglandin E_2 (PGE_2) levels were determined in culture medium by ELISA (514010, Cayman Chemical) following the manufacturer's instructions and subsequently corrected for explant weight. Cumulative GAG and PGE_2 release were calculated over the 21 day culture period.

Histology

Cartilage and synovial explants were fixed in neutral buffered formalin (NBF 4%, 4286, Klinipath) for at least 24 hours. The samples were embedded in paraffin and 5 µm sections were stained with Safranin O/Fast Green staining on cartilage and Haematoxylin and Eosin (H&E) staining on synovial tissue. Tissue sections were blindly scored for OA severity according to an adapted protocol of the Osteoarthritis Research Society International (OARSI) scoring for the assessment for osteoarthritis for the dog (KH, AMB) [3]. In this protocol the severity of cartilage, chondrocyte, and proteoglycan pathology were assessed. H&E stained sections were scored for the severity of synovitis in a blinded fashion by a scheme proposed by Krenn et al (KH, AT) [26]. Immunohistochemistry for collagen type I and II (cartilage quality), β-catenin (canonical Wnt pathway) [27] and COX-2 (inflammation marker) [28] was performed on explants collected on day 0 (supplementary file 3). Isotype controls, normal mouse IgG1 (3877; Santa Cruz Biotechnology) showed no specific staining. To quantify COX-2 and β-catenin immunopositivity, the percentage of positive cells over total amount of cells were calculated in ImageJ. Herein, cytoplasmic or nuclear staining for β-catenin were scored separately.

Canonical Wnt signalling activity at the cellular level

In order to determine canonical Wnt signalling activity at the cellular level, chondrocytes were isolated from healthy CD and NCD cartilage tissue and the level of Wnt activity was measured by a TCF-reporter assay (supplementary file 4).

Osteoarthritis and synovitis severity of canine joints with experimentally induced OA

In order to explore differences in OA susceptibility between CD and NCD dogs, articular cartilage sections and synovial tissues were analysed from young adult dogs that were employed in previous experiments where OA was induced and followed up in a standardized manner (table 1). These studies were approved by the Utrecht University Animal Ethics Committee, approval numbers 01065, 02070707 and 99029. OA had been induced by applying standardized grooves on the lateral and medial femoral condyles with a 1.5 mm diameter Kirschner-wire [29, 30] (*n*=11 CD dogs; *n*=6 NCD dogs)[31]. Cartilage was collected 10 weeks after OA induction as described previously [32]. Cartilage sections (*n*=2 per region) collected from the medial and lateral tibia plateaus and medial and lateral femur condyles of healthy contralateral and OA joints were assessed histologically. Sections were assessed blinded for osteoarthritis and synovitis (AT) [29, 31, 33] and average values calculated for each joint [3]. Furthermore, synovitis severity was scored in the synovial tissue collected from three locations in the joint (medial, middle and lateral infra-patellar) [26, 32]. For biochemical analysis, the cartilage samples were assayed as described previously [34]. Total cartilage GAG content (µg/mg wet weight), GAG synthesis, GAG release and retention of newly formed GAGs were determined and averaged for femoral condyles and tibial plateau for eight explants per donor per parameter [35].

Statistical analysis

Data were statistically analysed using R Studio v3.3.1. A normality check was performed using a bootstrapped Shapiro Wilks. Data that was not normally distributed, was subjected to the Kruskal Wallis and post-hoc Mann Whitney *U* test. Normally distributed data was subjected to the ANOVA and post-hoc tests (Benjamini & Hochberg) for multiple comparisons. Since multiple factors (donor, NCD-CD, treatment and day) could influence the outcome of the present results, a multivariate regression model, the COX proportional hazard model, was used, when necessary. For this purpose, donor and experiments as a random effect, and culture condition and breed as fixed effects, were tested for the *goodness of fit*. Then, the model that retrieved the lowest *Akaike Information Criterion* (AIC) values, assessed by a Likelihood Ratio Test under a Chi- square distribution, was chosen for the analysis of the corresponding data set. The effect size (ES) and ESs confident intervals (CI set at 95%) were also taken into consideration to evaluate the significances. Effect sizes (ES) were retrieved as *Hedge's g* for parametric data (medium, 0.5-0.8; large, 0.8-1.2; very large, 1.2-2; and huge, >2 [36]) and, for non-parametric data, Cliff's delta was assessed (0.28<ES<0.43, medium; 0.43≤ES<0.7, large; ES≥0.7, very large [37]). Differences were considered significant when $p<0.05$, or when $0.05<p$-value <0.1 and ES was medium or larger.

Table 1. Overview of canine donors used for retrospective analysis of joint histology in experimental OA. CD, chondrodystrophic; NCD, non-chondrodystrophic; ACLT, anterior cruciate ligament transection.

Type of model	No of animals	Period	Breed	Age (years)	Body weight	Sex	Reference
Groove & ACLT	5 ACLT, 4 groove	10 weeks	Labrador retriever (NCD)	2.5 ± 1.2	21 - 26 kg	Female	[31]
Groove & ACLT	7 ACLT, 6 groove	10 weeks	Beagle (CD)	1.5 - 3	10-15 kg	Female	[29]
Groove	5 groove	10 weeks	Beagle (CD)	2.4 ± 0.3	10-15 kg	Female	[33]

Results

Native cartilage from CD dogs differed from NCD cartilage

The *FGF4* retrogene insertion on CFA12 was present in samples of all CD dogs, but not in NCD dogs. The *FGF4* retrogene insertion on CFA18 was not present in any of the used donors (supplementary file 2). CD donors were significantly older and weighed significantly less than their NCD counterparts ($p<0.001$). Cartilage explants retrieved from healthy knee joints of NCD dogs showed a significantly higher OARSI score (Fig. 2A; $p<0.001$) than CD dogs (day 0). Protein expression of COX-2 was higher in NCD vs. CD cartilage at the same initial day (Fig. 2C; $p<0.001$), in line with histological changes, but no differences were found in synovitis score and COX-2 immunopositivity in the synovium (Fig. 2B, D; $p>0.15$). Total DNA was higher in NCD vs. CD cartilage (Fig 3A; $p=0.028$), suggesting higher cellularity. GAG/DNA and GAG/dry weight did not differ at day 0 (Fig. 3C,D; $p>0.15$). In both CD and NCD cartilage, collagen I protein expression was very low to absent, but abundant immunopositivity for collagen II was noted (supplementary file 3).

Cartilage explants of CD dogs were better capable of GAG retention

The DNA content remained significantly higher in NCD vs. CD cartilage after 21 days of culturing (Fig. 3A; $p=0.007$). During the entire culture period, GAG release was higher in NCD vs. CD cartilage (Fig. 3B; $p<0.001$). This led to a (borderline) significant lower GAG/dry weight and GAG/DNA in NCD cartilage at day 21 (Fig. 3C,D; $p=0.065$, small ES; $p=0.007$ respectively). PGE_2 production tended to increase by TNF-α stimulation only in NCD cartilage (Fig. 2E; $p=0.068$, medium ES), and was only effectively suppressed in NCD cartilage by the celecoxib ($p=0.032$). Although COX-2 protein expression in the synovial tissue was increased in both CD and NCD cartilage after the 21-day culture period compared to day 0 ($p<0.05$), OARSI score, synovitis score and COX-2 expression in cartilage explants did not differ between CD and NCD tissue (Fig. 2A-D). In the same line, gene expression levels of matrix genes *ACAN*, *COL1A1*, *COL2A1*, ADAMTS5 and *MMP13* were not significantly different between CD and NCD cartilage after one week of culture (supplementary file 2). Gene expression of *FZD1*, *IL1β*, *IL6*, *LRP5, PTGES1* and *WIF1* was undetectable.

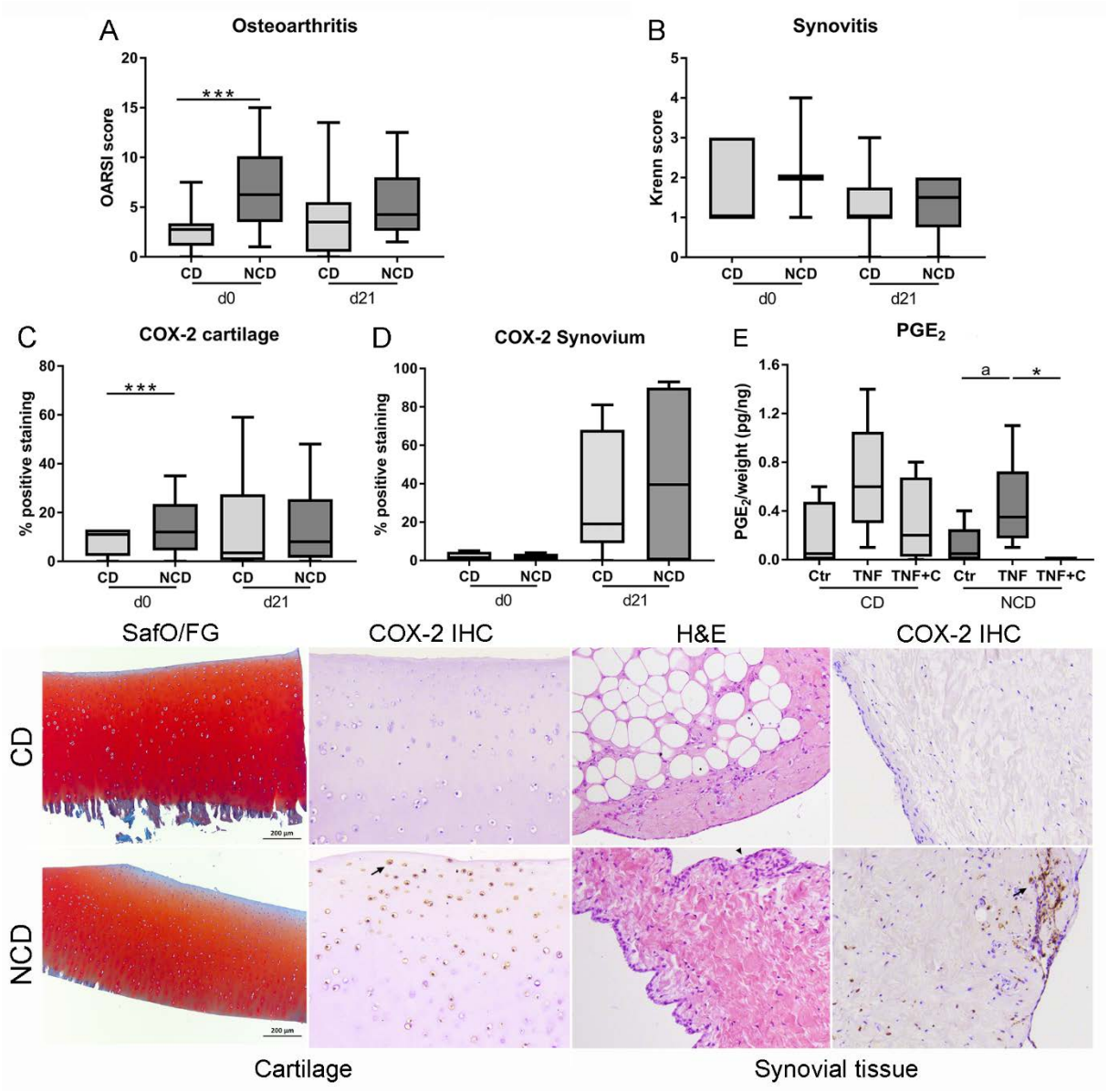

Figure 2. Histological scoring and COX-2 immunohistochemistry of cartilage and synovium explants obtained from healthy experimental non-chondrodystrophic (NCD) and chondrodystrophic (CD) dogs. Top: the OARSI score of native explants was higher in NCD vs. CD cartilage (p<0.001) at day 0 (**A**), while no differences were found with regard to synovial inflammation (**B**). NCD cartilage contained significantly more cyclooxygenase 2 (COX-2) expressing cells (p<0.001) than CD cartilage explants at day 0 (**C**). Although the overall COX-2 expression increased during the 21-day culture period, no differences were found between CD and NCD synovial tissue (**D**). Total prostaglandin E_2 (PGE_2) levels only increased in NCD explants in the presence of a pro-inflammatory stimulus (TNF-α) and were significantly suppressed by celecoxib (**E**). Bottom: Representative examples of Safranin O / Fast Green (SafO/FG) stained cartilage, haematoxylin & Eosin stained synovial tissue (H&E), and cartilage and synovial sections stained for COX-2. All samples were obtained at day 0 representing the state of native tissue. Arrows indicate immunopositive cells. Data depicted as boxplots with mean and 5-95 percentile. * p<0.05; *** p<0.001; a, medium effect size.

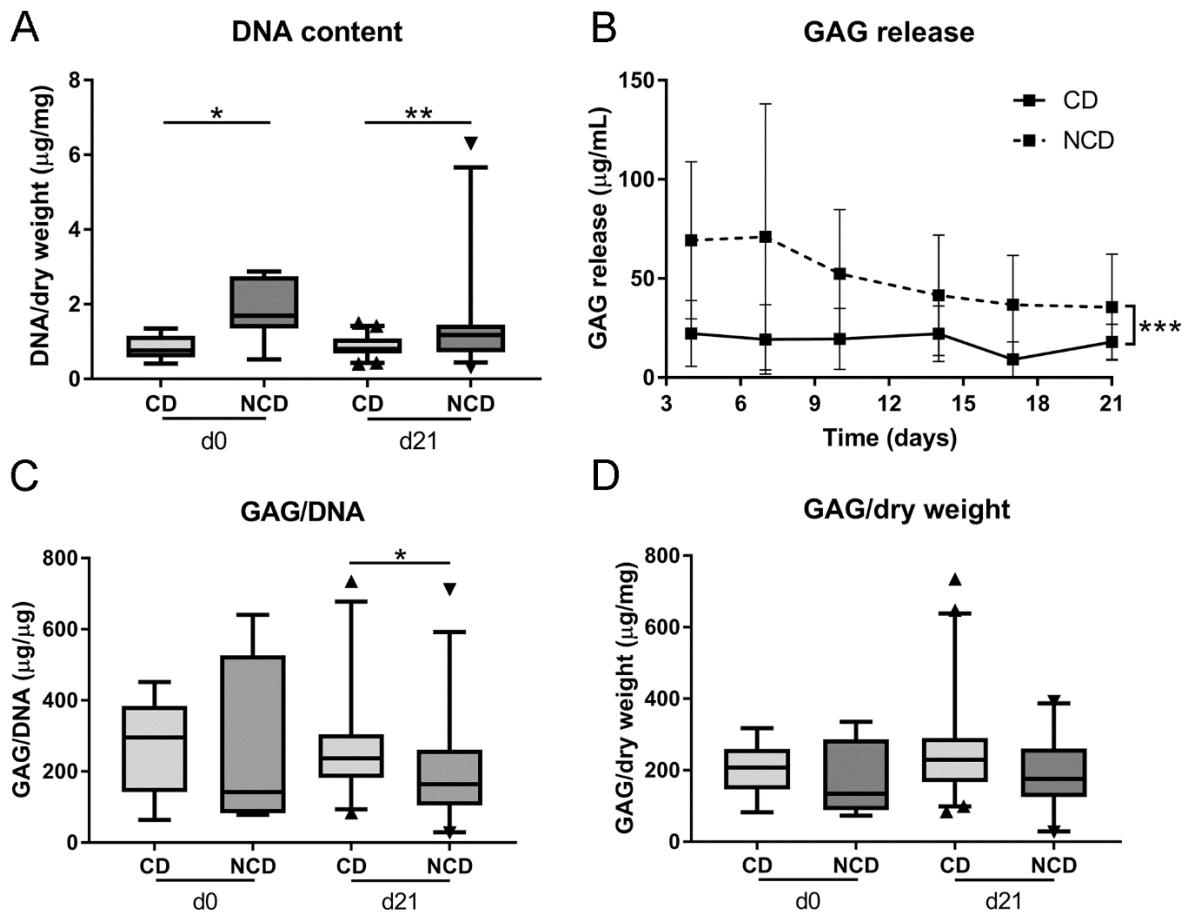

Figure 3. Biochemical analysis of cartilage explants derived from non-chondrodystrophic (NCD) and chondrodystrophic (CD) dogs. The DNA content (**A**) of NCD cartilage was higher at day 0 and 21 of culturing. The GAG release over the total culture period was higher in NCD cartilage (**B**). There was no difference in GAG/dry weight at day 0 and 21 (**C**), although GAG/DNA content was lower in NCD vs. CD cartilage after the 21 day culture period (**D**). Data depicted as boxplots with mean and 5-95 percentile. *n*=6 per condition. * $p<0.05$, ** $p<0.01$.

Canonical Wnt signalling in healthy cartilage explants of CD and NCD dogs did not differ

No significant differences were found in gene expression of downstream targets *AXIN2* and *CCND1* mRNA expression (Fig. 4A,B; $p=0.17$, $p=0.16$, respectively), although mRNA expression of the Wnt antagonist *DDK3* was increased ($p=0.01$; Fig. 4C) in NCD cartilage compared to their CD counterparts. There were no differences in β-catenin immunopositivity in the nuclear and / or cytoplasmic regions (Fig. 4D, $p>0.15$). Considering the complex canonical Wnt signalling regulation, a TCF-reporter assay was performed to explore Wnt signalling in CD and NCD chondrocytes cultured either in basic conditions alone and in the presence of a pro-inflammatory OA-like stimulus. There was a slightly higher canonical Wnt signalling in CD vs. NCD articular cartilage cells in chondrogenic medium only in the presence of TNF-α (Fig. 4E; $p=0.09$, medium ES). There also was a higher canonical

Wnt activity measured by the TCF reporter assay in chondrocytes retrieved from healthy female CD donors, as compared to healthy male donors (supplementary file 4).

Before and after experimental OA induction, joints of NCD dogs showed more severe histological cartilage degeneration and synovitis

There was no difference in overall OA severity between the two induction models, i.e. craniate cruciate ligament transection versus the groove model (p=0.156, data not shown). Therefore, the results of both OA models, pertaining to OA joints and contralateral controls in which OA was not induced, were combined to test for differences in OA susceptibility between CD and NCD experimental dogs. The severity of OA, as indicated by the OARSI score, was significantly higher in NCD vs CD control joints (Fig. 5A; p=0.0027) and was also significantly higher in knee joints from NCD vs. CD dogs 10 weeks after OA induction (Fig. 5A; p=0.0018). In both CD and NCD dogs, OARSI scores were significantly higher in OA joints compared to healthy control joints (p=0.02; p<0.001 respectively), as expected. Synovial inflammation increased after OA induction in both CD and NCD dogs (Fig. 5B; p<0.001). Synovial inflammation was higher in NCD vs CD joints, both in joints with induced OA and in the contralateral healthy controls (Fig. 5B; p=0.007, p=0.003, respectively).

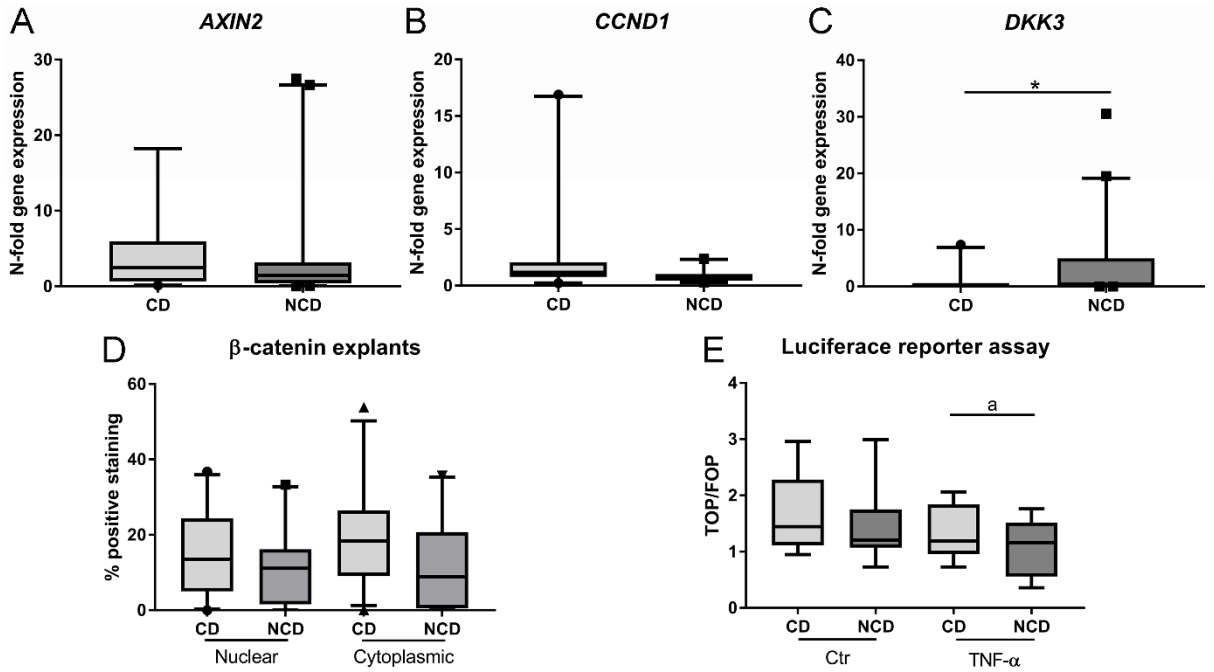

Figure 4. Analysis of the canonical Wnt-signalling in cartilage of non-chondrodystrophic (NCD) and chondrodystrophic (CD) dogs. No differences were found in *AXIN2* and cyclin-D1 (*CCND1*) mRNA expression (**A,B**), while dikkopf-3 (*DKK3*) mRNA expression was higher in NCD cartilage (**C**). B-catenin immunopositivity did not differ between NCD and CD donors (**D**). Wnt activity measured by the TCF reporter assay was slightly lower in NCD cartilage explants stimulated with TNF-α (**E**, medium ES). Data depicted as boxplots with mean and 5-95 percentile. * p<0.05. a, medium ES.

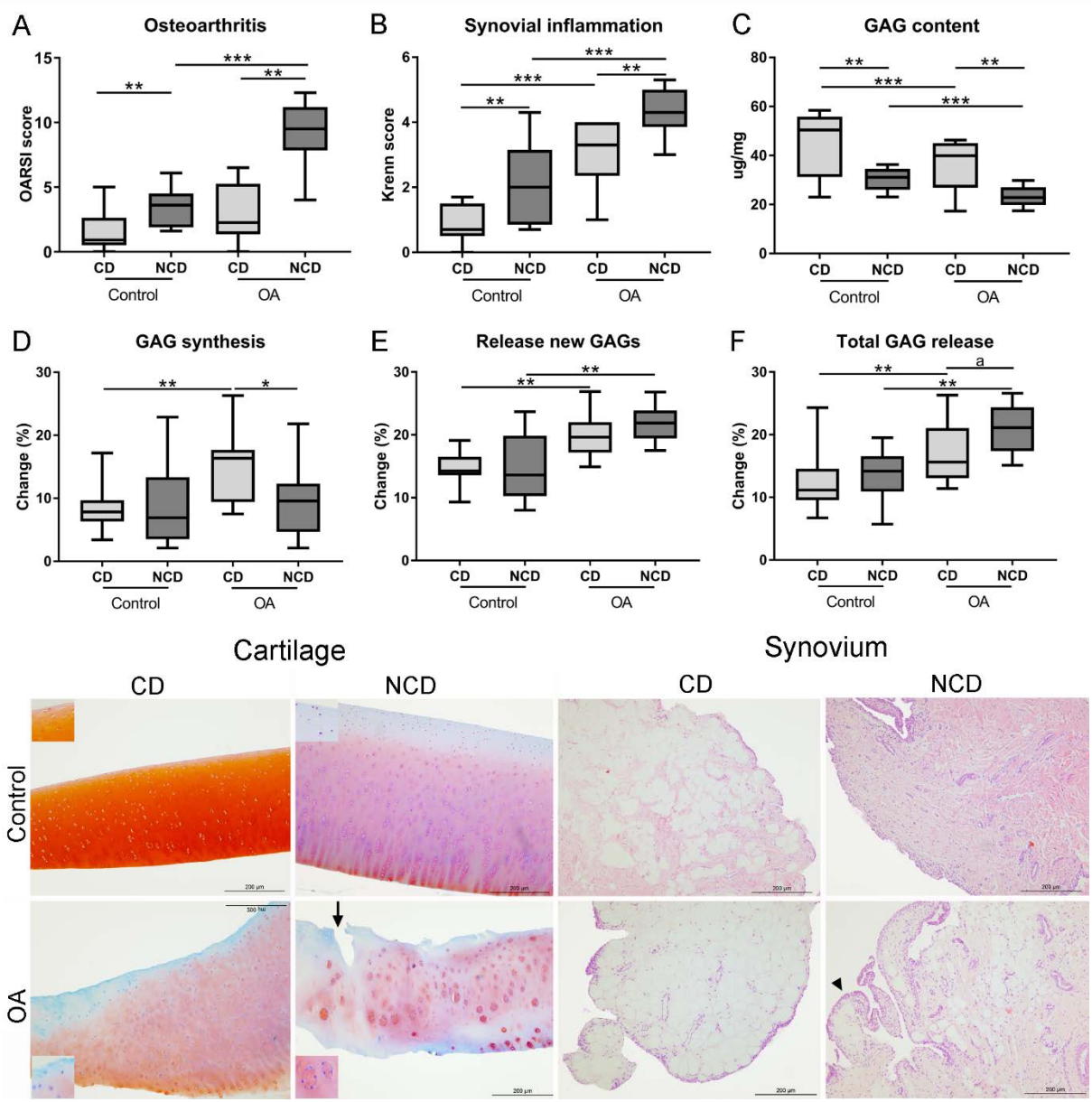

Figure 5. Top: OARSI scores (**A**) and synovial inflammation (Krenn) scores (**B**) were significantly higher in both healthy and OA cartilage of non-chondrodystrophic (NCD) dogs compared to chondrodystrophic (CD) cartilage. *n*=2 per location per donor. Glycosaminoglycan (GAG) content (**C**), changes in GAG synthesis rate (**D**), the percentage release of newly formed GAGs (**E**) and percentage total GAG release (**F**). *n*=10 per group. Data depicted as boxplots with mean and 5-95 percentile. * $p<0.05$, ** $p<0.01$, *** $p<0.001$, a medium effect size. Bottom: Representative examples of Safranin-O / Fast Green (SafO + FG) stained cartilage sections from the medial femoral condyle and Haematoxylin & Eosin stained infrapatellar synovium sections (H&E) of NCD and CD joints 10 weeks after unilateral OA induction and the healthy contralateral control joint. NCD-derived cartilage shows more severe degenerative changes after OA induction: large cellular clusters (*) and fissures (arrow) are present. Synovial hyperplasia also seems more evident in NCD-derived synovial tissue after OA induction (arrowheads).

In freshly collected cartilage explants from these experimental studies a meta-analysis was conducted to determine GAG content and synthesis. The total GAG content (Fig. 5C) was higher in healthy and OA cartilage of CD vs NCD donors (p<0.01) and declined in both dog breeds after OA induction (p<0.001). The rate of GAG synthesis only increased in CD-derived OA cartilage (p<0.001) and was significantly higher than the rate of GAG synthesis in NCD OA cartilage (p=0.02). The release of newly formed GAGs, as a measure of retention of newly formed GAGs in the cartilage, significantly increased in both CD and NCD cartilage compared to healthy controls (p<0.001). The total GAG release also increased after OA induction in both dog breeds (p<0.001) and was higher in NCD OA cartilage than CD OA cartilage (p=0.15, medium ES).

Discussion

To the authors' knowledge, this is the first study reporting on intrinsic differences between cartilage and synovium of different dog breeds that are often employed in experimental OA models, i.e. with and without chondrodysplasia based on genetic background leading to aberrant FGFR3 activation. Humans suffering from chondrodysplasia due to increased FGFR3 signalling often present with orthopaedic conditions, caused by bone and joint deformities, joint laxity, brittle bones and limb length inequality [38]. These abnormalities predispose patients to degenerative joint diseases and spinal conditions, but they surprisingly exhibit a lower incidence of OA [39]. In chondrodystrophic dogs, these bony deformities are seen as well [40], and are also accompanied by lower conventional OA rates [41]. These clinical observations match with the experimental results in the current study. Histological analysis of both untreated joints of young-adult dogs, and after standardized induction of OA, revealed more severe degenerative cartilage in NCD cartilage than in CD cartilage.

At the biochemical level, similar differences were observed. CD-derived cartilage contained less DNA than NCD-derived cartilage, which is in line with the observation that gain-of-function of FGFR3 caused decreased proliferation of chondrocytes [8, 9]. The total GAG release into the culture medium from NCD cartilage was higher. This could indicate a higher capability of CD dogs in retaining GAGs inside the cartilage [42], but could also reflect a lower total GAG production because of activated FGFR3 signalling [8, 9]. Indeed, after 21 days of culturing the total GAG production (content + release) was higher in NCD cartilage explants. The higher GAG content in cartilage for CD dogs than in NCD dogs could be one of the protective mechanisms against OA [43]. Similar results were found in the GAG incorporation assay of cartilage explants collected from experiments on models of induced OA. While there was no significant difference in GAG synthesis, cartilage of CD donors contained more GAGs compared to NCD donors. Moreover, total GAG release from CD cartilage was lower than in NCD OA cartilage. Altogether, these observation indicate a differential cartilage physiology between CD and NCD dogs pointing towards protective effects of carrying a FGFR3 polymorphism at CFA12.

It has become increasingly clear that OA is a disease of the whole joint, with interplay between cartilage, synovial lining and subchondral bone. In this respect, the synovial tissue and cartilage can influence each other and the development and progression of OA, possible resulting in more severe OA in the case of NCD dogs. In line with this assumption, the present study also indicated a differential susceptibility for joint inflammation between CD and NCD donors: synovitis scores were indeed higher in synovial tissue from healthy NCD vs. CD joints *in vivo* and aggravated further after OA induction. In agreement with this observation, *in vitro*, NCD-derived cartilage explants showed increased COX-2 immunopositivity and higher PGE_2 levels in the presence of a pro-inflammatory stimulus than CD cartilage, the main drivers of joint inflammation and degeneration [44]. Synovial inflammation affects *in vitro* cartilage metabolism by reducing GAG production [45]. Moreover, it is widely known that synovial inflammation is low-grade in OA, but does play an important role [46]. Synoviocytes become activated after an initial insult to the joint, after which synovial tissue drives the progression of cartilage loss and development of clinical signs, by producing inflammatory mediators, such as PGE_2 and degrading enzymes [1]. The tendency of NCD cartilage to show an aggravated response to degenerative or inflammatory stimuli, might predispose it to early OA.

Based on the above, we explored whether there were differences in Wnt signalling, related to the underlying possible differences in FGFR3 signalling [14]. In the current study, no significant differences were found in Wnt/β-catenin signalling based on IHC for β-catenin, qPCR for Wnt associated targets and Wnt activation on cartilage level, although NCD cartilage expressed higher *DKK3* mRNA levels in culture. Several studies reported an upregulation of *DKK3* and other DKKs in OA cartilage, and its upregulation has been associated with both OA progression and chondroprotection [21, 47-49]. Members of the *DKK* gene family demonstrated both inhibitory and potentiating actions on the Wnt signalling pathway, indicating a tissue-dependent effect [17]. Not much is known on how *DKK3* impacts Wnt signalling in cartilage, but given our findings, it could be inhibitory. It would therefore be tempting to speculate that upregulation of *DKK3* in NCD cartilage reflects early osteoarthritic changes, and might be an attempt to avert further progression of degeneration.

There are a few limitations to his study. Mostly female donors were used for both the *in vitro* experiments and the analysis of joint pathology in experimentally induced OA. Gene expression and biochemical analyses did not differ between female and male donors, but there was a higher canonical Wnt activity measured by the TCF reporter assay in chondrocytes retrieved from healthy female CD donors, as compared to healthy male donors. This could be due to a type I error because of small sample size. Nevertheless, it is known that females have a higher incidence of OA, although old age, obesity and physical activity are suggested to influence this difference [1]. Whether gender influences Wnt activity, is still to be determined. Moreover, due to the setup of the study, the median age of CD donors used for characterisation of joint tissues in healthy animals, was twice as high as NCD

donors. Notwithstanding, even though CD dogs were older, thus expecting a worse cartilage condition, their cartilage displayed less degenerative changes compatible with early OA than NCD donors, further supporting our findings.

To conclude, in both healthy and OA cartilage there are physio-pathological differences between dog breeds, presumably caused by the genotypic changes associated with chondrodystrophy. NCD-derived cartilage seems to be more sensitive to pro-inflammatory stimuli than cartilage from CD dogs, possibly predisposing NCD dogs to the development of OA. These differences should be taken into account when considering an *in vitro* or *in vivo* canine model to study OA, in order to avoid confounding effects. Therefore, differences in cartilage homeostasis, and possibly other relevant signalling pathways influenced by the genetic background of dog breeds can have implications for the choice of dog type to investigate OA for both veterinary and human OA patients.

Acknowledgements

The authors would also like to thank Harry van Engelen, Katja Coeleveld and Willem de Jong for their assistance with data acquisition.

References

1. Glyn-Jones S, Palmer AJ, Agricola R, Price AJ, Vincent TL, Weinans H*, et al*. Osteoarthritis. Lancet 2015;386:376-87.
2. Bendele AM. Animal models of osteoarthritis. J.Musculoskelet.Neuronal Interact. 2001;1:363-76.
3. Cook JL, Kuroki K, Visco D, Pelletier JP, Schulz L, Lafeber FP. The OARSI histopathology initiative - recommendations for histological assessments of osteoarthritis in the dog. Osteoarthritis Cartilage 2010;18 Suppl 3:S66-79.
4. Johnston SA. Osteoarthritis. Joint anatomy, physiology, and pathobiology. Vet.Clin.North Am.Small Anim.Pract. 1997;27:699-723.
5. King MD. Etiopathogenesis of canine hip dysplasia, prevalence, and genetics. Vet.Clin.North Am.Small Anim.Pract. 2017;47:753-67.
6. Brown EA, Dickinson PJ, Mansour T, Sturges BK, Aguilar M, Young AE*, et al*. FGF4 retrogene on CFA12 is responsible for chondrodystrophy and intervertebral disc disease in dogs. PNAS 2017;114:11476–11481.
7. Parker HG, VonHoldt BM, Quignon P, Margulies EH, Shao S, Mosher DS*, et al*. An expressed fgf4 retrogene is associated with breed-defining chondrodysplasia in domestic dogs. Science 2009;325:995-8.
8. Ornitz DM and Marie PJ. Fibroblast growth factor signaling in skeletal development and disease. Genes Dev. 2015;29:1463-86.
9. Teven CM, Farina EM, Rivas J, Reid RR. Fibroblast growth factor (FGF) signaling in development and skeletal diseases. Genes Dis. 2014;1:199-213.
10. Eswarakumar VP and Schlessinger J. Skeletal overgrowth is mediated by deficiency in a specific isoform of fibroblast growth factor receptor 3. Proc.Natl.Acad.Sci.U.S.A. 2007;104:3937-42.
11. Tang J, Su N, Zhou S, Xie Y, Huang J, Wen X*, et al*. Fibroblast Growth Factor Receptor 3 inhibits osteoarthritis progression in the knee joints of adult mice. Arthritis Rheumatol. 2016;68:2432-43.
12. Vincent TL. Explaining the fibroblast growth factor paradox in osteoarthritis: lessons from conditional knockout mice. Arthritis Rheum. 2012;64:3835-8.
13. Zhou S, Xie Y, Li W, Huang J, Wang Z, Tang J*, et al*. Conditional deletion of Fgfr3 in chondrocytes leads to osteoarthritis-like defects in temporomandibular joint of adult mice. Sci.Rep. 2016;6:24039.
14. Buchtova M, Oralova V, Aklian A, Masek J, Vesela I, Ouyang Z*, et al*. Fibroblast growth factor and canonical WNT/beta-catenin signaling cooperate in suppression of chondrocyte differentiation in experimental models of FGFR signaling in cartilage. Biochim.Biophys.Acta 2015;1852:839-50.
15. Nakamura Y, Nawata M, Wakitani S. Expression profiles and functional analyses of Wnt-related genes in human joint disorders. Am.J.Pathol. 2005;167:97-105.
16. Blom AB, Brockbank SM, van Lent PL, van Beuningen HM, Geurts J, Takahashi N*, et al*. Involvement of the Wnt signaling pathway in experimental and human osteoarthritis: prominent role of Wnt-induced signaling protein 1. Arthritis Rheum. 2009;60:501-12.
17. Usami Y, Gunawardena AT, Iwamoto M, Enomoto-Iwamoto M. Wnt signaling in cartilage development and diseases: lessons from animal studies. Lab.Invest. 2016;96:186-96.
18. Zhu M, Tang D, Wu Q, Hao S, Chen M, Xie C*, et al*. Activation of beta-catenin signaling in articular chondrocytes leads to osteoarthritis-like phenotype in adult beta-catenin conditional activation mice. J.Bone Miner.Res. 2009;24:12-21.
19. Yasuhara R, Ohta Y, Yuasa T, Kondo N, Hoang T, Addya S*, et al*. Roles of beta-catenin signaling in phenotypic expression and proliferation of articular cartilage superficial zone cells. Lab.Invest. 2011;91:1739-52.
20. Weng LH, Wang CJ, Ko JY, Sun YC, Wang FS. Control of Dkk-1 ameliorates chondrocyte apoptosis, cartilage destruction, and subchondral bone deterioration in osteoarthritic knees. Arthritis Rheum. 2010;62:1393-402.
21. Funck-Brentano T, Bouaziz W, Marty C, Geoffroy V, Hay E, Cohen-Solal M. Dkk-1-mediated inhibition of Wnt signaling in bone ameliorates osteoarthritis in mice. Arthritis Rheumatol. 2014;66:3028-39.
22. Loughlin J, Dowling B, Chapman K, Marcelline L, Mustafa Z, Southam L*, et al*. Functional variants within the secreted frizzled-related protein 3 gene are associated with hip osteoarthritis in females. Proc.Natl.Acad.Sci.U.S.A. 2004;101:9757-62.
23. Castano Betancourt MC, Cailotto F, Kerkhof HJ, Cornelis FM, Doherty SA, Hart DJ*, et al*. Genome-wide association and functional studies identify the DOT1L gene to be involved in cartilage thickness and hip osteoarthritis. Proc.Natl.Acad.Sci.U.S.A. 2012;109:8218-23.
24. Smolders LA, Bergknut N, Grinwis GC, Hagman R, Lagerstedt AS, Hazewinkel HA*, et al*. Intervertebral disc degeneration in the dog. Part 2: chondrodystrophic and non-chondrodystrophic breeds. Vet.J. 2013;195:292-9.
25. Farndale RW, Sayers CA, Barrett AJ. A direct spectrophotometric microassay for sulfated glycosaminoglycans in cartilage cultures. Connect.Tissue Res. 1982;9:247-8.

26. Krenn V, Morawietz L, Burmester GR, Haupl T. Synovialitis score: histopathological grading system for chronic rheumatic and non-rheumatic synovialitis. Z.Rheumatol. 2005;64:334-42.
27. Smolders LA, Meij BP, Riemers FM, Licht R, Wubbolts R, Heuvel D*, et al*. Canonical Wnt signaling in the notochordal cell is upregulated in early intervertebral disk degeneration. J.Orthop.Res. 2012;30:950-7.
28. Tellegen AR, Jansen I, Thomas R, de Visser H, Kik M, Grinwis G*, et al*. Controlled release of celecoxib inhibits inflammation, bone cysts and osteophyte formation in a preclinical model of osteoarthritis. 2018;25:1438-47.
29. Sniekers YH, Intema F, Lafeber FP, van Osch GJ, van Leeuwen JP, Weinans H*, et al*. A role for subchondral bone changes in the process of osteoarthritis; a micro-CT study of two canine models. BMC Musculoskelet.Disord. 2008;9:20.
30. Mastbergen SC, Marijnissen AC, Vianen ME, Zoer B, van Roermund PM, Bijlsma JW*, et al*. Inhibition of COX-2 by celecoxib in the canine groove model of osteoarthritis. Rheumatology (Oxford) 2006;45:405-13.
31. Frost-Christensen LN, Mastbergen SC, Vianen ME, Hartog A, DeGroot J, Voorhout G*, et al*. Degeneration, inflammation, regeneration, and pain/disability in dogs following destabilization or articular cartilage grooving of the stifle joint. Osteoarthritis Cartilage 2008;16:1327-35.
32. Marijnissen AC, van Roermund PM, TeKoppele JM, Bijlsma JW, Lafeber FP. The canine 'groove' model, compared with the ACLT model of osteoarthritis. Osteoarthritis Cartilage 2002;10:145-55.
33. Mastbergen SC, Marijnissen AC, Vianen ME, van Roermund PM, Bijlsma JW, Lafeber FP. The canine 'groove' model of osteoarthritis is more than simply the expression of surgically applied damage. Osteoarthritis Cartilage 2006;14:39-46.
34. Lafeber FP, Vander Kraan PM, Huber-Bruning O, Vanden Berg WB, Bijlsma JW. Osteoarthritic human cartilage is more sensitive to transforming growth factor beta than is normal cartilage. Br.J.Rheumatol. 1993;32:281-6.
35. van Valburg AA, van Roermund PM, Marijnissen AC, Wenting MJ, Verbout AJ, Lafeber FP*, et al*. Joint distraction in treatment of osteoarthritis (II): effects on cartilage in a canine model. Osteoarthritis Cartilage 2000;8:1-8.
36. Sawilowsky SS. New effect size rules of thumb. J. Mod. Appl. Stat. Meth. 2009;8:597-599.
37. Vargha A and Delaney HD. A Critique and Improvement of the CL Common Language Effect Size Statistics of McGraw and Wong. J. Educ. Behav. Stat. 2000;25:101-132.
38. Ireland PJ, Pacey V, Zankl A, Edwards P, Johnston LM, Savarirayan R. Optimal management of complications associated with achondroplasia. Appl.Clin.Genet. 2014;7:117-25.
39. Klag KA and Horton WA. Advances in treatment of achondroplasia and osteoarthritis. Hum.Mol.Genet. 2016;25:R2-8.
40. Martinez S, Fajardo R, Valdes J, Ulloa-Arvizu R, Alonso R. Histopathologic study of long-bone growth plates confirms the basset hound as an osteochondrodysplastic breed. Can.J.Vet.Res. 2007;71:66-9.
41. Karbe GT, Biery DN, Gregor TP, Giger U, Smith GK. Radiographic hip joint phenotype of the Pembroke Welsh Corgi. Vet.Surg. 2012;41:34-41.
42. Fujita Y, Hara Y, Nezu Y, Schulz KS, Tagawa M. Proinflammatory cytokine activities, matrix metalloproteinase-3 activity, and sulfated glycosaminoglycan content in synovial fluid of dogs with naturally acquired cranial cruciate ligament rupture. Vet.Surg. 2006;35:369-76.
43. Fenwick SA, Gregg PJ, Rooney P. Osteoarthritic cartilage loses its ability to remain avascular. Osteoarthritis Cartilage 1999;7:441-52.
44. Attur M, Al-Mussawir HE, Patel J, Kitay A, Dave M, Palmer G*, et al*. Prostaglandin E2 exerts catabolic effects in osteoarthritis cartilage: evidence for signaling via the EP4 receptor. J.Immunol. 2008;181:5082-8.
45. Beekhuizen M, Bastiaansen-Jenniskens YM, Koevoet W, Saris DB, Dhert WJ, Creemers LB*, et al*. Osteoarthritic synovial tissue inhibition of proteoglycan production in human osteoarthritic knee cartilage: establishment and characterization of a long-term cartilage-synovium coculture. Arthritis Rheum. 2011;63:1918-27.
46. Hugle T and Geurts J. What drives osteoarthritis?-synovial versus subchondral bone pathology. Rheumatology (Oxford) 2017;56:1461-71.
47. Honsawek S, Tanavalee A, Yuktanandana P, Ngarmukos S, Saetan N, Tantavisut S. Dickkopf-1 (Dkk-1) in plasma and synovial fluid is inversely correlated with radiographic severity of knee osteoarthritis patients. BMC Musculoskelet.Disord. 2010;11:257,2474-11-257.
48. Meng J, Ma X, Ma D, Xu C. Microarray analysis of differential gene expression in temporomandibular joint condylar cartilage after experimentally induced osteoarthritis. Osteoarthritis Cartilage 2005;13:1115-25.
49. Snelling SJ, Davidson RK, Swingler TE, Le LT, Barter MJ, Culley KL*, et al*. Dickkopf-3 is upregulated in osteoarthritis and has a chondroprotective role. Osteoarthritis Cartilage 2016;24:883-91.

50. Bach FC, de Vries SA, Krouwels A, Creemers LB, Ito K, Meij BP*, et al*. The species-specific regenerative effects of notochordal cell-conditioned medium on chondrocyte-like cells derived from degenerated human intervertebral discs. Eur.Cell.Mater. 2015;30:132,-47.

Supplementary file 1. Characteristics of the canine donors used in the *in vitro* cartilage explant experiment.

Breed	CD/NCD	Age (months)	Body weight (kg)	Sex
Beagle	CD	45	10	Female
Beagle	CD	48	11	Female
Beagle	CD	26	10	Female
Beagle	CD	54	10	Male
Beagle	CD	62	10	Male
Beagle	CD	50	10	Male
Beagle	CD	48	10	Male
Beagle	CD	21	10	Female
Beagle x Bedlington terrier	CD	49	15	Female
Beagle x Bedlington terrier	CD	49	16	Female
Hound type dog	NCD	29	25	Female
Hound type dog	NCD	20	23	Female
Hound type dog	NCD	22	22	Female
Hound type dog	NCD	29	28	Female
Hound type dog	NCD	24	24	Female
Hound type dog	NCD	26	24	Female
Hound type dog	NCD	24	32	Female
Hound type dog	NCD	36	23	Female
Hound type dog	NCD	19	22	Female
Hound type dog	NCD	19	21	Female
Hound type dog	NCD	21	23	Female

CD, Chondrodystrophic; NCD, non-chondrodystrophic.

Supplementary file 2. Description of the FGF4 genotyping PCR and PCR primers of the *in vitro* explant culture experiment.

FGF4 genotyping PCR

Four non-chondrodystrophic (NCD) donors and five chondrodystrophic (CD) dogs were assayed for the *FGF4* insertion on CFA12 and CFA18 using a PCR-based assay as described by Brown *et al* [1], with some modifications to optimize for the available thermal cycler (C1000, Biorad) and PCR reagents. Genomic DNA was isolated from papain digested samples (Qiagen DNeasy Mini Kit, 69504). As a control four different breeds (Dachshund, Cane Corso, Beagle, Labrador) were assayed in each of the genotyping assays.

Table 1. Gene-specific primer sequences with associated amplification temperatures.

Gene	Primer sequence (5'-'3)	Temp (°C)
CFA12	Fw ACAGCTGGCATGGTCAGTTA I GTCCGTGCGGTGAAATAAAA Rv TGCTGTAGATTTTGAGGTGTCTT	55
CFA18	Fw TTGGGAATGTCAAACCACTG I GTCCGTGCGGTGAAATAAAA Rv GTTCCCTCCATTTCGGTTT	55

The CFA12 insert assay for each reaction consisted of 6.4µL milliQ water, 1.5µL 10x Buffer, 0.6µL 50mM MgCl2, 0.3µL 10mM dNTP, 0.08µL of the external forward primer (100µM), 0.11µL of the internal forward primer (100µM), 0.12µL of the reverse primer (100µM), 0.15µL of PlatinumTaq DNA Polymerase (10966018, Invitrogen),3.75µL 4M Betaine, and 2µL of DNA. The CFA18 FGF4 insert assay consisted for each reaction of 6.4µl milliQ water, 1.5µL 10x Buffer, 0.6µL 50mM MgCl2, 0.3µL 10 mM dNTP, 0.08µl of the external forward primer (100µM), 0.09µl of the internal forward primer (100µM), 0.14µL of the reverse primer (100µM), 0.15µL of PlatinumTaq DNA Polymerase (Invitrogen), 3.75µL 4M Betaine, and 2µL of DNA. PCR products were visualized on a 2% agarose gel. The same band sizes were observed as described by Brown *et al* [1] and 8 of the dogs were genotyped accordingly. These were for the CFA12 FGF4 insertion assay: a single band of 333bp when no insert was present, a single 654bp band for the homozygous mutant and both bands for the heterozygous animals. For the CFA18 FGF4 insertion assay: a single 388bp band when the insert was not present, a single 168bp band for the homozygous mutant and the presence of both bands indicated a heterozygous animal.

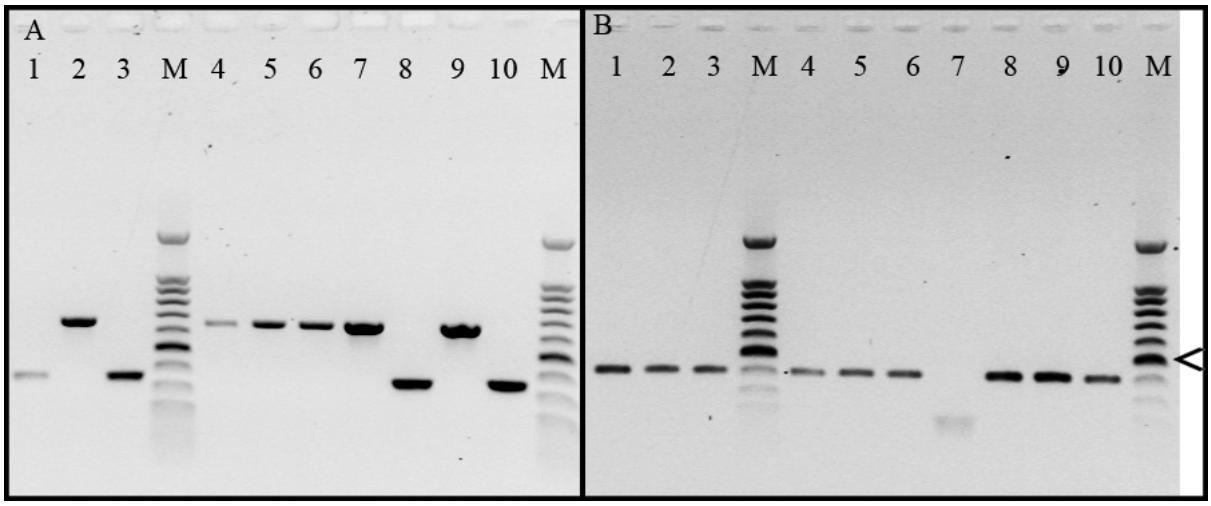

Figure 1. Gel electrophoreses on 2% agarose of the genotyping PCR for the presence of the FGF4 retrogene on CFA12 (**A**) and CFA18 (**B**). The 100 bp DNA ladder (G2101, Promega) marked by M allows to estimate the product size, the 500bp band is indicated by the arrowhead.

Table 2. Dog breeds and results of the genotyping PCR for the presence of the FGF4 retrogene on CFA12 (**A**) and CFA18 (**B**).

		CFA12		CFA18	
Lane	**CD/NCD**	**Band**	**Presence**	**Band**	**Presence**
1	NCD	333	-	388	-
2	CD	654	+	388	-
3	NCD	333	-	388	-
4	CD	654	+	388	-
5	CD	654	+	388	-
6	CD	654	+	388	-
7	CD *	654	+	168	+
8	NCD #	333	-	388	-
9	CD	654	+	388	-
10	NCD	333	-	388	-

CD, Chondrodystrophic; NCD, non-chondrodystrophic. * Positive (Dachshund) and # negative (Cane Corso) control sample.

Gene expression analysis of the in vitro explant culture

The snap frozen samples were folded in tinfoil were crushed by use of a hammer, and snap freezing. Subsequently, the sample was collected in 600 µL of Lysis solution (17209, Exiqon) and RNA was isolated (300110, Exiqon) according to the manufacturer's guidelines. DNA removal was safeguarded in this process by performing a DNAse on-column step (79254, Qiagen). cDNA was synthesized using the iScript™ cDNA Synthesis Kit (170-8891, Bio-Rad) according to the guidelines of the manufacturer. RT-qPCR was performed as described previously [50] with maximal RNA input. Briefly, RT-qPCR was performed using the iQT™ SYBR Green Supermix Kit (Bio-Rad) and the CFX384 Touch™ Real-Time PCR Detection System (Bio-Rad, Veenendaal, the Netherlands). For determination of relative gene expression, the Normfirst ($E^{\Delta\Delta Cq}$) method was used. For every target gene, the mean n-fold changes in gene expression was calculated. Six stably expressed reference genes were chosen to normalize target gene expression.

RT-qPCR primers of the in vitro explant culture

Genes were selected based on their role in anabolic and catabolic cartilage metabolism, apoptosis, transforming growth factor beta (TGF-β) pathway, inflammation, osteoarthritis, and Wnt signalling pathway (**Table 3**).

Table 3. Gene-specific primer sequences with associated amplification temperatures.

Gene	Primer sequence (5'-'3)	Amplicon size (bp)	Temp (°C)
Reference genes			
GAPDH	Fw TGTCCCCACCCCCAATGTATC	100	58
	Rv CTCCGATGCCTGCTTCACTACCTT		
HNRPH	Fw CTCACTATGATCCACCACG	151	61
	Rv TAGCCTCCATAACCTCCAC		
RPL13	Fw GCCGGAAGGTTGTAGTCGT	87	61
	GGAGGAAGGCCAGGTAATTC		
RPS19	Fw CCTTCCTCAAAAAGTCTGGG	95	61-63
	Rv GTTCTCATCGTAGGGAGCAAG		
SRPR	Fw GCTTCAGGATCTGGACTGC	81	61.5
	Rv GTTCCCTTGGTAGCACTGG		
YWHAZ	Fw CGAAGTTGCTGCTGGTGA	94	58
	Rv TTGCATTTCCTTTTTGCTGA		
Target genes			
ACAN	Fw GGACACTCCTTGCAATTTGAG	110	61-62
	Rv GTCATTCCACTCTCCCTTCTC		
ADAMTS5	Fw CTACTGCACAGGGAAGAG	148	61
	Rv GAACCCATTCCACAAATGTC		
AXIN2	Fw GGACAAATGCGTGGATACCT	128	60
	Rv TGCTTGGAGACAATGCTGTT		
CCND1	Fw ACTACCTGGACCGCT	151	60
	Rv CGGATGGAGTTGTCA		
COL1A1	Fw GTGTGTACAGAACGGCCTCA	109	61
	Rv TCGCAAATCACGTCATCG		
COL2A1	Fw GCAGCAAGAGCAAGGAC	150	60.5-65
	Rv TTCTGAGAGCCCTCGGT		
DKK3	Fw CATCCAGTCCAGTGCTCTCA	140	58
	Rv GGGCCAGGATTGTAAGTGAA		
FZD1	Fw GGCGCAGGGCACCAAGAAG	97	61.5
	Rv GAGCGACAGAATCACCCACCAGA		
IL1β	Fw: TGCTGCCAAGACCTGAACCAC	115	68
	Rv: TCCAAAGCTACAATGACTGACACG		
IL6	Fw: GAGCCCACCAGGAACGAAAGAGA	123	65
	Rv: CCGGGGTAGGGAAAGCAGTAGC		
LRP5A	Fw GCTCCATCCACGCCTGTAA	137	61
	Rv ACCATTGTCCTCCGCACAC		
MMP13	Fw CTGAGGAAGACTTCCAGCTT	250	65
	Rv -TTGGACCACTTGAGAGTTCG		
PTGES1	Fw CCAGTATTGCCGGAGTGACCAG	97	68
	Rv AAACGAAGCCCAGGAACAGGA		
WIF1	Fw CCGAAATGGAGGCTTTTGTA	135	61.5
	Rv ATGCAGAACCCAGGAGTGAC		

Reference genes: *GAPDH*, Glyceraldehyde 3-phosphate dehydrogenase; *HNRPH*, heterogeneous nuclear ribonucleoprotein H1; *RPL13*, ribosomal protein L13; *RPS19*, ribosomal protein S19; *SRPR*, signal recognition particle receptor; *YWHAZ*, tyrosine 3-monooxygenase/tryptophan 5-monooxygenase activation protein zeta. Target genes: *ACAN*, aggrecan; *ADAMTS5,* A disintegrin and metalloproteinase with thrombospondin motifs 5, *AXIN2,* Axis inhibition protein 2; *CCND1*, cyclin-D1; *COL1A1,* collagen type I; *COL2A1,* collagen type II; *DDK3*, dickkopf-3; *FZD1*, frizzled-1; *IL1β*, interleukin 1β; *IL6*, interleukin 6; *LRP5*, low-density lipoprotein receptor-related protein 5; *MMP13*, matrix metalloproteinase 13; *PTGES1,* prostaglandin E synthase ; *WIF1*, Wnt inhibitory factor 1.

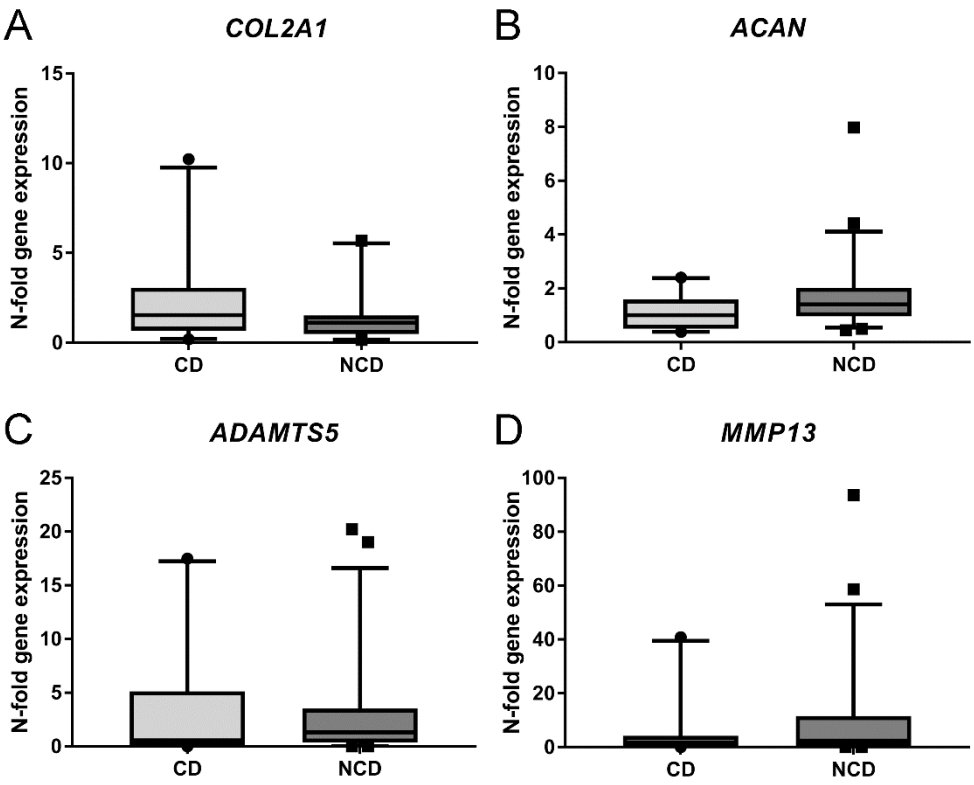

Figure 2. Gene expression analysis of cartilage explants derived from non-chondrodystrophic (NCD) and chondrodystrophic (CD) donors. There were no differences in mRNA expression of collagen 2α1 (*COL2A1*, **A**), aggrecan (*ACAN*, **B**); a disintegrin and metalloproteinase with thrombospondin motifs 5, (*ADAMTS5*, **C**) and matrix metalloproteinase 13 (*MMP13*; **D**) measured at day 7 of the culture period. Data depicted as boxplots with mean and 5-95 percentile. *N*= 6 per condition.

References

[1] Brown EA, Dickinson PJ, Mansour T, Sturges BK, Aguilar M, Young AE, et al. FGF4 Retrogene On CFA12 Is Responsible For Chondrodystrophy And Intervertebral Disc Disease In Dogs. PNAS 2017;114:11476–11481.

Supplementary file 3. Immunohistochemistry of canine cartilage explant samples.

Table 1. Details on immunohistochemistry protocols.

Name	Manu-facturer	Origin	Antibody Ig fraction	Antigen retrieval	Block	Dilution 1st antibody	Secondary antibody
Collagen I	ab6308, Abcam	Human recombinant	Mouse Mab	Pronase and HAse, 30 min @37°C each	PBS/BSA 5% 30 min @RT	1:500 in PBS/BSA 5%	K4001, Dako
Collagen II	ab21291, Abcam	Human recombinant	Mouse Mab	Pronase and HAse, 30 min @37°C each	PBS/BSA 5% 30 min @RT	1:2000 in PBS/BSA 5%	K4001, Dako
COX-2	160112, Cayman	Human recombinant	Mouse Mab IgG1	N/A	TBS-BSA 5%, 60 min @ RT	1:50 in TBS-BSA 5%	K4001, Dako
β-catenin	ab6302, Abcam	Human recombinant	Rabbit Pab	10 mM citrate (pH 6.0)	PBS/BSA 10% 30 min @ RT	1:000 in PBS/BSA 1%	K4002, Dako

Mab: monoclonal antibody; Pab, polyclonal antibody; HAse: bovine hyaluronidase 4 450 IU/mg, adjusted to pH 5 with 0.1M HCl.; PBST: Phosphate buffered saline 0.1% Tween-20. RT, room temperature.

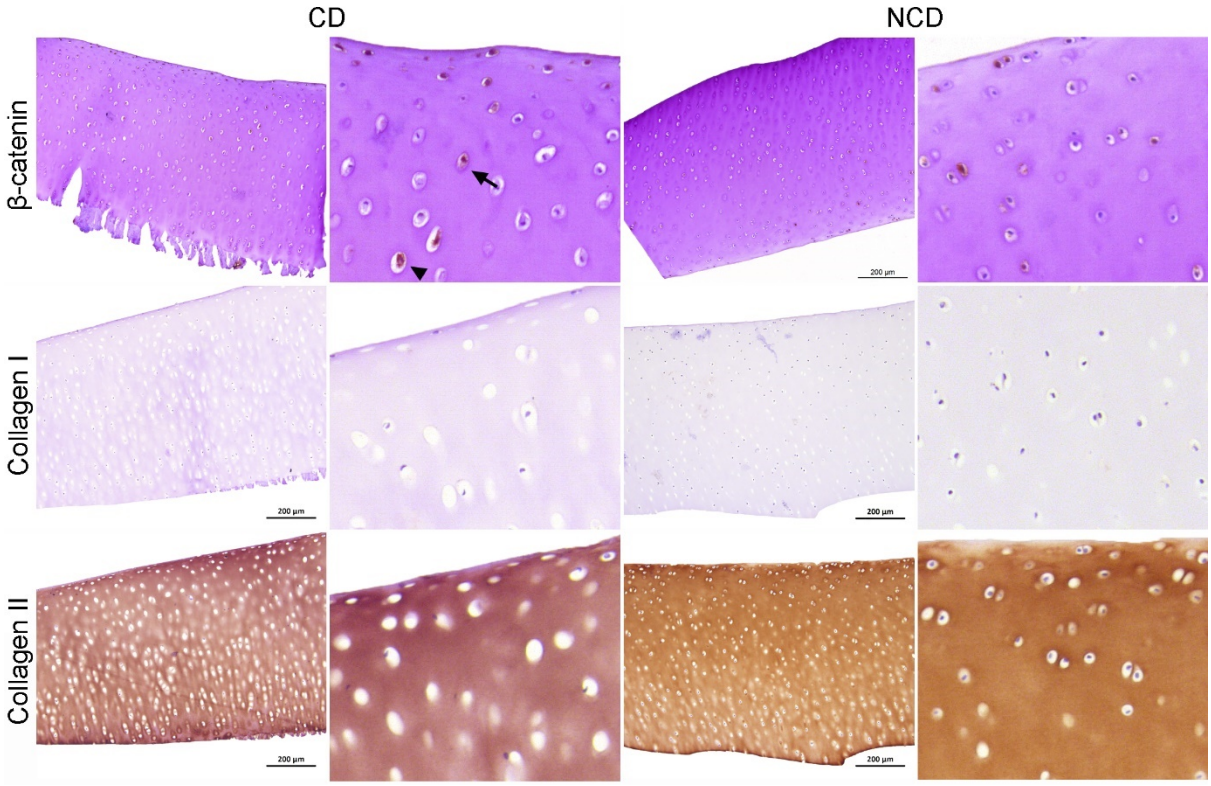

Figure 1. Typical examples of positive staining on immunohistochemical cartilage sections for β-catenin, collagen type 1 and collagen type 2. The arrow points to cytoplasmic immunopositivity, while the arrowhead illustrates nuclear immunopositivity for β-catenin. The left column shows 10x magnification, the right column 40x magnification. Left panel: CD, Chondrodystrophic; Right panel: NCD, non-chondrodystrophic.

Supplementary file 4. TCF-reporter assay.

Cryopreserved P1 articular cartilage cells (ACs) of non-chondrodystrophic (NCD, *n*=8) and chondrodystrophic (CD, *n*=8) were expanded for three days under normoxic conditions in a T75 flask (658175 Cellstar®, Greiner Bio-one) in expansion medium, consisting of hgDMEM, 10% FBS, 1% v/v p/s, 0.05% v/v fungizone, 0.1 mM ascorbic acid 2-phosphate, 10^{-9} M dexamethasone (D1756, Sigma), and 1 ng/mL basic fibroblast growth factor (PHP105, AbD Serotec). Monolayers of approximately 60.000 cells were seeded (*n*=2 per condition per donor) in a 24-wells primaria plate (353847, Corning) in expansion medium. After 24 hours, cells had reached a confluency of ~90% and were washed with 1 mL Hanks balanced salt solution (HBSS, 14025-050, Gibco® Life Technologies ™). Subsequently, 400 µL of hgDMEM was added. Wnt activation was measured using the dual-Glo Luciferace system (E2940, Promega). TOP (hgDMEM with 10 ng/mL TOP and 0.02 ng/mL β-actenine Renilla and FOP (hgDMEM with 10 ng/mL FOP and 0.02 ng/mL β-actenine Renilla) mixes, as well as the lipofectamine mixes (hgDMEM with 10 µL/mL Lipofectamine (11668-019, Lipofectamine® 2000 transfection reagent, Invitrogen, Thermo Fisher Scientific), were prepared and incubated 5 minutes at room temperature (RT). The lipofectamine mix was added to either the TOP or the FOP mix in a 1:1 ratio, followed by an incubation of 20 minutes at room temperature. Thereafter, either one of the mixes (100 µL) was added to the ACs. Cells were then incubated for 5 hours at 37 °C and 5% CO_2 under normoxic conditions. The transfection was halted by addition of 500 µL plain chondrogenic medium with 30% FBS. Cells only treated with plain chondrogenic medium served as a control (*n*=2). A proven Wnt activity active mammary gland tumour cell line (CMT5) served as a positive control (*n*=2 for TOP and *n*=2 for FOP). After additional incubation for 43 hours at 37 °C, 21% O2 and 5% CO_2, cells were washed with 1 mL HBBS. Then, 100 µL passive lysis buffer solution (200 µL/mL passive lysis buffer, E1910, Promega) diluted in milli-Q was added and cells were incubated for 15 minutes (37 °C and 5% CO_2). Subsequently, cells were frozen (at -70 °C) for 30 minutes. After thawing, 100 µL of the lysated cell suspension was plated in a 96-wells plate with a V-shaped bottom (651191, Greiner Bio-One) and centrifuged for 15 minutes (1900 rpm). After centrifugation, 25 µL of the supernatant was transferred to a flat bottomed 96-wells plate (3600, Corning). Finally, 36 µL Luciferase assay substrate (E151A, Promega) and 36 µL Stop & Glo® substrate (E640A, Promega), dissolved 1:50 in Stop & Glo® buffer (E641A, Promega), were added and the TOP, FOP, and β-actenine Renilla activities were measured in a luminometer (LUMIstar Galaxy luminometer, BMG Labtech GmbH). The β-actenine Renilla construct served as an internal control, after which the TOP/FOP ratio was determined.

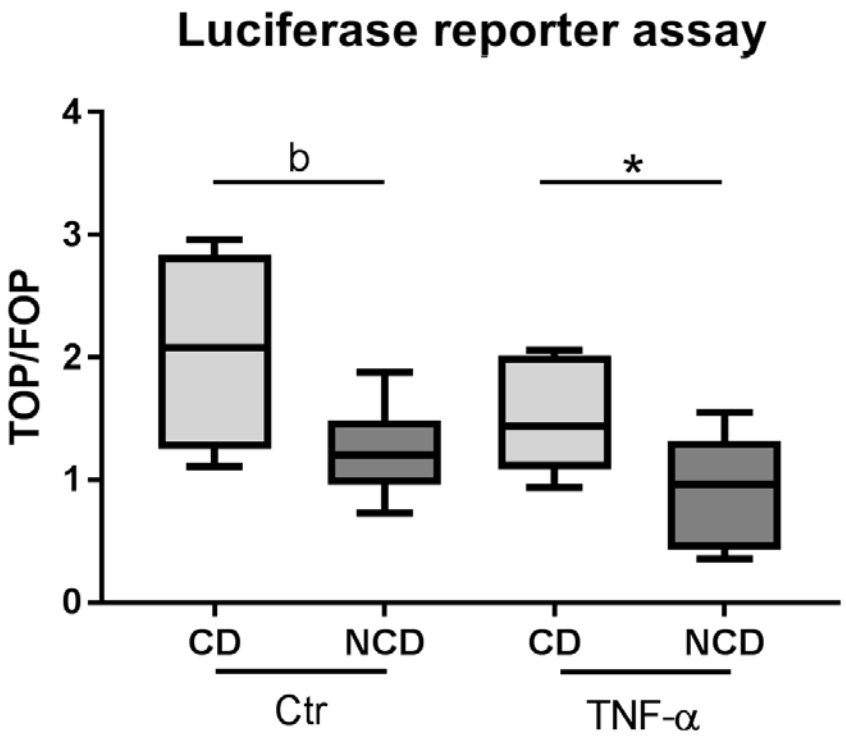

Figure 1. Canonical Wnt activity was measured by the TCF reporter assay. When only taking into account female donors, there is a substantially higher Wnt activity in CD chondrocytes than NCD chondrocytes in chondrogenic medium (Ctr, control) and in chondrogenic medium stimulated with 10 ng/mL TNF-α (p=0.06 with very large effect size and p=0.01, respectively). CD, Chondrodystrophic; NCD, non-chondrodystrophic. * p<0.05; b, very large effect size.

Chapter 3

Controlled release of celecoxib inhibits inflammation and subchondral bone changes in a preclinical model of osteoarthritis

A. R. Tellegen [1], I. Rudnik-Jansen [2], B. Pouran [3], H. M. de Visser [3], H. H. Weinans [2,3], R. E. Thomas [4], M. J. L. Kik [4], G. C. M. Grinwis [4], J. C. Thies [5], N. Woike [5], G. Mihov [5], P. J. Emans [6], B. P. Meij [1], L. B. Creemers [2]*, M. A. Tryfonidou [1],*

[1] Department of Clinical Sciences of Companion Animals, Faculty of Veterinary Medicine, Utrecht University, The Netherlands

[2] Department of Orthopaedics, University Medical Centre Utrecht, The Netherlands

[3] Department of Rheumatology & Clinical Immunology, University Medical Centre Utrecht, The Netherlands

[4] Department of Pathobiology, Faculty of Veterinary Medicine, Utrecht University, The Netherlands

[5] DSM Biomedical, The Netherlands

[6] Department of Orthopaedics, University Medical Centre Maastricht, The Netherlands

* Creemers and Tryfonidou contributed equally to this work

Drug Delivery (2018) 25:1

Abstract

Major hallmarks of osteoarthritis (OA) are cartilage degeneration, inflammation and osteophyte formation. COX-2 inhibitors counteract inflammation-related pain but their prolonged oral use entails the risk for side effects. Local and prolonged administration in biocompatible and biodegradable drug delivery biomaterials could offer an efficient and safe treatment for the long-term management of OA symptoms. Therefore, we evaluated the disease-modifying effects and the optimal dose of polyesteramide microspheres delivering the COX-2 inhibitor celecoxib in a rat OA model. Four weeks after OA induction by anterior cruciate ligament transection and partial medial meniscectomy, 8-week old female rats (*n*=6/ group) were injected intra-articular with celecoxib-loaded microspheres at three dosages (0.03, 0.23, or 0.39 mg). Unloaded microspheres served as control. During the 16-week follow-up, static weight bearing and plasma celecoxib concentrations were monitored. Post-mortem, micro-computed tomography and knee joint histology determined progression of synovitis, osteophyte formation, subchondral bone changes, and cartilage integrity. Systemic celecoxib levels were below the detection limit 6 days upon delivery. Systemic and local adverse effects were absent. Local delivery of celecoxib reduced the formation of osteophytes, subchondral sclerosis, bone cysts and calcified loose bodies, and reduced synovial inflammation, while cartilage histology was unaffected. Even though the effects on pain could not be evaluated directly in the current model, our results suggest the application of celecoxib-loaded microspheres holds promise as novel, safe and effective treatment for inflammation and pain in OA.

Introduction

Osteoarthritis (OA) is the most common form of arthritis in humans. It is estimated that 18% of women and 10% of men over the age of 60 years suffer from OA [1]. With aging of the population and the increasing prevalence of obesity, the incidence of OA is rising concurrently [2]. OA can result in joint pain, stiffness and functional limitations, negatively influencing quality of life [3].

Pain in OA is related to several associated disease processes, of which cartilage degeneration, synovial inflammation and peri-articular bone reaction, including bone cysts and osteophyte formation play an important role [4, 5]. Inflammation of the synovial lining results in the production of pro-inflammatory mediators and degradative enzymes, thereby mediating pain and facilitating further joint degeneration. These pro-inflammatory mediators are associated with the progression of OA pain [6] and disease [7]. Moreover, subchondral bone changes are considered increasingly important in OA. Bone marrow lesions (BML) and subchondral bone cysts appear early in the disease process [8] and are visible as regions of hyperintense marrow signal in fluid-sensitive MRI image sequences [9]. Both have been associated with joint pain [10] and disease progression [11, 12]. Other peri-articular bone changes include subchondral bone sclerosis and the formation of osteophytes [5]. Osteophytes may impair joint mobility and can cause pain by impinging surrounding structures [13]. As such, OA is considered a disease of the whole joint and successful therapeutic strategies should involve disease-modifying drugs that exert effects at multiple levels [14].

Oral nonsteroidal anti-inflammatory drugs (NSAIDs) are frequently used to inhibit pain and inflammation in OA [15, 16]. It has been suggested that celecoxib, a selective COX-2 inhibitor and the first drug to be approved for oral administration in OA, has disease-modifying properties. Cyclo-oxygenase-2 (COX-2) expression is upregulated in OA joints, resulting in pro-inflammatory mediators, such as prostaglandin E2 (PGE_2) [17]. The latter is associated with inflammation of the synovium, cartilage degeneration and the sensitization to pain [18]. Clinical studies have already proven that celecoxib is effective in relieving OA pain [19, 20]. *In vitro* studies even suggested a protective effect of celecoxib on OA cartilage [21, 22]. In line with this, cartilage of patients orally treated with celecoxib contained significantly more proteoglycans compared to cartilage of patients treated with the non-specific COX inhibitor indomethacin [22]. Moreover, celecoxib was able to prevent synovial hyperplasia and bone destruction both *in vitro* and *in vivo* [23]. A reduction in osteophytes was found when rats with surgically induced OA were treated with celecoxib orally [24].

Although COX-2 inhibition is effective in attenuating the symptoms of OA, longitudinal clinical studies associated oral COX-2 inhibitors at a higher oral dose with increased cardiovascular risk [25]. To overcome these issues, local biomaterial-based delivery of celecoxib can be a suitable treatment alternative, by providing prolonged drug exposure [26]. Local drug delivery not only prevents systemic side effects, it also ensures optimal exposure

in the joint cavity and avoids drug binding to systemic molecules and drug modifications that can limit efficacy when the drug is administered systemically [27].

To facilitate local delivery and sustained local exposure to drugs, biomaterial carriers can be used. Although a few *in vivo* studies have investigated intra-articular (IA) delivery systems of celecoxib in both healthy [28] and OA joints [29], the optimal dose range of celecoxib remains unknown. Polyesteramide (PEA) microspheres are very suitable for local sustained drug delivery, given their favorable mechanical and thermal properties and extended drug release profiles [30, 31]. The local safety of IA injection of celecoxib-loaded PEA microspheres (PEAMs) has previously been confirmed in healthy and OA rat knee joints 12 weeks after injection [32]. There, degradation of PEAMs was shown to be faster in OA compared to healthy joints, suggesting celecoxib-loaded PEAMs as a potent drug delivery system with autoregulatory behavior [32]. However, no therapeutic effects were noted, which may have been due to the dosage used. Therefore, the aim of this study was to assess the safety and efficacy of PEA microspheres loaded with a wide dose range of celecoxib *in vivo* in osteoarthritic rat joints, starting with twice the dosage used in the aforementioned study. By increasing the loading dose of celecoxib, we expect more pronounced tissue modulating effects on OA progression.

Materials and methods

Synthesis of the polyesteramide copolymer

The biomaterial in this study is a biodegradable poly(ester amide) (PEA) based on α-amino acids, aliphatic dicarboxylic acids and aliphatic α-ω diols. The selected PEA comprises three types of building blocks randomly distributed along the polymer chain. The polymer was synthesized according to a procedure reported previously [33]. Briefly, the polymer was prepared via solution polycondensation of di-p-toluenesulfonic acid salts of bis-(α-amino acid) α,ω- diol diesters, lysine benzyl ester and di-N-hydroxysuccinimide sebacate in anhydrous DMSO. The use of pre-activated acid in the reaction allows polymerization at low temperature (65 °C) affording side-product free polycondensates and predictable degradation products. The polymer was isolated from the reaction mixture in two precipitation steps.

Polymer characterization

^{1}H NMR spectra were obtained on a Bruker Avance 500 MHz Ultrashield NMR; samples were recorded in DMSO d_6. Molecular weight and molecular weight distributions of PEA were determined by GPC equipped with RI detector. Samples were dissolved in THF at a concentration of approximately 5 mg/mL and were run at a flow rate of 1 mL/min at 50 °C. The molecular weights were calibrated to a narrow polystyrene standard calibration curve, using Waters Empower software.

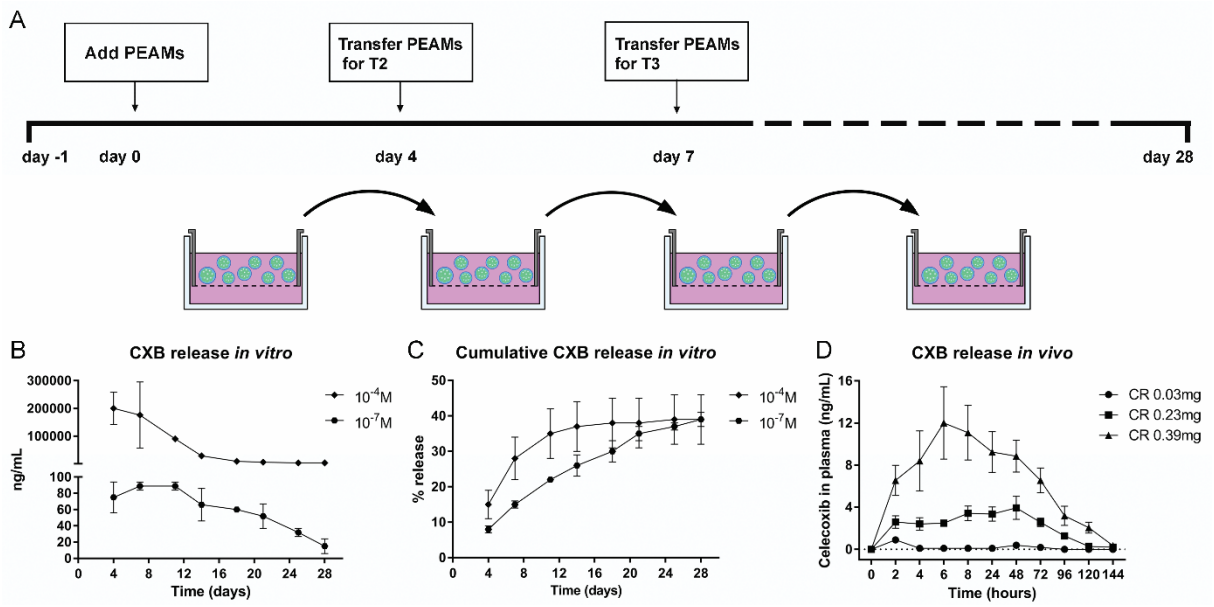

Figure 1. A. Setup of *in vitro* release of celecoxib (CXB). Absolute (**B**) and cumulative (**C**) celecoxib (CXB) release from PEA microspheres (PEAMs) in plain culture medium: after 28 days, 40% was released. *N*=2 per time point. (**D**) CXB release in plasma after intra-articular injection in osteoarthritic rat knee joints with three different loadings as indicated. *N*=6 per group. Plasma CXB concentrations were significantly different (p<0.001) between groups at all timepoints, except for T=144h. Data depicted as average ±SD.

Synthesis and characterization of (celecoxib-loaded) microspheres

Polyester amide polymer is dissolved in dichloromethane. To generate celecoxib (CXB) loaded PEA microspheres (PEAMs), the drug was added. After homogenization, the solution is sonicated in a water bath for 3 minutes. The PEA-CXB solution is then emulsified in 20ml of water phase (PVA 1 wt%, NaCl 2.5 wt%) by the use of an ultraturrax, stirring at 8000rpm for 3 minutes. After emulsification, particles are hardened overnight under air flow. Before washing, particles are cooled with an ice-bath for 1 hour and washed with Tween 80. Excess of surfactant is removed by centrifugation. Before freeze-drying to remove residual solvent, particles are suspended in Tween 80 in order to reach the right concentration of particles per volume. 15 and 70 mg/ml are aimed for CXB loaded- and unloaded PEAMs. Once dried, the particles are weighted in individual HPLC vials to the approximate amount of 15 or 70 mg respectively and γ-sterilized on dry ice.

Particle characteristics are described in Table 2. To measure celecoxib release in vitro, celecoxib-loaded PEAMs were dispersed in culture medium (hgDMEM+Glutamax, 1966; Invitrogen) and placed in Transwell® baskets (pore size 0.4 µm, polycarbonate membrane, 3413; Corning Life Sciences). Two concentrations, of celecoxib-loaded PEAMs were utilized: 10^{-7} M and 10^{-4} M corresponding to 1.33 µg CXB/mL and 1.33 mg CXB/mL. Medium was

changed twice a week, aliquots (700 µL) were obtained at day 4, 7, 11, 14, 18, 21, 25, and 28 and stored at -20 °C (Fig. 1A). For celecoxib measurements, medium samples were lyophilized for 3 hours and dissolved in 50 µL buffer (180719; Neogen Corporation) overnight at 4 °C prior to analysis. Celecoxib release from the PEAMs was measured by ELISA (180719; Neogen Corporation) following manufacturer's instructions.

Animal study

Study setup

This study was approved by the ethics committee for laboratory animal use (protocol #2014.III.10.086). Female, 8-week-old Sprague Dawley rats (Charles River laboratories, The Netherlands) were allowed to acclimatize for 7 days and housed in groups (3 to 4 rats) in polycarbonate cages with wire tops, wood chip bedding, and access to *ad libitum* food and tap water.

OA was induced unilaterally through anterior cruciate ligament transection (ACLT) and partial medial meniscectomy (pMMx) in the left knee of 24 rats [34]. Details on group size calculations are described in supplementary file 1. Completeness of ACLT was confirmed intra-operatively by a positive drawer sign. Pain management included 4 mg/kg carprofen and 0.03 mg/kg buprenorphine subcutaneously prior to surgery, buprenorphine was continued b.i.d. for three days. Animals were monitored daily for signs of discomfort and were weighed weekly. Four weeks later, rats were randomly divided into four groups with six rats per group (Table 1). On two consecutive days (day 0 and day 1), rats received IA injection with unloaded PEAMs (OA control) or PEAMs loaded with 0.015 mg/25 µL (low dose; LD), 0.115 mg/25 µL (medium dose; MD) or 0.195 mg/25 µL (high dose, HD) celecoxib. On day 0, 100 µL blood was collected five times every 2 hours (starting from directly prior to injection) to monitor systemic release of celecoxib. On day 1-7, blood was collected once daily (starting from 24 hours after injection) and thereafter once weekly until termination of the study. After sixteen weeks, rats were euthanized with CO_2.

Longitudinal measurements in vivo

EDTA-plasma was collected in capillary blood collection tubes (T-MQK Capiject, Terumo Medical Corporation) and stored at -80 °C until further use. Celecoxib was measured in plasma samples diluted 1:5 with buffer by ELISA (Neogen). A calibration curve ranging from 0.4 to 100 ng/mL celecoxib (C-1502, LC Laboratories) was measured in spiked EDTA-plasma of healthy rats from unrelated experiments.

Hind limb weight distribution as an index of pain was obtained with an incapacitance tester (Linton Instrumentation) before and 3 weeks after OA induction, and weekly after IA injections, as described previously [35]. The average of 5 measurements was used to calculate the weight on the affected limb as a percentage of total weight distributed by both hind limbs (Fig. 3A).

Table 1. Overview of experimental groups and microsphere loading.

Group	Treatment	Total dosage (mg/kg)	Particle concentration in formulation *[mg/ml]*	Loading drug *[wt%]*	Total drug injected *[mg]*	Mean particle size *[µm]*	Span
1	Unloaded	N/A	70	N/A	N/A	33.4	1.47
2	LD-CXB	0.13	15	4.1%	0.03	36.6	1.47
3	MD-CXB	0.99	70	6.5%	0.23	35.7	1.62
4	HD-CXB	1.67	70	11.2%	0.39	36.9	1.51

LD, low dose; MD, middle dose; HD, high dose; CXB, celecoxib; N/A, not applicable.

Post-mortem analysis

Directly post-mortem, micro-computed tomography (µ-CT) scans were acquired with a Quantum FX µ-CT Imaging System (Perkin Elmer, USA) to assess subchondral bone. Scans with an isotropic voxel size of 15 µm, at a voltage of 90 kV, a current of 180 µA and a field of view of 42 mm were created. Subchondral plate thickness, volume and porosity were measured in the cortical bone of the medial and lateral tibial plateau in coronal scans as previously described by De Visser et al [36]. With the use of ImageJ software, the regions of interest (ROI) were selected. Bone was segmented from the µ-CT datasets with a local threshold algorithm (Bernsen, radius 5) from the coronal sections. Regions of interests were manually drawn for a total of 90 slides, starting in the caudal side of the knee joint from the point where the medial and lateral compartments of the tibial epiphysis unite, onwards to the cranial side of the knee joint. ROIs were manually drawn in the subchondral bone of the lateral and medial compartments of the tibia plateau, resulting in data on mean subchondral plate thickness (mm) and subchondral bone volume fraction (BV/TV) representing the ratio of trabecular bone volume (BV, in mm^3) to endocortical tissue volume (TV, in mm^3), the mean trabecular bone thickness (mm) and trabecular bone volume fraction (BV/TV). The average distance (mm) between individual trabeculae ("spacing") was also recorded. In addition to subchondral bone changes, all knee joints were also assessed for the presence of subchondral bone sclerosis, osteophytes, subchondral bone cysts (SBCs) and loose bodies according to the method of Panahifar [24]. Briefly, SBCs were defined as round structures with no trabeculae, recognizable from black structures on µ-CT. Their presence was scored in the sagittal plane in the tibia, primarily on coronal plane, with grade 0 indicating absence of SBCs and grade I presence of SBCs. Loose bodies in the synovial capsule based on their number where 0 = none, 1 = 1 loose body, 2 = 2 loose bodies and 3 = 3 or more loose bodies. Subchondral sclerosis was evaluated at both medial and lateral sides in the femur and tibia in the sagittal plane based on a three scale score (a maximum score of six for each bone). Sclerosis was defined as a solid mineralized region with no distinct trabecular structure. The depth of sclerosis was measured on sagittal CT sections, from the articular surface along the diaphysis and the maximum value was reported. Baseline data were analysed and depth of up to 0.3 mm was considered normal thickness of subchondral bone plate. Osteophytes

were scored separately for femur, tibia and patella at four regions. The maximum depth of osteophyte perpendicular to bone was measured and scored in a two scale score (maximum of eight for each bone). Depth of less than 0.2 mm was considered ambiguous and scored 0. The reference plane for scoring femur and tibia was axial and for the patella, coronal. The diameter of SBCs was also measured in ImageJ (version 1.50e). All treated knees per treatment group were used for analyses by a blinded observer, together with six randomly selected non-treated control knees, leading to six knees per group. A blinded observer (AT) analyzed all µ-CT scans of the knees together.

Co-morbidities were explored with the aid of several parameters, including body weight reflecting well-being of the experimental animal during the study and post-mortem examination of the rats. Internal organs were assessed macroscopically and histologically to rule out systemic effects or co-morbidities, by blinded observers (RT, MK). Histopathologic analysis was performed according to standard protocols and tissue samples were fixed in 4% buffered formalin, embedded in paraffin and cut at 4 µm before routine staining with hematoxylin and eosin (H&E). Bacteriological testing was performed when there was macroscopic and cytological evidence of bacterial infection. Both necropsy and histological assessment were performed by operators blinded to the treatment administered. All organs were reviewed by RT and MK and the degree of hepatic vacuolisation was subsequently scored using the grading scheme proposed by Hardisty and Eustis (1990). Briefly, grades 1 (mild) to 5 (severe) based on the number of fields affected out of the fourteen randomly chosen high-powered fields that were viewed. Cytoplasmic vacuolisation was identified as being lacey (glycogen) or micro- or macro-vacuolar (fat).

All hind limbs were dissected and fixed in 4% v/v formalin for 7 days at RT. The histological preparations and analysis were performed according to the OARSI guidelines and scored on coronal 5 µm thick sections of EDTA-decalcified knee joints at 100 µm intervals [34]. Cartilage quality was assessed focusing on the following OARSI components: cartilage matrix loss width, cartilage degeneration, cartilage degeneration width, osteophytes, synovial inflammation and calcified cartilage, subchondral bone damage and growth plate thickness. To detect macrophages, CD68 immunohistochemistry (IHC) was performed (supplementary file 2). Collagen X IHC was performed to visualize hypertrophic differentiation of chondrocytes. The growth plate served as an internal positive control. The expression patterns of inducible nitric oxide synthase (i-NOS) and folate receptor beta (FR-β) were used to distinguish between M1 and M2 macrophages. Photographs were obtained of cartilage and synovial tissue adjacent to the medial tibia plateau. In ImageJ the total surface (pixels) of the synovial tissue or cartilage on digital photographs was obtained by manually selecting the region of interest. Positive DAB staining was quantified in that ROI. Expression was quantified by the % of positive surface.

Statistical analysis

Statistical analysis was conducted using IBM SPSS statistics 24.0 and R studio (*RStudio* 3.3.1). Normality of the data was checked by assessing Q-Q plots, histograms and Shapiro-Wilk tests. The effect of treatment on weight distribution was analysed using the Wilcoxon's signed rank test. One-way ANOVA and Kruskall-Wallis tests were used to analyse µ-CT data and histological scores. Differences in plasma celecoxib concentration were analyzed by a Cox proportional hazard model, considering "donor" as random effect and "time" and "treatment" as fixed effects. $P<0.05$ was considered significant after correcting for multiple testing with Benjamini&Hochberg False Discovery Rate *post-hoc* tests. Effect sizes (ES) were retrieved as *Hedge's g* for parametric data*:* medium; 0.5-0.8, large; 0.8-1.2 very large and >2 huge [37]. Differences were considered as relevant when $p< 0.05$ and/ or ES was medium or larger when p-value was <0.1. For non-parametric data, Cliff's delta was assessed: 0.28<ES<0.43, medium; 0.43≤ES<0.7, large; ES≥0.7, extra large [38]. *P*-values and effect sizes for all comparisons made in this study are provided in supplementary file 3.

Results

Polymer characterization

The relative ratio between the polymer building blocks was determined by 1H NMR. Tg of the polymer was determined under dry conditions. The average molecular weight of the polymer was 70 kDa, the polydispersity index (PDI) 1.70, the glass transition temperature (Tg) 54 °C and the relative monomer ratio of A:B:C was 0.30:0.27:0.43. The polymer used for this study is depicted in Figure 2.

Table 2. Polymer characterization.

	Mn (kDa)	**Polydispersity index (PDI)**	**Glass transition temperature (Tg)**	**Relative monomer ratio A:B:C**
PEA III Ac Bz	70	1.70	54°C	0.30:0.27:0.43

The relative ratio between the polymer building blocks was determined by 1H NMR. Tg of the polymer was determined under dry conditions.

In vitro and *in vivo* release of celecoxib

In vitro, CXB-PEAMs demonstrated a sustained drug release (Fig. 1B) with cumulative release of 40% after 28 days (Fig. 1C). *In vivo*, the small volume of synovial fluid in rat knees did not allow for sampling to monitor local celecoxib release from PEAMs. Therefore, systemic plasma celecoxib concentrations were determined. Celecoxib was, dose-dependently, detectable until 120 hours after IA injection (Fig. 1D).

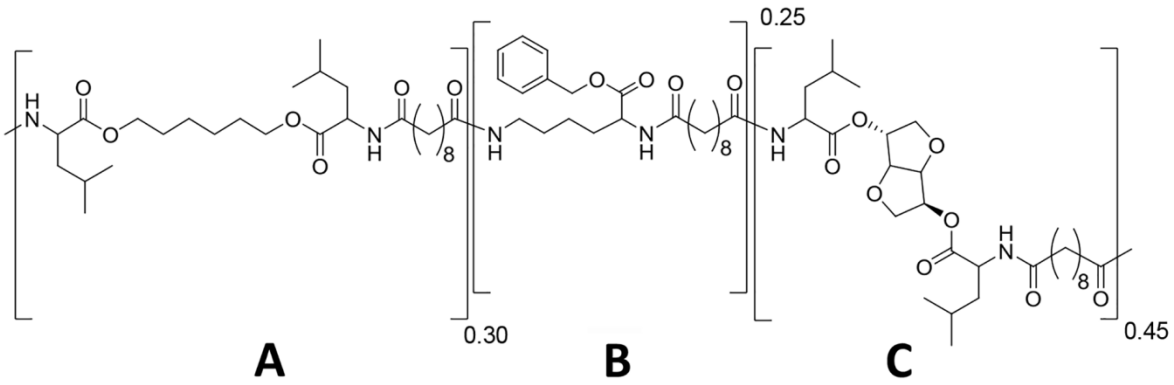

Figure 2. Structure of PEA III Ac Bz, random copolymer consisting of building blocks A, B and C.

Hind limb weight distributions seemed to restore as a result of treatment with LD-celecoxib-PEAMs

During the study period, average body weight increased gradually from 233 g (range 196-290 g) to 321 g (274–405 g), as expected. No differences were observed in body weight between treatment groups (Figure 3B). No treatment-related systemic abnormalities were found on necropsy confirming systemic safety. Before OA induction, rats bore weight on both hind limbs equally: 50.8%±6.7% (mean±SD) (Fig. 3C). Three weeks after ACLT+pMMx, weight distribution on the operated leg was significantly lower than the pre-operative situation (Fig. 3C, p=0.013). One week after IA injection of (un)loaded-PEAMs and throughout the whole study period, only borderline significant differences compared to pre-treatment values were found (p=0.058). Post hoc tests revealed a significant increase in weight bearing of the affected leg only with LD-CXB-PEAMs (p=0.044) vs. unloaded-PEAMs (Fig. 3D).

Ex vivo µ-CT revealed protective effects of prolonged celecoxib exposure on OA progression at the subchondral bone level

Ex vivo µ-CT was used to quantitatively evaluate the subchondral bone of the medial tibial plateau. All measured µ-CT parameters were significantly different in OA vs. healthy contralateral knees (Fig. 4A-L), confirming the typical hallmarks of OA at subchondral bone level, i.e. increase in subchondral sclerosis (Fig. 4A,B; p<0.001), osteophyte formation (Fig. 4C,D; p<0.001), the presence of calcified loose bodies (Fig. 4E,F; p<0.001) SBCs (Fig. 4G,H; p=0.001), whereas healthy knees had none. Moreover, lower porosity of the subchondral bone plate (Fig. 4J, p=0.059, medium ES) and a decrease in bone volume of the trabecular bone (Fig. 4L; p=0.027) beneath the subchondral plate, with a concurrent increase in trabecular spacing (Fig. 4K, p=0.003) were detectable in OA joints.

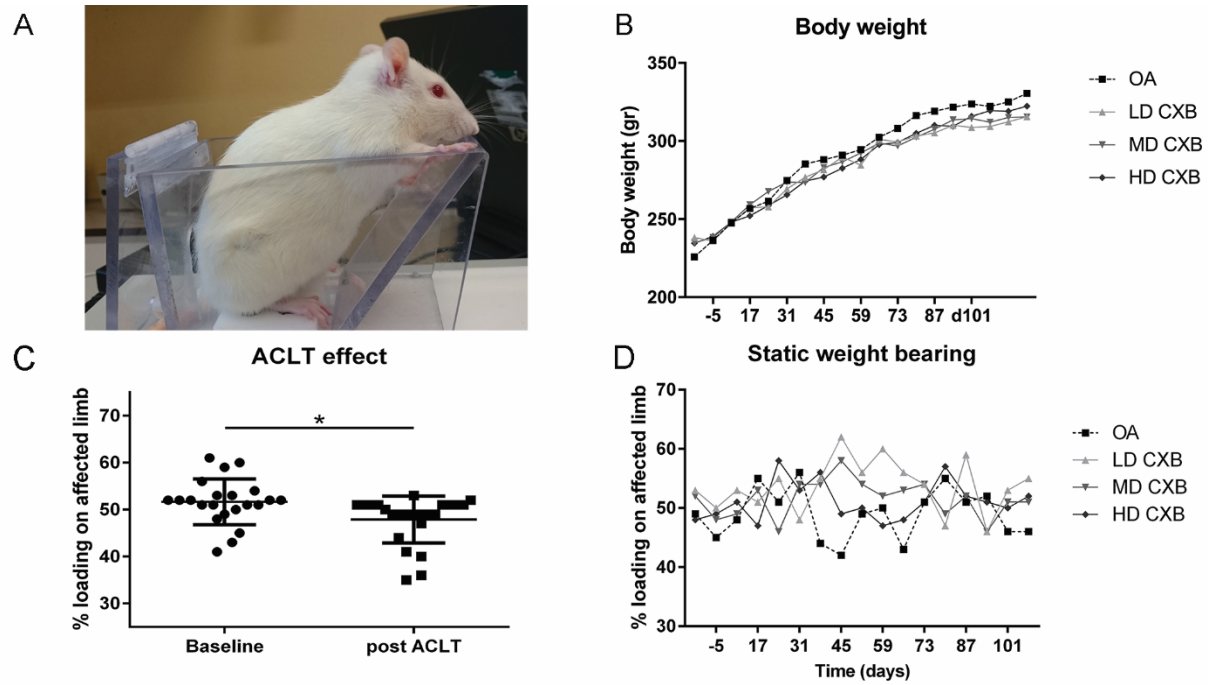

Figure 3. **A**. Setup of the pressure plate measurements. **B**. Body weight increased gradually in all groups during the course of the study. **C**. Load bearing significantly decreased (p=0.013) in operated joints 3 weeks after anterior cruciate ligament transection and partial medial meniscectomy (ACLT+pMMx). **D**. Static weight bearing improved 6 weeks after OA induction, but only the LD-CXB-PEAMs could significantly enhanced weight bearing compared to OA control joints (p=0.044). ACLT, Anterior cruciate ligament transection; OA, osteoarthritis (unloaded PEAM control group); LD CXB, low dose celecoxib; MD CXB, middle dose CXB; HD CXB, high dose CXB.

Less subchondral sclerosis was demonstrated in OA knees treated with LD-, MD- and HD-CXB-PEAMs (Fig. 4A), vs. unloaded-PEAMs (p<0.001). Knee joints that received celecoxib-PEAMs contained significantly less osteophytes (Fig 4C, p<0.05 for LD-, MD- and HD-CXB-PEAMs) vs. unloaded-PEAMs. In OA knees treated with unloaded-PEAMs, significantly more SBCs were scored compared to knees treated with CXB-PEAMs (Fig. 4G, p<0.05 for all dosages). Furthermore, SBC size was significantly smaller in OA knees treated with celecoxib-loaded-PEAMs vs. unloaded-PEAMs (Fig. 4I; p<0.05 for all dosages). In OA knees loose bodies were present (Fig. 4E,F); LD-CXB-PEAMs lowered their numbers vs. unloaded PEAMs (Fig. 4E, p=0.011). Furthermore, HD-CXB-PEAMs inhibited increase in subchondral BV/TV (Fig. 4J, p=0.09, large ES), and tended to counteract an increase in trabecular bone spacing (Fig. 4L, p=0.063, medium ES). No significant differences between treatment groups were detected in trabecular thickness of subchondral nor trabecular bone. Growth plate thickness was unaffected by OA induction and treatment with celecoxib (data not shown).

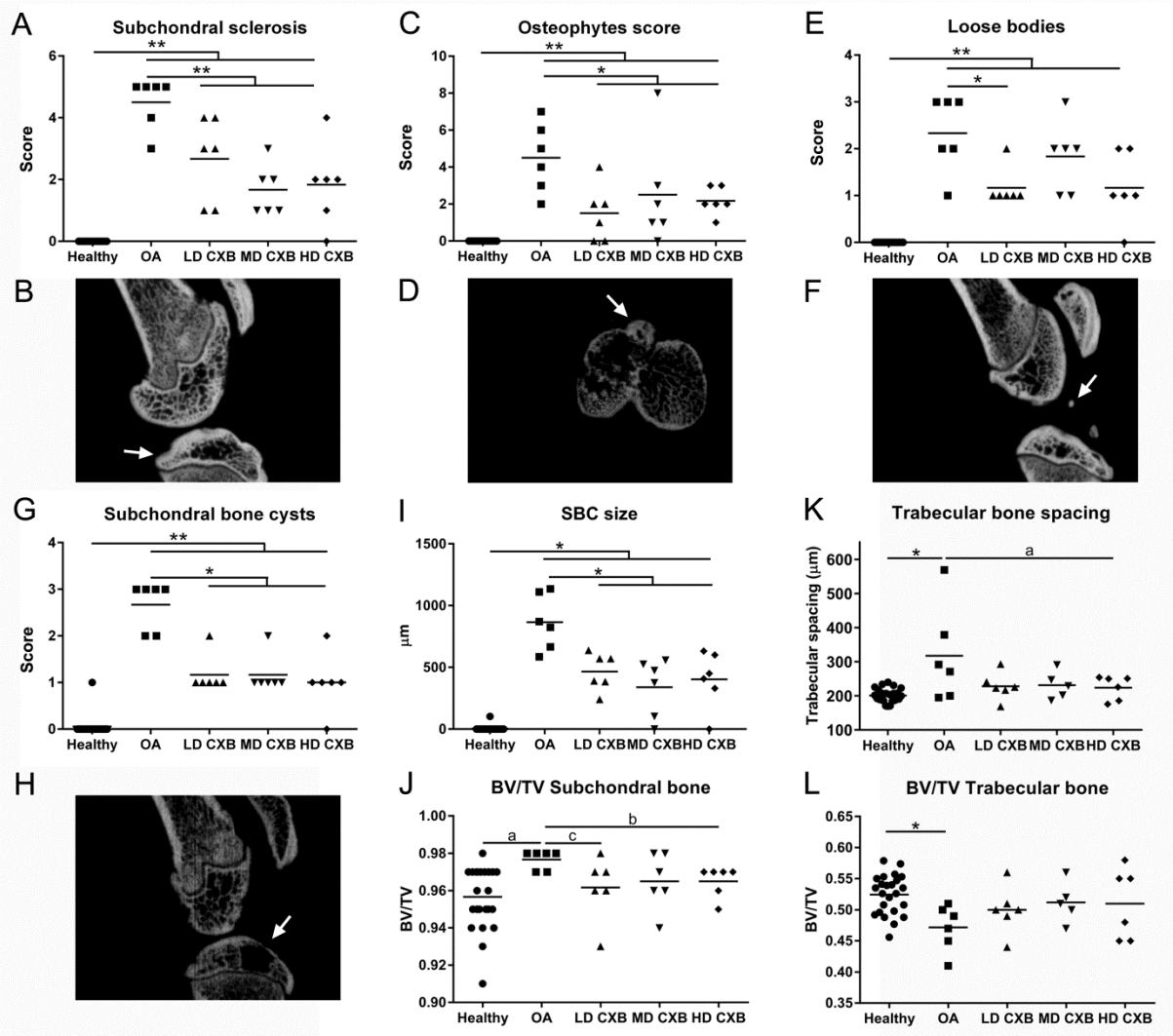

Figure 4. *Ex vivo* micro computed tomography (µ-CT) analysis of the medial tibia plateau. The induction of osteoarthritis (OA) led to an increase in subchondral sclerosis (**A**,**B**; $p<0.001$), which was inhibited by the controlled release (CR) of celecoxib (CXB) (**A**; $p=0.007$, $p=0.063$, $p=0.003$ for low, middle and high dose CXB (LD-, MD- and HD-CXB)). CXB-PEAMs exerted a protective effect on the formation of osteophytes (**C**,**D**; $p=0.006$, $p=0.036$ and $p=0.019$ for LD-, MD- and HD-CXB) and the presence of loose bodies (**E**,**F**; $p=0.011$, $p=0.24$, $p=0.142$) in OA joints. CR of celecoxib reduced the number of subchondral bone cysts (**G**,**H**; LD-CXB $p=0.002$; MD-CXB $p=0.037$; HD-CXB $p=0.002$) in OA joints, and also resulted in smaller cysts (**I**; $p=0.0015$, $p=0.002$, $p=0.0018$). The induction of OA resulted in increased bone volume of the subchondral bone plate (**J**; $p=0.059$, ES 0.7), which was decreased by HD-CXB-PEAMs (**J**, $p=0.09$, ES 0.8). HD-CXB-PEAMs tended to prevent increase of trabecular bone spacing (**K**; $p=0.063$, ES 0.65). *$p<0.05$, **$p<0.01$, a=medium effect size (ES), b=large ES, c=very large ES.

Histologic evaluation of cartilage integrity and synovial inflammation showed anti-inflammatory effects of celecoxib-releasing microspheres but no inhibition of cartilage degeneration

Histomorphometrical measurements were performed in the most affected region, *i.e.* the medial tibia plateau. The OARSI score (Fig. 5) was significantly higher in OA vs. healthy contralateral knees ($p<0.01$). Treatment with celecoxib-loaded PEAMs had no effect within the OA joints. The synovitis score was significantly increased in OA knees treated with unloaded-PEAMs vs. healthy ($p<0.001$) and HD-CXB-PEAMs ($p=0.028$). CD68 immunopositive cells, a general macrophage marker, were rarely seen in healthy knees. In OA control joints treated with unloaded-PEAMs, significantly more CD68 immunopositivity was found in the synovial perivascular regions vs. healthy controls ($p<0.001$). There was a dose-dependent decrease in CD68 immunopositivity with increasing celecoxib loading dose as indicated by the significantly lower CD68 immunopositivity in MD-CXB ($p=0.016$) and HD-CXB-PEAMs ($p=0.005$) vs. unloaded-PEAMs. Given these distinct differences, the presence of M1/M2 macrophages was further profiled by evaluating iNOS and FR-β immunopositivity in consecutive sections. The expression of M1 related iNOS was upregulated in OA vs. healthy contralateral joints ($p=0.012$) and there was a substantive significant decrease in iNOS expression in the HD-CXB-PEAMs ($p=0.068$, large ES). No significant differences in M2 related FR-β expression was noted between treatment groups, although FR-β expression seemed increased in OA vs healthy contralateral joints ($p=0.072$, large ES).

Collagen X immunopositivity in the tibial cartilage of OA knees injected with unloaded-PEAMs was increased ($p=0.047$) vs. healthy contralateral joints ($p=0.04$), indicating hypertrophic differentiation. Controlled release of celecoxib seemed to inhibit collagen X deposition ($p<0.1$; very large ES for LD-, MD- and huge ES for HD-CXB-PEAMs).

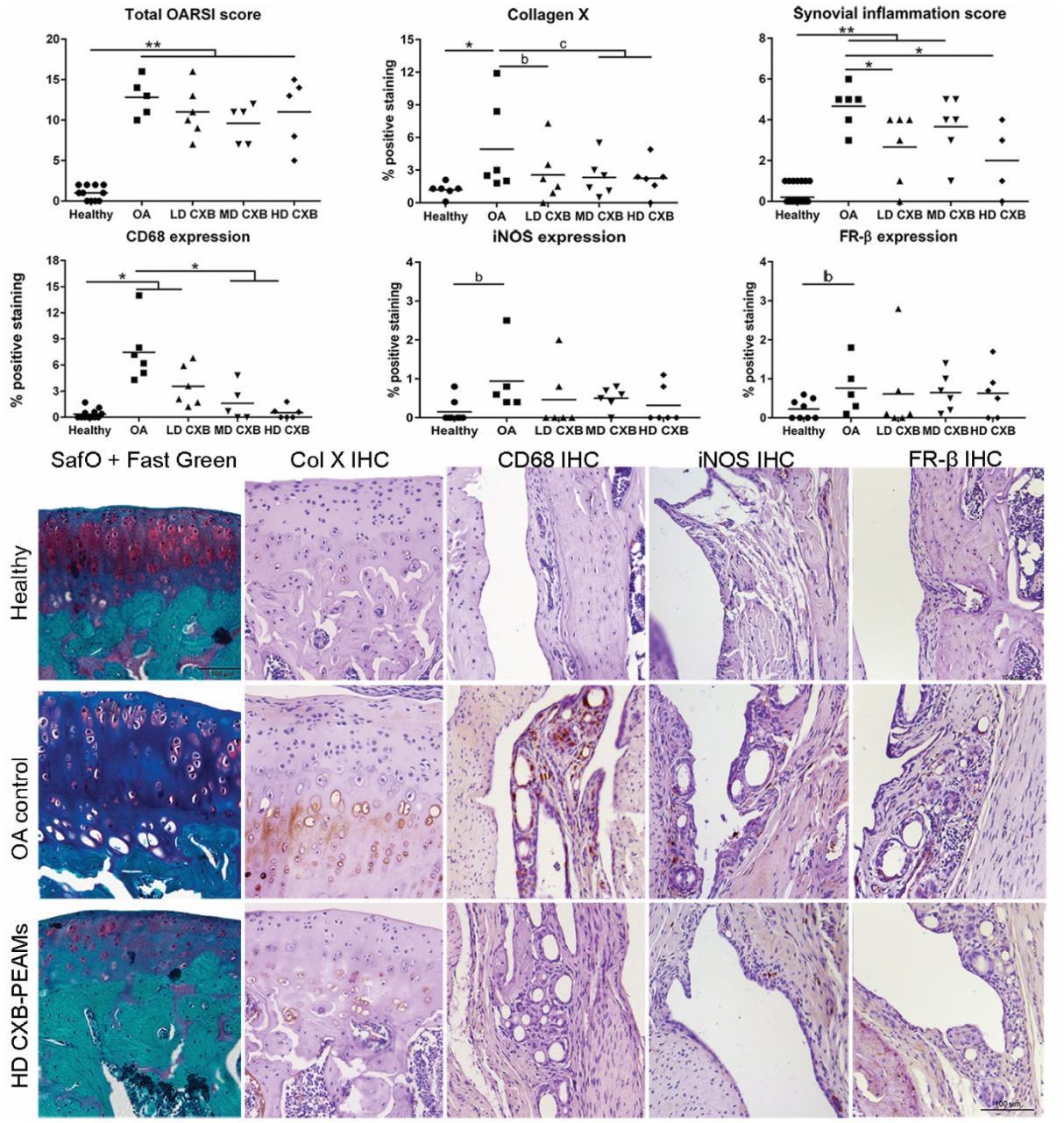

Figure 5. Histological grading and immunohistochemical analysis of the medial tibial. OA induction led to an increase in OARSI score, collagen X deposition and synovial inflammation. Celecoxib-loaded PEAMs were able to decrease synovial inflammation, macrophage presence and collagen X deposition. *p<0.05; ** p<0.01; a=medium effect size (ES), b=large ES, c=very large ES. OA, osteoarthritic control knees; LD; low dose; MD, middle dose; HD, high dose celecoxib. HD CXB-PEAMs, high dose celecoxib-polyesteramide microspheres; IHC, immunohistochemistry.

Discussion

In the present *in vivo* study, the effects of sustained release of celecoxib from PEAMs, administered intra-articular in a rat OA model were evaluated. Local or systemic adverse effects were absent in the (celecoxib-)PEAM-injected joints, indicating that the platform is safe to apply over a wide range of celecoxib loading. Systemic exposure of celecoxib after intra-articular injection was only detectable in the first 5 days after IA delivery, with substantially lower circulatory values than after oral administration [39]. In addition, local treatment with celecoxib-loaded PEAMs inhibited the OA bone phenotype as demonstrated by a decrease in subchondral bone sclerosis, osteophytes, calcified loose body formation, and SBCs. Even more so, celecoxib-loaded PEAMs reduced local joint inflammation. Considering the demonstrated role of synovial inflammation and peri-articular bone changes in OA-related pain, local sustained delivery of celecoxib is a disease modifying drug that could alleviate pain.

Prolonged local exposure to celecoxib inhibited subchondral bone changes and osteophyte formation, characteristic for OA. An increasing body of evidence points to an interplay between bone and cartilage in OA [14], even suggesting a key role for subchondral bone in OA development [40]. Targeting bone changes may be an effective strategy to reduce symptoms and disease progression in OA, as bone marrow lesions, bone cysts, osteophytes and bone shape were associated with structural progression and pain in patients with knee OA [12, 41]. The mechanism by which CXB inhibits OA bone changes may at least partially be related to its inhibitory effect on hypertrophic differentiation[42]. The process of OA at least partially recapitulates chondrocyte hypertrophic differentiation during endochondral ossification [43], which was also observed in the present OA model where significantly more collagen X in the degenerating cartilage was found. Notably, local delivery of CXB-PEAMs partially counteracted cartilage collagen type X deposition, while it was even more effective in slowing progression of OA-related subchondral bone changes and osteophyte formation. This is in accordance with previous reports exploring the disease-modifying effects of oral celecoxib administration [24].

In parallel to beneficial effects at the subchondral level, local delivery of celecoxib reduced the number and size of SBCs. SBCs are cavitary lesions that contain fibrous tissue and fluid, but can ossify in later stages. [9]. They arise at locations where cartilage damage is most severe and are associated with activated osteoclasts and osteoblasts [44]. Notably, human patients suffering from OA with associated BMLs/SBCs appear to have more pain and an increased risk for joint replacement surgery [9, 41]. The inhibition of cyst formation by local sustained delivery of celecoxib suggests a second route towards inhibition of OA-associated pain in addition to the inhibition of synovial inflammation. As celecoxib exerts direct effects on bone by inhibiting NF-κB-dependent osteoclastogenesis and osteoclast activation and indirect effects by reducing RANKL production by OA chondrocytes [23], this mechanism may account for the decreased number and size of SBCs in the present study.

This study also provided evidence for the inhibitory effect of local and sustained drug celecoxib delivery on osteophyte formation. From a clinical perspective, osteophytes can cause a decrease in joint range of motion and can also be a source of pain, by vascularization and associated innervation, and by impinging adjacent structures. Pain due to impingement can be an indication for surgical intervention for several joints such as the hip, shoulder and ankle joint, and it is recommended to remove osteophytes during arthroplasty surgery. Short-term outcome for cheilectomies is favorable, but osteophytes tend to recur in the long-term [45]. In this respect, local prolonged exposure to celecoxib could slow down osteophyte formation or prevent recurrence after surgical removal.

Corroborating to the observed effects at the subchondral bone and peri-articular level, a single injection of CXB-PEAMs seemed to harness the synovial inflammatory process on the long term as indicated by the improvement of the synovitis score and reduction of infiltrating inflammatory macrophages 16 weeks after injection. In line with these findings, a previous study employing the same rat OA model and CXB-PEAMs demonstrated reduction of total PGE_2 levels in knee homogenates, although improvement of synovitis at the histological level was not detected [32]. The latter could be attributed to the fact that half the loading dose of celecoxib per knee joint was used, compared to the lowest concentration employed in the current study. Indeed, celecoxib can inhibit synovial inflammation and proteolytic enzyme production through inhibition of the COX-2 and the NF-κB pathway *in vivo* [23]. In addition, celecoxib also inhibits proliferation of synovial fibroblasts, reducing synovial hyperplasia and potentially slowing down synovitis-mediated OA progression [23].

Although beneficial effects of celecoxib on subchondral bone, osteophytes and synovium were found, protective effects on cartilage histology were absent. We cannot exclude that the absence of a chondroprotective effect could be attributed to the specific OA rat model used. In contrast to the monosodium iodoacetate (MIA) model, the ACLT model does not give rise to significant differences in gait parameters and pain-related behavior, while quick irreversible degenerative changes at the tissue level do occur [46, 47]. Moreover, lately evidence has been accumulating that inflammation may play a minor role in OA-associated cartilage degeneration. In a collagenase-induced OA model, IL-1α and IL-1β were not involved in cartilage destruction [48] and in clinical trials, where inhibition of TNF-α or IL-1β, key players in inflammation, had disappointing effects [49]. In line with this, inflammation in the present rat OA model is low-grade, indicating that the role of inflammatory mediators in cartilage degeneration could be of minor importance.

Altogether, the present study showed that by fine-tuning the loading dose of the PEAM-based drug delivery platform, the disease modifying effects of celecoxib were further improved. Clear beneficial effects were exerted on the bone phenotype of OA. It remains to be investigated whether the controlled and local release of celecoxib also effectively inhibits pain-related inflammation. However, the inhibition of synovial inflammation and the

inhibition of bone cysts and osteophyte formation suggests local delivery of celecoxib may be an effective treatment for both disease-modifying as well as OA-associated pain.

Acknowledgements

The authors would also like to thank Maarten Jansen, Joyce Bestebroer, Frances Bach, Arie Doornenbal, and Saskia Plomp for their assistance with data acquisition from the *in vivo* experiment and Silvia Pluis for aiding in microsphere preparation. We would also like to acknowledge dr. Louis Penning for his critical revision of the manuscript.

References

1. Cross M, Smith E, Hoy D, Nolte S, Ackerman I, Fransen M*, et al*. The global burden of hip and knee osteoarthritis: estimates from the global burden of disease 2010 study. Ann.Rheum.Dis. 2014;73:1323-30.
2. Holt HL, Katz JN, Reichmann WM, Gerlovin H, Wright EA, Hunter DJ*, et al*. Forecasting the burden of advanced knee osteoarthritis over a 10-year period in a cohort of 60-64 year-old US adults. Osteoarthritis Cartilage 2011;19:44-50.
3. Lane NE, Brandt K, Hawker G, Peeva E, Schreyer E, Tsuji W*, et al*. OARSI-FDA initiative: defining the disease state of osteoarthritis. Osteoarthritis Cartilage 2011;19:478-82.
4. Glyn-Jones S, Palmer AJ, Agricola R, Price AJ, Vincent TL, Weinans H*, et al*. Osteoarthritis. Lancet 2015;386:376-87.
5. Loeser RF, Goldring SR, Scanzello CR, Goldring MB. Osteoarthritis: a disease of the joint as an organ. Arthritis Rheum. 2012;64:1697-707.
6. Baker K, Grainger A, Niu J, Clancy M, Guermazi A, Crema M*, et al*. Relation of synovitis to knee pain using contrast-enhanced MRIs. Ann.Rheum.Dis. 2010;69:1779-83.
7. Roemer FW, Guermazi A, Felson DT, Niu J, Nevitt MC, Crema MD*, et al*. Presence of MRI-detected joint effusion and synovitis increases the risk of cartilage loss in knees without osteoarthritis at 30-month follow-up: the MOST study. Ann.Rheum.Dis. 2011;70:1804-9.
8. Alliston T, Hernandez CJ, Findlay DM, Felson DT, Kennedy OD. Bone Marrow Lesions in Osteoarthritis: What Lies Beneath. J.Orthop.Res. 2017;.
9. Kon E, Ronga M, Filardo G, Farr J, Madry H, Milano G*, et al*. Bone marrow lesions and subchondral bone pathology of the knee. Knee Surg.Sports Traumatol.Arthrosc. 2016;24:1797-814.
10. Yusuf E, Kortekaas MC, Watt I, Huizinga TW, Kloppenburg M. Do knee abnormalities visualised on MRI explain knee pain in knee osteoarthritis? A systematic review. Ann.Rheum.Dis. 2011;70:60-7.
11. Taljanovic MS, Graham AR, Benjamin JB, Gmitro AF, Krupinski EA, Schwartz SA*, et al*. Bone marrow edema pattern in advanced hip osteoarthritis: quantitative assessment with magnetic resonance imaging and correlation with clinical examination, radiographic findings, and histopathology. Skeletal Radiol. 2008;37:423-31.
12. Tanamas SK, Wluka AE, Pelletier JP, Martel-Pelletier J, Abram F, Wang Y*, et al*. The association between subchondral bone cysts and tibial cartilage volume and risk of joint replacement in people with knee osteoarthritis: a longitudinal study. Arthritis Res.Ther. 2010;12:R58.
13. Sofat N, Ejindu V, Kiely P. What makes osteoarthritis painful? The evidence for local and central pain processing. Rheumatology (Oxford) 2011;50:2157-65.
14. Karsdal MA, Leeming DJ, Dam EB, Henriksen K, Alexandersen P, Pastoureau P*, et al*. Should subchondral bone turnover be targeted when treating osteoarthritis? Osteoarthritis Cartilage 2008;16:638-46.
15. Wolfe F, Zhao S, Lane N. Preference for nonsteroidal antiinflammatory drugs over acetaminophen by rheumatic disease patients: a survey of 1,799 patients with osteoarthritis, rheumatoid arthritis, and fibromyalgia. Arthritis Rheum. 2000;43:378-85.
16. Moskowitz RW, Abramson SB, Berenbaum F, Simon LS, Hochberg M. Coxibs and NSAIDs--is the air any clearer? Perspectives from the OARSI/International COX-2 Study Group Workshop 2007. Osteoarthritis Cartilage 2007;15:849-56.
17. Pincus T. Clinical evidence for osteoarthritis as an inflammatory disease. Curr.Rheumatol.Rep. 2001;3:524-34.
18. Wang P, Guan PP, Guo C, Zhu F, Konstantopoulos K, Wang ZY. Fluid shear stress-induced osteoarthritis: roles of cyclooxygenase-2 and its metabolic products in inducing the expression of proinflammatory cytokines and matrix metalloproteinases. FASEB J. 2013;27:4664-77.
19. McCormack PL. Celecoxib: a review of its use for symptomatic relief in the treatment of osteoarthritis, rheumatoid arthritis and ankylosing spondylitis. Drugs 2011;71:2457-89.
20. Pincus T, Koch G, Lei H, Mangal B, Sokka T, Moskowitz R*, et al*. Patient Preference for Placebo, Acetaminophen (paracetamol) or Celecoxib Efficacy Studies (PACES): two randomised, double blind, placebo controlled, crossover clinical trials in patients with knee or hip osteoarthritis. Ann.Rheum.Dis. 2004;63:931-9.
21. Mastbergen SC, Lafeber FP, Bijlsma JW. Selective COX-2 inhibition prevents proinflammatory cytokine-induced cartilage damage. Rheumatology (Oxford) 2002;41:801-8.
22. de Boer TN, Huisman AM, Polak AA, Niehoff AG, van Rinsum AC, Saris D*, et al*. The chondroprotective effect of selective COX-2 inhibition in osteoarthritis: ex vivo evaluation of human cartilage tissue after in vivo treatment. Osteoarthritis Cartilage 2009;17:482-8.

23. Zweers MC, de Boer TN, van Roon J, Bijlsma JW, Lafeber FP, Mastbergen SC. Celecoxib: considerations regarding its potential disease-modifying properties in osteoarthritis. Arthritis Res.Ther. 2011;13:239-250.
24. Panahifar A, Jaremko JL, Tessier AG, Lambert RG, Maksymowych WP, Fallone BG*, et al*. Development and reliability of a multi-modality scoring system for evaluation of disease progression in pre-clinical models of osteoarthritis: celecoxib may possess disease-modifying properties. Osteoarthritis Cartilage 2014;22:1639-50.
25. Solomon DH, Husni ME, Libby PA, Yeomans ND, Lincoff AM, Lupsilonscher TF*, et al*. The Risk of Major NSAID Toxicity with Celecoxib, Ibuprofen, or Naproxen: A Secondary Analysis of the PRECISION Trial. Am.J.Med. 2017;130:1415-1422.
26. Larsen C, Ostergaard J, Larsen SW, Jensen H, Jacobsen S, Lindegaard C*, et al*. Intra-articular depot formulation principles: role in the management of postoperative pain and arthritic disorders. J.Pharm.Sci. 2008;97:4622-54.
27. Evans CH, Kraus VB, Setton LA. Progress in intra-articular therapy. Nat.Rev.Rheumatol. 2014;10:11-22.
28. Petit A, Redout EM, van de Lest CH, de Grauw JC, Muller B, Meyboom R*, et al*. Sustained intra-articular release of celecoxib from in situ forming gels made of acetyl-capped PCLA-PEG-PCLA triblock copolymers in horses. Biomaterials 2015;53:426-36.
29. Dong J, Jiang D, Wang Z, Wu G, Miao L, Huang L. Intra-articular delivery of liposomal celecoxib-hyaluronate combination for the treatment of osteoarthritis in rabbit model. Int.J.Pharm. 2013;441:285-90.
30. Andres-Guerrero V, Zong M, Ramsay E, Rojas B, Sarkhel S, Gallego B*, et al*. Novel biodegradable polyesteramide microspheres for controlled drug delivery in Ophthalmology. J.Control.Release 2015;211:105-17.
31. Rudnik-Jansen I, Colen S, Berard J, Plomp S, Que I, van Rijen M*, et al*. Prolonged inhibition of inflammation in osteoarthritis by triamcinolone acetonide released from a polyester amide microsphere platform. J.Control.Release 2017;253:64-72.
32. Janssen M, Timur UT, Woike N, Welting TJ, Draaisma G, Gijbels M*, et al*. Celecoxib-loaded PEA microspheres as an auto regulatory drug-delivery system after intra-articular injection. J.Control.Release 2016;244:30-40.
33. Katsarava R, Beridze Z, Arabuli N, Kharadze D, Chu CC, Won CY. Amino acid- based bioanalogous polymers. Synthesis, and study of regular poly(ester amide)s based on bis(α-amino acid) α, ω-alkylene diesters, and aliphatic dicarboxylic acids. 1999;37:391-407.
34. Gerwin N, Bendele AM, Glasson S, Carlson CS. The OARSI histopathology initiative - recommendations for histological assessments of osteoarthritis in the rat. Osteoarthritis Cartilage 2010;18 Suppl 3:S24-34.
35. van Buul GM, Siebelt M, Leijs MJ, Bos PK, Waarsing JH, Kops N*, et al*. Mesenchymal stem cells reduce pain but not degenerative changes in a mono-iodoacetate rat model of osteoarthritis. J.Orthop.Res. 2014;32:1167-74.
36. de Visser HM, Weinans H, Coeleveld K, van Rijen MH, Lafeber FP, Mastbergen SC. Groove model of tibia-femoral osteoarthritis in the rat. J.Orthop.Res. 2016;35:496-505.
37. Sawilowsky SS. New effect size rules of thumb. 2009;8:597-599.
38. Vargha A and Delaney HD. A Critique and Improvement of the CL Common Language Effect Size Statistics of McGraw and Wong. 2000;25:101-132.
39. Ma Y, Gao S, Hu M. Quantitation of celecoxib and four of its metabolites in rat blood by UPLC-MS/MS clarifies their blood distribution patterns and provides more accurate pharmacokinetics profiles. J.Chromatogr.B.Analyt Technol.Biomed.Life.Sci. 2015;1001:202-11.
40. Botter SM, van Osch GJ, Clockaerts S, Waarsing JH, Weinans H, van Leeuwen JP. Osteoarthritis induction leads to early and temporal subchondral plate porosity in the tibial plateau of mice: an in vivo microfocal computed tomography study. Arthritis Rheum. 2011;63:2690-9.
41. Barr AJ, Campbell TM, Hopkinson D, Kingsbury SR, Bowes MA, Conaghan PG. A systematic review of the relationship between subchondral bone features, pain and structural pathology in peripheral joint osteoarthritis. Arthritis Res.Ther. 2015;17:228.
42. Welting TJ, Caron MM, Emans PJ, Janssen MP, Sanen K, Coolsen MM*, et al*. Inhibition of cyclooxygenase-2 impacts chondrocyte hypertrophic differentiation during endochondral ossification. Eur.Cell.Mater. 2011;22:420-436.
43. Dreier R. Hypertrophic differentiation of chondrocytes in osteoarthritis: the developmental aspect of degenerative joint disorders. Arthritis Res.Ther. 2010;12:216.
44. Li G, Yin J, Gao J, Cheng TS, Pavlos NJ, Zhang C*, et al*. Subchondral bone in osteoarthritis: insight into risk factors and microstructural changes. Arthritis Res.Ther. 2013;15:223.
45. Wong SH, Chiu KY, Yan CH. Review Article: Osteophytes. J.Orthop.Surg.(Hong Kong) 2016;24:403-10.
46. Ferland CE, Laverty S, Beaudry F, Vachon P. Gait analysis and pain response of two rodent models of osteoarthritis. Pharmacol.Biochem.Behav. 2011;97:603-10.

47. Maerz T, Newton MD, Kurdziel MD, Altman P, Anderson K, Matthew HW*, et al*. Articular cartilage degeneration following anterior cruciate ligament injury: a comparison of surgical transection and noninvasive rupture as preclinical models of post-traumatic osteoarthritis. Osteoarthritis Cartilage 2016;24:1918-27.
48. van Dalen SC, Blom AB, Sloetjes AW, Helsen MM, Roth J, Vogl T*, et al*. Interleukin-1 is not involved in synovial inflammation and cartilage destruction in collagenase-induced osteoarthritis. Osteoarthritis Cartilage 2017;25:385-96.
49. Philp AM, Davis ET, Jones SW. Developing anti-inflammatory therapeutics for patients with osteoarthritis. Rheumatology (Oxford) 2017;56:869-81.

Supplementary file 1. Power analysis and group size calculation for the *in vivo* experiment.

To determine the total number of animals used in the *in vivo* experiment, and the number of animals in each experimental group, a power analysis was performed in G*Power 3.1.9.2. An a priori analysis was performed using an ANOVA, to compute the required sample size, given an effect size of 1, and an α of 0.008. An α of 0.008 was used as we had to correct for multiple comparisons: 6 comparisons in total results in an α of 0.05/6 = 0.008. A total of 24 animals was calculated (6 animals per experimental group), with a power of 0.85.

Supplementary file 2. Details of the primary antibodies and the immunohistochemistry protocols employed.

Deparaffinization was established through xylene (2x5 min) and graded ethanol (96, 80, 70, 60%, 5 min each), followed by two rinses of TBS+0.1% Tween (TBST0.1%, 2x5 min). Antigen retrieval was performed, followed by endogenous peroxidase inhibition for 5 min and pre-incubation with blocking buffer for 30 min at RT. Thereafter, sections were incubated with primary antibody at 4°C overnight (table 1). The EnVision-HRP detection system (Dako) was applied for 30 min at RT followed by incubation with streptavidin conjugated with horseradish peroxidase for 30 min at RT. All antibodies were visualized with the liquid DAB+ substrate chromogen (Dako). With the aid of ImageJ, immunopositivity was calculated as the % of positive staining in the total synovial area. Respective isotype controls confirmed specificity for the staining.

Table 2. Details on immunohistochemistry protocols.

Name	Manufacturer	Origin	Antibody Ig fraction	Antigen retrieval	Block	Dilution 1st antibody	Secondary antibody
CD68	Abcam, ab31630	Human recombinant	Mouse Mab	None	1:10 goat serum / PBST	0.2 µg/mL	EnVision K4001, Dako
Collagen X	Quartett, 2031501005	Human recombinant	Mouse Mab IgG1	0.1% Pepsin, 20 min @37°C and HAse 10mg/mL, 30 min @37°C	1:10 goat serum / PBST		EnVision K4001, Dako
Folate receptor β		Human recombinant	Rabbit Pab IgG	0.01M citrate buffer pH 6.0 30 min @70°C	PBS-BSA 5%	1:500	X0903, Dako
NOS2 (iNOS)	Santa Cruz Bio-technology, SC-7271	Human recombinant	Mouse Mab IgG1	0.1% Pepsin, 20 min @37°C	0.3% H_2O_2; PBS-BSA 5%	1:1000	EnVision K4001, Dako

Mab: monoclonal antibody; Pab: polyclonal antibody; HAse: bovine hyaluronidase 4 450 IU/mg, adjusted to pH 5 with 0.1M HCl.; PBST: 6 Phosphate buffered saline 0.1% Tween-20.

Supplementary file 3. Effect sizes (ES), ES's confident intervals (99.9%, between brackets) and P values for the different analyses performed in the study with P-values between 0.05 and 0.1.

Experiment	Comparison	Effect size	P value	Type
Trabecular thickness subchondral bone	OA vs healthy	0.21		Hedge's G
	OA vs LD-PEAMs	0.04		
	OA vs MD-PEAMs	0.15		
	OA vs HD-PEAMs	0.87		
Trabecular thickness trabecular bone	OA vs healthy	0.27		Hedge's G
	OA vs LD-PEAMs	0.49		
	OA vs MD-PEAMs	0.18		
	OA vs HD-PEAMs	0.30		
BV/TV subchondral bone	OA vs healthy	0.68 (0.85-2.20)	0.059 #	Hedge's G
	OA vs LD-PEAMs	1.27 (0.36-2.90)	0.08 #	
	OA vs MD-PEAMs	0.48 (-1.99-1.03)	0.09 #	
	OA vs HD-PEAMs	0.85 (0.70-2.41)	0.08 #	
BV/TV trabecular bone	OA vs healthy	0.37 (-1.13-1.87)	0.027 *	Hedge's G
	OA vs LD-PEAMs	0 (-1.49-1.49)	0.86	
	OA vs MD-PEAMs	0.19 (-1.30-1.68)	0.79	
	OA vs HD-PEAMs	0.16 (-1.33-1.65)	0.78	
Trabecular bone spacing	OA vs healthy	0.82 (0.73-2.37)	0.003 **	Hedge's G
	OA vs LD-PEAMs	0.50 (-2.01-1.01)	0.093 #	
	OA vs MD-PEAMs	0.47 (-1.98-1.04)	0.128	
	OA vs HD-PEAMs	0.65 (0.95-2.08)	0.071 #	
Collagen X IHC	OA vs healthy	1.26 (0.37-2.88)	0.047 *	Hedge's G
	OA vs LD-PEAMs	0.67 (-2.20-0.86)	0.380	
	OA vs MD-PEAMs	0.82 (0.73-2.73)	0.064 #	
	OA vs HD-PEAMs	0.87 (0.69-2.43)	0.052 #	
iNOS IHC	OA vs healthy	0.60	0.012 *	Cliff's delta
	OA vs LD-PEAMs	0.40	0.177	
	OA vs MD-PEAMs	0.34	0.126	
	OA vs HD-PEAMs	0.34	0.068 #	
FR-β IHC	OA vs healthy	1.01 (0.57-2.14)	0.072 #	Hedge's G
	OA vs LD-PEAMs	0.22 (-1.71-1.27)	0.63	
	OA vs MD-PEAMs	0.28 (-1.77-1.22)	0.81	
	OA vs HD-PEAMs	0.31 (-1.80-1.19)	0.56	

Color labels for Hedge's g: *none* (ES≤0.01), no fill; *very small* (0.01≤ES<0.2), purple; *small* (0.2≤ES<0.5), light blue; *medium* (0.5≤ES<0.8), yellow; *large* (0.8≤ES<1.2), green; *very large* (1.2≤ES<2), orange; and *huge* (ES≥2), red. Color labels for Cliff's delta: *small* (ES<0.28), light blue; *medium* (0.28≤ES<0.43), yellow; *large* (0.43≤ES<0.7), green; and very l*arge* (ES≥0.7), red. (# p<0.1; * p<0.05; ** p<0.01.

Chapter 4

Sustained release of locally delivered celecoxib provides pain relief for osteoarthritis in dogs: a prospective, randomized controlled clinical trial

A. R. Tellegen [1], M. Beukers [1], R. J. Maarschalkerweerd [2], C. D. van Zuilen [2], N. J. van Klaveren [2], K. Houben [1], E. Teske [1], R. van Weeren [3], N. Woike [4], G. Mihov [4], J. Thies [4], L. B. Creemers [5], B. P. Meij [1*], M. A. Tryfonidou [1*]

[1] Department of Clinical Sciences of Companion Animals, Faculty of Veterinary Medicine, Utrecht University, The Netherlands.
[2] Orthopedie, Medisch Centrum voor Dieren, The Netherlands.
[3] Department of Equine Sciences, Faculty of Veterinary Medicine, Utrecht University, The Netherlands.
[4] DSM Biomedical, The Netherlands.
[5] Department of Orthopaedics, University Medical Centre Utrecht, The Netherlands.

* Shared senior authorship

In review at The Veterinary Journal

Abstract

Osteoarthritis (OA) is a common cause of pain and lameness in companion animals. Non-steroidal anti-inflammatory drugs are effective against OA pain, but may be accompanied by side effects. Local administration via drug delivery platforms could offer a suitable treatment strategy for long-term OA management. The aim of this prospective, randomized controlled study was to investigate the efficacy of an intra-articular sustained release platform containing celecoxib, a COX-2 selective inhibitor, in client-owned dogs with established OA. Celecoxib release profiles and its anti-inflammatory properties were investigated in canine primary chondrocytes in monolayer culture for 28 days. Thirty dogs with clinical and radiological OA were included: 20 patients received celecoxib-loaded microspheres, 10 received unloaded microspheres (placebo). Weight-bearing was assessed by visual lameness scoring, kinetic gait analysis prior to, and 1 and 2 months after treatment; radiographs were scored for OA and synovial fluid was analysed after 2 months. Pain-related behaviour was scored by the owner. *In vitro*, celecoxib release was shown for 28 days and suppressed prostaglandin E_2 (PGE_2), a biomarker of inflammation, during the entire culture period, without negatively influencing cellular homeostasis. Intra-articular administration of celecoxib-loaded microspheres improved lameness and pain-related behaviour. PGE_2 content in the synovial fluid of dogs treated with celecoxib-loaded microspheres was significantly lowered. Radiographic OA scores were not influenced by treatment. Canine OA patients improved clinically after local application of celecoxib-loaded microspheres. These results provide a proof-of-concept for further translation of intra-articular administration of celecoxib-loaded microspheres from bench to bedside.

Introduction

Osteoarthritis (OA) occurs in most mammalian species. Over 20% of the canine population is affected by OA, in geriatric this is as high as 80% [1]. Pain and joint stiffness, the most common signs of OA, are the result of degeneration of articular cartilage, synovial inflammation, and changes in subchondral and peri-articular bone [2]. Pro-inflammatory mediators produced by articular chondrocytes (ACs) and cells in the synovial lining are known to influence OA progression and the severity of symptoms [3]. Considering the inflammatory component of OA, non-steroidal anti-inflammatory drugs (NSAIDs) provide suitable and effective therapy [4]. However, long-term systemic NSAIDs use can lead to adverse effects [5]. Intra-articular (IA) corticosteroid injections have a limited duration of action and occasional adverse effects [6]. Recently developed IA therapies include hyaluronic acid, autologous blood products and mesenchymal stromal cells, evidence on effectiveness is inconclusive to date [7].

A more straightforward and cost-effective method could be the local and extended delivery of well-known disease-modifying drugs. One of such drugs is celecoxib, a selective COX-2 inhibitor, originally developed as an oral NSAID for musculoskeletal diseases in man. Evidence is increasing that celecoxib has disease-modifying effects [8, 9]. Less osteophyte formation and bone marrow lesions occurred in a post-traumatic rat OA model after oral or IA treatment with celecoxib [10, 11]. In a post-traumatic rabbit OA model, IA celecoxib inhibited expression of pro-inflammatory mediators and improved cartilage repair, which did not occur after IA delivery of hyaluronic acid or saline [12].

To facilitate IA application and achieve sustained local drug levels, delivery platforms based on biomaterial carriers can be applied to release small molecule drugs over a prolonged period of time. Drug delivery platforms that release celecoxib have been studied *in vitro* [13, 14] and *in vivo* [15] for application in cartilaginous tissues. *In vitro* release of celecoxib in PBS from α-amino acid based polyesteramide microspheres (PEAMs), a biodegradable and non-toxic platform [16], was shown for over 80 days. In addition, IA injected celecoxib-PEAMs were present in femorotibial OA joints for over 12 weeks and lowered local prostaglandin E_2 (PGE_2) levels [17]. Furthermore, IA delivery in a preclinical rat OA model of PEAMs with 2-13x higher celecoxib loading doses, was not only able to attenuate synovial inflammation, but also inhibited the progression of subchondral bone changes [11].

These preclinical studies on the safety and disease-modifying effects of celecoxib at tissue level have been very promising. Therefore, the aim of this prospective, randomized controlled clinical trial was to assess the clinical efficacy of IA celecoxib-PEAMs in client-owned dogs suffering from OA. This was preceded by evaluation of release of celecoxib from PEAMs on primary canine ACs, showing release kinetics and bioactivity of the released celecoxib.

Materials and methods

Microsphere preparation and celecoxib release in vitro

PEAMs were synthesized as reported [18]. Suspensions of 70 PEAMs /mL for 20 wt% CXB-loaded (16 mg/mL) and unloaded PEAMs were prepared. Directly prior to IA injection, PEAMs were re-suspended in 1.5 mL sterile 2% lidocaine injection solution (B. Braun Medical), to avoid pain from the arthrocentesis procedure. To assess the release behaviour and bioactivity of (celecoxib-)PEAMs were cultured with and without ACs for 28 days (Figure 1A). Celecoxib, PGE_2, DNA measurements and gene expression analysis were used as read out parameters. Methods are described in Supplementary file 1.

Veterinary patient study design

This study was conducted with the approval of the Ethical Committee of the Department of Clinical Sciences of Companion Animals, Utrecht University (trial number AVR 17-06, approval date 18-12-2016). A power analysis was performed on historical data from our institution *a priori*, to calculate minimal required group size with an α of 0.05, power of 0.9 and an effect size of 1.18. Written consent was obtained from all dog owners before study enrolment. Dogs were randomly allocated (random sequences generated by Excel 2016, Microsoft) to the treatment (*n*=20) or placebo group (*n*=10). The owners and assessing veterinarians were blinded to the treatment. For the purpose of the arthrocentesis and IA injection dogs were sedated, and the affected joint(s) were clipped and prepared aseptically. Arthrocentesis was performed, and synovial fluid (SF) was collected for cytology and stored at -20 °C, if there was sufficient SF. This was followed by IA injection of the PEAMs. Dogs with a body weight of 15-30 kg received 0.5 mL, dogs weighing 30-45 kg received 1 mL and dogs weighing over 45 kg received 1.5 mL microsphere solution, corresponding with 8, 16 and 24 mg celecoxib per injection, respectively. Dogs were evaluated after 1 and 2 months. Follow-up consisted of clinical examination, force plate analysis and owner questionnaires, plain radiographs and SF analysis (Fig. 2).

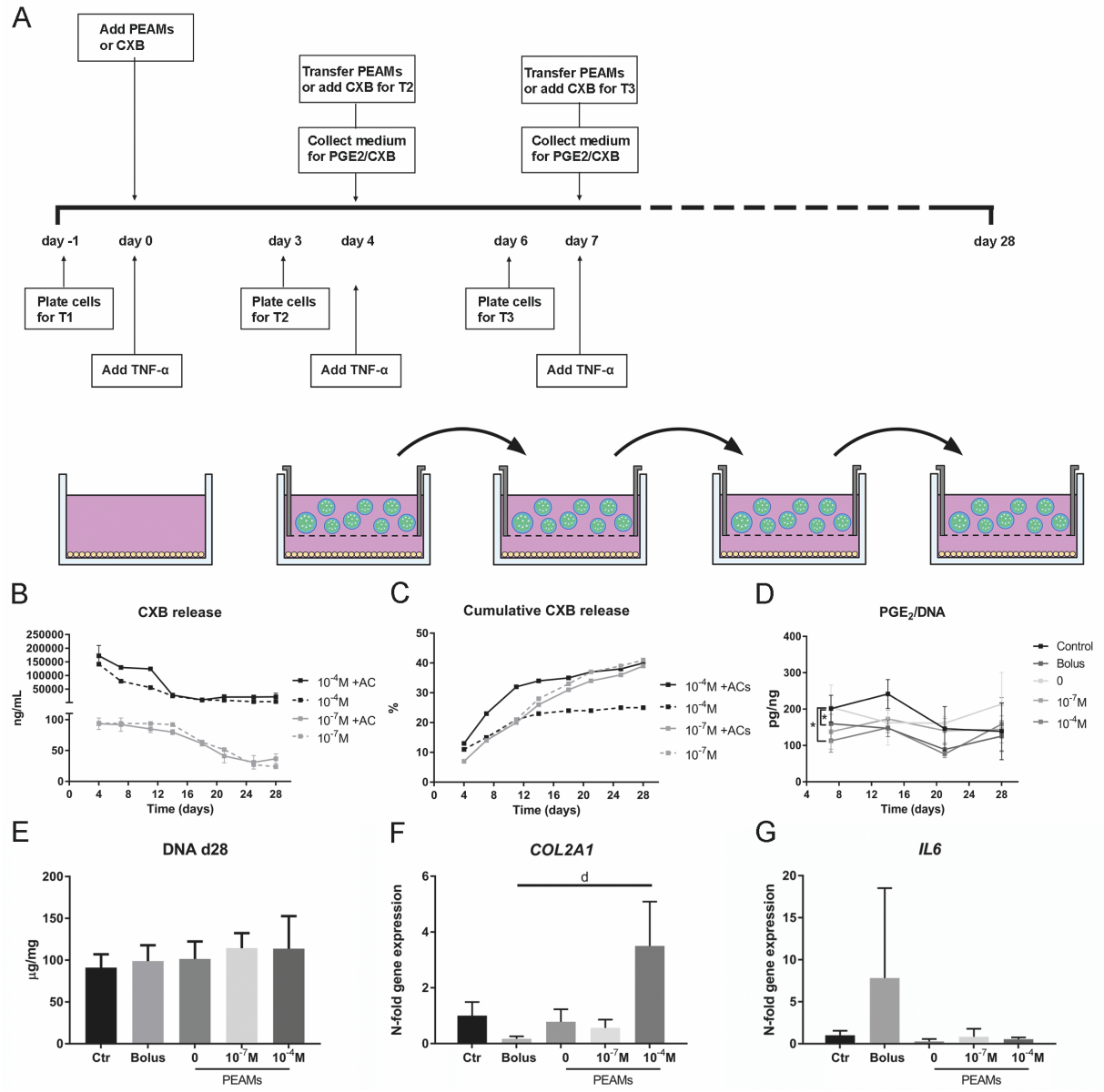

Figure 1. Setup and results of the *in vitro* release experiment. A. Schematic overview of the assay used for evaluating bioactivity of released celecoxib (CXB) on prostaglandin E_2 (PGE_2) production in primary articular chondrocytes (ACs) cultured with 10 ng/mL tumour necrosis factor alpha (TNF-α) during a 28 days culture period. Release profile (B) and cumulative (C) celecoxib release from two concentrations microspheres (10^{-4} M, 10^{-7} M) in chondrogenic medium with (+ACs) or without chondrocytes. The high concentration microspheres (10^{-4} M) and the bolus celecoxib condition (equivalent to 10^{-6}M) effectively suppressed PGE_2 levels throughout the culture period (D). Total DNA content was not affected by any of the treatments (E), although an increase in *COL2A1* gene expression was observed in the presence of 10^{-4}M celecoxib-PEAMs (F). Interleukin-6 (*IL6*) was highly variable in the presence of a pro-inflammatory stimulus and was not influenced by the CXB-conditions (G). *N*=6 per condition (mean ± 95% confidence interval). * Significant different from baseline ($p<0.05$). d, Very large effect size with $0.05<p<0.1$.

Read out parameters

All dogs underwent a full clinical and orthopaedic examination by a board-certified veterinary surgeon (BM) to document overall health and the presence of orthopaedic abnormalities. Lameness was recorded on a 4-point scale, with categories 0 (none), 1 (intermittent mild lameness after rest and exercise), 2 (mild lameness / intermittent moderate lameness after rest and exercise), 3 (moderate lameness / non-weight bearing after exercise) and 4 (non-weight bearing lameness at all times). All examinations were repeated during the 1- and 2- month follow-up visits.

Dogs were considered eligible for the study if they met the inclusion criteria (Table 1). Any pain medication was discontinued 4 days prior to baseline measurements and inclusion in the study. Owners were provided with a diary to document medications administered during the study ('additional pain relief medication') and note adverse reactions. Physical activity was limited to leash walks on the first two days after treatment. Thereafter, owners could gradually take up activity as before the start of the study, if the dog tolerated this.

Table 1. Inclusion- and exclusion criteria for participation in the clinical study.

Inclusion criteria	**Exclusion criteria**
A medical history, clinical signs, physical examination findings and radiographic findings consistent with OA	Orthopaedic or neurologic diseases other than OA, such as fractures or neoplasia of the affected limb
Dogs that are treated with long term medication for OA may be included when owner is willing to test alternative	Prior orthopaedic surgeries within 6 weeks of the affected limb or other limbs than the affected joint
Dogs that are unresponsive to conservative treatment methods for OA for at least 1 week	Prior orthopaedic surgery in the affected joint within 3-6 months
Grade 1-3 lameness due to OA	Prior orthopaedic surgery in the affected joint with techniques that include intra-articular non-resorbable materials (e.g. Tightrope)
Body weight more than 15 kg	NSAIDS, glucocorticoids or opioid therapy within 3 days prior to visit 2
The owner of the dog states availability and willingness to perform all follow-up examinations, and has signed the informed consent form	Active infection at the surgical site, for example chronic pyoderma, or septic arthritis

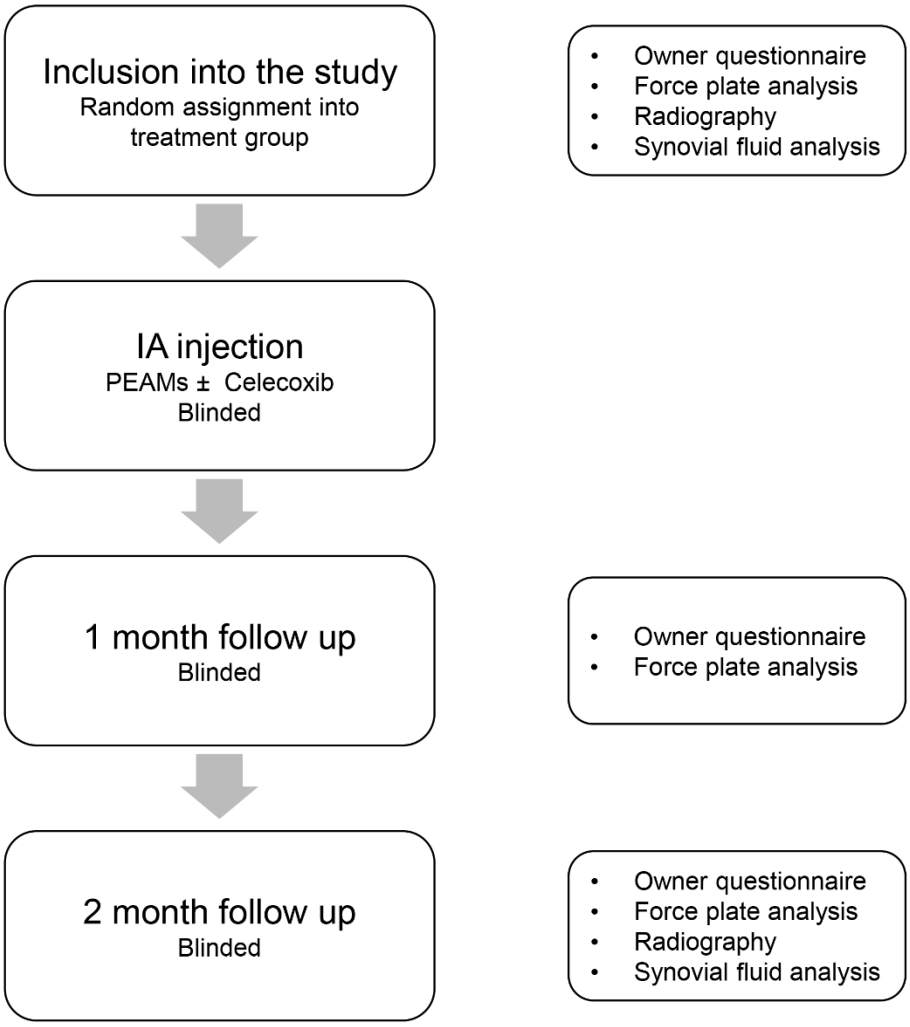

Figure 2. Flow chart of the prospective, randomized controlled study evaluating the clinical efficacy of intra-articular injection of celecoxib-loaded or unloaded polyesteramide microspheres (PEAMs). *N*=20 dogs in the treatment group, *n*=10 dogs in the placebo group.

Radiographs of affected joints were obtained within three months prior to inclusion in the study to confirm the presence of OA (Fig. 3A-F) and were repeated two months after IA injection to monitor for adverse effects and progression of OA. Mediolateral and craniocaudal or caudocranial radiographic projections of each joint were and scored (AT) following previously reported criteria [19]: 0 (normal), 1 (mild OA), 2 moderate OA, 3 (severe OA). To assess OA more quantitatively, the height of osteophytes was measured and graded as described previously [20]: 0 = no OA, 1 (osteophytes <2 mm), 2 (2-5 mm) or 3 (>5 mm). The highest value was entered in the analysis.

During each visit, ground reaction forces (GRFs) were measured (9261 Kistler Instrumente) as described previously [21]. GRFs in the mediolateral (Fx), craniocaudal (Fy) and vertical (Fz) direction were normalized for body weight. Asymmetry indices (ASI) were calculated according the following formula:

$$\frac{Left - Right}{0.5\ (Left + Right)} * 100$$

ASIs were determined for peak propulsive force (PPF), peak vertical force (PVF) and area under the force-time curve of Fz+, which is equal to the vertical impulse (VI) during the stance phase, [22, 23]. Stance time was recorded as well.

Questionnaires were dispatched to owners regarding behaviour and function of their dog, asking for the owner's perspective of treatment outcome (Table 2). These questionnaires were partially adapted from the Canine Brief Pain Inventory [24]. If owners perceived lameness that was of similar (or worse) severity compared to pre-treatment which lasted for at least 1-2 days, they were allowed to administer pain medication that the dog received prior to inclusion. The owner contacted the study coordinator (AT) for guidance by phone or email, and if necessary, could book an extra in-house check-up. The owners were asked to assess their dog at least twice a day and note down the severity of lameness and the administration of analgesic drugs in the log diary.

Macroscopic assessment of the SF was performed to evaluate volume, colour, viscosity and turbidity. Direct smears of SF were stained using Pappenheim staining evaluated on the following parameters: number and type of cells (degenerative vs inflammatory) and presence of cell clusters. Furthermore, several biomarkers were investigated, i.e. PGE_2, C-C motif chemokine ligand 2 (CCL2) and glycosaminoglycans (GAG). PGE_2 was measured using ELISA following the manufacturer's instructions (1:10 diluted in assay buffer), CCL2 concentration was determined by ELISA (DIY0934D-003, Kingfisher Biotech) (1:10 diluted in assay buffer). The SF GAG concentration was determined using a dimethyl methylene blue (DMMB) assay after incubation with 1:1 0.1 mg/mL hyaluronidase (H2126, Sigma-Aldrich) at 37°C for 30 minutes, diluted 50x in PBS-EDTA [25]. The total cell count of the SF was determined using a TC20 Automatic Cell Counter (1450102, Bio-Rad) with trypan blue dye. To aid in the interpretation of SF biomarker levels, SF of healthy joints collected post-mortem from six experimental dogs in unrelated experiments (approved by the Dutch Central Committee for Animal experimentation, experimental number: #AVD108002015282, approval date 25/11/2015) and six client-owned dogs with OA presented for orthopedic surgery was performed were analysed concurrently with the samples of the present study.

Figure 3. Radiographs obtained prior to or two months after intra-articular injection with celecoxib-loaded or unloaded polyesteramide microspheres. Arrows indicate locations for osteophyte measurements. A, B. Mediolateral (A) and craniocaudal (B) radiographic projections obtained of the elbow joint of dog 19 prior to inclusion in the study. Osteophytes were measured at the cranial aspect of the radial head, the caudal surface of the lateral condylar ridge, the medial contour of the humeral condyle and the medial contour of the medial coronoid process. C and D show mediolateral and caudocranial radiographs of the femorotibial joint of dog 1 prior to inclusion in the study. Osteophytes were measured at the proximal trochlear edge, the distal patella and the lateral and medial tibial plateau. E, F. Ventrodorsal radiographs of the pelvis of dog 28 prior to (E) and 2 months after treatment with unloaded microspheres (F), respectively. Osteophytes on the cranial and caudal edge of the acetabulum and at the femoral neck were recorded.

Statistical analysis

The statistical software IBM SPSS Statistics 24 was used. Normality of the data was checked by assessing the Q-Q plots, histograms and Shapiro-Wilks tests. First, differences regarding dog characteristics between treatment groups were assessed. For the parameters 'age', and 'weight', a one-way ANOVA test was applied. To test differences in sex and joint distribution between groups, a Mann-Whitney *U* test was performed. To compare the questionnaire, force plate analysis data, visual lameness score and celecoxib release *in vitro*, repeated-measures ANOVAs were performed to test for differences within group (CXB-PEAMs and unloaded PEAMs), between time points, and between groups within time points. To compare the proportions of dogs that received additional pain relief medication between treatment- and placebo group, a Fisher's exact test was performed. *P* values <0.05 were considered statistically significant. Effect sizes (ES) were retrieved as *Hedge's g* for parametric data*:* medium, 0.5-0.8; large, 0.8-1.2; 1.2-2, very large and >2 huge [26]. Differences were considered as relevant when *P*<0.05 and/ or ES was medium or larger with a *P*-value of <0.1.

Results

Celecoxib release in vitro

After 28 days ±40% of celecoxib was released, independent of the microsphere concentration in the medium (Fig. 1B,C). The presence of cells in a pro-inflammatory environment accelerated celecoxib release in the culture condition with the 10^{-4}M PEAMs (*P*<0.001). The bolus celecoxib and the 10^{-4}M celecoxib-PEAMs suppressed PGE_2 production (Fig. 1D) during the 28-day culture period (*p*=0.002, *P*<0.001, respectively). There was no significant change in DNA content, indicating no effect of (un)loaded PEAMs on cell death or proliferation (Fig 1E). This effect was corroborated by steady *BAX/BCL2* ratios on RT-qPCR (Supplementary file 1), indicating no increase in apoptosis. No significant differences in gene expression levels of matrix components *ACAN, COL1A1, TIMP1*, *ADAMTS5* (Supplementary file 1), or inflammatory mediators interleukin-6 (*IL6*, Fig. 1G) and *NGF* (Supplementary file 1) were found, although a slight increase *COL2A1* by 10^{-4}M PEAMs was seen (Fig 1F).

Veterinary patient study

Thirty dogs met the inclusion criteria and were enrolled in the study (Supplementary file 2). Fourteen elbow joints, 11 femorotibial joints and 6 coxofemoral joints were included (dog 6 received IA injections in 2 joints simultaneously). The median age was 6 years (range 9 months – 13 years), the mean body weight was 33 kg (range 16-68 kg), without significant changes in body weight during the follow-up period. There were 16 females (14/16 spayed) and 14 males (9/14 castrated). There were no differences regarding age (*p*=0.52), body weight (*p*=0.88), sex (*p*=0.94) and joint distribution (*p*=0.27) between treatment- and placebo groups. The mean visual lameness score was 2 in both the treatment- and placebo group prior to the start of the study (range 1-3 for both groups; *p*=0.75). There were no

major adverse effects noted during the study period. Peri-articular swelling of the joint 1-3 days after IA injection with unloaded PEAMs occurred in dog 2 and dog 26, but this resolved after a few days without additional treatment.

Only in the dogs that were injected with the celecoxib-PEAMs, there was an improvement from baseline in overall questionnaire score at 1 (P<0.0001) and 2 months (P=0.001) after treatment (Fig 4A). Compared to the dogs in the placebo group, treatment with celecoxib-PEAMs led to a significantly higher questionnaire score at both 1 (P=0.009) and 2 months (P=0.007) after injection indicative of clinical improvement (Table 2). Additional pain relief medication was provided by 9/10 owners of dogs that were allocated to the treatment with unloaded PEAMs, vs 3/20 owners of dogs that received celecoxib-PEAMs (P<0.001 and P=0.001 at 1 and 2 months follow-up).

The visual lameness score was significantly lower in the animals treated with celecoxib-PEAMs, compared to baseline at 1 (p<0.001) and 2 months (p<0.001) after IA injection (Fig 4B). There was a significant improvement of kinetic gait parameters at 1 and 2 months after IA injection with celecoxib-PEAMs (Table 3): PPF and VI improved substantially at 1-month post injection (p=0.03 and p=0.024, respectively) together with the PVF at 2 months (p=0.007; p=0.059, medium ES and p=0.07, medium ES, respectively for PPF, PVF and VI). No significant differences were found between time-points in the placebo group. There were no significant differences between treatment groups and time-points for the stance time.

Radiographs were scored for OA severity and osteophyte size prior to and 2 months after treatment (Fig. 3A-F; supplementary file 3) in a fashion blinded to the treatment. Osteoarthritis severity and osteophyte size did not change during the follow-up period (p>0.15).

Table 2. Responses to owners' questionnaires of dogs with osteoarthritis before and at 1 and 2 months after intra-articular injection with celecoxib-loaded (Celecoxib) or unloaded ("Placebo") polyesteramide microspheres.

Questions	**Before treatment**		**After 1 month**		**After 2 months**	
	Celecoxib	**Placebo**	**Celecoxib**	**Placebo**	**Celecoxib**	**Placebo**
Does your dog show lameness, and in which severity?	4 (2-9)	5 (2-8)	**6 (2-10) *** ***P*<0.001**	5 (2-9) *p*=0.85	**9 (3-10) *** ***p*<0.001**	4 (2-9) *p*=0.92
Does your dog have pain as a result of its osteoarthritis?	4 (2-7)	4.5 (2-7)	**7 (1-10) *** ***p*=0.001**	5 (3-10) *p*=0.34	**8 (3-10) *** ***p*<0.001**	4 (1-9) *p*=0.86
Does your dog show any weakness in its affected leg?	8 (2-10)	7 (1-10)	9 (4-10) *p*=0.246	7.5 (4-10) *p*=0.59	8 (4-10) *p*=0.405	5 (2-10) *p*=0.90
Does your dog have difficulty rising up?	4 (1-9)	4.5 (2-9)	**7.5 (3-10) *** ***p*<0.001**	5.5 (3-10) *p*=0.64	**8 (3-10) *** ***p*=0.001**	5 (2-9) *p*=0.83
Does your dog have difficulty lying down?	5 (3-10)	7 (1-10)	**8.5 (3-10) *** ***p*=0.007**	8.5 (4-10) *p*=0.373	**8 (4-10) *** ***p*=0.028**	9 (2-10) *p*=0.66
Does the pain interfere with normal activities in and around the house?	4.5 (2-10)	6 (1-9)	**7.5 (2-10) *** ***p*=0.014**	5 (3-10) *p*=0.68	**7 (3-10)** [a] ***p*=0.09**	4 (2-9) *p*=0.83
Does the pain interfere with the quality of life of your dog?	5 (2-10)	4 (1-9)	**8.5 (2-10) *** ***p*<0.001**	4.5 (3-9) *p*=0.63	**8 (3-10) *** ***p*=0.001**	4 (2-9) *p*=0.78
Does the pain interfere with the ability to walk?	4 (1-10)	4.5 (2-9)	**7.5 (2-10) *** ***p*=0.012**	4 (2-9) *p*=0.46	**8 (2-10) *** ***p*=0.014**	4 (1-9) *p*=0.63
Does the pain interfere with the ability to run?	3.5 (1-10)	6.5 (1-9)	**8 (3-10) *** ***p*=0.001**	3 (1-8) *p*=0.32	**8 (2-10) *** ***p*=0.014**	4 (1-9) *p*=0.47
Does the pain interfere with the ability to climb stairs?	4 (1-10)	4.5 (1-10)	**7.5 (3-10) *** **p=0.016**	4.5 (2-9) *p*=0.94	**8 (3-10) *** **p=0.014**	4 (1-9) *p*=0.36

Data represented as median (range). *N*=20 animals in the celecoxib-treated group and *n*=10 for the placebo group at all time points. *Indicates significantly different from baseline ($p<0.05$). [a], Medium effect size with $0.05<p<0.1$.

Table 3. Results of force plate measurements of dogs with osteoarthritis before and at 1 and 2 months after intra-articular injection with celecoxib-loaded (Celecoxib) or unloaded (Placebo) polyesteramide microspheres.

Parameter	Before treatment		After 1 month		After 2 months	
	Celecoxib	Placebo	Celecoxib	Placebo	Celecoxib	Placebo
PVF ASI	19 (18)	19 (27)	13 (15)	18 (20)	**9 (9) ***	23 (27)
			p=0.137	*p*=0.874	***p*=0.025**	*p*=0.450
PVF (Improvement from baseline)	N/A	N/A	26%	-7%	**128%**	-29%
			p=0.634	*p*=0.901	***p*=0.059** [a]	*p*=0.664
PPF ASI	37 (25)	44 (37)	**18 (10) ***	41 (32)	**10 (11) ***	37 (31)
			***p*=0.003**	*p*=0.659	***p*=0.001**	*p*=0.120
PPF (Improvement from baseline)	N/A	N/A	**73% ***	-142%	**103% ***	-28%
			***p*<0.001**	*p*=0.587	***p*=0.007**	*p*=0.261
VI ASI	17 (21)	28 (29)	14 (25)	26 (29)	**9 (10) ***	22 (28)
			p=0.20	*p*=0.31	***p*=0.018**	*p*=0.86
VI (Improvement from baseline)	N/A	N/A	**143% ***	39%	**60%**	33%
			***p*=0.024**	*p*=0.07	***p*=0.07** [a]	*p*=0.61
Stance time ASI	6.7 (6.1)	7.5 (5.2)	4.7 (3.9)	7.8 (5.8)	4.4 (4.2)	8.9 (5.8)
			p=0.26	*p*=0.72	*p*=0.21	*p*=0.48
Stance time (Improvement from baseline)	N/A	N/A	2%	-2%	-29%	-37%
			p=0.30	*p*=0.89	*p*=0.15	*p*=0.31

PVF, peak vertical force; ASI, asymmetry index; PPF, peak propulsive force; VI, vertical impulse. Data represented as mean (SD). *N*=20 animals in the celecoxib-treated group and *n*=10 for the placebo group at all time points. * Indicates significant difference from baseline ($p<0.05$). [a], Medium effect size with $0.05<p<0.1$.

Prior to IA injection, sufficient SF could be obtained and was subsequently analysed from 21/30 joints (14 CXB; 7 placebo), and 20/30 (13 CXB; 7 placebo) joints at the 2 months check-up visit. Prior to treatment, all SF samples contained an excessive number of cells, of a degenerative phenotype (mainly synoviocytes and macrophages). Two months after IA injection, cytology confirmed degenerative arthritis in all dogs. In two dogs that had received CXB-PEAMs and one dog that was administered unloaded microspheres an increase in polymorphonuclear cells was observed. PGE_2 levels were significantly lower in the celecoxib-treated group two months after treatment, compared to baseline (Fig. 4C, $p=0.003$). Total GAG (Fig. 4E) and CCL2 (Fig 4F) concentrations were not significantly different between time-points or treatment groups.

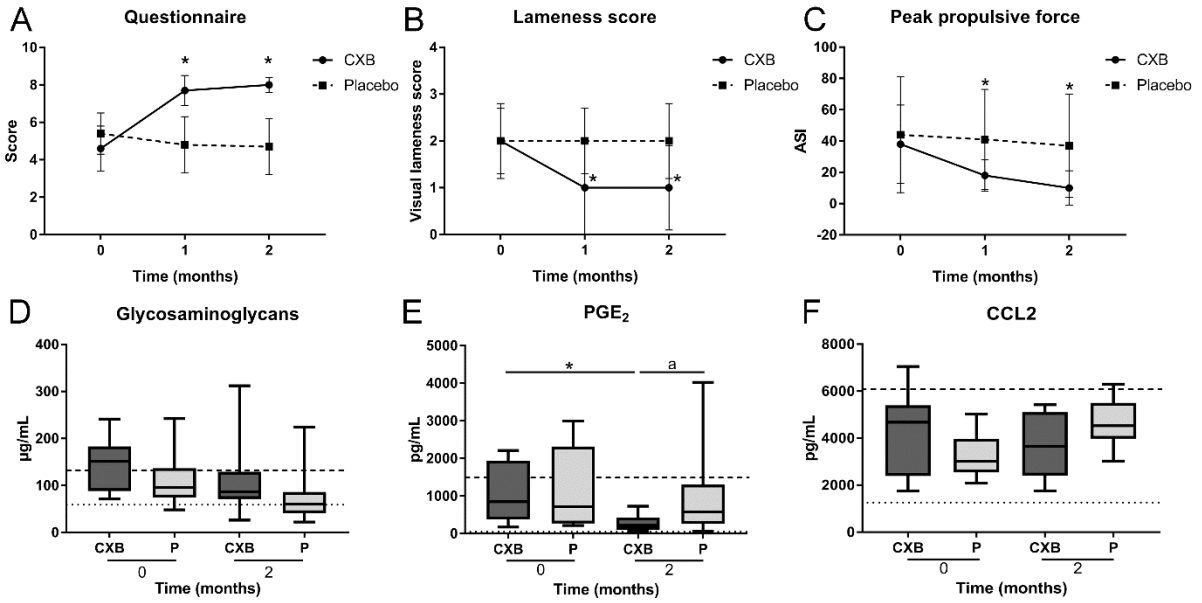

Figure 4. Combined results of the veterinary patient study. A. The overall owner questionnaire score was significantly higher in the dogs that received celecoxib-loaded polyesteramide microspheres (CXB-PEAMs) than in the dogs that received unloaded microspheres (P; placebo), at the 1- and 2-month follow-up visits. B. Visual lameness scores only improved in dogs that received CXB-loaded microspheres. C. The peak propulsive force (PPF) asymmetry only improved in dogs treated with CXB-PEAMs during the follow-up period. Glycosaminoglycan content of the synovial fluid (SF) was not affected by treatment (D), while prostaglandin E_2 (PGE_2) was significantly lower in SF of the celecoxib-treated group 2 months post injection compared to pre-treatment values (E). The synovial fluid C-C motif chemokine ligand 2 (CCL2) concentration was not affected by intra-articular injection of (celecoxib-loaded) microspheres (F). Dotted lines indicate SF control samples of 6 healthy joints, dashed lines indicate average SF biomarker values for osteoarthritic joints of 6 donors (D-F). * Significant different from baseline (p<0.05).

Discussion

Drug delivery platforms that gradually release anti-inflammatory drugs after intra-articular administration are a promising approach towards long-term relief of OA-associated pain. For the purpose of translation from bench-to-bedside of a drug delivery platform employing the selective COX-2 inhibitor celecoxib, a prospective randomized controlled trial was conducted in client-owned dogs with OA. The present study showed prolonged COX-2 inhibition resulting in significant reduction of PGE_2 levels both *in vitro* in canine ACs and *in vivo* in SF of osteoarthritic joints of client-owned dogs without affecting the other two SF biomarkers, i.e. CCL2 and GAGs. In this respect, an increase in the COX-2 mediated PGE_2 has been consistently found in SF of OA joints [27], and PGE_2 seems to clearly correlate with pain and OA progression in humans [28, 29] and dogs [30, 31]. Therefore, long-term inhibition of PGE_2 might be a solution for effective relief of OA-related pain and disease modification. Accordingly, the group treated with celecoxib-PEAMs showed significant clinical improvement on both

subjective and objective read out parameters, also reflected in significantly less additional pain relief medication administered by the owner.

Previous research showed a substantial caregiver placebo effect in the evaluation of veterinary patient response to treatment for OA by both the owner and the assessing veterinarian [32]. Therefore, to assess clinical effectivity, a placebo group was included in the study design to show superiority of the celecoxib-PEAMs over treatment with unloaded PEAMs where both the assessing veterinarian and the owner were blinded to the treatment. Significant improvement in questionnaire scores and lameness were only seen in the treatment group, indicating no substantial caregiver placebo effect. These results were underscored by objective gait analysis; only in the dogs treated with celecoxib-PEAMs a decrease in PVF, VI and PPF asymmetry were noted during the 2-month follow-up period. Stance time has been associated with changes in PVF and VI but was not significantly influenced by treatment in this study [33]. Earlier research already confirmed that the use of multiple parameters increases the reliability of force plate analysis [34, 35], but gait analysis still only registers a fraction of the total mobility pattern of an individual. Altogether, the majority of the gait parameters improved upon IA delivery of celecoxib-PEAMs further supporting the more subjective improvement in clinical signs as perceived by the owner and the assessing veterinarian.

Osteophytes visualized on radiography were not affected by IA delivery of celecoxib-PEAMs within two months follow-up. In preclinical studies employing early OA animal models and micro-CT imaging, an inhibitory effect of celecoxib on osteophyte formation was demonstrated, suggesting it as a disease-modifying OA [10, 11]. It is plausible that the absence of a disease-modifying effect at osteophyte level is due to the fact that in a clinical OA population osteophytes are already present, and radiography could be unable to detect subtle changes. More advanced imaging modalities such as CT or MRI might be capable of more detailed analysis of cartilage and subchondral bone [36]. Considering the promising data in the current study, studies with longer follow-up time and predefined rescue analgesia protocols are warranted to demonstrate that prolonged local exposure of celecoxib to the joint may result in less progression in osteophyte formation in veterinary patients with early or established OA.

This prospective, randomized controlled clinical trial confirmed improved limb function and quality of life after intra-articular administration of celecoxib-loaded biodegradable microspheres during the 2-month follow-up period without of substantial adverse effects.

Acknowledgements

We wish to thank Mandy van de Vooren, Willem de Jong and Arie Doornenbal for their technical assistance.

References

Appleton, C.T., Pitelka, V., Henry, J., Beier, F., 2007. Global analyses of gene expression in early experimental osteoarthritis. Arthritis and Rheumatism 56, 1854-1868.

Bockstahler, B.A., Vobornik, A., Muller, M., Peham, C., 2009. Compensatory load redistribution in naturally occurring osteoarthritis of the elbow joint and induced weight-bearing lameness of the forelimbs compared with clinically sound dogs. The Veterinary Journal 180, 202-212.

Brenner, S.S., Klotz, U., Alscher, D.M., Mais, A., Lauer, G., Schweer, H., Seyberth, H.W., Fritz, P., Bierbach, U., 2004. Osteoarthritis of the knee--clinical assessments and inflammatory markers. Osteoarthritis and cartilage 12, 469-475.

Brown, D.C., Boston, R.C., Coyne, J.C., Farrar, J.T., 2008. Ability of the canine brief pain inventory to detect response to treatment in dogs with osteoarthritis. Journal of the American Veterinary Medical Association 233, 1278-1283.

Cokelaere, S.M., Plomp, S.G.M., de Boef, E., de Leeuw, M., Bool, S., van de Lest, C.H.A., van Weeren, P.R., Korthagen, N.M., 2018. Sustained intra-articular release of celecoxib in an equine repeated LPS synovitis model. European journal of pharmaceutics and biopharmaceutics : official journal of Arbeitsgemeinschaft fur Pharmazeutische Verfahrenstechnik e.V 128, 327-336.

Conzemius, M.G., Evans, R.B., 2012. Caregiver placebo effect for dogs with lameness from osteoarthritis. Journal of the American Veterinary Medical Association 241, 1314-1319.

de Boer, T.N., Huisman, A.M., Polak, A.A., Niehoff, A.G., van Rinsum, A.C., Saris, D., Bijlsma, J.W., Lafeber, F.J., Mastbergen, S.C., 2009. The chondroprotective effect of selective COX-2 inhibition in osteoarthritis: ex vivo evaluation of human cartilage tissue after in vivo treatment. Osteoarthritis and cartilage 17, 482-488.

Farndale, R.W., Sayers, C.A., Barrett, A.J., 1982. A direct spectrophotometric microassay for sulfated glycosaminoglycans in cartilage cultures. Connective tissue research 9, 247-248.

Glyn-Jones, S., Palmer, A.J., Agricola, R., Price, A.J., Vincent, T.L., Weinans, H., Carr, A.J., 2015. Osteoarthritis. Lancet 386, 376-387.

Hazewinkel, H.A., van den Brom, W.E., Theyse, L.F., Pollmeier, M., Hanson, P.D., 2008. Comparison of the effects of firocoxib, carprofen and vedaprofen in a sodium urate crystal induced synovitis model of arthritis in dogs. Research in veterinary science 84, 74-79.

Heikkila, H.M., Hielm-Bjorkman, A.K., Innes, J.F., Laitinen-Vapaavuori, O.M., 2017. The effect of intra-articular botulinum toxin A on substance P, prostaglandin E2, and tumor necrosis factor alpha in the canine osteoarthritic joint. BMC veterinary research 13, 74-017-0990-y.

Hogberg, E., Stalman, A., Wredmark, T., Tsai, J.A., Arner, P., Fellander-Tsai, L., 2006. Opioid requirement after arthroscopy is associated with decreasing glucose levels and increasing PGE2 levels in the synovial membrane. Acta orthopaedica 77, 657-661.

Hugle, T., Geurts, J., 2017. What drives osteoarthritis?-synovial versus subchondral bone pathology. Rheumatology (Oxford, England) 56, 1461-1471.

Janssen, M., Timur, U.T., Woike, N., Welting, T.J., Draaisma, G., Gijbels, M., van Rhijn, L.W., Mihov, G., Thies, J., Emans, P.J., 2016. Celecoxib-loaded PEA microspheres as an auto regulatory drug-delivery system after intra-articular injection. Journal of Controlled Release 244, 30-40.

Jiang, D., Zou, J., Huang, L., Shi, Q., Zhu, X., Wang, G., Yang, H., 2010. Efficacy of intra-articular injection of celecoxib in a rabbit model of osteoarthritis. International journal of molecular sciences 11, 4106-4113.

Johnston, S.A., 1997. Osteoarthritis. Joint anatomy, physiology, and pathobiology. The Veterinary clinics of North America.Small animal practice 27, 699-723.

Joles, J.A., Rijnberk, A., van den Brom, W.E., Dogterom, J., 1980. Studies on the mechanism of polyuria induced by cortisol excess in the dog. Tijdschrift voor diergeneeskunde 105, 199-205.

Kropp, M., Morawa, K., Mihov, G., Salz, A.K., Harmening, N., Franken, A., Kemp, A., Dias, A.A., Thies, J.C., Johnen, S. et al., 2014. Biocompatibility of Poly(ester amide) (PEA) microfibrils in ocular tissues. Polymers 6, 243-260.

Lavrijsen, I.C., Heuven, H.C., Voorhout, G., Meij, B.P., Theyse, L.F., Leegwater, P.A., Hazewinkel, H.A., 2012. Phenotypic and genetic evaluation of elbow dysplasia in Dutch Labrador Retrievers, Golden Retrievers, and Bernese Mountain dogs. The Veterinary Journal 193, 486-492.

Lineberger, J.A., Allen, D.A., Wilson, E.R., Tobias, T.A., Shaiken, L.G., Shiroma, J.T., Biller, D.S., Lehenbauer, T.W., 2005. Comparison of radiographic arthritic changes associated with two variations of tibial plateau leveling osteotomy. Veterinary and Comparative Orthopaedics and Traumatology 18, 13-17.

Meijer, E., Oosterlinck, M., van Nes, A., Back, W., van der Staay, F.J., 2014. Pressure mat analysis of naturally occurring lameness in young pigs after weaning. BMC veterinary research 10, 193-014-0193-8.

Nakata, K., Hanai, T., Take, Y., Osada, T., Tsuchiya, T., Shima, D., Fujimoto, Y., 2018. Disease-modifying effects of COX-2 selective inhibitors and non-selective NSAIDs in osteoarthritis: a systematic review. Osteoarthritis and cartilage 10.1016/j.joca.2018.05.021.

Oosterlinck, M., Bosmans, T., Gasthuys, F., Polis, I., Van Ryssen, B., Dewulf, J., Pille, F., 2011. Accuracy of pressure plate kinetic asymmetry indices and their correlation with visual gait assessment scores in lame and nonlame dogs. American Journal of Veterinary Research 72, 820-825.

Panahifar, A., Jaremko, J.L., Tessier, A.G., Lambert, R.G., Maksymowych, W.P., Fallone, B.G., Doschak, M.R., 2014. Development and reliability of a multi-modality scoring system for evaluation of disease progression in pre-clinical models of osteoarthritis: celecoxib may possess disease-modifying properties. Osteoarthritis and Cartilage 22, 1639-1650.

Roush, J.K., McLaughlin, R.M.,Jr, 1994. Effects of subject stance time and velocity on ground reaction forces in clinically normal greyhounds at the walk. American Journal of Veterinary Research 55, 1672-1676.

Rychel, J.K., 2010. Diagnosis and treatment of osteoarthritis. Topics in companion animal medicine 25, 20-25.

Sanderson, R.O., Beata, C., Flipo, R.M., Genevois, J.P., Macias, C., Tacke, S., Vezzoni, A., Innes, J.F., 2009. Systematic review of the management of canine osteoarthritis. The Veterinary record 164, 418-424.

Sawilowsky, S.S., 2009. New effect size rules of thumb. Journal of modern applied statistical methods 8, 597-599.

Sellam, J., Berenbaum, F., 2010. The role of synovitis in pathophysiology and clinical symptoms of osteoarthritis. Nature reviews.Rheumatology 6, 625-635.

Tellegen, A.R., Jansen, I., Thomas, R., de Visser, H., Kik, M., Grinwis, G., Woike, N., Mihov, G., Emans, P., Meij, B. et al., 2018. Controlled release of celecoxib inhibits inflammation, bone cysts and osteophyte formation in a preclinical model of osteoarthritis. Drug Delivery 25, 1438-47.

Theyse, L.F.H., Hazewinkel, H.A., Van den Brom, W.E., 2000. Force plate analyses before and after surgical treatment of unilateral fragmented coronoid process. Veterinary and Comparative Orthopaedics and Traumatology 13, 135-40.

Trumble, T.N., Billinghurst, R.C., McIlwraith, C.W., 2004. Correlation of prostaglandin E2 concentrations in synovial fluid with ground reaction forces and clinical variables for pain or inflammation in dogs with osteoarthritis induced by transection of the cranial cruciate ligament. American Journal of Veterinary Research 65, 1269-1275.

Willems, N., Mihov, G., Grinwis, G.C., van Dijk, M., Schumann, D., Bos, C., Strijkers, G.J., Dhert, W.J., Meij, B.P., Creemers, L.B. et al., 2015. Safety of intradiscal injection and biocompatibility of polyester amide microspheres in a canine model predisposed to intervertebral disc degeneration. Journal of biomedical materials research.Part B, Applied biomaterials 105, 707-714.

Yang, H.Y., van Dijk, M., Licht, R., Beekhuizen, M., van Rijen, M., Janstal, M.K., Oner, F.C., Dhert, W.J., Schumann, D., Creemers, L.B., 2015. Applicability of a newly developed bioassay for determining bioactivity of anti-inflammatory compounds in release studies--celecoxib and triamcinolone acetonide released from novel PLGA-based microspheres. Pharmaceutical research 32, 680-690.

Yu, S.P., Hunter, D.J., 2016. Intra-articular therapies for osteoarthritis. Expert opinion on pharmacotherapy 17, 2057-2071.

Zweers, M.C., de Boer, T.N., van Roon, J., Bijlsma, J.W., Lafeber, F.P., Mastbergen, S.C., 2011. Celecoxib: considerations regarding its potential disease-modifying properties in osteoarthritis. Arthritis research & therapy 13, 239-250.

Supplementary file 1. Materials and methods and supplementary qPCR results of the *in vitro* experiment.

Healthy articular cartilage was collected post-mortem under aseptic conditions from six experimental dogs in unrelated experiments (approved by the Dutch Central Committee for Animal experimentation, experimental number: #AVD108002015282, approval date 25/11/2015). Cartilage was digested by 0.15% w/v pronase (45 min, 37°C) and 0.15% w/v collagenase (overnight, 37°C). The cells were expanded at 37°C, 21% O_2 and 5% O_2, culture medium (hgDMEM+Glutamax, Gibco Life Technologies) was refreshed every 3-4 days. At passage 2, cells were cryopreserved in aliquots of 1 million cells per vial in hgDMEM containing 10% v/v DMSO and 10% v/v Fetal Bovine Serum (16000-044, Gibco Life Technologies). One day prior to the start of the experiment, cells were seeded on a 24-wells plate at a density of 60,000 cells per well with chondrogenic medium (hgDMEM) containing 1% v/v P/S (GE healthcare Life Sciences), 1% v/v ITS+ premix (Corning Life Sciences), 0.04 mg/mL bovine serum albumin (Sigma-Aldrich), 0.1 mM ascorbic acid (A8960, Sigma-Aldrich). On day 0, the medium was renewed and both the unloaded or CXB-loaded PEAMs were dispersed in culture medium and placed in Transwell® baskets (pore size 0.4 µm, polycarbonate membrane, Costar Corning). Two concentrations, of CXB-loaded microspheres were utilized: 10^{-7}M and 10^{-4}M, in order to achieve partial and complete inhibition of COX-2 activity within the culture system and thereby determine dose-dependent bioactivity. Cells and microspheres were co-incubated at 37°C, 21% O_2, 5% CO_2. After four hours, tumor necrosis factor alpha (TNF-α; 210-TA, R&D Systems) was added at a final concentration of 10 ng/mL to the culture medium as a pro-inflammatory stimulus. Cells treated with celecoxib (equivalent to 1 µM) were included as comparisons at each medium change. Cells and PEAMs were co-incubated for 72 hours before the PEAMs were transferred to a new 24-well culture plate containing cells seeded according to the procedure described above (*n*=6 donors, in duplicates). This procedure was repeated 8 times amounting to a release period of 28 days (Fig. 1A) where bioactivity of the released celecoxib was determined. Every 72 hours, medium was collected and stored at -20 °C. Celecoxib medium levels were measured using ELISA (180719, Neogen Corporation) following manufacturer's instructions. PGE_2 and CCL2 levels in the medium, as a measure of the inflammatory response, were measured using a commercial ELISA kit (514010, Cayman Chemical; DIY0934D-003, Kingfisher Biotech, respectively). DNA content was measured using the Qubit® dsDNA High Sensitivity Assay Kit (Q32851; Invitrogen). RNA was isolated using the RNeasy® microkit (74004, Qiagen, Valencia, USA) according to the manufacturer's instructions, including a DNAse (RNAse-Free DNase Set, 79254, Qiagen, Valencia, USA) step. cDNA was synthesized using the iScript™ cDNA Synthesis Kit (170-8891, Bio-Rad) according to the manufacturer's instructions. Primer sequences were designed using PerlPrimer. RT-qPCR was performed using the iQT™ SYBR Green Supermix Kit and the CFX384 Touch™ Real-Time PCR Detection System (both from Bio-Rad). For determination of relative gene expression, the Normfirst (EΔΔCq) method was used. For each target gene, the mean n-fold

changes and standard deviations in gene expression were calculated. Four reference genes shown to be stable were chosen to normalize gene expression of target genes.

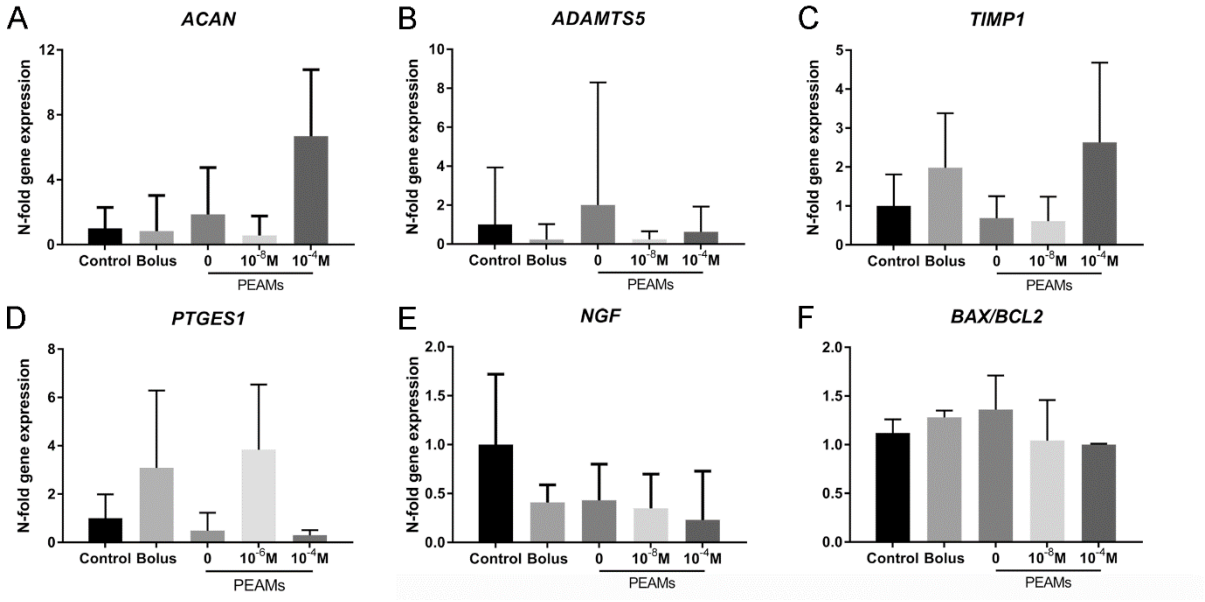

Figure 1. Relative gene expression (mean ± 95% confidence interval) of aggrecan (*ACAN*, **A**), a disintegrin-like and metallopeptidase (*ADAMTS5*, **B**), tissue inhibitor of metalloproteinase 1 (*TIMP1*, **C**), prostaglandin E synthase-1 (*PTGES1*, **D**), neuronal growth factor (*NGF*, **E**) and the ratio of pro-apoptotic Bax and anti-apoptotic gene BCL2 (*BAX/BCL2*,**F**). PEAMs, polyesteramide microspheres.

Table 1. Gene-specific primer sequences with associated amplification temperatures.

Gene	Primer sequence (5'-'3)	Amplicon size (bp)	Temp (°C)
Reference genes			
GAPDH	Fw TGTCCCCACCCCCAATGTATC	100	58
	Rv CTCCGATGCCTGCTTCACTACCTT		
HPRT	Fw AGCTTGCTGGTGAAAAGGAC	104	56-58
	Rv TTATAGTCAAGGGCATATCC		
RPS19	Fw CCTTCCTCAAAAAGTCTGGG	95	61-63
	Rv GTTCTCATCGTAGGGAGCAAG		
SDHA	Fw GCCTTGGATCTCTTGATGGA	92	61
	Rv TTCTTGGCTCTTATGCGATG		
Target genes			
Extracellular matrix			
ACAN	Fw GGACACTCCTTGCAATTTGAG	110	61-62
	Rv GTCATTCCACTCTCCCTTCTC		
ADAMTS5	Fw CTACTGCACAGGGAAGAG	148	61
	Rv GAACCCATTCCACAAATGTC		
COL1A1	Fw GTGTGTACAGAACGGCCTCA	109	61
	Rv TCGCAAATCACGTCATCG		
COL2A1	Fw GCAGCAAGAGCAAGGAC	150	60.5-65
	Rv TTCTGAGAGCCCTCGGT		
MMP13	Fw CTGAGGAAGACTTCCAGCTT	250	65
	Rv -TTGGACCACTTGAGAGTTCG		
TIMP1	Fw GGCGTTATGAGATCAAGATGAC	120	66
	Rv ACCTGTGCAAGTATCCGC		
Inflammatory markers			
IL1β	Fw: TGCTGCCAAGACCTGAACCAC	115	68
	Rv: TCCAAAGCTACAATGACTGACACG		
IL6	Fw: GAGCCCACCAGGAACGAAAGAGA	123	65
	Rv: CCGGGGTAGGGAAAGCAGTAGC		
IL10	Fw: CCCGGGCTGAGAACCACGAC	91	63
	Rv: AAATGCGCTCTTCACCTGCTCCAC		
PTGES1	Fw CCAGTATTGCCGGAGTGACCAG	97	68
	Rv AAACGAAGCCCAGGAACAGGA		
Markers for apoptosis			
BAX	Fw CCTTTTGCTTCAGGGTTTCA	108	58-59
	Rv CTCAGCTTCTTGGTGGATGC		
BCL2	Fw GGATGACTGAGTACCTGAACC	80	61.5-63
	Rv CGTACAGTTCCACAAAGGC		
CASP3	Fw CGGACTTCTTGTATGCTTACTC	89	61
	Rv CACAAAGTGACTGGATGAACC		

Primers used for qPCR analysis of target genes aggrecan (ACAN), a disintegrin and metalloproteinase with thrombospondin motifs 5 (ADAMTS5); Bcl-2-associated protein (BAX); B-Cell lymphoma 2 (BCL2), Caspase 3 (CASP3), collagen type II α1 (COL2A1), collagen type I α1 (COL1A1), interleukin 1β (IL1B), interleukin 6 (IL6), interleukin 10 (IL10), matrix metalloproteinase 13 (MMP13), prostaglandin E synthase 1 (PTGES1), tissue inhibitor of metalloproteinases 1 (TIMP1) and reference genes glyceraldehyde 3-phosphate dehydrogenase (GAPDH), hypoxanthine-guanine phosphoribosyltransferase (HPRT), ribosomal protein S19 (RPS19) and succinate dehydrogenase complex, subunit A (SDHA).

Supplementary file 2. Overview of dogs included in the study.

Dog	Group	Joint	Breed	Age (years)	Body weight (BCS)	Diagnosis	Treatment history
1	C	R knee	Cane Corso	2	46 (4/9)	OA, partial ACL rupture	Carprofen (4 mg/kg 1dd)
2	P	R knee	Galgo Español	10	28 (4/9)	OA	Cimicoxib (2 mg/kg 1dd), IA ACS injection 3x 1 yrs earlier, physical therapy
3	C	L knee	Boerboel	3	40 (4/9)	OA	Carprofen (2 mg/kg 2dd), arthrotomy 3 yrs prior
4	P	R knee	Cocker Spaniel cross	10	18 (6/9)	ACL rupture, OA	Carprofen (4 mg/kg 1dd)
5	C	L knee	Basset Fauve de Bretagne	13	16 (5/9)	OA	Firocoxib (4 mg/kg1dd)
6	P	L elbow + L knee	German Shepherd dog	8	32 (5/9)	OA	Carprofen (4 mg/kg1dd), arthrotomy knee 6 mo prior
7	C	R knee	Labrador retriever	5	28 (5/9)	ACL rupture, OA	Carprofen (4 mg/kg1dd), Tramadol (2 mg/kg 3dd), arthrotomy 6 mo prior, extracapsular imbrication 2 yrs earlier
8	C	R elbow	Bouvier cross	11	37 (5/9)	OA	Carprofen (4 mg/kg1dd)
9	C	L knee	Bracco Italiano	3	29 (5/9)	ACL rupture, OA	Carprofen (4 mg/kg 1dd) 3x IA ACS 1 yr earlier, TTA + MMx 2 yrs prior
10	C	R elbow	Australian Cattle dog	8	22 (5/9)	FCP, OA	Cimicoxib (2 mg/kg 1dd), arthrotomy L+R elbow 1.5 yr earlier, 3x IA ACS injection 9 mo earlier
11	P	R elbow	Crossbreed	7	32 (6/9)	FCP, OA	Meloxicam (0.1 mg/kg, 1dd), arthrotomy 5 yrs prior, 2x IA methylprednisolone 3 yrs earlier
12	P	R elbow	German Shepherd dog	8	36 (5/9)	FCP, OA	Cimicoxib (2 mg/kg 1dd), IA hyaluronic acid 6 mo earlier
13	C	R elbow	Dutch Shepherd dog	6	41 (6/9)	FCP, OA	Firocoxib (4 mg/kg 1dd)
14	C	L hip	Belgian Shepherd dog	4	32 (5/9)	HD, OA	Carprofen (4 mg/kg 1dd)
15	C	R elbow	German shepherd dog	10 mo	36 (5/9)	UAP, OA	Carprofen (4 mg/kg 1dd)
16	C	L hip	Border Collie	11 mo	16 (4/9)	HD, OA	Meloxicam (0.1 mg/kg

			cross				1dd)
17	P	R knee	Labrador retriever cross	10	34 (5/9)	ACL rupture, OA	Carprofen (2 mg/kg 2dd), extracapsular imbrication 3 yrs earlier
18	C	R hip	German pointer	7	32 (5/9)	HD, OA	Meloxicam (0.1 mg/kg 1dd)
19	P	L elbow	German Shepherd dog	5	40 (6/9)	FCP, UAP	Carprofen (4 mg/kg 1dd), arthrotomy for FCP removal 4 yrs earlier
20	P	R knee	American Staffordshire Terrier	4	40 (6/9)	Partial ACL rupture, OA	Carprofen (4 mg/kg 1dd)
21	C	R hip	Wetterhoun	5	25 (5/9)	HD, OA	Tramadol (2 mg/kg 3dd), phenylbutazone (6 mg/kg 2dd), prednisolone (0.2 mg/kg 2dd), TPO 4 yrs earlier, implant removal after infection 3.5 yrs earlier
22	C	R hip	Crossbreed	12	18 (4/9)	HD, OA	Meloxicam (0.1 mg/kg 1dd), pectineus myotomy 10 years ago
23	C	R elbow	Border Collie	10	22 (6/9)	FCP, OA	Carprofen (4 mg/kg 1dd)
24	C	L knee	Fila Brasileiro	3	44 (5/9)	ACL degeneration, OA	Carprofen (4 mg/kg 1dd)
25	C	R elbow	Newfoundland dog	4	69 (8/9)	FCP, OA	Tramadol (2 mg/kg 2dd), meloxicam (0.2 mg/kg 1dd), arthrotomy 3 yrs earlier
26	P	R elbow	Rottweiler	2	54 (5/9)	FCP, OA	Meloxicam (0.1 mg/kg 1dd), arthrotomy 1 yr earlier
27	C	R elbow	American Staffordshire Terrier	8	34 (5/9)	FCP, OA	Cimicoxib (2 mg/kg 1dd)
28	P	L Hip	Border Collie	4	24 (5/9)	HD, OA	Carprofen (4 mg/kg 1dd)
29	C	R elbow	Rottweiler cross	4	40 (6/9)	FCP, OA	Carprofen (2 mg/kg 2dd), Arthroscopy 3 years ago
30	C	R elbow	Labrador Retriever	8	35 (7/9)	FCP, OA	Meloxicam (0.1 mg/kg 1dd)

Abbreviations: C, Celecoxib; mo, months; P, Placebo; BCS, body condition score; R, right; L, left; OA, osteoarthritis; ACL, anterior cruciate ligament; yrs, years; TTA, tibial tuberosity advancement; MMX, medial meniscectomy; ACS, autologous conditioned serum; FCP, fragmented coronoid process; UAP, ununited anconeal process, HD, hip dysplasia; TPO, triple pelvic osteotomy.

Supplementary file 3. Results of radiographic osteoarthritis (OA) score and scoring of osteophyte measurements at baseline and 2 months after intra-articular injection with celecoxib (C) loaded and unloaded (P, placebo) polyesteramide microspheres.

Dog	Group	Joint	OA Score [a]		Osteophyte score [b]	
			Baseline	2 months	Baseline	2 months
1	C	Knee	2	2	2	2
2	P	Knee	3	3	2	2
3	C	Knee	2	2	2	2
4	P	Knee	3	3	2	2
5	C	Knee	1	1	2	2
6	P	Knee + elbow	3 + 2	3 + 2	2	3
7	C	Knee	3	3	2	2
8	C	Elbow	3	3	3	3
9	C	Knee	2	2	2	2
10	C	Elbow	3	3	2	2
11	P	Elbow	3	3	3	3
12	P	Elbow	3	3	3	3
13	C	Elbow	3	3	2	2
14	C	Hip	3	3	2	2
15	C	Elbow	1	1	1	1
16	C	Hip	2	2	1	1
17	P	Knee	3	3	2	2
18	C	Hip	2	2	2	2
19	P	Elbow	3	3	3	3
20	P	Knee	2	2	1	1
21	C	Hip	3	3	2	2
22	C	Hip	3	3	3	2
23	C	Elbow	3	3	3	3
24	C	Knee	3	3	3	3
25	C	Elbow	3	3	3	3
26	P	Elbow	2	2	2	2
27	C	Elbow	1	1	1	1
28	P	Hip	2	2	1	2
29	C	Elbow	3	3	3	3
30	C	Elbow	3	3	3	3

[a] OA score: normal = 0, mild OA = 1, moderate OA = 2, severe OA = 3. [b] Osteophyte scoring: 0 = no OA, 1 (osteophytes <2 mm), 2 (2-5 mm) or 3 (>5 mm).

Chapter 5

A novel intra-articular slow-release formulation of triamcinolone acetonide effectively reduces symptoms in dogs with osteoarthritis

A. R. Tellegen [1], M. Beukers [1], N. J. van Klaveren [2], K.L. How [3], N. Woike [4], G. Mihov [4], J.C. Thies [4], E. Teske [1], L. B. Creemers [5], M. A. Tryfonidou [1*], B. P. Meij [1*]

[1] Department of Clinical Sciences of Companion Animals, Faculty of Veterinary Medicine, Utrecht University, The Netherlands

[2] Orthopedie, Medisch Centrum voor Dieren, The Netherlands

[3] Diergeneeskundig Specialisten Centrum Den Haag, The Netherlands

[4] DSM Biomedical, The Netherlands

[5] Department of Orthopaedics, University Medical Centre Utrecht, The Netherlands

* Shared senior authorship.

Submitted to Acta Veterinaria Scandinavica

Abstract

Osteoarthritis (OA) is a common cause of pain and lameness in dogs. Local injections of corticosteroids are effective in treating OA pain, but have a short period of action. The aim of this prospective study was to assess the safety and efficacy of intra-articular (IA) applied microspheres gradually releasing triamcinolone acetonide (TA) in client-owned dogs with OA. OA was diagnosed by clinical examination and radiography. TA-microspheres were injected in the affected joint (10-20 mg TA per joint, dependent on body weight). Outcome parameters were determined before treatment and at 1, 2 and 6 months after IA injection and included clinical examination, force plate gait analysis, radiographs, synovial fluid analysis, and questionnaires to owners regarding the pain-related behaviour of their dog. OA was confirmed in 14 articular joints of 12 dogs (8 elbow-, 3 hip-, 2 knee– and 1 tarsal joint). Treatment resulted in clinical improvement in 10/12 dogs during the two months follow-up period which persisted in 6/10 dogs after 6 months. Radiographic examination at 2 and 6 months follow-up showed no changes in OA severity. Synovial fluid prostaglandin E2, a pro-inflammatory marker, was decreased 2 months after treatment. This study showed safety and efficacy of intra-articular administered TA-microspheres in dogs with OA. The inclusion of more dogs in a double blind randomized placebo-controlled study should confirm these results.

Introduction

Osteoarthritis (OA) is the most common form of arthritis in dogs. Twenty percent of adult dogs and 80% of geriatric dogs suffer from OA [1]. OA is a multifactorial disease, caused by an interplay between environmental factors, such as trauma and obesity, and hereditary factors. Elbow and hip dysplasia (ED and HD) are such hereditary disorders and inevitably lead to degenerative joint disease. ED has a prevalence between 0-64%, dogs can be treated medically or surgically, although over 40% will have an unsatisfactory long-term outcome due to development of OA [1-3]. The prevalence of HD also varies between dog breeds; prevalences over 50% were reported in certain breeds [2, 3]. Medical and surgical treatment can be effective in managing HD, but OA progresses nevertheless [4-6].

OA is characterized by degeneration of articular cartilage, accompanied by subchondral bone changes and synovitis. Pain, swelling and stiffness of the affected joint are the main clinical signs of OA [7]. Oral (non-steroidal) anti-inflammatory drugs and analgesics such as gabapentin and tramadol are frequently used to treat OA-related pain and can be administered safely for prolonged periods, with appropriate monitoring. However, they all are accompanied by drug-related side effects [8]. Also, delivery of drugs to the joint by the oral route my not be that effective [9]. An alternative route is via intra-articular (IA) injections. Steroidal anti-inflammatory drugs are known to be effective against OA pain for decades, but IA administration has a limited duration of action. Additional drawbacks of IA injections include the need for reinjection under sedation [10], risk of septic arthritis, and the high initial burst release of corticosteroids that can cause systemic side effects directly after each administration [10, 11]. Moreover, negative effects of IA corticosteroid injections on articular cartilage have been described in humans and horses [11, 12]. Sustained release formulations which lower the frequency of re-injections and decreased peak levels of corticosteroid formulations would therefore be preferred [13].

A novel drug delivery platform facilitating sustained drug release, consisting of biodegradable amino-acid based polyesteramide microspheres (PEAMs) was shown to gradually release triamcinolone acetonide (TA) over a period of 3-6 months. PEAMs loaded with TA were capable of inhibiting inflammation both in vitro and in vivo [13, 14]. In a rat OA model, retention of PEAMs in the joint was confirmed for up to 70 days. Moreover, synovial inflammation was lowered in OA joints injected with TA-PEAMs after 7 weeks [13]. Based on this promising preclinical data, the aim of this prospective study was to assess safety and efficacy of injection of TA-PEAMs in joints with chronic OA in client-owned dogs.

Materials and methods

Preparation of microspheres

PEA polymer and PEA microspheres were synthesized according to previously reported protocols [15, 16]. TA was loaded in PEAMs at 30wt%. Once dried, the PEAMs were weighed in individual HPLC vials to the approximate amount of 40 mg PEAMs and γ-sterilized on dry ice. Directly prior to injection, PEAMs were re-suspended in 2 mL (20 mg/mL) sterile 2% lidocaine HCl injection solution (B. Braun Medical), to avoid pain from the arthrocentesis procedure.

Inclusion criteria

Dogs were considered eligible for the study if they were otherwise healthy, weighed at least 15 kg, had a history of chronic lameness and were diagnosed with OA on orthopaedic examination and radiographic evaluation. Dogs were excluded if they had undergone surgery in the affected or contralateral limb in the past three months, if there was evidence of a fracture or tumour in the affected limb, or if the dog had received IA injections in the affected joint in the past three months. Dogs with clear joint instability on clinical examination were also excluded from the study. Pain medication was discontinued 4 days prior to the study, to obtain baseline levels of the read-out parameters. Physical activity was limited to leash walks on the first two days after treatment. Thereafter, owners could gradually take up activity as before the start of the study. In case there was insufficient control of OA pain, rescue analgesia was permitted during the study period, starting from three weeks after the IA injection.

Study design

This study was conducted with the approval of the Ethical Committee of the Department of Clinical Sciences of Companion Animals, Utrecht University. Owners were informed, and written consent was obtained before study enrolment. The study design is illustrated in Figure 1. After baseline clinical evaluation, dogs were sedated, and the affected joint(s) were clipped and prepared aseptically. Arthrocentesis was performed, and synovial fluid (SF) was collected for cytology and when there was sufficient volume, stored at -20 °C. This was followed by IA administration of the TA-PEAMs through the same needle. Dogs with a body weight of 15-30 kg received 0.5 mL PEAM solution (10 mg TA), dogs weighing 30-45 kg received 1 mL (20 mg TA) and dogs weighing over 45 kg received 1.5 mL (30 mg TA). The dogs were evaluated after 1 and 2 months, and if possible, 6 months after IA injection.

Read out parameters

Physical examination and lameness score. All dogs underwent a full clinical and orthopaedic examination by a board-certified veterinary surgeon (BM). Lameness was recorded on a 4-point scale, ranging from 0 (none), 1 (intermittent mild lameness after rest and exercise), 2 (mild lameness / intermittent moderate lameness after rest and exercise), 3 (moderate lameness / non-weight bearing after exercise) or 4 (non-weight bearing lameness).

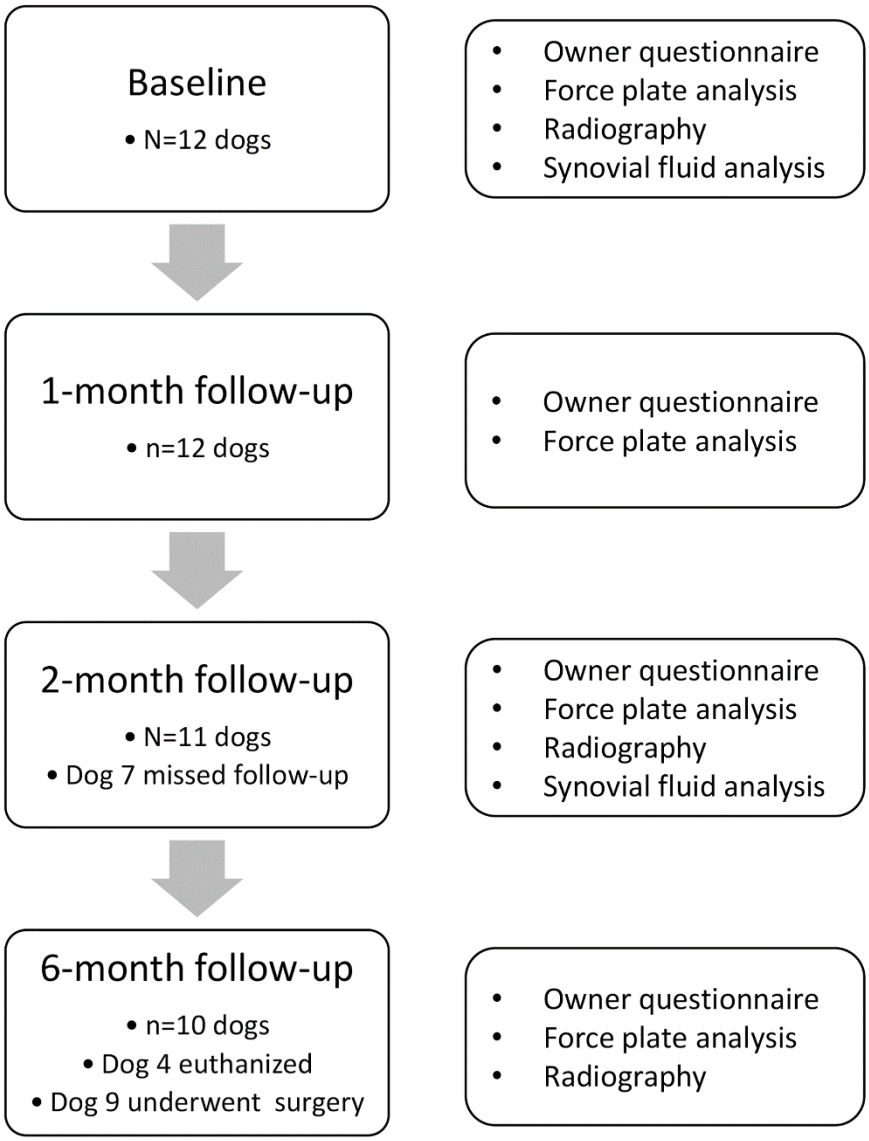

Figure 1. Schematic overview of the study setup.

Kinetic gait analysis. Ground reaction forces (GRFs) were measured by force plate analysis (FPA) with a quartz crystal piezoelectric force plate (9261, Kistler Instrumente) together with the Kistler 9865E charge amplifiers as described previously [17, 18]. GRFs in the mediolateral (Fx), craniocaudal (Fy) and vertical (Fz) direction were normalized for body weight. Asymmetry indices (ASI) were calculated according the following formula:

$$\frac{Left - Right}{0.5\ (Left + Right)} * 100$$

ASIs were determined for peak propulsive force (PPF), peak vertical force (PVF) and area under the force-time curve of Fz+, which is equal to the vertical impulse (VI) during the stance phase, as previously described [19, 20]. Stance time was recorded as well.

Owner assessment of pain and lameness. A questionnaire to owners regarding pain-related behaviour and function of their dog, assessed the owner's perspective of treatment outcome (Table 2), and was partially adapted from the Canine Brief Pain Inventory [21]. Rescue analgesia in case of recurrence or persistence of clinical signs was recorded by the owners.

Radiographic evaluation. Radiographs of the affected joints were obtained within three months prior to inclusion in the study and at 2 and 6 months after injection to monitor for adverse effects and OA progression. Images were examined by a board-certified veterinary radiologist (MB). Each radiograph was scored for OA severity as follows: 0 (none); 1 (minimal), 2 (mild), 3 (moderate) or 4 (marked) as previously reported [22] and was adjusted for use in the other joints. To assess OA more quantitatively, the height of osteophytes was measured and graded as described previously for the elbow joint [23]: 0 (no OA), 1 (osteophytes <2 mm), 2 (2-5 mm) or 3 (>5 mm). Osteophytes in elbow joints were measured at the cranial aspect of the radial head, the caudal surface of the lateral condylar ridge, the medial contour of the humeral condyle and the medial contour of the medial coronoid process. For hip joints, osteophytes on the edge of the cranial and caudal acetabulum or at the femoral neck were taken into account. For knee joints, osteophytes were measured at the proximal trochlear edge, the distal patella and the lateral and medial tibia plateau. Osteophytes in the tarsal joint were measured at the medial and lateral aspect of the distal tibia (Fig. 2A-G). The highest value was taken into account into the analysis.

Synovial fluid analysis. Before treatment, and 2 months after IA injection, arthrocentesis was performed to collect SF. This was directly assessed macroscopically on volume, colour, turbidity and viscosity. Direct impression smears were obtained, stained with Hemacolor® and smears were assessed for number of cells, the type of cells (synoviocytes, macrophages, polymorphonuclear leukocytes (PML), lymphocytes), the presence of cell clusters and the presence of micro-organisms. Cells were counted with an automatic cell counter (1450102 Bio-Rad) with trypan blue dye. Remaining SF was aliquoted and stored at -20°C for biochemical analysis. Glycosaminoglycan (GAG) concentration was determined after incubation with 1:10 0.1 mg/mL hyaluronidase (H2126, Sigma-Aldrich) at 37°C for 30 minutes, by using chondroitin sulphate from shark cartilage (C4384, Sigma-Aldrich) as a standard. The absorbance was read at 540/595 nm [24]. Prostaglandin E2 (PGE2) and C-C motif chemokine ligand 2 (CCL2) levels were determined by ELISA (514010, Cayman Chemical; DIY0934D-003, Kingfisher Biotech, respectively) following manufacturer's instructions.

Figure 2. Representative examples of radiographs obtained 6 months after intra-articular injection with triamcinolone acetonide-loaded microspheres. Radiological OA findings remained unchanged at 6 months follow up compared to recordings prior to treatment. Arrows indicate locations for osteophyte measurements. **A** and **B** show the mediolateral and craniocaudal radiographs of the elbow joint of dog 6. Mediolateral (**C**) and caudocranial (**D**) radiograph of the knee joint of dog 7. **E** and **F** depict the mediolateral and plantarodorsal radiographs of the tarsal joint of dog 5. **G** and **H** show a ventrodorsal radiograph of the pelvis of dog 3 prior to and 6 months after treatment, respectively.

Statistical analysis

Statistical software (IBM SPSS Statistics 24) was used for all comparisons. Normality of the data was checked by assessing the Q-Q plots, histograms and Shapiro-Wilks tests. A repeated measures ANOVA was used to assess difference in the body weight, questionnaire scores and force plate parameters at baseline, 1, 2, and 6 months. PGE2, GAGs and CCL2 SF levels at baseline and 2 months were compared using a one-way ANOVA. The visual lameness scores obtained at baseline, 1, 2 and 6 months were compared using the Wilcoxon's signed rank test. P values <0.05 were considered statistically significant after correction for multiple testing (Benjamini-Hochberg method). Effect sizes (ES) were retrieved as Hedge's g for parametric data: medium, 0.5-0.8; large, 0.8-1.2; 1.2-2, very large and >2 huge [25]. For non-parametric data, Cliff's delta was assessed: 0.28<ES<0.43, medium;

0.43≤ES<0.7, large; ES≥0.7, extra-large [26]. Differences were considered as relevant when $p<0.05$ and/ or ES was medium or larger when the p-value was <0.1.

Results

Study population

Twelve dogs met the inclusion criteria and were enrolled in the study (Table 1). The median age at inclusion was 8 years (range 1-12 years) and the average body weight 30 kg (range 21-36 kg). Body weight did not substantially change during the course of the study (p=0.74). The visual lameness scores included mild (2/4; *n*=7), moderate (3/4; *n*=5) and non-weight bearing (4/4; *n*=1) lameness. Clinical and radiological findings were compatible with OA. No serious adverse events were reported by the owners after IA injection. Transient polyuria (± 1 week) was reported in 5 dogs.

Visual lameness scores were significantly decreased at 1 month (p=0.031), 2 months (p=0.011), and 6 months (p=0.016) after IA injection of TA-PEAMs (Fig. 3A). At 1 month after IA injection, lameness was absent in 4 limbs, intermittent/mild in 2 limbs, mild-moderate in 2 limbs and moderate in 2 limbs (Fig. 3A). In 3 dogs, lameness shifted to the contralateral limb (dog 6, 8 and 9). At the 2-month follow-up visit, lameness was absent in 3 dogs, intermittent/mild in 5 limbs, mild-moderate in 2 limbs and moderate in 2 limbs. After 6 months, lameness was absent in 2 dogs, mild in 4 limbs, mild-moderate in 4 limbs and moderate in 2 limbs.

The owners of 2 of the 12 dogs (dog 4 and dog 5) noticed no marked clinical improvement during the two months after treatment, although there was slight improvement noticed in the PVF in both dogs. These dogs both suffered from severe OA secondary to ED and both dogs already had undergone arthroscopy prior to inclusion in the study. Three months after inclusion in the study, dog 4 underwent arthrotomy and a large fragmented coronoid process was removed. Clinical signs did not improve after surgery and the dog was eventually euthanized. Dog 5 had severe OA in the left tarsal and right elbow joint and was able to function to the owner's satisfaction with the aid of oral NSAID therapy and a tarsal brace, applied 3 and 7 months after the start of this study, respectively. Dog 9 was lost for the six months follow-up, since a proximal abducting ulnar osteotomy was performed 5 months after IA TA injection.

Table 1. Overview of dogs included in the study.

Dog	Joint	Breed	Age	Body weight (BCS)	Diagnosis	Treatment history
1	R Hip	Rottweiler	1	35 (5/9)	HD, OA	Conservative (NSAIDs)
2	R elbow	Labrador retriever	3	32 (6/9)	OA	Arthrotomy 6 months earlier
3	R knee, R hip	Bouvier de Flandres	9	36 (5/9)	OA	PLO 10 months earlier, MMX 4 months earlier
4	L elbow	Labrador retriever	9	32 (7/9)	OA	Arthroscopy 3 years earlier
5	R elbow, L tarsus	Cesky fousek	12	22 (5/9)	OA	Conservative
6	R elbow	Labrador retriever	11	29 (6/9)	FCP, OA	Conservative
7	R knee	Siberian husky	8	30 (5/9)	ACL rupture, OA	TPLO
8	R elbow	Shar Pei	4	33 (6/9)	FCP, MCD, OA	Arthrotomy 4 years earlier, arthroscopy 3 months earlier
9	R elbow	Belgian Shepherd dog	6	29 (7/9)	MCD, OA	Arthroscopy
10	R elbow	Australian cattle dog	8	21 (6/9)	FCP, MCD, OA	Arthrotomy 1 year earlier,
11	R elbow	German Shepherd dog	8	36 (5/9)	FCP, OA	Conservative
12	R hip	Wetterhoun	5	25 (6/9)	HD, OA	TPO 4 years earlier with implant removal 3 months later due to implant infection

Abbreviations: BCS, body condition score; R, right; L, left; HD, hip dysplasia; OA, osteoarthritis; ACL, anterior cruciate ligament; NSAIDs, non-steroidal anti-inflammatory drugs; TPLO, tibial plateau leveling osteotomy; MMX, medial meniscectomy; ACP, autologous conditioned plasma; FCP, fragmented coronoid process; MCD, medial compartment disease; TPO, triple pelvic osteotomy.

Owner assessment of pain and lameness

Questionnaires were completed by owners prior to treatment, and 1, 2 and 6 months after IA injection (table 2). There was a significant improvement in total questionnaire scores (Fig. 3B) after 1 ($p=0.0008$), 2 ($p=0.023$), and 6 months ($p=0.018$).

Table 2. Responses to owners' questionnaires before and 1, 2 and 6 months after intra-articular injection with triamcinolone acetonide-loaded microspheres.

Questions	Before treatment (*n*=12)	After 1 month (*n*=11)	After 2 months (*n*=12)	After 6 months (*n*=10)
Does your dog show lameness, and in which severity?	3.5 (2-10)	8 (1-10) *	7 (3-10) [c]	5.5 (3-10)
Does your dog have pain as a result of its osteoarthritis?	4 (1-10)	8 (1-10) *	7 (1-10)	6 (3-10)
Does your dog show any weakness in its affected leg?	6.5 (1-10)	9.5 (3-10) *	9 (3-10)	8 (3-10)
Does your dog have difficulty rising up?	4 (1-10)	8 (2-10) *	8 (2-10) [b]	6.5 (1-10)
Does your dog have difficulty lying down?	4.5 (1-10)	9 (4-10) *	9 (4-10) *	8.5 (1-10)
Does the pain interfere with normal activities in and around the house?	5.5 (2-10)	9 (5-10) *	9 (3-10)	8 (1-10)
Does the pain interfere with the quality of life of your dog?	4.0 (1-10)	8 (2-10) *	8 (2-10) *	8 (3-10) *
Does the pain interfere with the ability to walk?	3.5 (1-7)	6 (2-10) *	6 (1-10) [a]	6 (2-10) *
Does the pain interfere with the quality to run?	3.5 (1-6)	7 (1-10) *	5 (1-10) *	5.5 (2-10) *
Does the pain interfere with the ability to walk stairs?	4.0 (1-10)	7 (1-10)	8 (1-10)	5.5 (1-10)

Data represented as median (range). * Indicates significant difference from baseline (p<0.05). a, medium size (ES); b, large ES; c, very large effect ES when 0.05>p<0.1.

Kinetic gait analysis

Force plate analysis was performed in dogs prior to treatment and after 1 month, and after 2 and 6 months (Fig. 3C-F, Supplementary file 1). The asymmetry of the PPF and PVF were significantly improved at the 1-month post injection (p=0.041, p=0.04) and PVF improved during the 2-month follow-up visits (p=0.027). There was a borderline significant decrease in VI asymmetry (p=0.053, medium ES; p=0.062, medium ES). Stance time did not differ between time-points. Six months after IA injection, force plate parameters did not significantly differ from baseline values.

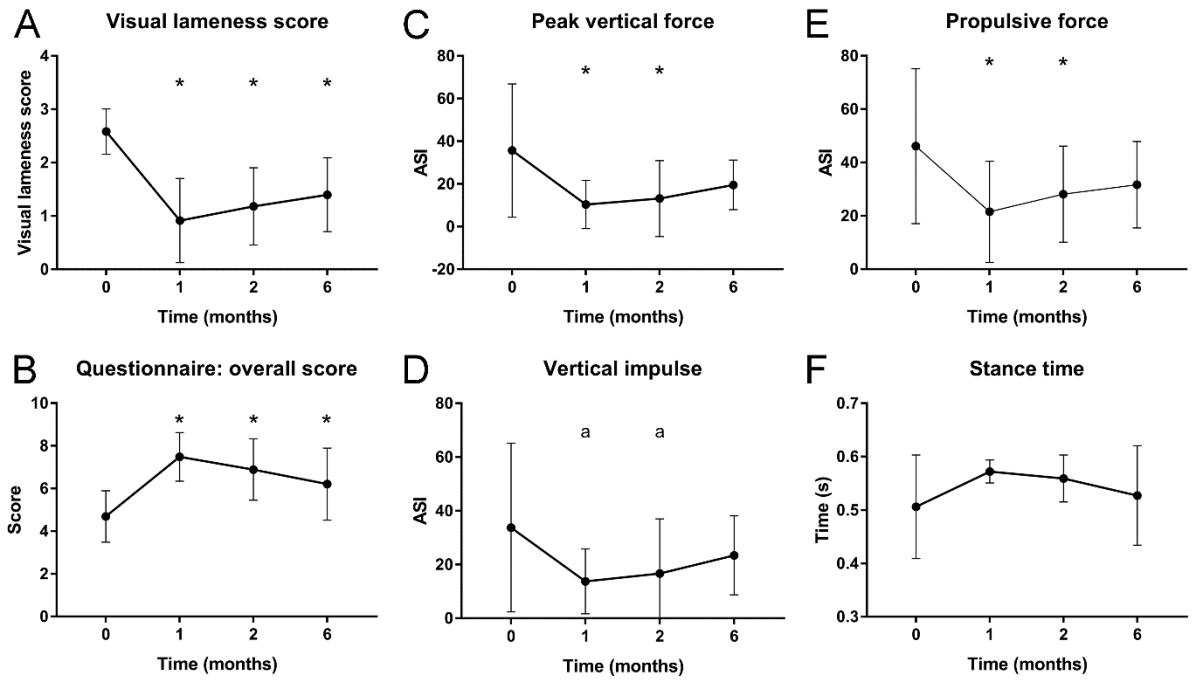

Figure 3. Clinical and kinematic outcome parameters. Visual lameness score (**A**) and average overall questionnaire score (**B**) improved significantly during the 6-moth follow-up period. Asymmetry indices (ASI) of the peak vertical force (**C**), vertical impulse (**D**), the propulsive force (**E**) improved during the first 2- months after treatment. Stance time remained similar throughout the 6-month period (**F**). * Indicates significant difference from baseline value (p<0.05). a, medium effect size with 0.05>p<0.1.

Radiographic evaluation

Severity of OA and osteophyte size were evaluated in the subset of patients that completed the follow-up period, at 2 and 6 months after IA administration of TA-PEAMs and compared with pre-treatment radiographs. No significant changes in OA severity or osteophytes were detected in any of the dogs (Fig. 2, Table 3).

Table 3. Blinded evaluation of severity of osteoarthritis and osteophyte size on radiographs before, and 2 and 6 months after intra-articular injection with triamcinolone acetonide-loaded microspheres.

		Osteoarthritis score			Osteophyte size (largest, mm)		
Dog	**Joint**	**Before treatment**	**After 2 months**	**After 6 months**	**Before treatment**	**After 2 months**	**After 6 months**
1	Hip	3	3	3	6.0	6.0	5.8
2	Elbow	2	2	2	3.7	4.4	4.5
3	Knee	3	3	3	4.9	4.8	3.9
3	Hip	3	3	3	4.4	3.5	5.2
4	Elbow	3	3	N/A	4.5	4.8	N/A
5	Elbow	3	3	3	7.2	7.1	7.5
5	Tarsus	3	3	3	5.0	4.9	5.6
6	Elbow	3	3	3	6.0	6.2	6.4
7	Knee	2	N/A	2	4.9	N/A	4.8
8	Elbow	2	2	2	3.4	3.7	3.7
9	Elbow	3	3	N/A	5.8	5.9	N/A
10	Elbow	3	3	3	5.5	5.8	5.8
11	Elbow	3	3	3	5.7	6.1	6.2
12	Hip	1	1	1	1.7	1.9	1.9

N/A, not available.

Synovial fluid analysis

Prior to IA injection, SF from 9 joints was available for analysis. Cytology confirmed the presence of degenerative OA (9/9) and showed an increased number of synoviocytes and macrophage-like cells (8/9; Fig. 4A,B), and the presence of cellular clusters (4/9; Fig. 4C) were observed. In dog 8 there was also an abundance of PML (Fig. 4B). The mean total cell count was 6.3*106 (range 1.3 – 10.4*106) cells/mL. At the 2-month follow-up visit, 7 samples were available for analysis and in 1/7 samples, degenerative OA had shifted to inflammatory arthritis with an increased presence of PMLs (knee joint, dog 3) but no (intracellular) bacteria were observed on cytology or culture. The average total cell count was 4.3*106 cells/mL (range 1.7 – 9.9*106), which was not significantly different from the baseline (p=0.34). PGE2 was lower 2 months after IA injection, compared to pre-treatment values (p=0.045). No significant changes in total GAG and CCL2 values in the SF were detected 2 months after IA injection compared to baseline measurements (Fig. 4D-F).

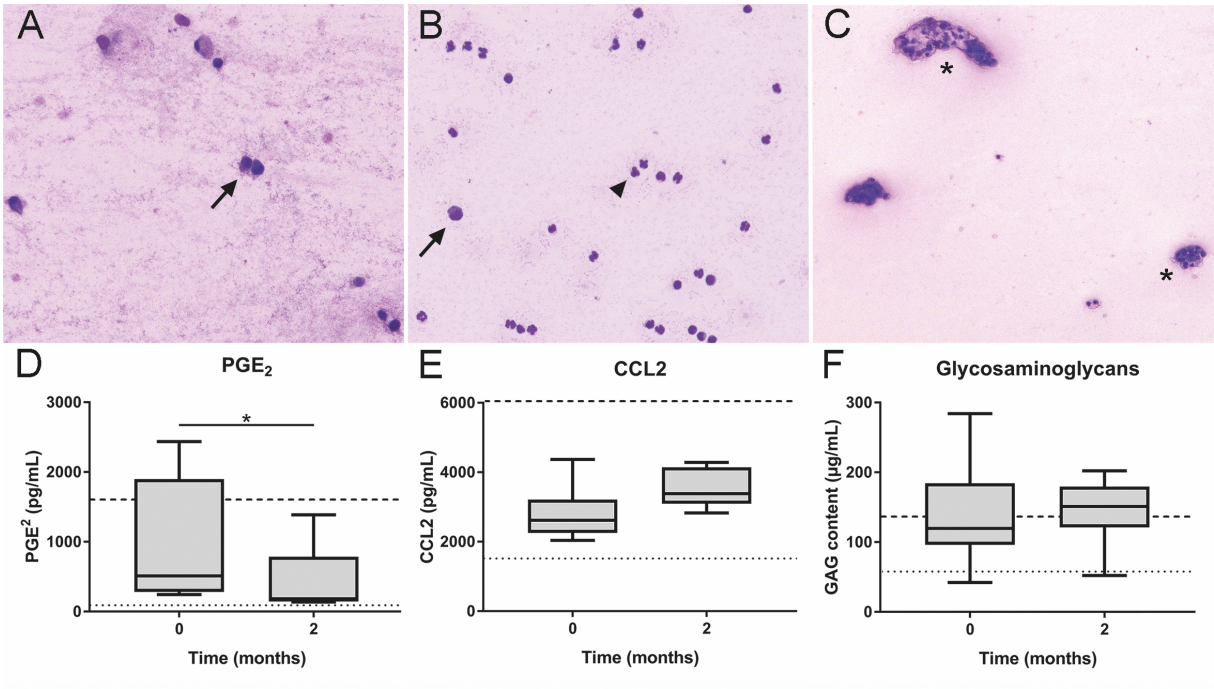

Figure 4. Results of the synovial fluid analysis. **A**. Synovial aspirate of dog 5 6 months after intra-articular injection with triamcinolone acetonide-loaded microspheres. A few synoviocyte-like cells are present (arrow). **B.** Cytological smear of synovial fluid of dog 3, 6 months after treatment. Abundant polymorphonuclear cells are present (arrowhead), along with some macrophage-like cells (arrow). No (intra)-cellular bacteria were found. **C.** Contact smear of the synovial fluid of dog 1 prior to treatment. Clusters of synovial lining cells are present (asterisks). Concentrations of prostaglandin E_2 (PGE_2, **D**), C-C motif chemokine ligand 2 (CCL2), **E**) and glycosaminoglycans (GAGs, **F**) in synovial fluid before and 2 months after intra-articular injection with triamcinolone-acetonide-loaded microspheres. Dotted lines indicate SF control samples of 6 healthy joints, dashed lines indicate average SF biomarker values for osteoarthritic joints of 6 donors. * Indicates significant (p<0.05).

Discussion

The goal of this prospective clinical study was to investigate safety and preliminary efficacy of the controlled release of TA in dogs with established OA. There were no adverse effects or complications in the six-month follow-up period after local injection with TA-PEAMs. Ten out of twelve dogs improved clinically, according to the owner questionnaire, and objective and subjective gait analyses. Clinical improvement was most apparent during the first two months. Six months after IA treatment with TA-loaded PEAMs, significant improvement was only apparent in 6/10 owner questionnaires but not on force plate analysis. A discrepancy between owner assessment and force plate analysis could be explained by the fact that the owners were focused on other behaviours than lameness, when making efficacy evaluations in their dogs [21]. Also, force plate measurements reflect a single moment in time, whereas the owners monitor their dogs' behaviour on a daily basis.

Joint health was monitored with the aid of biomarkers indicative for inflammation and cartilage degradation. The pro-inflammatory mediator PGE2 was increased in patients with symptomatic OA [27], and known to directly influence nociceptors, mediating OA pain [28]. In dogs with experimentally induced OA, PGE2 concentrations in SF correlated well with force plate analysis and subjective lameness scores [29], providing evidence for the use of PGE2 as a valuable biomarker in the evaluation of canine OA. Indeed, in this study, total SF PGE2 levels tended to decrease, consistent with improvement in clinical lameness. Several studies showed an increase in (fragments of) GAGs in the SF of OA joints, compared to healthy joints in dogs [30, 31] and horses [32, 33], reflecting the increased activity of proteases in OA cartilage, leading to cartilage matrix loss. In the SF samples in our study, no changes in GAG concentration were present in the SF two months after IA injection, which could indicate no (long term) change in cartilage breakdown.

Owners were also asked to report side effects after IA injection of TA-PEAMs. Five out of twelve owners mentioned transient polyuria. No relationship was apparent between the occurrence of polyuria and body weight or SF PGE2 values. Polyuria is commonly reported after administration of corticosteroids in dogs [34] and in this case were due to the initial burst release reaching the systemic circulation from the synovial space. Lower burst release of TA was indeed demonstrated after IA administration in PEAMs, compared to a commercially available TA formulation (Kenalog® in rats [13]. An additional benefit of the PEAMs employed in this study, is that they seem to possess autoregulatory properties [35]. As biomaterial degradation mainly occurs through enzymatic degradation, degradation of PEAMs and thus drug release is accelerated in OA joints vs healthy joints. In joints with higher inflammation grades, degradation could be faster, thereby limiting the period of sustained release, but increasing its effectivity, tapered to the specific joint. The results of the current study confirm the need for a sustained release formulation for IA corticosteroid application, as a higher loading dose can be achieved with less side effects, and reinjections would be required on a less frequent basis, limiting the well-known drawbacks of frequent reinjection of corticosteroids.

There are different types of corticosteroids and their biologic effects differ dependent on the type used. A recent review on the use of IA corticosteroids in the horse concluded that results of different corticosteroids should not be generalised as methylprednisolone acetate consistently caused deleterious effects, while IA TA demonstrated favourable effects on clinical, synovial and cartilage parameters [11, 36]. Moreover, negative effects also seemed to be dose-dependent, as higher doses of corticosteroids were associated with gross cartilage damage and chondrotoxicity, although both in vitro and in vivo experimental studies found beneficial effects of TA at low doses and durations [37]. TA inhibited loss of proteoglycans in co-culture of human cartilage tissue with synovium [38], and also decreased COX-2 and matrix metalloproteinase gene expression after IL-1β in equine cartilage [39]. It should be noted that the reviewed studies of corticosteroids in dogs were unanimously positive [12]. The majority of these studies was performed in experimental animal models and not much is published on

IA corticosteroid therapy in companion dogs. The currently available injectable corticosteroid formulations in human medicine were more effective than placebo but have limited duration of action [37]. As such, IA formulations that provide longer drug release are warranted.

This study showed safety and clinical efficacy of IA treatment with controlled release of TA from a biomaterial-based platform in client-owned dogs with OA. To gain more insight into the effect of IA treatment with controlled release of TA from PEMs, a study with a larger patient group should be performed. Moreover, to circumvent any caregiver placebo-effect, TA-microspheres should ideally be compared to a placebo treatment or the standard-of-care IA corticosteroid injection.

References

1. Johnston SA. Osteoarthritis. Joint anatomy, physiology, and pathobiology. Vet.Clin.North Am.Small Anim.Pract. 1997;27:699-723.
2. Coopman F, Broeckx B, Verelst E, Deforce D, Saunders J, Duchateau L*, et al*. Combined prevalence of inherited skeletal disorders in dog breeds in Belgium. Vet.Comp.Orthop.Traumatol. 2014;27:395-7.
3. Lavrijsen IC, Heuven HC, Meij BP, Theyse LF, Nap RC, Leegwater PA*, et al*. Prevalence and co-occurrence of hip dysplasia and elbow dysplasia in Dutch pure-bred dogs. Prev.Vet.Med. 2014;114:114-22.
4. Guevara F and Franklin SP. Triple Pelvic Osteotomy and Double Pelvic Osteotomy. Vet.Clin.North Am.Small Anim.Pract. 2017;47:865-84.
5. Kirkby KA and Lewis DD. Canine hip dysplasia: reviewing the evidence for nonsurgical management. Vet.Surg. 2012;41:2-9.
6. Theyse LFH, Hazewinkel HA, Van den Brom WE. Force plate analyses before and after surgical treatment of unilateral fragmented coronoid process. 2000;13:135-40.
7. Glyn-Jones S, Palmer AJ, Agricola R, Price AJ, Vincent TL, Weinans H*, et al*. Osteoarthritis. Lancet 2015;386:376-87.
8. Rychel JK. Diagnosis and treatment of osteoarthritis. Top.Companion Anim.Med. 2010;25:20-5.
9. Evans CH, Kraus VB, Setton LA. Progress in intra-articular therapy. Nat.Rev.Rheumatol. 2014;10:11-22.
10. Van Vynckt D, Polis I, Verschooten F, Van Ryssen B. A review of the human and veterinary literature on local anaesthetics and their intra-articular use. Relevant information for lameness diagnosis in the dog. Vet.Comp.Orthop.Traumatol. 2010;23:225-30.
11. McIlwraith CW. The use of intra-articular corticosteroids in the horse: what is known on a scientific basis? Equine Vet.J. 2010;42:563-71.
12. Vandeweerd JM, Zhao Y, Nisolle JF, Zhang W, Zhihong L, Clegg P*, et al*. Effect of corticosteroids on articular cartilage: have animal studies said everything? Fundam.Clin.Pharmacol. 2015;29:427-38.
13. Rudnik-Jansen I, Colen S, Berard J, Plomp S, Que I, van Rijen M*, et al*. Prolonged inhibition of inflammation in osteoarthritis by triamcinolone acetonide released from a polyester amide microsphere platform. J.Control.Release 2017;253:64-72.
14. Yang HY, van Dijk M, Licht R, Beekhuizen M, van Rijen M, Janstal MK*, et al*. Applicability of a newly developed bioassay for determining bioactivity of anti-inflammatory compounds in release studies--celecoxib and triamcinolone acetonide released from novel PLGA-based microspheres. Pharm.Res. 2015;32:680-90.
15. Katsarava R, Beridze Z, Arabuli N, Kharadze D, Chu CC, Won CY. Amino acid- based bioanalogous polymers. Synthesis, and study of regular poly(ester amide)s based on bis(α-amino acid) α, ω-alkylene diesters, and aliphatic dicarboxylic acids. 1999;37:391-407.
16. Willems N, Mihov G, Grinwis GC, van Dijk M, Schumann D, Bos C*, et al*. Safety of intradiscal injection and biocompatibility of polyester amide microspheres in a canine model predisposed to intervertebral disc degeneration. J.Biomed.Mater.Res.B.Appl.Biomater. 2015;105:707-714.
17. Suwankong N, Meij BP, Van Klaveren NJ, Van Wees AM, Meijer E, Van den Brom WE*, et al*. Assessment of decompressive surgery in dogs with degenerative lumbosacral stenosis using force plate analysis and questionnaires. Vet.Surg. 2007;36:423-31.
18. Hazewinkel HA, van den Brom WE, Theyse LF, Pollmeier M, Hanson PD. Comparison of the effects of firocoxib, carprofen and vedaprofen in a sodium urate crystal induced synovitis model of arthritis in dogs. Res.Vet.Sci. 2008;84:74-9.
19. Bockstahler BA, Vobornik A, Muller M, Peham C. Compensatory load redistribution in naturally occurring osteoarthritis of the elbow joint and induced weight-bearing lameness of the forelimbs compared with clinically sound dogs. Vet.J. 2009;180:202-12.
20. Meijer E, Oosterlinck M, van Nes A, Back W, van der Staay FJ. Pressure mat analysis of naturally occurring lameness in young pigs after weaning. BMC Vet.Res. 2014;10:193,014-0193-8.
21. Brown DC, Boston RC, Coyne JC, Farrar JT. Ability of the canine brief pain inventory to detect response to treatment in dogs with osteoarthritis. J.Am.Vet.Med.Assoc. 2008;233:1278-83.
22. Lineberger JA, Allen DA, Wilson ER, Tobias TA, Shaiken LG, Shiroma JT*, et al*. Comparison of radiographic arthritic changes associated with two variations of tibial plateau leveling osteotomy. Vet.Comp.Orthop.Traumatol. 2005;18:13-7.
23. Lavrijsen IC, Heuven HC, Voorhout G, Meij BP, Theyse LF, Leegwater PA*, et al*. Phenotypic and genetic evaluation of elbow dysplasia in Dutch Labrador Retrievers, Golden Retrievers, and Bernese Mountain dogs. Vet.J. 2012;193:486-92.

24. Farndale RW, Sayers CA, Barrett AJ. A direct spectrophotometric microassay for sulfated glycosaminoglycans in cartilage cultures. Connect.Tissue Res. 1982;9:247-8.
25. Sawilowsky SS. New effect size rules of thumb. J. Mod. Appl. Stat. Meth. 2009;8:597-599.
26. Cliff N. Dominance statistics: Ordinal analyses to answer ordinal questions. 1993;114:494-509.
27. Attur M, Krasnokutsky S, Statnikov A, Samuels J, Li Z, Friese O*, et al*. Low-grade inflammation in symptomatic knee osteoarthritis: prognostic value of inflammatory plasma lipids and peripheral blood leukocyte biomarkers. Arthritis Rheumatol. 2015;67:2905-15.
28. Lee AS, Ellman MB, Yan D, Kroin JS, Cole BJ, van Wijnen AJ*, et al*. A current review of molecular mechanisms regarding osteoarthritis and pain. Gene 2013;527:440-7.
29. Trumble TN, Billinghurst RC, McIlwraith CW. Correlation of prostaglandin E2 concentrations in synovial fluid with ground reaction forces and clinical variables for pain or inflammation in dogs with osteoarthritis induced by transection of the cranial cruciate ligament. Am.J.Vet.Res. 2004;65:1269-75.
30. Fujita Y, Hara Y, Nezu Y, Schulz KS, Tagawa M. Proinflammatory cytokine activities, matrix metalloproteinase-3 activity, and sulfated glycosaminoglycan content in synovial fluid of dogs with naturally acquired cranial cruciate ligament rupture. Vet.Surg. 2006;35:369-76.
31. Carlson CS, Guilak F, Vail TP, Gardin JF, Kraus VB. Synovial fluid biomarker levels predict articular cartilage damage following complete medial meniscectomy in the canine knee. J.Orthop.Res. 2002;20:92-100.
32. Kawcak CE, Frisbie DD, McIlwraith CW. Effects of extracorporeal shock wave therapy and polysulfated glycosaminoglycan treatment on subchondral bone, serum biomarkers, and synovial fluid biomarkers in horses with induced osteoarthritis. Am.J.Vet.Res. 2011;72:772-9.
33. Koenig TJ, Dart AJ, McIlwraith CW, Horadagoda N, Bell RJ, Perkins N*, et al*. Treatment of experimentally induced osteoarthritis in horses using an intravenous combination of sodium pentosan polysulfate, N-acetyl glucosamine, and sodium hyaluronan. Vet.Surg. 2014;43:612-22.
34. Joles JA, Rijnberk A, van den Brom WE, Dogterom J. Studies on the mechanism of polyuria induced by cortisol excess in the dog. Tijdschr.Diergeneeskd. 1980;105:199-205.
35. Janssen M, Timur UT, Woike N, Welting TJ, Draaisma G, Gijbels M*, et al*. Celecoxib-loaded PEA microspheres as an auto regulatory drug-delivery system after intra-articular injection. J.Control.Release 2016;244:30-40.
36. Frisbie DD, Kawcak CE, Trotter GW, Powers BE, Walton RM, McIlwraith CW. Effects of triamcinolone acetonide on an in vivo equine osteochondral fragment exercise model. Equine Vet.J. 1997;29:349-59.
37. Wernecke C, Braun HJ, Dragoo JL. The Effect of Intra-articular Corticosteroids on Articular Cartilage: A Systematic Review. Orthop.J.Sports Med. 2015;3:.
38. Beekhuizen M, Bastiaansen-Jenniskens YM, Koevoet W, Saris DB, Dhert WJ, Creemers LB*, et al*. Osteoarthritic synovial tissue inhibition of proteoglycan production in human osteoarthritic knee cartilage: establishment and characterization of a long-term cartilage-synovium coculture. Arthritis Rheum. 2011;63:1918-27.
39. Caron JP, Gandy JC, Schmidt M, Hauptman JG, Sordillo LM. Influence of corticosteroids on interleukin-1beta-stimulated equine chondrocyte gene expression. Vet.Surg. 2013;42:231-7.

Supplementary file 1. Results of force plate analysis before and 1, 2, and 6 months after intra-articular injection with triamcinolone acetonide-loaded microspheres.

Parameter	Before treatment	After 1 month	After 2 months	After 6 months
PVF ASI	30 (51)	**11 (18) ***	**14 (26) ***	20 (16)
		***p*=0.04**	***p*=0.027**	*p*=0.86
PVF (Improvement from baseline)	N/A	**61% ***	**67% ***	3%
		***p*=0.003**	***p*=0.008**	*p*=0.3
VI ASI	34 (50)	**14 (19)**	**18 (30)**	23 (21)
		***p*=0.053**[a]	***p*=0.062** [a]	*p*=0.347
VI (Improvement from baseline)		**59%**	**63%**	32%
		***p*=0.022**	***p*=0.033**	*p*=0.3
PPF ASI	40 (48)	**22 (32)**	34 (42)	41 (37)
		***p*=0.041**	*p*=0.086	*p*=0.27
PPF (improvement from baseline)	N/A	**58% ***	27%	-12%
		***p*=0.049**	*p*=0.09	*p*=0.3
Stance time (s)	0.51 (0.15)	0.57 (0.03)	0.57 (0.07)	0.53 (0.13)
		p=0.141	*p*=0.245	*p*=0.649

PVF, peak vertical force; ASI, asymmetry index; PPF, peak propulsive force. Data represented as mean (SD). *Indicates significantly different from baseline ($p<0.05$). a, medium effect size (ES) when $0.05>p<0.1$.

Part II

Development of novel treatment strategies for low back pain in humans and canines

Chapter 6
Inflammatory profiles in canine intervertebral disc degeneration

N. Willems [1], A. R. Tellegen [1], N. Bergknut [1], L. B. Creemers [2], J. Wolfswinkel [1], C. Freudigmann [3], K. Benz [3], G. C. M. Grinwis [4], M. A. Tryfonidou [1], B. P. Meij [1]

[1] Department of Clinical Sciences of Companion Animals, Faculty of Veterinary Medicine, Utrecht University, The Netherlands.
[2] Department of Orthopaedics, University Medical Centre Utrecht, The Netherlands.
[3] NMI Natural and Medical Sciences Institute, University of Tuebingen, Germany.
[4] Department of Pathobiology, Faculty of Veterinary Medicine, Utrecht University, The Netherlands.

BMC Veterinary Research (2016) 12:10

Abstract

Intervertebral disc (IVD) disease is a common spinal disorder in dogs and degeneration and inflammation are significant components of the pathological cascade. Only limited studies have studied the cytokine and chemokine profiles in IVD degeneration in dogs, and mainly focused on gene expression. A better understanding is needed in order to develop biological therapies that address both pain and degeneration in IVD disease. Therefore, in this study, we determined the levels of prostaglandin E2 (PGE_2), cytokines, chemokines, and matrix components in IVDs from chondrodystrophic (CD) and non-chondrodystrophic (NCD) dogs with and without clinical signs of IVD disease, and correlated these to degeneration grade (according to Pfirrmann), or herniation type (according to Hansen). In addition, we investigated cyclooxygenase 2 (COX-2) expression and signs of inflammation in histological IVD samples of CD and NCD dogs. PGE_2 levels were significantly higher in the nucleus pulposus (NP) of degenerated IVDs compared with non-degenerated IVDs, and in herniated IVDs from NCD dogs compared with non-herniated IVDs of NCD dogs. COX-2 expression in the NP and annulus fibrosus (AF), and proliferation of fibroblasts and numbers of macrophages in the AF significantly increased with increased degeneration grade. GAG content did not significantly change with degeneration grade or herniation type. Cytokines interleukin (IL)-2, IL-6, IL-7, IL-8, IL-10, IL-15, IL-18, immune protein (IP)-10, tumour necrosis factor (TNF)-α, and granulocyte macrophage colony-stimulating factor (GM-CSF) were not detectable in the samples. Chemokine (C-C) motif ligand (CCL)2 levels in the NP from extruded samples were significantly higher compared with the AF of these samples and the NP from protrusion samples. PGE_2 levels and CCL2 levels in degenerated and herniated IVDs were significantly higher compared with non-degenerated and non-herniated IVDs. COX-2 expression in the NP and AF and reactive changes in the AF increased with advancing degeneration stages. Although macrophages invaded the AF as degeneration progressed, the production of inflammatory mediators seemed most pronounced in degenerated NP tissue. Future studies are needed to investigate if inhibition of PGE_2 levels in degenerated IVDs provides effective analgesia and exerts a protective role in the process of IVD degeneration and the development of IVD disease.

Introduction

Intervertebral disc (IVD) disease is a common spinal disorder in dogs and humans and is characterized by clinical signs ranging from back pain to neurological deficits. IVD disease is preceded by IVD degeneration with a similar etiopathogenesis in dogs and humans [1]. Chondrodystrophic (CD) dogs are predisposed to explosive extrusion of the nucleus pulposus (NP) (Hansen type I) of degenerated thoracolumbar and cervical IVDs, mainly between 3 and 7 years of age. Non-chondrodystrophic (NCD) dogs are predisposed to protrusion of the annulus fibrosus (AF) (Hansen type II) of degenerated lumbosacral and caudal cervical IVDs at 6 to 8 years of age, and NP extrusion of degenerated thoracolumbar IVDs [2-5]. Hansen type II annular protrusion does occur in CD dogs, but less commonly [6, 7].

The onset of IVD degeneration at a cellular level is characterized by a gradual replacement of notochordal cells by chondrocyte-like cells in the NP. In this respect, the NP of CD dogs contains primarily chondrocyte-like cells already by one year of age, while notochordal cells remain the predominant cell type in the NP of NCD dogs during their lifetime. In the latter, notochordal cells in some IVDs are substituted and degeneration occurs at a much later age [1, 8, 9]. In both types of dogs, a decrease in proteoglycan content, a shift in collagen type II to collagen type I in the extracellular matrix of the NP, together with a disruption of the lamellae in the annulus fibrosus (AF) is seen during IVD degeneration [10, 11]. Furthermore, in degenerated discs, nerve endings extend into the deeper layers of the AF and into the NP, in contrast to healthy discs, in which only the outer third of the AF is innervated. Stimulation of nociceptors in the AF and dorsal longitudinal ligament is related to pain [12, 13]. A nociceptive response can either be evoked by a mechanical or inflammatory stimulus. Various inflammatory mediators have also been suggested to play a role in the catabolic processes in human NP and AF tissue, including prostaglandin E_2 (PGE_2), interleukins (IL-1α, IL-1β IL-6, IL-8), and tumour necrosis factor α (TNF-α)) [14-16]. In NP cells from experimental CD dogs with surgically induced IVD degeneration increased levels of TNF-α and IL-1β were shown in vitro [17]. While knowledge of the involvement of inflammatory mediators in human IVD degeneration has substantially increased over the last years [14-16, 18-34], only limited studies have focused on cytokine and chemokine profiles in IVD degeneration in dogs, and mainly focused on gene expression [17, 35, 36].

PGE_2 is the most common prostanoid and plays an important regulatory role in physiological as well as pathological processes. It is synthesized by two cyclooxygenase (COX) isoforms, COX-1 and COX-2, by conversion of arachidonic acid into prostaglandin H_2 (PGH_2) and isomerization of PGH_2 to PGE_2 by prostaglandin E synthases. COX-2 expression is highly restricted under physiological conditions, but can be rapidly induced in response to inflammatory stimuli and is therefore believed to play an important role in the PGE_2 production involved in degenerative processes [27, 37]. Current therapies of IVD disease aim at alleviating pain by administration of corticosteroids, non-steroidal anti-inflammatory drugs (NSAIDs), and/or opioids, by physical therapy, or by surgery. Among the numerous NSAIDs available, oral selective COX-2 inhibitors are primarily used for managing clinical signs, as

they reduce inflammation and relieve pain, but cause less gastrointestinal side effects [38, 39]. Delivery of COX-2 inhibitors directly into the avascular IVD has been suggested as an alternative route of administration to enhance the local efficacy and to minimalize systemic side effects. A recent study in experimental CD dogs has shown the biocompatibility and safety of intradiscal injection of a hydrogel loaded with a selective COX-2 inhibitor [40]. As PGE_2 is one of the inflammatory mediators in human IVD herniation that has been shown to sensitize nerves and induce pain, the efficacy of intradiscal delivery of NSAIDs is likely to be limited to IVD disease with a clear inflammatory profile [41]. We hypothesize that PGE_2 levels are higher in degenerated and herniated (protruded or extruded) IVDs of CD and NCD dogs compared with non-degenerated or non-herniated IVDs. Therefore, we determined the levels of PGE_2, cytokines, chemokines, and matrix components in IVDs from CD and NCD dogs with and without clinical signs of IVD disease and correlated these to degeneration grade or herniation type. In addition, we investigated COX-2 expression in histological IVD samples of CD and NCD dogs.

Materials and methods

Collection and preparation of samples for biochemical analyses

IVDs collected post-mortem

A total of 19 IVDs, with a Thompson grade I and II, were collected from 7 laboratory (3 CD, 4 NCD) dogs that were euthanized in unrelated animal experiments (experiment numbers: DEC 2007.III.08.110, DEC 2009.III.06.050),and a total of 34 samples, with a Pfirrmann grade II, were collected from 15 laboratory (CD) dogs from previous animal experiments (DEC 2012.III.05.046, DEC 2013.III.02.017). All animal experiments were approved by the Ethics Committee of Animal Experiments (DEC) of Utrecht University. None of the dogs had a history of clinical signs of IVD disease. NP and AF tissues were isolated from the spine and collected separately, snap frozen in liquid nitrogen, and stored at -80 ˚C until further analysis.

IVDs collected during surgical treatment

A total of 123 IVDs were collected from 76 client-owned dogs that were referred to the University Clinic for Companion Animals in Utrecht with IVD disease that required surgical intervention. The diagnosis of IVD disease was confirmed on MRI or CT. Dogs were classified as CD and NCD and divided into subgroups, based on the Pfirrmann grade on T2-weighted MR images [42, 43]. In 10 samples of 6 dogs, in which no MRI was available, grading of the IVD was performed on CT images [43]. The medical history and records of the dogs were screened for information on prior medical treatment of IVD disease and the duration of this treatment.

Diagnostic imaging

Diagnostic imaging was performed in fully anesthetized client-owned dogs, according to standard practice. MRI images were obtained with a 0.2 Tesla open MRI system (Magnetom Open Viva, Siemens AG, Erlangen, Germany) by using multipurpose flex coils until 2013, and thereafter with a 1.5 Tesla scanner (Ingenia, Philips Healthcare, Best, The Netherlands) by using a small-extremity or a posterior coil. For each examination a coil was chosen that fitted around the body of the patient as closely as possible. Sagittal T2-weighted (T2W) images were acquired using a turbo-spin echo pulse sequence with the following parameters: repetition time = 2500 - 3048 ms, echo time = 110 - 120 ms, field of view = 50 x 160/160 x 350 mm, acquisition matrix = 100 x 256/200 x 235 mm, voxel size = 0.6 x 0.8/0.8 x 1.03 mm slice thickness = 2 – 2.5 mm. CT images were obtained with a third-generation single-slice helical CT-scanner (Philips Secura). Contiguous 2 mm thick slices with 1 mm overlap were obtained with exposure settings of 120 kV and 260 mA.

Surgical treatment

Client-owned dogs were anesthetized according to standard of care. Collection of IVDs was achieved through standard surgical procedures, depending on the location of disc herniation: ventral decompression in the cervical area, dorsolateral hemilaminectomy in the thoracolumbar area, and dorsal laminectomy in the lumbosacral area. In dogs with nuclear extrusion (Hansen type I), free NP material was collected from the epidural space in the spinal canal, and AF material was collected during ventral fenestration preceding the ventral decompression for cervical disc herniations, or when an additional lateral fenestration was performed after hemilaminectomy for thoracolumbar disc herniations. In dogs with lumbosacral annular protrusion (Hansen type II), partial discectomy consisting of annulotomy and nucleotomy, allowed separate collection of NP and/or AF tissue. In 3 dogs, an adjacent IVD was fenestrated, and AF and/or NP material was collected. The treatment decision (discectomy, nucleotomy, fenestration) was taken during surgery and depended on the state of the AF and the position of the NP. Each surgeon documented the type of herniation (NP extrusion (Hansen type I) or AF protrusion (Hansen type II)) and type of collected material (NP or AF) in the surgical report.

NP and/or AF tissues were collected in separate vials during surgery, snap frozen into liquid nitrogen within minutes after collection, and subsequently stored at -80 ˚C until further analysis. Details of the samples are shown in Table 1 and in Additional file 1.

Table 1. Sample classification details.

Samples biochemistry					**Samples histopathology**		
	CD dogs		NCD dogs			CD dogs	NCD dogs
#Dogs	58		40		#Dogs	15	10
Age – median (range(mths – yrs))	5 yrs (1 – 11)		2 yrs (8 – 12)		Age – median (range(yrs))	10 yrs (2 – 10)	7 yrs (1– 10)
Spinal location	**NP**	**AF**	**NP**	**AF**	**Spinal location**		
# IVDs	52	47	36	41	# IVDs	19	18
Cervical (C1 – T1)	13	21	10	16	Cervical (C1 – T1)	NA	NA
Thoracolumbar (T1-L1)	21	12	2	NA	Thoracolumbar (T1-L1)	5	8
Lumbar (L1 – S1)	11	7	23	25	Lumbar (L1 – S1)	14	10
Unknown	7	7	1		Unknown		
Degeneration					**Degeneration**		
Grade I (non-surgical)	NA	NA	9[a]	10[a]	Grade I	2	8
Grade II	32[b]	32[c]	9	9	Grade II	4	7
Grade III	7	6	8	8	Grade III	3	3
Grade IV + V	13[d]	9[d]	10	12 + 2	Grade IV + V	3 + 3	3
Displacement					**Displacement**		
NP in situ (non-surgical)	27[d,e]	27[d,e]	9[a]	10[a]	NP in situ	NA	
Nuclear extrusion	24	18	12	7	Nuclear extrusion	NA	
Annular protrusion	1	2	15	24	Annular protrusion	NA	
Treatment					**Treatment**		
No treatment	26	26	14	20	No treatment	NA	
Treatment	24	21	20	20			
NSAID < 1 wk	7	8	7	4	NSAID < 1 wk	NA	
NSAID > 1 wk	6	7	8	9	NSAID > 1 wk	NA	
Steroids < 1 wk	4	2	1	-	Steroids < 1 wk	NA	
Steroids > 1 wk	4	3	2	2	Steroids > 1 wk	NA	
Other medication	3	1	2	5	Other medication	NA	
Unknown	2	-	2	1	Unknown	NA	

[a] samples collected from experimental dogs

[b] 9 samples collected from experimental dogs (non-surgical); 17 samples collected in a previous study [44]

[c] 4 samples collected from experimental dogs (non-surgical); 17 samples collected in a previous study [44]

[d] 1 sample collected via fenestration

[e] samples collected from experimental dogs;17 samples collected in a previous study [44]

CD, chondrodystrophic; NCD, non-chondrodystrophic; mths, months; yrs, years; NA, not available

Biochemical analyses of IVDs collected post-mortem and intra-operatively

Prior to analyses, samples were weighed, and 400 µl and 750 µl lysis buffer (cOmplete lysis M EDTA buffer, Roche diagnostics Nederland B.V., Almere, The Netherlands) was added to NP and AF tissue, respectively. Tissues were lysed in a TissueLyser II (Qiagen, Venlo, The Netherlands) for 2x 60 s at 20 kHz. After centrifugation for 15 minutes at 14.000 g, the volume of the supernatant of each sample was measured and separated from its pellet. A volume of 80 µl was filtered over a 0.22 µm nylon spin-X centrifuge tube filter (8169, Costar, Corning Incorporated, NY, USA) and stored at -80˚C in aliquots for cytokine measurements.

Glycosaminoglycan and DNA assays

To determine GAG and DNA, supernatants and pellets were digested in a papain buffer (250 µg/ml papain (P3125-100 mg, Sigma-Aldrich) + 1.57 mg cysteine HCL (C7880, Sigma-Aldrich)) at 60 ˚C overnight. The 1.9-dimethylmethylene blue (DMMB) assay was used to determine GAG content.[44] A volume of 16 mg DMMB (341088 Sigma-Aldrich) was added to 5 ml 100% ethanol and incubated overnight on a roller bench. A solution of 2.37 g NaCl and 3.04 g glycine in 1 l distilled water with a pH set at 3.00 was sterilized by using a 0.22 µm syringe filter (SLGSV255F Millex-GS Syringe Filter Unit, Merck Millipore, Darmstadt, Germany), added to the DMMB solution, and stored at 4 ˚C, protected from light. Pellets were diluted 1:1000 and supernatants 1:150 in PBS-EDTA. A volume of 100 µl of the dilutions and standards was pipetted into a 96-wells microplate (655199 PS microplate, Greiner Bio-One, Alphen aan den Rijn, Netherlands), and prior to spectrophotometric analysis, 200 µl of DMMB was added to each well. The ratio of absorption at 540 to 595 nm was measured by using a microplate reader (Multimode detector DTX 880, Beckman Coulter). Chondroitin sulphate from shark cartilage (C4384, Sigma-Aldrich) was used as a standard to calculate GAG concentrations. The Quant-iT^{TM} dsDNA Broad-Range assay kit in combination with a Qubit Fluorometer (Invitrogen, Carlsbad, USA) was used according to the manufacturer's protocol to determine the DNA content.

PGE_2 and cytokine assays

PGE_2 levels were determined in the supernatants by using a colorimetric competitive enzyme immunoassay kit (PGE_2 high sensitivity EIA kit, ENZO Life Sciences BVBA, Antwerp, Belgium). A magnetic canine cytokine bead panel based on Luminex® xMAP® technology (#CCYTOMAG-90K/CCYTOMAG-90K-PX13); Milliplex® MAP kit, Millipore Corporation, Billerica, USA) was used to measure twelve different cytokines and chemokines in supernatants: TNF-α, granulocyte-macrophage colony-stimulating factor (GM-CSF), IL-2, IL-6, IL-7, IL-8, IL-10, IL-15, IL-18, chemokine (C-C motif) ligand 2 (CCL2), chemokine (C-X-C motif) ligand 1 (CXCL1), chemokine (C-X-C motif) ligand 10 (CXCL10). Supernatants were diluted 1:2 and were measured according to the manufacturer's instructions. All biochemical values were corrected for weight of the sample.

Collection of post-mortem IVDs for histology

IVDs collected post-mortem

Post-mortem, 37 IVDs were collected from vertebral columns of 16 client-owned dogs that were euthanized for diseases other than IVD disease and submitted for necropsy to the Department of Pathobiology at the Faculty of Veterinary Medicine, Utrecht University, and from 9 experimental dogs in unrelated cardiovascular experiments (DEC 2007.II.01.029, DEC 2011.07.065). Permission to collect material from the client-owned dogs was granted by the owners. None of the dogs had a reported history of back problems. Details of the dogs of which material was collected for histology are shown in Table 1.

Diagnostic imaging

Within 24 hours after euthanasia or death, the vertebral column (T11 – S1) was harvested by using an electric multipurpose saw (Bosch, Stuttgart, Germany). Within 1 hour after dissection, sagittal T2W MR images were obtained with a 0.2 Tesla open MRI system (Magnetom Open Viva, Siemens AG) as described earlier. All lumbar IVDs were graded on midsagittal T2W images according to the Pfirrmann score by two independent investigators (NW, AT) [46].

Histology and immunohistochemistry

After scanning, all muscles were removed and the vertebrae were transected transversely with a band saw (EXAKT tape saw, EXAKT Advanced Technologies GmbH, Norderstedt, Germany), resulting in spinal units (endplate – IVD – endplate). These units were then transected sagittally into two halves by using a diamond band pathology saw (EXAKT 312 saw; EXAKT diamond cutting band 0.1 mm D64; EXAKT Advanced Technologies GmbH, Norderstedt, Germany). Midsagittal slices (3 – 4 mm) were cut from one half and fixed in 4% neutral buffered formaldehyde and decalcified in EDTA. Samples were dehydrated in graded alcohol series, rinsed in xylene, and embedded in paraffin. Sections (5 µm) were cut, deparaffinized and rehydrated, and stained with both hematoxylin (109249, Merck)/eosin (115935, Merck), and with picrosirius red (saturated aqueous picric acid: 36011, Sigma-Aldrich, sirius red: 8015, Klinipath)/alcian blue (alcian blue: 05500, Sigma-Aldrich; glacial acetic acid: 100063, Merck). Histological sections were assessed for the presence of inflammatory cells, and evaluated according to a histological grading scheme described by Bergknut et al [42].

Immunohistochemistry for COX-2 was performed on 5 µm sections mounted on KP plus glass slides (Klinipath B.V., Duiven, The Netherlands). After deparaffinization and rehydration sections were treated with Dual Endogenous Enzyme Block (S2003, Dako, California, USA) for 10 min at room temperature to block nonspecific endogenous peroxidase, followed by 2 washing steps of each 5 min with tris buffered saline containing 1% Tween 20® (TBS-T). Sections were treated with TBS bovine serum albumin (BSA) 5% solution to block non-specific binding for 60 minutes at room temperature. Subsequently they were incubated

with a primary mouse anti-human monoclonal COX-2 antibody (#160112 Clone CX229, Cayman, Ann Arbor, USA) diluted 1:800 in TBS-BSA 5% overnight at 4°C. The following day sections were incubated with peroxidase-labelled polymer (K4007; Envision anti-mouse, Dako) and antibody binding was visualized by using diaminobenzidine (DAB; K4007; Dako). Sections were counterstained with hematoxylin solution (Hematoxylin QS, Vector, Peterborough, UK), rehydrated and mounted in permanent mounting medium. The percentage of COX-2 positive chondrocytes in the NP, and in the dorsal AF (DAF) was determined by manual counting by a blinded independent investigator (AT).

Statistical analyses

Data were analyzed by using R statistical software, package 2.15.2 (http://r-project.org/). A multiple linear regression model was used to analyze the effect of multiple explanatory variables on corrected PGE_2, GAG, and DNA levels for the wet weight of the tissues. Furthermore, in order to be able to compare this study with previous reports [40], PGE_2 levels were also corrected for DNA content. Data were logarithmically transformed to achieve normality. Two separate models were employed to investigate the association of explanatory variables 'grade' (Pfirrmann grade I – IV) and 'herniation' (NP in situ, NP extrusion, AF protrusion) with inflammatory parameters. Variables incorporated into both models were 'dog' (CD, NCD), 'tissue' (NP and AF), 'treatment' (no treatment, NSAID administered less than (<) 1 wk, NSAID administered more than (>) 1 wk, corticosteroids (cort) < 1 wk, cort > 1 wk, other) and their interaction. Residual plots and quantile-quantile (QQ)-plots were used to check the critical assumptions of linearity, equal variance at all fitted values and the assumption of normally distributed residuals. The Cox proportional hazards regression model was used for analysis of the COX-2 values, that did not approximate a normal distribution after log transformation. 'Grade' (Pfirrmann grade I – IV) and 'breed' (CD, NCD) and their interaction were incorporated into this model. Calculations were performed on values distracted from 100%. In the absence of COX-2 positive cells the sample was set at 100% and right censored. Histological reactive changes in the IVDs were statistically evaluated by using the nonparametric Kruskal-Wallis test, followed by a Mann-Whitney U-test. The Spearman's correlation coefficient was calculated to estimate the correlation between the presence of inflammatory cells ('yes' or 'no') and COX-2 positive cells. For all statistical models, regression coefficients were estimated by the maximum likelihood method. Model selection was based on the lowest Akaike Information Criterion (AIC). Confidence intervals were calculated and stated at the 99% confidence level to correct for multiple comparisons. Differences between treatments were considered significant if the confidence interval did not include 0, whereas hazard ratios were considered significant if the confidence interval did not include 1. Significant differences and the corresponding confidence intervals are represented in Additional file 2.

Results

Extracellular matrix components and inflammatory profiles in relation to stage of degeneration

GAG content normalized for wet weight did not significantly change with degeneration grade according to Pfirrmann (Figure 1A and 1B). In grade IV + V samples the GAG content in the NP was significantly lower than in the AF (Figure 1A). DNA expressed as µg/mg wet weight was significantly lower in grade II samples compared with grade IV + V samples (Figure 1B). Due to sample limitations, samples that were above the upper range of the PGE_2 assay (> 1000 pg/ml) were set at 1000 pg/ml. PGE_2 levels normalized for wet weight were significantly lower in grade I NP samples compared with those in grade II, III, and IV + V NP samples (Figure 2A). PGE_2 levels normalized for DNA were significantly lower in grade I samples compared with grade II, III, and IV + V samples regardless of the tissue origin (NP/AF), dog type (CD/NCD), or treatment group (no treatment, NSAID < 1 wk, NSAID > 1 wk, cort < 1 wk, cort > 1 wk, other) (Figure 2B). Cytokines IL-2, IL-6, IL-7, IL-8, IL-10, IL-15, IL-18, IP-10, TNF-α, and GM-CSF were not detectable in the samples. Chemokine CCL2 was measured in 66/120 samples and chemokine CXCL1 in 119/120 samples. CXCL1 and CCL2 expressed as pg/gram wet weight did not significantly change with degeneration (Figure 2C and 2D). There were no significant differences between treatment groups.

Extracellular matrix components and inflammatory profiles in relation to herniation of NP and AF

GAG and DNA (Figure 1C and 1D) and CXCL1 (Figure 2D and 2E) expressed as pg/gram wet weight were not significantly different between herniation groups. PGE_2 levels normalized for either DNA content or wet weight, were significantly lower in non-herniated samples compared with extruded and protruded samples of NCD dogs, regardless of the tissue origin (NP/AF), or treatment group (no treatment, NSAID < 1 wk, NSAID > 1 wk, cort < 1 wk, cort > 1 wk, other). CCL2 levels in the NP from extruded samples were significantly higher compared with the AF of these samples and the NP from protrusion samples regardless of the dog breed (CD/NCD) (Figure 2F). There were no significant differences between biochemical parameters of CD and NCD dogs or treatment groups. Pfirrmann grade II samples from this study were compared with Pfirrmann grade II samples obtained from experimental CD dogs (Figure 3A) [40]. As sample weights were not available in the previous study, PGE_2 was normalized for DNA. In this combined Pfirrmann grade II dataset, PGE_2/DNA in the NP was significantly higher in extruded samples compared with Pfirrmann grade II IVDs with the NP in situ. To compare this combined Pfirrmann grade II dataset to the complete dataset, we have normalized PGE_2 for DNA (Figure 3b and 3c).

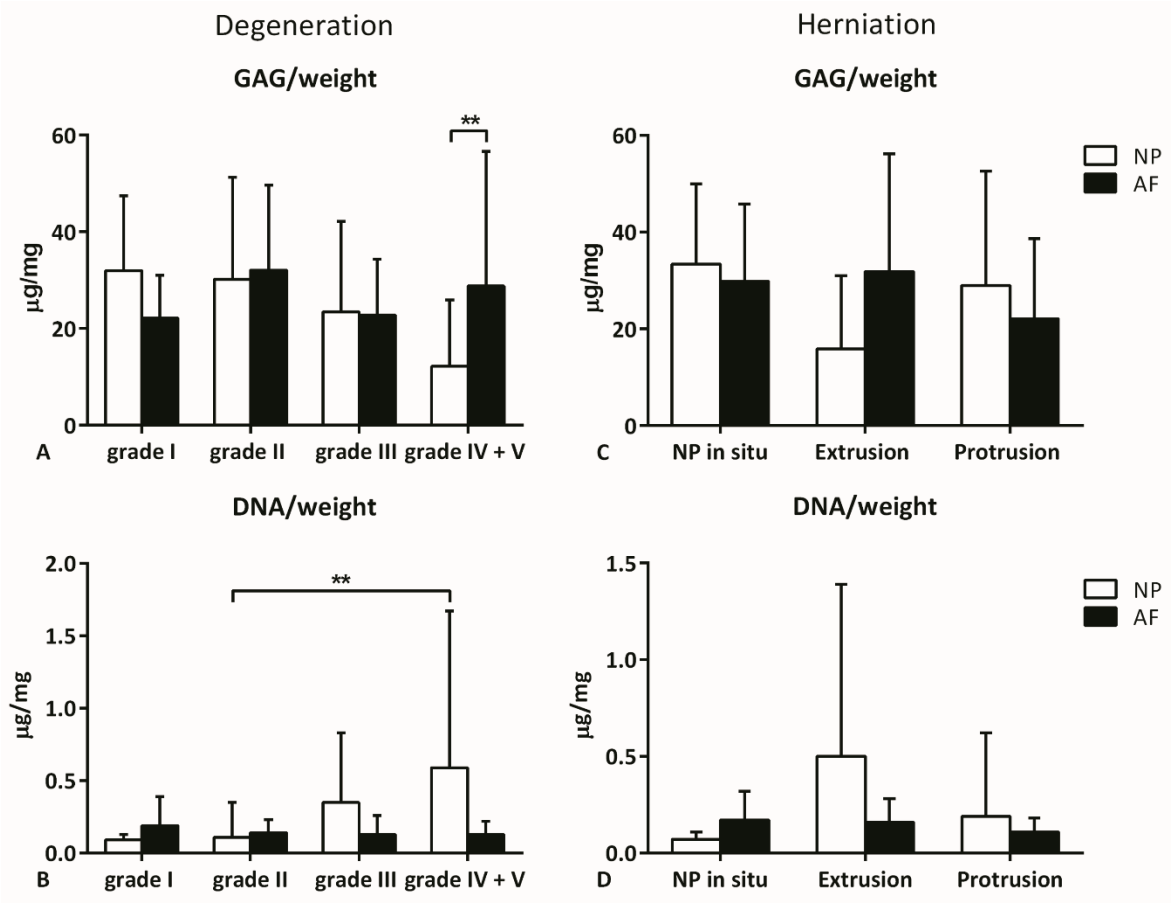

Figure 1. Mean + standard deviation glycosaminoglycan (GAG) and DNA content normalized for weight in the nucleus pulposus (NP) and annulus fibrosus (AF) per Pfirrmann grade (**A and B**) and per herniation (**C and D**). **A**. GAG/weight levels were significantly higher in the AF compared with the NP in grade IV + V samples. **B.** DNA/weight was significantly lower in the NP of grade II samples compared with grade IV + V. **C** and **D**. Normalized GAG and DNA levels did not significantly differ between herniation groups. No significant differences were shown between dog (chondrodystrophic, non-chondrodystrophic) or treatment (no treatment, NSAID < 1 wk, NSAID > 1 wk, corticosteroids (cort) < 1 wk, cort > 1 wk, other) groups, hence these groups are not shown separately. *** Indicates significant difference at a 99% confidence level.*

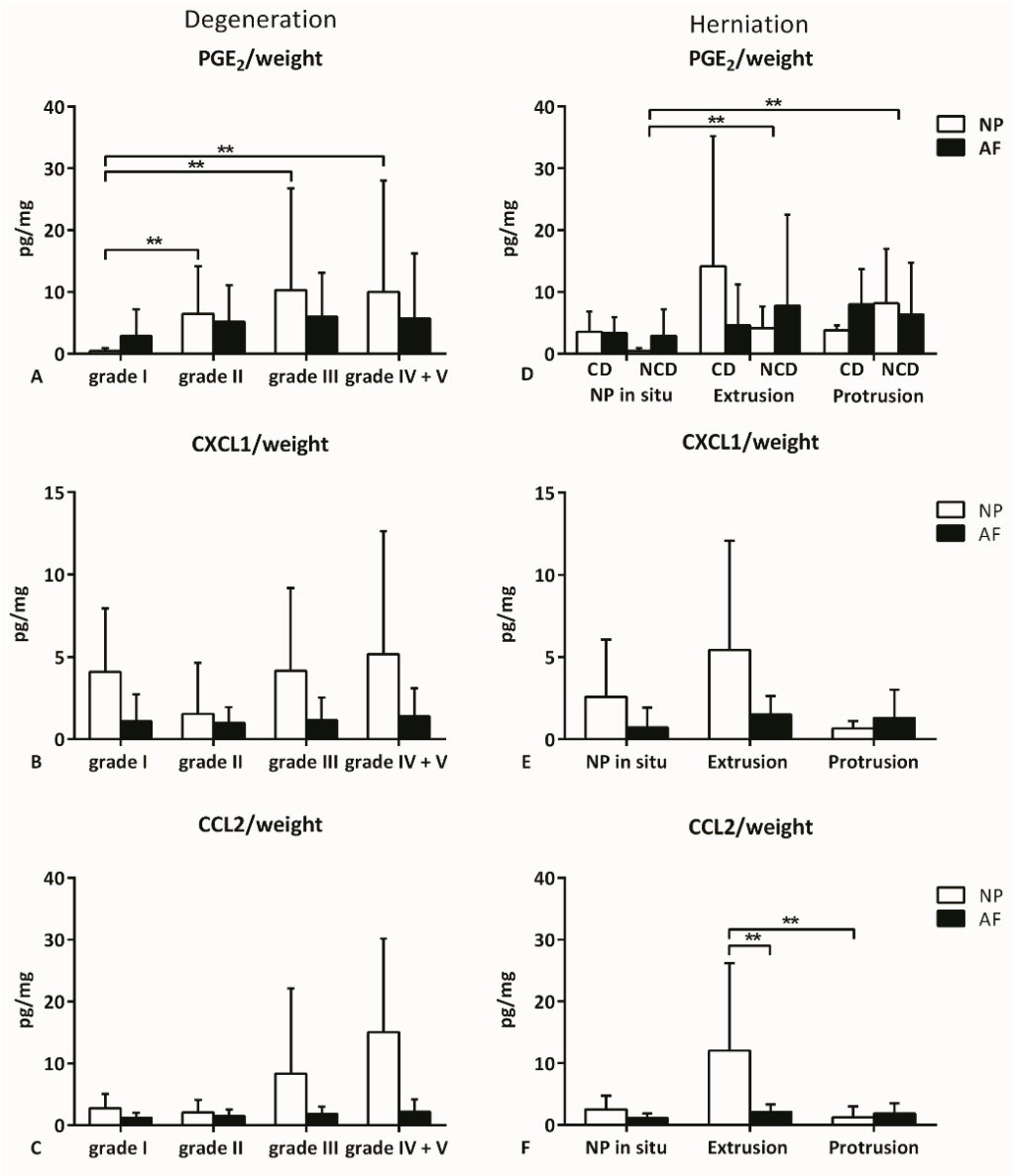

Figure 2. Mean + standard deviation prostaglandin E_2 (PGE_2) and chemokine (C-C motif) ligand 2 (CCL2) and chemokine (C-X-C motif) ligand 1 (CXCL1) levels normalized for weight in the nucleus pulposus (NP) and annulus fibrosus (AF) per Pfirrmann grade (**A, B, C**) and per herniation (**D, E, F**). **A.** PGE_2 levels expressed as pg/mg wet weight in grade I NP samples were significantly lower compared with grade II, III, and IV + V NP samples. **B** and **C.** CCL2 and CXCL1 levels normalized for weight did not significantly change with degeneration. **D.** PGE_2 levels did not significantly differ in the NP and AF between the three herniation groups. **E.** CXCL1 levels did not significantly differ between herniation groups. **F.** CCL2 levels normalized for weight in the NP from extruded samples were significantly higher compared with the AF of these samples and the NP from protruded samples. No significant differences were shown between treatment (no treatment, NSAID < 1 wk, NSAID > 1 wk, corticosteroids (cort) < 1 wk, cort > 1 wk, other) groups, hence these groups are not shown separately. *** Indicates significant difference at a 99% confidence level.*

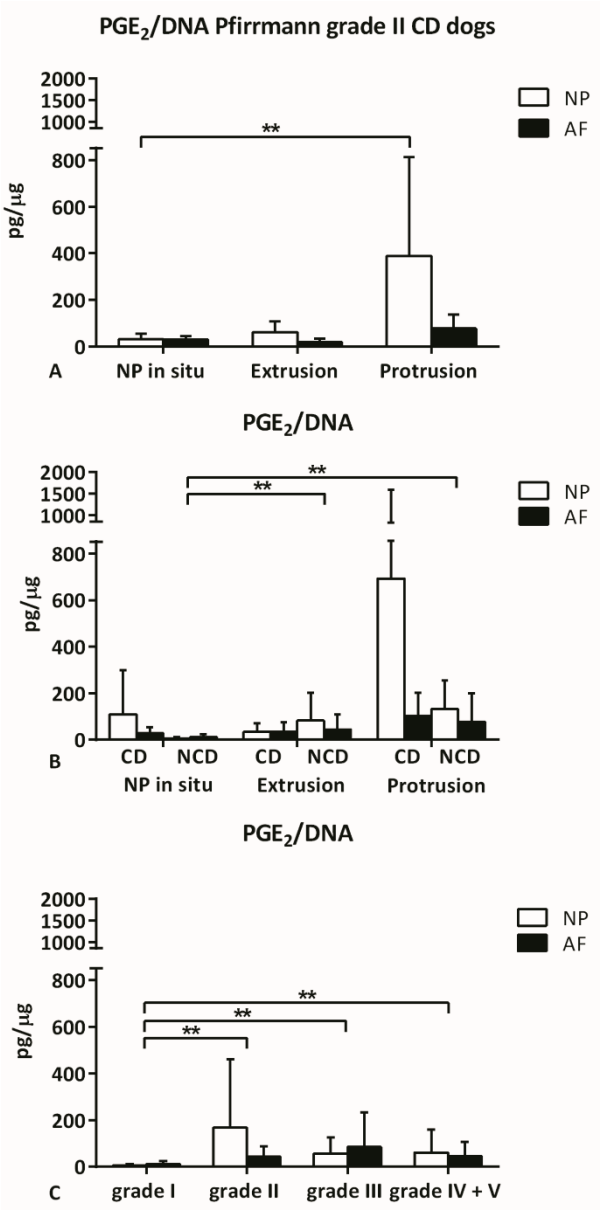

Figure 3. Mean + standard deviation PGE_2 levels normalized for DNA content in the nucleus pulposus (NP) and annulus fibrosus (AF) in Pfirrmann grade II samples obtained from experimental chondrodystrophic (CD) dogs (**A**), and in the complete dataset (CD and non-chondrodystrophic (NCD) dogs) per Pfirrmann grade (**B**), and per herniation (**C**). **A**. PGE_2 levels expressed as pg/µg DNA in the NP of CD dogs were significantly higher in protruded grade II samples compared with NP in situ samples. **B.** PGE_2 levels normalized for DNA were significantly lower in grade I samples compared with grade II, III, and IV + V samples regardless of the tissue origin (NP/AF), dog group (CD/NCD), or treatment group (no treatment, NSAID < 1 wk, NSAID > 1 wk, corticosteroids (cort) < 1 wk, cort > 1 wk, other). **C.** PGE_2 levels expressed as pg/µg DNA were significantly lower in non-herniated samples compared with extruded and protruded samples in NCD dogs, regardless of the tissue origin (NP/AF), or treatment group (no treatment, NSAID < 1 wk, NSAID > 1 wk, corticosteroids (cort) < 1 wk, cort > 1 wk, other). *** Indicates significant difference at a 99% confidence level.*

Histology and COX-2 expression

Histological scores according to the grading scheme by Bergknut et al. ranged from 7 – 12 (median = 8) for Pfirrmann grade I, 8 – 27 (median = 14) for Pfirrmann grade II, 14 – 20 (median =19) for Pfirrmann grade III, and 18 – 26 (median = 21) for Pfirrmann grade IV + V. In 5/37 IVDs from 3/16 dogs ventral bone formation was seen in grade I – V IVDs. Histology revealed no inflammatory cells or fibroblasts in the NP of Pfirrmann grade I – V IVDs, and in the dorsal AF of Pfirrmann grade I IVDs. However, in higher degeneration grades, focal infiltration of macrophages, proliferation of fibroblasts and capillaries were detected in the dorsal and/or the ventral ligament, extending into the outer layers of the dorsal and ventral AF, respectively (Figure 4). Macrophages and proliferation of fibroblasts were present in 0% (0/10), 10% (1/10), 83% (5/6) and 55% (6/11) of the IVDs scored a Pfirrmann grade I, II, III, IV + V, respectively. Numbers of macrophages and fibroblasts in grade IV + V IVDs were significantly higher than in grade I, and in grade III significantly higher than in grade I and II. Protrusion of the AF was seen in a grade II and a grade IV + V IVD.

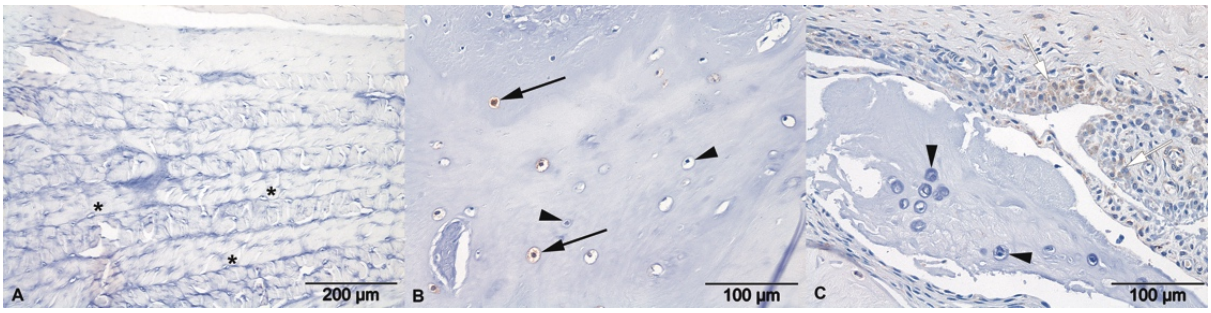

Figure 4. Representative histological images of the annulus fibrosus (AF) of intervertebral discs (IVDs) graded according to Pfirrmann stained with a cyclooxygenase-2 (COX-2) antibody and counterstained with hematoxylin. **A.** The dorsal AF of a non-degenerated Pfirrmann grade 1 IVD consisted of well-organized lamellae with COX-2 negative spindle-shaped fibroblasts (asterisks). **B**. In the dorsal AF of a degenerated Pfirrmann grade IV IVD lamellar organization was lost and COX-2 negative chondrocytes (arrowheads) as well as COX-2 positive chondrocytes (arrows) were present. **c**. The dorsal AF of a Pfirrmann grade V IVD consisted of COX-2 negative chondrocytes (arrowheads), whereas COX-2 positive macrophages (open arrows) were situated in the dorsal ligament. Percentages of COX-2-positive cells in the NP and dorsal AF of grade I and grade II tissue were significantly lower compared with the NP and dorsal AF of grade IV + V samples (Figure 5). The presence of macrophages and fibroblasts in the dorsal AF was moderately correlated (Spearman's ρ = 0.4, *p*-value = 0.003) with COX-2 positive cells in the dorsal AF.

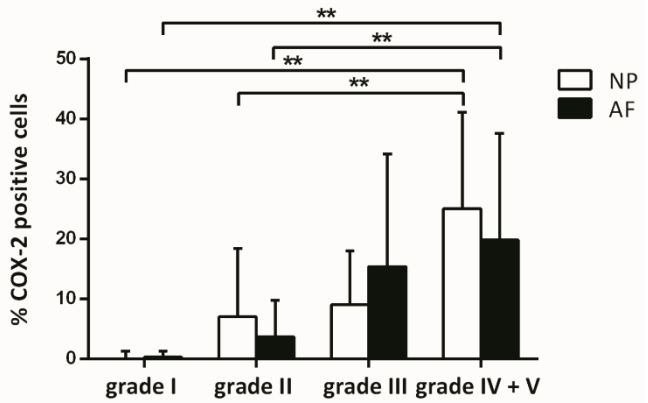

Figure 5. Percentage of COX-2-positive cells in the nucleus pulposus (NP) and annulus fibrosus (AF) per Pfirrmann grade. The NP and AF of grade I and grade II samples were significantly lower compared with the NP and AF grade IV + V samples. *** Indicates significant difference at a 99% confidence level.*

Discussion

To our knowledge this is the first study that describes levels of COX-2, PGE_2, cytokines, chemokines, and matrix components in IVDs from CD and NCD dogs with and without clinical signs of IVD disease and degeneration. PGE_2 levels were significantly higher in degenerated IVDs compared with non-degenerated IVDs, and they were also higher in herniated (protruded and extruded) IVDs from NCD dogs compared with non-herniated IVDs of NCD dogs. In contrast to PGE_2 levels in Pfirrmann grade II IVDs from CD dogs with (a limited number of) protruded IVDs, PGE_2 levels in extruded IVDs were not significantly different from IVDs with the NP in situ. Furthermore, COX-2 protein expression was significantly higher in degenerated IVDs compared with non-degenerated IVDs. These results are

consistent with findings in herniated human lumbar IVD cells that produced increased PGE_2 levels spontaneously *in vitro* compared with PGE_2 levels in control IVD cells [15].

Contrary to PGE_2 levels, COX-2 expression in the NP and AF and numbers of macrophages in the dorsal and ventral ligaments were increased in advanced stages of degeneration. Histological results of non-herniated degenerated IVDs in our study are consistent with histological findings described in studies on canine herniated IVDs. In extruded IVDs an acute inflammatory reaction has been described, characterized by neutrophils and macrophages, while in protruded IVDs a more chronic inflammatory reaction has been described, characterized by macrophages, lymphocytes and plasma cells [47, 48]. Macrophages do not only have a phagocytic function, but secret next to cytokines also a number of growth factors, e.g. fibroblast growth factor, transforming growth factor beta, that can induce neovascularization and mediate cell proliferation and differentiation [49]. The focal infiltrates of macrophages, proliferation of fibroblasts and capillaries, and the new bone formation as was seen histologically in some IVDs are reactive tissue changes that might reflect a process of tissue repair. Although a physiological inflammatory response to aseptic tissue injury primarily serves to promote tissue repair, macroscopic findings may reflect an excessive inflammatory response. This response may have detrimental effects on tissue integrity, and may contribute to the pathogenesis of IVD degeneration and/or disease.

Significantly higher PGE_2 levels in degenerated NP tissues compared with non-degenerated IVDs were observed. Although not significantly different, PGE_2 levels and COX-2 expression in grade II and IV + V IVDs were consistently higher in the NP of degenerated IVDs compared with AF, while the contrary was true for non-degenerated IVDs. In Pfirrmann grade II samples from CD dogs, PGE_2 levels in the NP were significantly higher in Pfirrmann grade II IVDs with protrusion compared with IVDs with the NP in situ. This may indicate that the production of inflammatory mediators is more pronounced at the NP level. We cannot exclude that NP and AF cells respond differently to inflammatory stimuli and mechanic stress and hence produce different levels of PGE_2, as also suggested by others based on *in vitro* experiments in rat IVD cells [50]. Cytokine and chemokine profiles in this study are largely consistent with limited veterinary publications. The significantly increased CCL2 levels in NP tissue of dogs with Hansen type I herniation compared with AF tissue and NP tissue in dogs with Hansen type II herniation are in line with other studies reporting upregulated gene expression levels of CCL2 in dogs with extrusion of the NP [36]. Furthermore, increased CCL2 protein expression and CCL2 production levels have been reported in human prolapsed IVDs [28]. No studies in canine tissues, and only limited studies in human tissues, have determined cytokine and/or chemokine levels by using a (multiplex) sandwich immunoassay, and have shown increased levels of IFN-γ, IL-1, TNF-α, and CCL2, in epidural lavage fluid and in cell culture media, which complicates comparison of results [51-53]. Cytokine levels of IL-2, IL-6, IL-7, IL-8, IL-10, IL-15, IL-18, IP-10, TNF-α, and GM-CSF were not detected in NP and AF tissues of this study, consistent with downregulated gene expression levels of IL-2, IL-6, IL-10, and TNF-α in herniated canine IVDs [36]. Nevertheless, our findings seem to be in contrast with

increased protein and gene expression levels of TNF-α and IL-1 in human IVDs [22, 23, 25, 28, 29, 54]. Given the short half-life of TNF- α and cytokines [55, 56], and that all samples collected from degenerated IVDs were obtained during surgery and in several cases after flushing of the spinal canal, we cannot rule out degradation of cytokines/chemokines by the collection, preparation, and storage process. Although several studies have shown that IVD cells have the capacity to produce PGE_2, we cannot rule out that PGE_2 levels were influenced by infiltration from the epidural space.

Despite elevated PGE_2 levels in degenerated NP tissue in this study, GAG content was not significantly different between healthy and degenerated IVDs, while severely degenerated AFs (grade IV + V) had a higher GAG content compared with the NP. The latter may be explained by the presence of GAG-producing chondrocytes in the AF, known to be present in later stages of degeneration [46], or by the presence of unidentified GAG-rich herniated NP and/or inner AF material in AF samples. These findings are in contrast with the decrease in GAG content with increasing IVD degeneration described in literature [1, 11]. One plausible explanation for this discrepancy lies in the scoring system of degeneration prior to surgery and the matrix heterogeneity of the degenerated NP tissue, discussed in detail below. Interestingly, cell density (DNA/weight) in our study was significantly higher in the NP of severely degenerated IVDs compared with mildly degenerated IVDs. These findings touch upon findings in human IVD degeneration, in which cell density in the inner AF and NP of severely degenerated (Thompson grade V) specimens was significantly higher compared with lower grades [57, 58].

The results on the effects of PGE_2 on proteoglycan metabolism are conflicting. PGE_2 at concentrations much lower than those involved in inflammation have been demonstrated to be chondroprotective [59]. PGE_2 has been described to have anti-catabolic effects by downregulating the expression and synthesis of IL-1, TNF- α, and matrix metalloproteinases (MMPs), and to have anabolic effects by to inducing the expression, synthesis and secretion of IGF-I, and stimulating collagen and proteoglycan synthesis, important factors in anabolic processes [16, 60, 61]. *In vitro*, low concentrations of PGE_2 have been described to stimulate proteoglycan synthesis in rat chondrocytes, whereas higher doses have been described to decrease proteoglycan synthesis in NP cells [16, 61]. Furthermore, degradation of proteoglycans was not inhibited by a range of PGE_2 concentrations in osteoarthritic chondrocytes [62]. These possible protective effects of PGE_2 might have resulted in preservation of GAG content in the course of IVD degeneration. Nevertheless, these results should be interpreted with care, as GAG content of the studied tissues may have been affected by confounding factors explained below.

There are several confounding factors that may affect the results in the current study, including the factors that influence the scoring system of degeneration and the matrix heterogeneity of the degenerated NP tissue. Extruded NP tissue displaced into the vertebral canal results in narrowing of the disc space and a T2-hypointense area within the IVD on

MRI. Hence, we cannot exclude that prior to the extrusion incident the IVD may have been assessed with a lower Pfirrmann score. Moreover, in CD dogs, calcification of the NP could have negatively influenced the signal intensity in the NP [63, 64]. In addition, in both CD and NCD dogs, IVDs may have been graded falsely higher due to hemorrhage or inflammation, that may have influenced the appearance of the IVD on MR images. Matrix heterogeneity is common in degenerating NP tissue. In human IVDs several disc-specific locations are described with a high variation in GAG and water content, suggestive of focal damage and degeneration [65]. Although this has not yet been described in dogs, we cannot rule out that tissues collected during surgery may have originated from specific GAG-rich areas in the IVD, that inherently are more prone to extrusion/protrusion compared with degenerated fibrotic tissue. Furthermore, due to sample limitations PGE_2 values higher than 1000 pg/ml could not be measured reliably, but could have resulted in an underestimation of the highest samples. Lastly, a relatively high percentage of dogs in this study was treated prior to surgery with anti-inflammatory drugs, e.g. NSAIDs and corticosteroids. Dogs that did not respond to anti-inflammatory drugs initially, were treated with other drugs, e.g. opioids, GABA-agonists. Although treatment groups were categorized, duration of treatment and dosages used showed a high variation, and might have had an influence on the results.

From a clinical perspective, decompression surgery is recommended if dogs present with clinical signs, and diagnostic work-up indicates compression of neural tissue (spinal cord and/or nerve roots) due to extruded material. With regard to an intradiscal application that provides controlled release of an anti-inflammatory drug, future studies should focus on protruded IVDs. Obviously, this would indicate development of an application in NCD dogs, as disc protrusion rarely occurs in CD dogs. IVDs ideally should be early degenerated (Pfirrmann grade II – III), without irreversible anatomical malformations due to degenerative changes.

In this study we have shown that PGE_2 levels, and CCL2 levels in degenerated and herniated tissues were significantly higher compared with non-degenerated and non-herniated tissues. COX-2 expression in the NP and AF and numbers of macrophages in the AF increased with advancing degeneration stages. Although macrophages invade the dorsal and ventral AF as degeneration progresses, the production of inflammatory mediators seems most pronounced in degenerated NP tissue. Future studies are needed to investigate if inhibition of PGE_2 levels in degenerated IVDs provide effective analgesia and exerts a protective role in the process of IVD degeneration and the development of IVD disease.

Acknowledgements

We would like to thank Arie Doornenbal and Elise Petersen for their technical assistance.

References

1. Bergknut N, Rutges JP, Kranenburg HJ, Smolders LA, Hagman R, Smidt HJ*, et al*. The dog as an animal model for intervertebral disc degeneration? Spine (Phila Pa.1976) 2012;37:351-8.
2. Cudia SP and Duval JM. Thoracolumbar intervertebral disk disease in large, nonchondrodystrophic dogs: a retrospective study. J.Am.Anim.Hosp.Assoc. 1997;33:456-60.
3. Macias C, McKee WM, May C, Innes JF. Thoracolumbar disc disease in large dogs: a study of 99 cases. J.Small Anim.Pract. 2002;43:439-46.
4. Schmied O, Golini L, Steffen F. Effectiveness of cervical hemilaminectomy in canine Hansen Type I and Type II disc disease: a retrospective study. J.Am.Anim.Hosp.Assoc. 2011;47:342-50.
5. Suwankong N, Meij BP, Voorhout G, de Boer AH, Hazewinkel HA. Review and retrospective analysis of degenerative lumbosacral stenosis in 156 dogs treated by dorsal laminectomy. Vet.Comp.Orthop.Traumatol. 2008;21:285-93.
6. Brisson BA. Intervertebral disc disease in dogs. Vet.Clin.North Am.Small Anim.Pract. 2010;40:829-58.
7. Levine JM, Levine GJ, Kerwin SC, Hettlich BF, Fosgate GT. Association between various physical factors and acute thoracolumbar intervertebral disk extrusion or protrusion in Dachshunds. J.Am.Vet.Med.Assoc. 2006;229:370-5.
8. Hansen HJ. A pathologic-anatomical study on disc degeneration in dog, with special reference to the so-called enchondrosis intervertebralis. Acta Orthop.Scand.Suppl. 1952;11:1-117.
9. Smolders LA, Bergknut N, Grinwis GC, Hagman R, Lagerstedt AS, Hazewinkel HA*, et al*. Intervertebral disc degeneration in the dog. Part 2: chondrodystrophic and non-chondrodystrophic breeds. Vet.J. 2013;195:292-9.
10. Adams MA and Roughley PJ. What is intervertebral disc degeneration, and what causes it? Spine (Phila Pa.1976) 2006;31:2151-61.
11. Roughley PJ. Biology of intervertebral disc aging and degeneration: involvement of the extracellular matrix. Spine (Phila Pa.1976) 2004;29:2691-9.
12. Brisby H. Pathology and possible mechanisms of nervous system response to disc degeneration. J.Bone Joint Surg.Am. 2006;88 Suppl 2:68-71.
13. Freemont AJ, Peacock TE, Goupille P, Hoyland JA, O'Brien J, Jayson MI. Nerve ingrowth into diseased intervertebral disc in chronic back pain. Lancet 1997;350:178-81.
14. Ahn SH, Cho YW, Ahn MW, Jang SH, Sohn YK, Kim HS. mRNA expression of cytokines and chemokines in herniated lumbar intervertebral discs. Spine (Phila Pa.1976) 2002;27:911-7.
15. Kang JD, Georgescu HI, McIntyre-Larkin L, Stefanovic-Racic M, Donaldson WF,3rd, Evans CH. Herniated lumbar intervertebral discs spontaneously produce matrix metalloproteinases, nitric oxide, interleukin-6, and prostaglandin E2. Spine (Phila Pa.1976) 1996;21:271-7.
16. Vo NV, Sowa GA, Kang JD, Seidel C, Studer RK. Prostaglandin E2 and prostaglandin F2alpha differentially modulate matrix metabolism of human nucleus pulposus cells. J.Orthop.Res. 2010;28:1259-66.
17. Li W, Liu T, Wu L, Chen C, Jia Z, Bai X*, et al*. Blocking the function of inflammatory cytokines and mediators by using IL-10 and TGF-beta: a potential biological immunotherapy for intervertebral disc degeneration in a beagle model. Int.J.Mol.Sci. 2014;15:17270-83.
18. Burke JG, Watson RW, McCormack D, Dowling FE, Walsh MG, Fitzpatrick JM. Spontaneous production of monocyte chemoattractant protein-1 and interleukin-8 by the human lumbar intervertebral disc. Spine (Phila Pa.1976) 2002;27:1402-7.
19. Hoyland JA, Le Maitre C, Freemont AJ. Investigation of the role of IL-1 and TNF in matrix degradation in the intervertebral disc. Rheumatology (Oxford) 2008;47:809-14.
20. Hughes SP, Freemont AJ, Hukins DW, McGregor AH, Roberts S. The pathogenesis of degeneration of the intervertebral disc and emerging therapies in the management of back pain. J.Bone Joint Surg.Br. 2012;94:1298-304.
21. Kepler CK, Markova DZ, Hilibrand AS, Vaccaro AR, Risbud MV, Albert TJ*, et al*. Substance P stimulates production of inflammatory cytokines in human disc cells. Spine (Phila Pa.1976) 2013;38:E1291-9.
22. Le Maitre CL, Hoyland JA, Freemont AJ. Catabolic cytokine expression in degenerate and herniated human intervertebral discs: IL-1beta and TNFalpha expression profile. Arthritis Res.Ther. 2007;9:R77.
23. Le Maitre CL, Pockert A, Buttle DJ, Freemont AJ, Hoyland JA. Matrix synthesis and degradation in human intervertebral disc degeneration. Biochem.Soc.Trans. 2007;35:652-5.
24. Le Maitre CL, Binch AL, Thorpe AA, Hughes SP. Degeneration of the intervertebral disc with new approaches for treating low back pain. J.Neurosurg.Sci. 2015;59:47-61.

25. Le Maitre CL, Hoyland JA, Freemont AJ. Interleukin-1 receptor antagonist delivered directly and by gene therapy inhibits matrix degradation in the intact degenerate human intervertebral disc: an in situ zymographic and gene therapy study. Arthritis Res.Ther. 2007;9:R83.
26. Le Maitre CL, Freemont AJ, Hoyland JA. The role of interleukin-1 in the pathogenesis of human intervertebral disc degeneration. Arthritis Res.Ther. 2005;7:R732-45.
27. Park JY, Pillinger MH, Abramson SB. Prostaglandin E2 synthesis and secretion: the role of PGE2 synthases. Clin.Immunol. 2006;119:229-40.
28. Phillips KL, Chiverton N, Michael AL, Cole AA, Breakwell LM, Haddock G*, et al*. The cytokine and chemokine expression profile of nucleus pulposus cells: implications for degeneration and regeneration of the intervertebral disc. Arthritis Res.Ther. 2013;15:R213.
29. Purmessur D, Walter BA, Roughley PJ, Laudier DM, Hecht AC, Iatridis J. A role for TNFalpha in intervertebral disc degeneration: a non-recoverable catabolic shift. Biochem.Biophys.Res.Commun. 2013;433:151-6.
30. Shamji MF, Setton LA, Jarvis W, So S, Chen J, Jing L*, et al*. Proinflammatory cytokine expression profile in degenerated and herniated human intervertebral disc tissues. Arthritis Rheum. 2010;62:1974-82.
31. Takahashi H, Suguro T, Okazima Y, Motegi M, Okada Y, Kakiuchi T. Inflammatory cytokines in the herniated disc of the lumbar spine. Spine (Phila Pa.1976) 1996;21:218-24.
32. Wang J, Markova D, Anderson DG, Zheng Z, Shapiro IM, Risbud MV. TNF-alpha and IL-1beta promote a disintegrin-like and metalloprotease with thrombospondin type I motif-5-mediated aggrecan degradation through syndecan-4 in intervertebral disc. J.Biol.Chem. 2011;286:39738-49.
33. Wang J, Tian Y, Phillips KL, Chiverton N, Haddock G, Bunning RA*, et al*. Tumor necrosis factor alpha- and interleukin-1beta-dependent induction of CCL3 expression by nucleus pulposus cells promotes macrophage migration through CCR1. Arthritis Rheum. 2013;65:832-42.
34. Weiler C, Nerlich AG, Bachmeier BE, Boos N. Expression and distribution of tumor necrosis factor alpha in human lumbar intervertebral discs: a study in surgical specimen and autopsy controls. Spine (Phila Pa.1976) 2005;30:44,53; discussion 54.
35. Iwata M, Ochi H, Asou Y, Haro H, Aikawa T, Harada Y*, et al*. Variations in gene and protein expression in canine chondrodystrophic nucleus pulposus cells following long-term three-dimensional culture. PLoS One 2013;8:e63120.
36. Karli P, Martle V, Bossens K, Summerfield A, Doherr MG, Turner P*, et al*. Dominance of chemokine ligand 2 and matrix metalloproteinase-2 and -9 and suppression of pro-inflammatory cytokines in the epidural compartment after intervertebral disc extrusion in a canine model. Spine J. 2014;14:2976-84.
37. Brock TG, McNish RW, Peters-Golden M. Arachidonic acid is preferentially metabolized by cyclooxygenase-2 to prostacyclin and prostaglandin E2. J.Biol.Chem. 1999;274:11660-6.
38. Clark TP. The clinical pharmacology of cyclooxygenase-2-selective and dual inhibitors. Vet.Clin.North Am.Small Anim.Pract. 2006;36:1061,85, vii.
39. Nell T, Bergman J, Hoeijmakers M, Van Laar P, Horspool LJ. Comparison of vedaprofen and meloxicam in dogs with musculoskeletal pain and inflammation. J.Small Anim.Pract. 2002;43:208-12.
40. Willems N, Yang HY, Langelaan ML, Tellegen AR, Grinwis GC, Kranenburg HJ*, et al*. Biocompatibility and intradiscal application of a thermoreversible celecoxib-loaded poly-N-isopropylacrylamide MgFe-layered double hydroxide hydrogel in a canine model. Arthritis Res.Ther. 2015;17:214,015-0727-x.
41. Samad TA, Moore KA, Sapirstein A, Billet S, Allchorne A, Poole S*, et al*. Interleukin-1beta-mediated induction of Cox-2 in the CNS contributes to inflammatory pain hypersensitivity. Nature 2001;410:471-5.
42. Bergknut N, Auriemma E, Wijsman S, Voorhout G, Hagman R, Lagerstedt AS*, et al*. Evaluation of intervertebral disk degeneration in chondrodystrophic and nonchondrodystrophic dogs by use of Pfirrmann grading of images obtained with low-field magnetic resonance imaging. Am.J.Vet.Res. 2011;72:893-8.
43. Harder L, Ludwig D, Galindo-Zamora V, Wefstaedt P, Nolte I. Classification of canine intervertebral disc degeneration using high-field magnetic resonance imaging and computed tomography. Tierarztl.Prax.Ausg.K.Kleintiere Heimtiere 2014;42:374-82.
44. Johnston SA, McLaughlin RM, Budsberg SC. Nonsurgical management of osteoarthritis in dogs. Vet.Clin.North Am.Small Anim.Pract. 2008;38:1449,70, viii.
45. Farndale RW, Sayers CA, Barrett AJ. A direct spectrophotometric microassay for sulfated glycosaminoglycans in cartilage cultures. Connect.Tissue Res. 1982;9:247-8.
46. Bergknut N, Meij BP, Hagman R, de Nies KS, Rutges JP, Smolders LA*, et al*. Intervertebral disc disease in dogs - Part 1: A new histological grading scheme for classification of intervertebral disc degeneration in dogs. Vet.J. 2013;195:156-63.

47. Kranenburg HJ, Grinwis GC, Bergknut N, Gahrmann N, Voorhout G, Hazewinkel HA*, et al*. Intervertebral disc disease in dogs - Part 2: Comparison of clinical, magnetic resonance imaging, and histological findings in 74 surgically treated dogs. Vet.J. 2013;195:164-71.
48. Royal AB, Chigerwe M, Coates JR, Wiedmeyer CE, Berent LM. Cytologic and histopathologic evaluation of extruded canine degenerate disks. Vet.Surg. 2009;38:798-802.
49. Varol C, Mildner A, Jung S. Macrophages: development and tissue specialization. Annu.Rev.Immunol. 2015;33:643-75.
50. Miyamoto H, Doita M, Nishida K, Yamamoto T, Sumi M, Kurosaka M. Effects of cyclic mechanical stress on the production of inflammatory agents by nucleus pulposus and anulus fibrosus derived cells in vitro. Spine (Phila Pa.1976) 2006;31:4-9.
51. Schroeder M, Viezens L, Schaefer C, Friedrichs B, Algenstaedt P, Ruther W*, et al*. Chemokine profile of disc degeneration with acute or chronic pain. J.Neurosurg.Spine 2013;18:496-503.
52. Scuderi GJ, Brusovanik GV, Anderson DG, Dunham CJ, Vaccaro AR, Demeo RF*, et al*. Cytokine assay of the epidural space lavage in patients with lumbar intervertebral disk herniation and radiculopathy. J.Spinal.Disord.Tech. 2006;19:266-9.
53. Scuderi GJ, Cuellar JM, Cuellar VG, Yeomans DC, Carragee EJ, Angst MS. Epidural interferon gamma-immunoreactivity: a biomarker for lumbar nerve root irritation. Spine (Phila Pa.1976) 2009;34:2311-7.
54. Risbud MV and Shapiro IM. Role of cytokines in intervertebral disc degeneration: pain and disc content. Nat.Rev.Rheumatol. 2014;10:44-56.
55. Oliver JC, Bland LA, Oettinger CW, Arduino MJ, McAllister SK, Aguero SM. Cytokine kinetics in an in vitro whole blood model following an endotoxin challenge. 1993;12:115-20.
56. Tarrant JM. Blood cytokines as biomarkers of in vivo toxicity in preclinical safety assessment: considerations for their use. Toxicol.Sci. 2010;117:4-16.
57. Hastreiter D, Ozuna RM, Spector M. Regional variations in certain cellular characteristics in human lumbar intervertebral discs, including the presence of alpha-smooth muscle actin. J.Orthop.Res. 2001;19:597-604.
58. Zhao CQ, Wang LM, Jiang LS, Dai LY. The cell biology of intervertebral disc aging and degeneration. Ageing Res.Rev. 2007;6:247-61.
59. Tchetina EV, Di Battista JA, Zukor DJ, Antoniou J, Poole AR. Prostaglandin PGE2 at very low concentrations suppresses collagen cleavage in cultured human osteoarthritic articular cartilage: this involves a decrease in expression of proinflammatory genes, collagenases and COL10A1, a gene linked to chondrocyte hypertrophy. Arthritis Res.Ther. 2007;9:R75.
60. Knudsen PJ, Dinarello CA, Strom TB. Prostaglandins posttranscriptionally inhibit monocyte expression of interleukin 1 activity by increasing intracellular cyclic adenosine monophosphate. J.Immunol. 1986;137:3189-94.
61. Lowe GN, Fu YH, McDougall S, Polendo R, Williams A, Benya PD*, et al*. Effects of prostaglandins on deoxyribonucleic acid and aggrecan synthesis in the RCJ 3.1C5.18 chondrocyte cell line: role of second messengers. Endocrinology 1996;137:2208-16.
62. Di Battista JA, Dore S, Martel-Pelletier J, Pelletier JP. Prostaglandin E2 stimulates incorporation of proline into collagenase digestible proteins in human articular chondrocytes: identification of an effector autocrine loop involving insulin-like growth factor I. Mol.Cell.Endocrinol. 1996;123:27-35.
63. Jensen VF, Beck S, Christensen KA, Arnbjerg J. Quantification of the association between intervertebral disk calcification and disk herniation in Dachshunds. J.Am.Vet.Med.Assoc. 2008;233:1090-5.
64. Jensen VF and Arnbjerg J. Development of intervertebral disk calcification in the dachshund: a prospective longitudinal radiographic study. J.Am.Anim.Hosp.Assoc. 2001;37:274-82.
65. Iatridis JC, MacLean JJ, O'Brien M, Stokes IA. Measurements of proteoglycan and water content distribution in human lumbar intervertebral discs. Spine (Phila Pa.1976) 2007;32:1493-7.

Additional file1. A more detailed representation of included samples in addition to Table 1 in the original article

NP = nucleus pulposus, CD = chondrodystrophic, Extr = nuclear extrusion, Protr = annular protrusion, NCD = non-chondrodystrophic, AF = annulus fibrosus, NSAID = non-steroidal anti-inflammatory drug, Cort = corticosteroids, NA = not available.

	NP CD	NP in situ/ Extr/Protr	Treatment	NP NCD	NP in situ/ Extr/Protr	Treatment	AF CD	NP in situ/ Extr/Protr	Treatment	AF NCD	NP in situ/ Extr/Protr	Treatment
Grade I	**17**	**17**	17: No	**1**	**9**	9: No	**17**	**17**	17: No	**10**	**10**	10: No
		0			**0**			**0**			**0**	
		0			**0**			**0**			**0**	
Grade II	**15**	**8**	7: No	**9**	**0**		**15**	**6**	6: No	**9**	**0**	
			1: NSAID>1 wk		**3**	1: NSAID<1 wk		**6**	3: NSAID<1 wk		**2**	1: NSAID<1 wk
		6	2: NSAID<1 wk			2: NSAID>1 wk			1: NSAID>1 wk			1: NSAID>1 wk
			2: NSAID>1 wk		**6**	4: No			1: Cort<1 wk		**7**	4: No
			1: Cort<1 wk			1: NSAID>1 wk			1: Cort>1 wk			2: NSAID>1 wk
			1: Cort>1 wk			1: Cort>1 wk		**3**	1: No			1: Cort>1 wk
		1	1: Cort>1 wk						2: NSAID>1 wk			
Grade III	**7**	**0**		**8**	**0**		**6**	**0**		**8**	**0**	
		6	2: NSAID<1 wk		**2**	1: NSAID<1 wk		**5**	3: NSAID<1 wk		**1**	1: Other
			1: Cort<1 wk			1: Cort<1 wk			2: NSAID>1 wk		**7**	2: No
			1: Cort>1 wk		**6**	1: No		**1**	1: Cort>1 wk			1: NSAID<1 wk
			1: Other			2: NSAID<1 wk						2: NSAID>1 wk
			1: NA			2: NSAID>1 wk						2: Other
		1	1: Cort>1 wk			1: Cort<1 wk						

Continuation table Additional file 1.

	NP CD	NP in situ/ Extr/Protr	Treatment	NP NCD	NP in situ/ Extr/Protr	Treatment	AF CD	NP in situ/ Extr/Protr	Treatment	AF NCD	NP in situ/ Extr/Protr	Treatment
Grade IV+V	**13**	**1**	1: NSAID<1 wk	**10**	**0**		**9**	**1**	1: Cort<1 wk	**14**	**0**	
		12	2: NSAID<1 wk		**7**	3: NSAID<1 wk		**8**	2: No		**4**	1: NSAID<1 wk
			4: NSAID>1 wk			3: NSAID>1 wk			2: NSAID<1 wk			1: NSAID>1 wk
			2: Cort<1 wk			1: Cort>1 wk			2: NSAID>1 wk			1: Cort>1 wk
			1: Cort>1 wk		**3**	1: Other			1: Cort>1 wk			1: Other
			2: Other			2: NA			1: Other		**10**	4: No
			1: NA					**0**				1: NSAID<1 wk
		0										3: NSAID>1 wk
												1: Other
												1: NA
	Total			**Total**			**Total**			**Total**		
	52	**26**		**36**	**9**		**47**	**24**		**41**	**10**	
		24			**12**			**19**			**7**	
		2			**15**			**4**			**24**	

NP = nucleus pulposus, CD = chondrodystrophic, Extr = extrusion, Protr = protrusion, NCD = non-chondrodystrophic, AF = annulus fibrosus, NSAID = non-steroidal anti-inflammatory drug, Cort = corticosteroids, NA = not available

Additional file 2. Significant differences and confidence intervals of statistical analyses

Tables 1, 2, 3, and 4 represent significant differences and confidence intervals of statistical analyses. Figure numbers in the tables correspond to figures shown in the main article.

Table 1. Significant differences and confidence intervals of statistical analyses of glycosaminoglycan (GAG) and DNA content normalized for weight in the nucleus pulposus (NP) and annulus fibrosus (AF) per degeneration grade and per herniation type, corresponding to Figure 1 in the main article.

Condition	vs	Condition	Estimated coefficient	Confidence interval (CI)	CI (%)
Degeneration					
1A. GAG/weight					
NP grade IV+V	**vs**	AF grade IV+V	0.65	0.05 – 1.25	99
Degeneration					
1B. DNA/weight					
NP grade II	**vs**	NP grade IV+V	1.13	0.22 – 2.04	99

Table 2. Significant differences and confidence intervals of statistical analyses of prostaglandin E_2 (PGE_2) and chemokine (C-C motif) ligand 2 (CCL2) and chemokine (C-X-C motif) ligand 1 (CXCL1) levels normalized for weight in the nucleus pulposus (NP) and annulus fibrosus (AF) per Pfirrmann grade and per herniation type, corresponding to Figure 2 in the main article.

Condition	vs	Condition	Estimated coefficient	Confidence interval (CI)	CI (%)
Degeneration					
2A. PGE_2/weight					
NP grade II		NP grade I	2.54	1.10 – 3.99	99
NP grade III		NP grade I	2.84	1.28 – 4.41	99
NP grade IV		NP grade I	2.67	1.20 – 4.14	99
Herniation					
2D. PGE_2/weight					
Extrusion NCD		In situ NCD	1.85	0.31 – 3.40	99
Protrusion NCD		In situ NCD	1.98	0.79 – 3.17	99
2F. CCL2/weight					
NP extrusion		AF extrusion	2.07	0.64 – 3.51	99
NP extrusion		NP protrusion	1.33	0.21 – 2.45	99

NCD = non-chondrodystrophic

Table 3. Significant differences and confidence intervals of statistical analyses of prostaglandin E_2 (PGE_2) normalized for DNA content in the nucleus pulposus (NP) and annulus fibrosus (AF) in Pfirrmann grade II samples obtained from experimental chondrodystrophic (CD) dogs, and in the complete dataset (CD and nonchondrodystrophic (NCD) dogs) per Pfirrmann grade, and per herniation type, corresponding to Figure 3 in the main article.

Condition	vs	Condition	Estimated coefficient	Confidence interval (CI)	CI (%)
3A. PGE_2/DNA grade II CD dogs					
NP protrusion		NP in situ	2.08	1.06 – 3.10	99
Degeneration					
3B. PGE_2/DNA					
Grade II		Grade I	2.17	1.18 – 3.17	99
Grade III		Grade I	2.13	1.04 – 3.21	99
Grade IV		Grade I	1.47	0.46 – 2.48	99
Herniation					
3C. PGE_2/DNA					
Extrusion NCD		In situ NCD	1.85	0.31 – 3.40	99
Protrusion NCD		In situ NCD	1.98	0.79 – 3.17	99

Table 4. Significant differences and confidence intervals of statistical analyses performed on cyclooxygenase-2 (COX-2) expression data in the nucleus pulposus (NP) and annulus fibrosus (AF) per Pfirrmann grade, corresponding to Figure 5 in the main article.

Condition	vs	Condition	Estimated hazard ratio (HR)	Confidence interval (CI)	CI (%)
NP grade IV + V		NP grade I	34.3	2.09 – 562.54	99
NP grade IV + V		NP grade II	7.40	1.39 – 39.46	99
AF grade IV + V		AF grade I	27.32	1.78 – 419.75	99
AF grade IV + V		AF grade I	4.92	1.64 – 14.79	99

Chapter 7

Intradiscal application of a PCLA-PEG-PCLA hydrogel loaded with celecoxib for the treatment of back pain in canines: What's in it for humans?

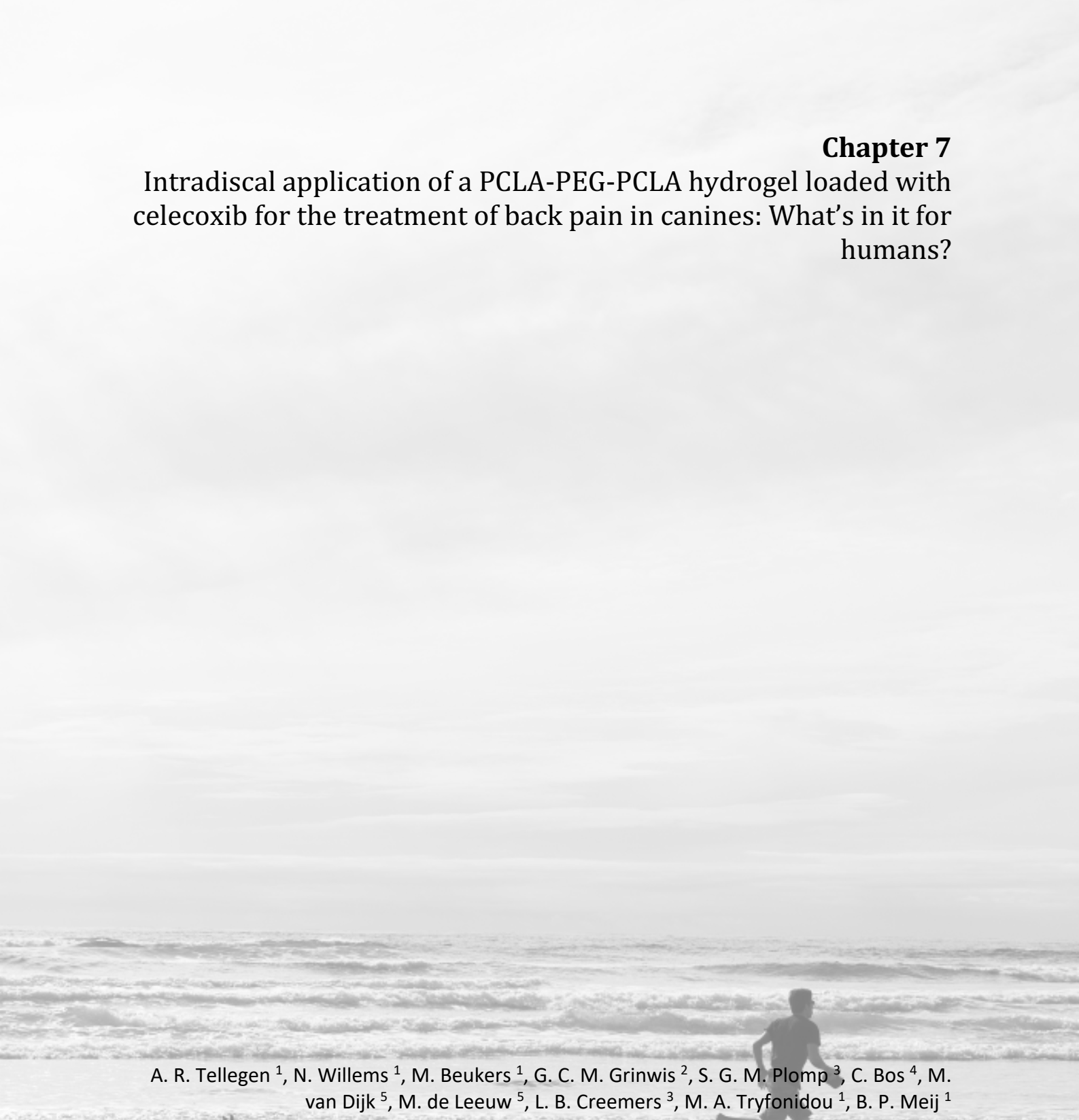

A. R. Tellegen [1], N. Willems [1], M. Beukers [1], G. C. M. Grinwis [2], S. G. M. Plomp [3], C. Bos [4], M. van Dijk [5], M. de Leeuw [5], L. B. Creemers [3], M. A. Tryfonidou [1], B. P. Meij [1]

[1] Department of Clinical Sciences of Companion Animals, Faculty of Veterinary Medicine, Utrecht University, The Netherlands.
[2] Department of Pathobiology, Faculty of Veterinary Medicine, Utrecht University, The Netherlands.
[3] Department of Orthopaedics, University Medical Centre Utrecht, The Netherlands.
[4] Imaging Division, University Medical Centre Utrecht, The Netherlands.
[5] InGell Labs BV, The Netherlands.

Journal of Tissue Engineering and Regenerative Medicine (2017) 1:11

Abstract

Chronic low back pain is a common clinical problem in both the human and canine population. Current pharmaceutical treatment often consists of oral anti-inflammatory drugs to alleviate pain. Novel treatments for degenerative disc diseases focus on local application of sustained released drug formulations. The aim of this study was to determine safety and feasibility of intradiscal application of a PCLA-PEG-PCLA hydrogel releasing celecoxib, a COX-2 inhibitor. Biocompatibility was evaluated after subcutaneous injection in mice and safety of intradiscal injection of the hydrogel was evaluated in experimental dogs with early spontaneous intervertebral disc (IVD) degeneration. COX-2 expression was increased in IVD samples surgically obtained from canine patients indicating a role of COX-2 in clinical IVD disease. Ten client-owned dogs with chronic low back pain related to IVD degeneration received an intradiscal injection with the celecoxib-loaded hydrogel. None of the dogs showed adverse reactions after intradiscal injection. The hydrogel did not influence MRI signal at long term follow up. Clinical improvement was achieved by reduction of back pain in 9/10 dogs, as was shown by clinical examination and owner questionnaires. In 3/10 dogs back pain recurred after 3 months. This study showed the safety and effectiveness of intradiscal injections *in vivo* with a thermoresponsive PCLA-PEG-PCLA hydrogel loaded with celecoxib. In this setup, the dog can be used as a model for the development of novel treatment modalities in both canine and human patients with chronic low back pain.

Introduction

Low back pain is a common clinical problem in both the human and canine population [1, 2]. In both species, it is often related to degeneration of the intervertebral disc (IVD) [3]. As the most common type of pain restricting daily activity, chronic low back pain has a huge impact on quality of life and productivity [4]. IVD degeneration in dogs resembles the human situation at the molecular, histological, radiological and clinical level and therefore, dogs are a suitable model to study IVD disease in humans [5, 6].

IVD degeneration involves the production of pro-inflammatory molecules by cells of the nucleus pulposus (NP) and annulus fibrosus (AF) and subsequent recruitment of inflammatory cells [7, 8]. Production of pro-inflammatory mediators such as tumor necrosis factor α (TNF-α), interleukin 1β (IL-1β) and prostaglandin E_2 (PGE_2) can lead to a shift from an anabolic- to a catabolic environment by upregulating matrix metalloproteinases (MMP-3 and MMP-13) and a disintegrin and metalloproteinase with thrombospondin motifs (ADAMTS-1, -4 and -5) [9]. In the NP this leads to an increase in collagen type I and a decrease in collagen type II and proteoglycans. This results in a decrease in hydrostatic pressure and further degenerative changes like tears and clefts, bulging of the AF or herniation of NP tissue into the spinal canal [8, 10]. During the process of degeneration vascular and neural ingrowth is related to discogenic pain mediated by IL-1β and TNF-α [8, 9, 11, 12]. COX-2 expression can be induced in response to inflammatory stimuli, mechanical stress [13] and COX-2 expression and its major downstream product, PGE_2, were found to be increased in both degenerated human [14] and canine IVDs [15]. PGE_2 can sensitize nerve endings evoking discogenic pain in the degenerated IVD [16, 17].

Current conservative and surgical treatments aim at relieving clinical signs of back pain, rather than interfering with the degenerative process to achieve biologic repair [5, 18]. Although COX-2 inhibitors can be effective in reducing back pain in humans and canine patients [19, 20], their systemic delivery is associated with various side- and co-morbidity effects, drug-drug incompatibility [19, 21, 22], and limited tissue penetration into the avascular IVD [23, 24]. Local delivery of sustained release drug formulations may accomplish higher local dosing and prolonged exposure of the target tissue to the released drug without systemic side effects. Indeed, after intra-articular (IA) injection of a controlled release system loaded with celecoxib, a COX-2 inhibitor, celecoxib levels were higher and more sustained in synovial fluid compared to serum levels [25]. Temperature-dependent hydrogels are suitable for intradiscal injection, since they are liquid at room temperature, therefore easy to inject, and form solid gels at body temperature, thereby preventing leakage out of the IVD [26, 27]. Controlled release platforms such as acetyl-capped PCLA-PEG-PCLA hydrogels loaded with the COX-2 inhibitor celecoxib are safely applied *in vivo* in small and large animal models [25, 28]. In the current study, the main aim was to demonstrate the safety and effectivity of prolonged release of the COX-2 inhibitor celecoxib *in vivo* in several translational animal models as outlined in Figure 1. In this setup, the dog functions as a model for the

development of treatments against low back pain for both the canine and human patient population.

Materials and methods

Synthesis of and preparation of the propionyl-capped PCLA-PEG-PCLA hydrogel

The propionyl-capped PCLA-PEG-PCLA thermoreversible hydrogel was synthesized and loaded with 0.016mg/mL celecoxib and was prepared according to a previously described two-step synthesis protocol [28, 29]. The tri-block copolymer PCLA-PEG-PCLA was prepared by standard stannous ethylhexanoate catalyzed ring opening polymerization, followed by the modification of the hydroxyl end groups with propionic anhydride. The polymer was characterized by ^{1}H NMR and GPC (supplementary file 1). For the celecoxib stock solution, 8.0 g of phosphate buffer pH 7.4 (43 mM Na_2HPO_4, 9 mM NaH_2PO_4 76 mM NaCl) was added to polymer (2.0 g) and celecoxib (26 mg) in a 20 mL glass crimp cap vial. A second formulation without celecoxib was prepared by adding polymer (2.0 g) to the phosphate buffer (8.0 g). Subsequently, both formulations were autoclaved for 20 min at 120 °C. The warm formulations were vortexed for 1 min and incubated at 4 °C for 48 h to yield fully dissolved polymer solutions. Next 60 mg celecoxib stock solution was mixed with 10 g polymer only solution to yield a formulation with a final concentration of 0.016 mg/g (43 µM) celecoxib and 20 wt% polymer. The gelation properties and the celecoxib concentration in the final formulation were verified by rheology and reverse phase HPLC-UV [25].

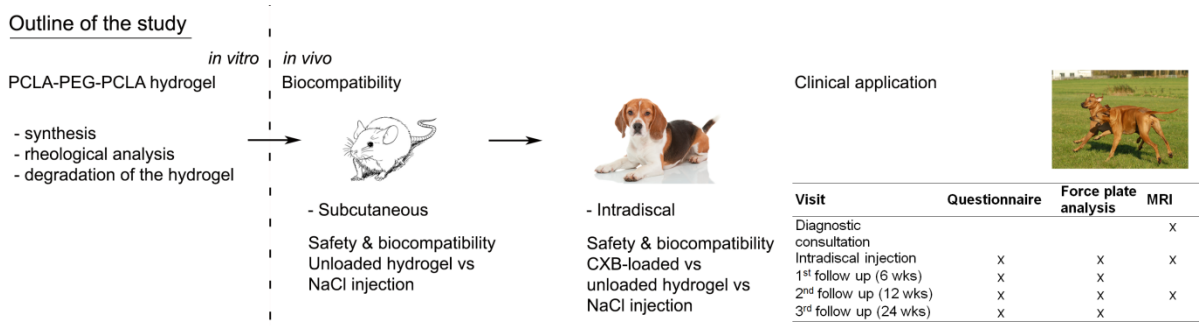

Figure 1. Outline of the study.

In vivo biocompatibility after subcutaneous injection in mice

Animal procedures were approved and performed in accordance with the guidelines set by the Animal Experiments Committee (DEC) of Utrecht University (DEC 2010.III.03.046). Twelve healthy female 8-10 weeks old BALB/c mice (Harlan-Olac Ltd., Bicester, UK) were used to test the PCLA-PEG-PCLA hydrogel together with 7 other biomaterials for biocompatibility. The mice received 100 µg/kg buprenorphine intraperitoneally and were subsequently anesthetized with 2.5% isoflurane in a 1:1 oxygen:air mixture. In each mouse,

200 µL of four different biomaterials were randomly injected into the dorsal subcutaneous tissue with a 27G needle, at least 1 cm apart. 200 µL PBS served as a control. Immediately after injection, Dermabond® (Ethicon, Cornelia, GA, USA) was applied to prevent leakage and the injection site was heated by an infrared lamp for 1 min. Mice were monitored daily for signs of distress or pain and injection sites were monitored for inflammation (e.g., swelling, redness, pain, and heat). Six animals were sacrificed 7 days after injection, and six after 28 days, resulting in *n*=3 implantation sites per biomaterial per time point. At the end of the experimental period, animals were anesthetized with isoflurane, blood was collected by cardiac puncture for white blood cell count and differentiation, and euthanasia was performed by cervical dislocation. The injection sites were fixed in 10% neutral buffered formaldehyde (Klinipath B.V., Duiven, The Netherlands) and embedded in paraffin. Infiltration of inflammatory cells, giant cells, necrosis, neovascularization, fatty infiltration, and the encapsulation of the biomaterial by a fibrotic capsule were histologically assessed on hematoxylin / eosin stained sections as parameters for a biological response at the injection site (supplementary file 2) by a blinded board-certified veterinary pathologist (GG) and the principal investigator (AT).

Intradiscal application of the celecoxib-loaded hydrogel in a canine model of spontaneous IVDD

Animal procedures were approved and performed in accordance with the guidelines set by the Animal Experiments Committee of Utrecht University (DEC 2012.III.05.046). Nine female Beagle dogs (Harlan, Gannat, France) with a median age of 1.6 years (1.3-1.8 years) and a median body weight of 8.2 kg (6.2 – 11 kg) were included. All dogs underwent general physical, neurologic and orthopaedic examination by a board-certified veterinary surgeon (BM). The IVD degeneration grade was determined before intradiscal injection on MR images of the lumbar spine using a 0.2 Tesla open magnet (Magnetom Open Viva, Siemens AG, Munich, Germany) [30]. A detailed description of the procedure has been published elsewhere [31, 32]. Briefly, dogs were positioned in right recumbent position to expose the 9 IVDs between T12 and L6 via a left lateral approach, and the L6-L7 and L7-S1 IVDs via a mini-dorsal laminectomy. A 100 µL syringe (7638-01 Model 710 RN, Hamilton Company USA, Reno, NV, USA) with a 29G needle (25mm, 12° bevelled point; Hamilton Company USA, Reno, NV, USA) was used to inject 30 µL of the following compounds through the AF into the NP in a random order, i.e. NaCl 0.9% (control treatment), 2.93 µg/mL celecoxib (single bolus), unloaded hydrogel, and loaded hydrogel containing 2.93 µg/mL celecoxib. Dogs were euthanized 4 weeks post injection to assess biocompatibility and PGE_2 tissue levels. After macroscopic grading (Thompson score) [33], spinal units (endplate – IVD – endplate) were collected. One half was snap-frozen in liquid nitrogen and stored at -80°C for biomolecular analysis, the other half was fixed in 4% neutral buffered formaldehyde, decalcified in 35% formic acid and 6.8% sodium formate in a microwave oven (Milestone Microwave Laboratory Systems, Bergamo, Italy) overnight at 37°C for 7 nights and embedded in paraffin. Five µm hematoxylin / eosin and Alcian Blue / Picrosirius Red stained sections were evaluated in a blinded and random fashion (AT, NW) using an Olympus microscope (Olympus

Nederland, Zoeterwoude, The Netherlands). Of the snap frozen tissues, on 60 µm cryosections, the NP and AF tissues were separated and half of the cryosections were collected in, respectively, 400 and 750 µL Ambion KDalert lysis buffer solution for measurements of GAG, DNA and PGE_2 content (Life Technologies). The other half of the NP and AF cryosections were collected in 300 µL RLT buffer containing 1% β-mercaptoethanol for RT-qPCR (Qiagen, Venlo, The Netherlands) and stored at -80°C until further analysis, described elsewhere [26]. Detailed description of qPCR primers is provided in supplementary file 3.

COX-2 Immunohistochemistry of surgically obtained canine IVD tissues

With the owner's consent, COX-2 immunostaining was performed on formalin-fixed paraffin embedded IVD tissues obtained from 44 canine patients, diagnosed with IVD degeneration and herniation and treated with routine veterinary surgical decompression and microdiscectomy at the Utrecht University Small Animal Clinic between March 2008 and September 2010. COX-2 mouse monoclonal antibody, (10 µg/mL5% TBS-BSA; 160112, Cayman, Michigan, USA) was used as described previously [15]. The percentage of COX-2 positive cells over the total number of cells in the NP and AF was determined.

Prospective clinical trial in canine patients with low back pain

Canine patients

Ten dogs with chronic low back pain referred to the Utrecht University Small Animal Clinic underwent a full clinical examination (consisting of a general physical, orthopaedic and neurologic examination) by a board-certified orthopaedic surgeon (BM) prior to inclusion (table 1). MR images were obtained on a high field 1.5T MRI (Ingenia Philips, Eindhoven, The Netherlands) in fully anesthetized dogs to confirm the presence of IVD degeneration. The owners consented to the use and disclosure of patient- and questionnaire data for the current study. The setup is shown in Figure 1.

Table 1. Criteria for in- and exclusion of canine patients.

Inclusion criteria	Exclusion criteria
History of low back pain for at least 6 weeks	Previously performed surgery on IVD of interest
No improvement on oral pain medication for at least 4 weeks	Discospondylitis or active infection on surgical site (i.e. pyoderma)
Body weight > 15 kg	Lumbosacral fracture
Pfirrmann grade II-IV on T2-weighted MRI	Spinal neoplasia
	Chondrodystrophic breed
	More than one IVD affected

IVD, intervertebral disc.

Intradiscal injection

Premedication consisted of intravenous (i.v.) administration of butorphanol (0.1 mg/kg) and dexmedetomedine (10 µg/kg), followed by induction of anaesthesia with propofol (i.v., 1

mg/kg). Maintenance of anaesthesia was achieved by administration of isoflurane (2%). Carprofen (i.v., 4 mg/kg) was administered prior to the start of the procedure to cover any discomfort as a result of positioning for the MRI and intradiscal injection. The patient was placed in sternal recumbency with the hind limbs extended cranially and a 20G epidural needle (4509757-13, Braun, Melsungen, Germany) was aseptically inserted. Correct placement of the needle was checked by fluoroscopic digital images (Omnidiagnost Eleva, Philips, Eindhoven, The Netherlands) and digital radiography (DX-D100 Mobile DR, Agfa Healthcare, Rijswijk, The Netherlands) in ventrodorsal and laterolateral projections. The 20G needle was advanced through the ligamentum flavum until the dorsal AF was reached. Thereafter, the stylet was removed and a 12 cm long, 27G needle (7803-01 Hamilton, Bonaduz, Switzerland) was inserted through the epidural needle that acted as a guide to position the tip of the 27G needle on top of the AF. The 27G needle was subsequently advanced through the dorsal AF into the centre of the NP and positioning was confirmed with imaging (figure 5A,B). Finally, a 100 µL gastight syringe (7656-01 Hamilton, Bonaduz, Switzerland) was connected to the 27G needle and the celecoxib-loaded hydrogel was slowly injected.

Read out parameters

All 10 canine patients were evaluated by clinical examination and underwent measurements of ground reaction forces (GRFs) by force plate analysis (FPA). GRFs in the mediolateral (Fx), craniocaudal (Fy) and vertical (Fz) direction were normalized for body weight. Ratios between pelvic (P) and thoracic (T) limbs were calculated: P/T Fy-, P/T Fy+ and P/T Fz+ and were compared to historic values from a cohort of sound dogs with similar constitution and body weight [34]. FPA was performed prior to the intradiscal injection, and at 6, 12 (*n*=10), and 24 (*n*=4) weeks after intradiscal injection. GRFs were measured with a quartz crystal piezoelectric force plate (Kistler type 9261, Kistler Instrumente) together with the Kistler 9865E charge amplifiers as described previously [34, 35]. Pain medication (if applicable) was discontinued for at least three days prior to FPA. Validated questionnaires to owners regarding behaviour and function of their dog, assessed the owner's perspective of treatment outcome [34, 35] (table 2). Rescue analgesia in case of recurrence of clinical signs was recorded by the owners.

Magnetic resonance imaging was performed directly prior to and directly after injection and repeated at 12 weeks after treatment. Four dogs were available for follow up at 24 weeks after intradiscal injection and underwent clinical evaluation and FPA. The MR protocol included a sagittal T2-weighted Turbo Spin Echo, a Fat-suppressed T1-weighted Turbo Spin Echo using spectral pre-saturation, and a quantitative multiple spin-echo T2-mapping sequence. The scans were carried out with the dogs under general anaesthesia, positioned in dorsal recumbency with the pelvic limbs extended caudally. All images were assessed by a board-certified veterinary radiologist (MB). The amount of disc protrusion into the spinal canal was categorized as mild (<25% of spinal canal), moderate (25-50%) or severe (>50%) protrusion. The disc height index (DHI) was measured on the MR images using the method

described by An *et al* [36]. The grade of IVD degeneration was determined on T2-weighted images by the Pfirrmann grading [30] for use in dogs. Mean T2 relaxation times were determined in an oval region of interest (ROI) in the lumbosacral IVDs on midsagittal T2-mapping images. ROIs were also drawn in fat and muscle tissue to serve as an internal control.

Table 2. Questionnaire to the owners of dogs before and at 6, 12, and 24 weeks after intradiscal application of PCLA–PEG–PCLA hydrogel with celecoxib.

Question	Before treatment / Baseline	After 6 weeks (*n*=10)	After 12 weeks (*n*=10)	After 24 weeks (*n*=4)
Pelvic limb lameness	3 (2-10)	10 (6-10)	9 (2-10)	10 (10-10)
Pelvic limb weakness	6 (2-10)	10 (3-10)	9.5 (3-10)	9.5 (9-10)
Caudal lumbar pain	2.5 (2-9)	9 (5-10)	9 (2-10)	8.5 (8-10)
Difficulty rising up	3.5 (2-9)	9 (7-10)	9 (2-10)	9.5 (9-10)
Difficulty lying down	7 (2-10)	10 (8-10)	10 (2-10)	10 (9-10)
Muscle volume	7.5 (3-10)	8 (5-10)	9 (5-10)	9 (9-9)
Position of the tail	6 (1-10)	10 (3-10)	9 (2-10)	9 (9-10)
Movement of the tail	8.5 (2-10)	10 (5-10)	9.5 (5-10)	9 (9-10)
Urinary and faecal continence	9.5 (4-10)	10 (6-10)	10 (5-10)	10 (10-10)
Hypersensitivity of the skin of the lower back	5 (1-10)	10 (4-10)	9.5 (4-10)	9 (9-10)

Histological and biochemical evaluation of IVD samples collected after intradiscal injection

After the three months follow up period, two dogs underwent decompressive surgery due to recurrence of clinical signs. One dog was euthanized due to recurrence of clinical signs on request of the owner. AF and NP samples were collected in 10% neutral buffered formalin and liquid nitrogen for histological and biochemical evaluation as described in section 2.4.

Statistical analysis

Statistical analysis was performed using SPSS 22 (SPSS Inc., Chicago, IL) and R statistical software, package 2.15.2. Normality was tested with the Shapiro Wilks test. Biochemical and biomolecular data of the Beagle study described in section 2.4 were analysed using a linear mixed effect model as previously described [26]. The relation of histological- and MRI scores with the expression of COX-2 was analysed with multiple linear regression analyses and with nonparametric Kruskal-Wallis followed by Mann-Whitney U-tests, in the NP and AF respectively. The reliability of the responses to the questionnaires was investigated by calculation of Cronbach's α. A value of >0.70 was considered reliable. Comparison of the mean scores of the questionnaires before intradiscal injection, at 6 and 12 weeks after treatment was conducted using Friedman's test, followed by Wilcoxon's signed rank tests for each time point. To investigate the effect of treatment on GRFs, DHI and T2 relaxation times, a repeated measures ANOVA was performed followed by pairwise dependent t-tests with

Bonferroni corrections. Data obtained from the four dogs that had follow-up visits performed at 24 weeks following treatment were treated as descriptive data only, because of the small sample size.

Results

In vivo biocompatibility was shown after subcutaneous injection in mice

No systemic effects were recorded after subcutaneous injection of the PCLA-PEG-PCLA hydrogel. At 7 days post injection, the injection site was infiltrated by inflammatory cells, mainly macrophages, and in smaller numbers neutrophils (figure 2C,D). Slight neovascularization surrounding the injected hydrogel was visible. Necrosis was noted in the centre of the biomaterial area at 4/6 injection sites. At 28 days post injection (figure 2G,H), tissues showed slightly more vascularization compared with day 7. The injection area was mostly infiltrated by macrophages, neutrophils and some eosinophilic granulocytes. A thin capsule-like structure was present surrounding the granulomatous inflammation consistent with a subacute reaction. Giant cells, lymphocytes, plasma cells, fibrous capsule formation and fatty infiltration were not observed at either time point. In control samples that were injected with PBS, only a few macrophages were present in two tissue explants at 7 days and in four at day 28 (supplementary file 2).

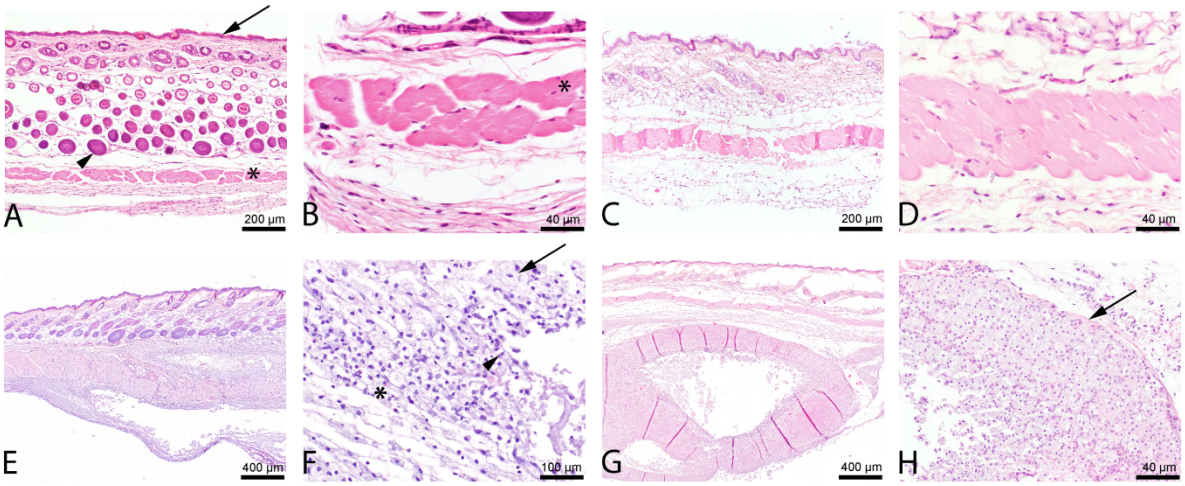

Figure 2. Representative histological images of subcutaneous injection sites with the PCLA-PEG-PCLA hydrogel in mice (hematoxylin / eosin staining). **A-B:** 7 days after injection with PBS revealing the epidermis (arrow), hair follicles (arrowhead) and striated muscle (asterisk). **C-D:** 28 days after injection with PBS. **E-F:** 7 days after hydrogel injection. Cellular infiltrate is visible with macrophages (arrow), neutrophils (arrowhead) and an occasional eosinophilic granulocyte (asterisk **F**). **G-H:** 28 days after hydrogel injection a thin capsule-like structure is evident (arrow).

Good biocompatibility and improved matrix composition was seen after intradiscal application of the (un)loaded hydrogel in early degenerated IVDs of experimental dogs

Before surgery, all IVDs in all experimental Beagle dogs were graded Pfirrmann grade II on MRI. All dogs showed uneventful recovery from surgery, were ambulant the next day and showed minor deficiencies in spinal reflexes that recovered within 7 days. Post mortem, Thompson score II was assigned to all IVDs of all dogs. Histological scores ranged from 4 to 12 compatible with mild IVD degeneration and did not differ between treatment groups (figure 3A). Normalized GAG content (GAG/DNA) and PGE_2 levels of the NP and AF did not differ between treatment groups (Figure 3B). Gene expression levels of extracellular matrix components (*ACAN, COL2A1* and *COL1A1*) and the anti-catabolic gene *TIMP1* were not significantly different between treatments. Gene expression levels of the catabolic genes *ADAMTS5* and *MMP13* were significantly downregulated in the NP samples treated with the hydrogel loaded with celecoxib compared with saline injection (p=0.047 and p=0.019, respectively) (figure 3C). Gene expression levels of NP cell markers (*T*, *CTK8* and *CTK18*) (figure 3D), genes associated with the Wnt-pathway (*AXIN, C-Myc* and *CCDN1*) and pro-inflammatory mediators (*TNFα, IL1β*, *IL6* and *IL10*) did not differ between treatment groups. The expression of *CASP3* was significantly upregulated (p=0.04, data not shown) in the unloaded hydrogel compared to the saline control. Gene expression levels of other apoptotic markers, i.e. *FasL* and *BCL2* did not differ between treatment groups.

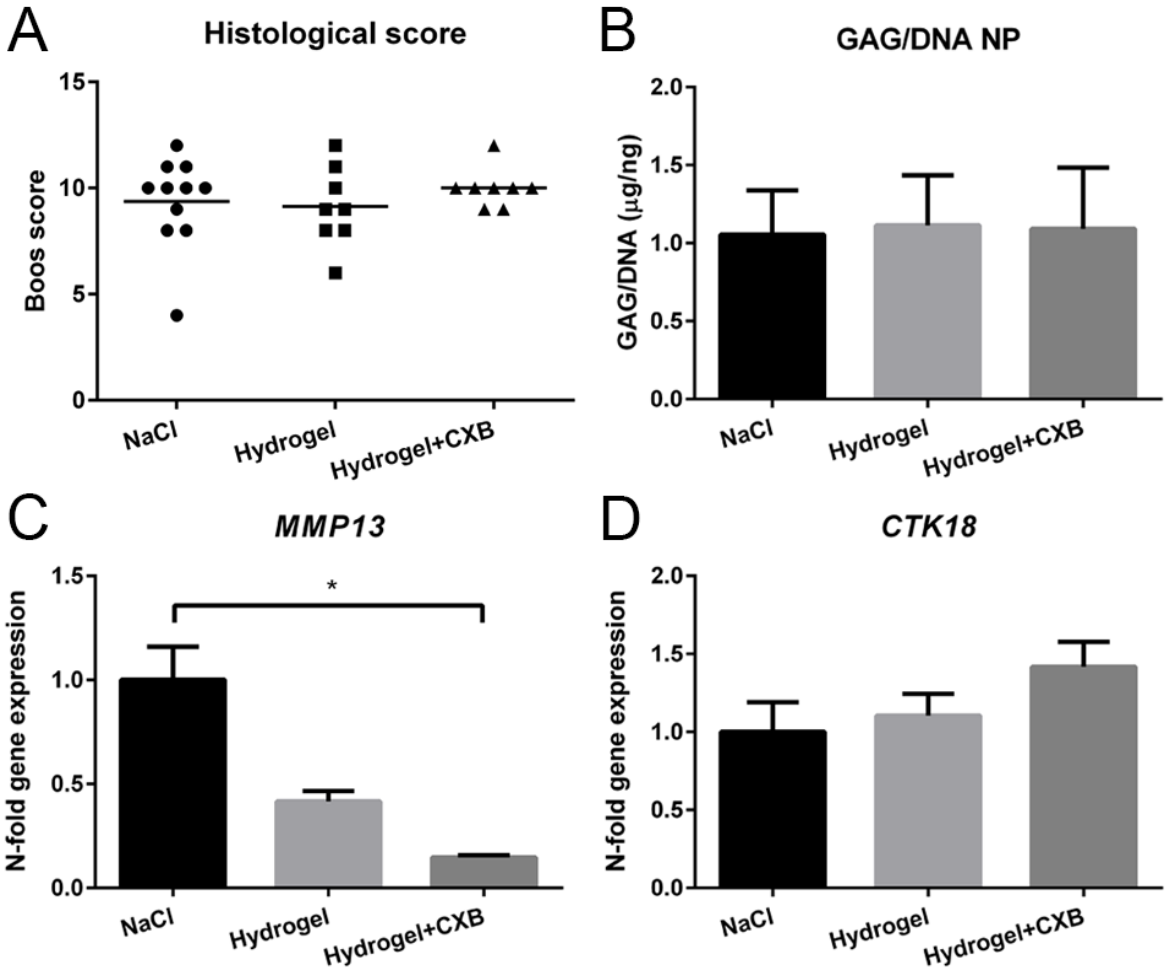

Figure 3. Results of *in vivo* beagle study. There was no difference in histological score of the IVDs (**A**) and the GAG content, normalized for DNA content, did not change after treatment with celecoxib-loaded hydrogel (**B**). MMP13 mRNA expression was significantly downregulated in the celecoxib-loaded hydrogel, compared to NaCl control (*: p=0.019) (**C**), cytokeratin 18 expression (**D**) did not differ between treatment groups.

COX-2 protein expression increased with degenerative grade in surgically obtained canine IVD tissues

The percentage of COX-2 positive NP cells was significantly higher in Pfirrmann grade III and IV+V IVDs compared to grade I and II IVDs (B=20.6, 95%CI=[0.003-0.408], p<0.05) (figure 4A,C). COX-2 expression in the AF was not different between MRI grade II, III, and IV+V IVDs and the histological score (figure 4B,D).

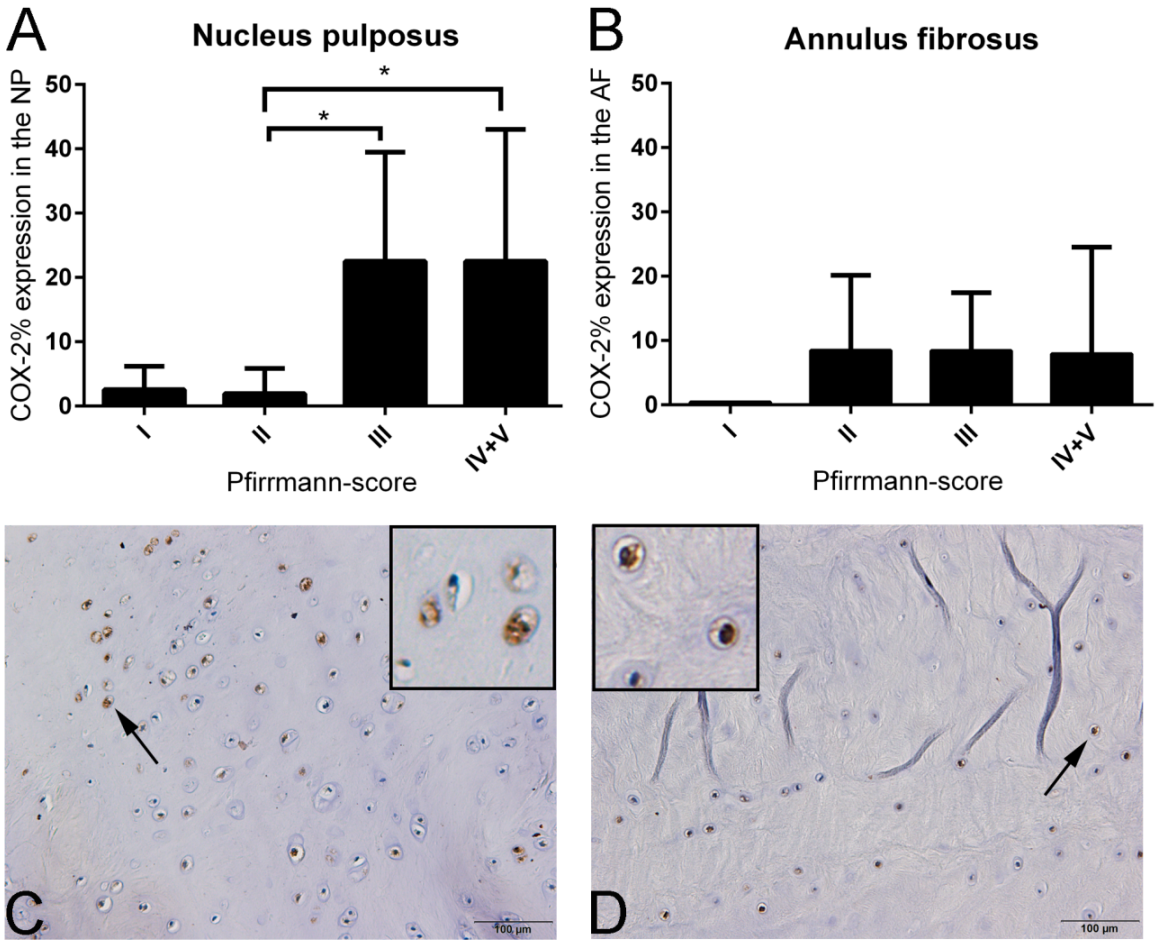

Figure 4. COX-2 expression in surgically obtained nucleus pulposus (NP, **A,C**) and annulus fibrosus (AF, **B,D**) tissue samples in relation to the histological degeneration grade.

Intradiscal injection with the celecoxib-loaded hydrogel was safe in canine patients with chronic low back pain and IVD degeneration

Ten canine patients with chronic low back pain referred to the Utrecht University Small Animal Clinic (table 3) received the celecoxib-loaded hydrogel intradiscally under fluoroscopy guidance (figure 5A, B).

Table 3. Overview of patient details and history of 10 dogs with low back pain related to intervertebral disc degeneration.

Dog	Breed	Sex	Age	BW (kg)	Purpose	Clinical signs	Radiological signs	Pfirrmann grade
1	Rhodesian ridgeback	FC	5	37.5	Companion	Caudal lumbar pain, difficulty defecating, urinary incontinence	Moderate AF protrusion with compression of CE	III
2	Newfoundland	MC	4	75	Companion	Caudal lumbar pain, muscle atrophy hind legs, reluctance to jump	Moderate AF protrusion, LF hypertrophy	II
3	Retriever cross breed	FC	4	26.7	Guide dog	Caudal lumbar pain, difficulty rising up	Moderate protrusion of the AF with compression of the CE, mild compression of the left S1 nerve root	III
4	Gordon Setter	FC	2	23.7	Companion	Caudal lumbar pain, difficulty lying down	Mild AF protrusion L7-S1	II
5	Bull terrier	MC	5	30.4	Companion	Caudal lumbar pain	Mild protrusion of AF L7-S1	II
6	Stabyhoun	FC	9	16.6	Companion	Caudal lumbar pain, left hind leg lameness, muscle atrophy left hind leg	Moderate protrusion AF L7-S1 disc, compression and dislocation of the CE	IV
7	Labrador retriever	FC	3	26.7	Guide dog	Caudal lumbar pain, right hind leg lameness	Mild protrusion of AF L7-S1 disc, hypertrophy LF	II
8	Leonberger	FC	5	55.6	Companion	Caudal lumbar pain, difficulty rising up and lying down	Osteochondrosis cranial end plate S1, moderate AF protrusion R>L, LF hypertrophy	IV
9	Labrador retriever	M	7	37	Companion	Intermittent caudal lumbar pain, difficulty jumping and walking stairs	6 lumbar vertebrae, severe protrusion of AF L6-S1 disc, cystic structure within spinal canal	IV
10	Border collie	M	7	23	Agility	Caudal lumbar pain, difficulty rising up	Left side L7 nerve thickening, mild protrusion of AF	II

Degree of disc protrusion: mild (<25%), moderate (25-50%), severe (>50%) protrusion of the disc into the spinal canal; Abbreviations: BW, body weight; AF, annulus fibrosus; CE, cauda equina; LF, ligamentum flavum.

Magnetic resonance imaging

MRI was performed prior to and directly after intradiscal injection and 12 weeks after treatment in all canine patients (figure 5C). Radiologic abnormalities prior to injection included mild protrusion (*n*=4), moderate protrusion (*n*=5) and severe protrusion (*n*=1) (table 3). In dog 9, there was a cystic structure visible within the spinal canal. No abnormalities were detected directly after injection on any of the MRI sequences, except small air bubbles within the spinal canal in 5 dogs that were hypointense on all sequences. The extent of protrusion was not different after injection in all injected IVDs and this remained the same after 12 weeks in eight dogs. In dog 9, the protrusion decreased slightly and the cystic structure in the spinal canal dorsal to the protrusion also decreased in size. In dog 3, the extent of protrusion after 3 months increased from 47% to 53%. Both Pfirrmann grade and DHI remained unchanged over time (p=0.264 and p=0.123, respectively). T2 relaxation times measured in the NP directly after injection were significantly higher compared to just prior to injection (p=0.012) and 3 months after intradiscal injection (p=0.006) (figure 5B). There were no significant differences in T2 relaxation times for fat and muscle tissue at the three different time points (p=0.119 and p=0.281 respectively).

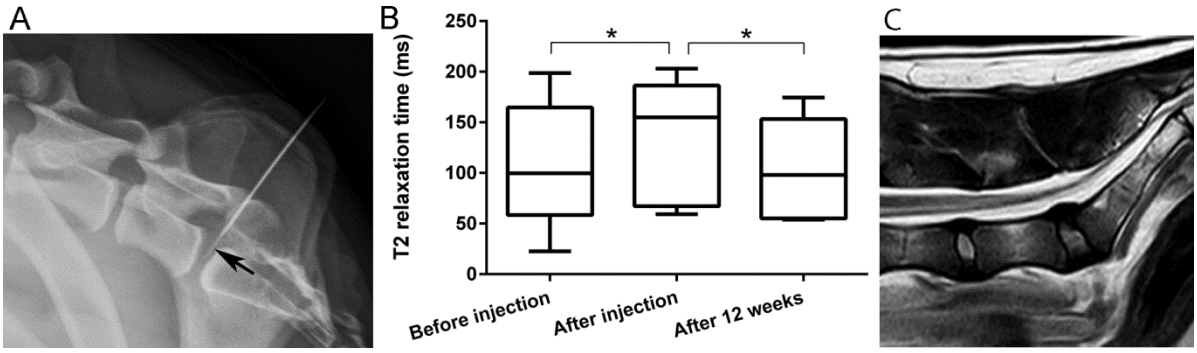

Figure 5. Laterolateral (**A**) radiographic images obtained during fluoroscopy guided intradiscal injection. Note the 20G needle advanced into the epidural space and the 27G needle (arrow) positioned in the centre of the nucleus pulposus. The T2 mapping values of the nucleus pulposus were significantly higher after injection compared to pre-injection and 3 months follow up (**B**). Representative T2 magnetic resonance image 3 months after intradiscal injection with the celecoxib-loaded hydrogel (**C**).

Force plate analysis

FPA was performed in 10 dogs prior to intradiscal injection and at the 6- and 12-week follow up visits. In 4 dogs, FPA was repeated at 24 weeks after treatment. The P/T Fy-, P/T Fy+ and P/T Fz+ values before, at 6 and at 12 weeks after injection were not statistically different. GRFs in 4 dogs at 24 weeks after intradiscal injection were not different from the values at 6- and 12-weeks post treatment (figure 6A).

Owner questionnaires

Questionnaires were completed by owners prior to treatment, 6 and 12 weeks (*n*=10) and 24 weeks (*n*=4) after intradiscal injection (table 4). The Cronbach's alpha value of the responses to the questionnaire was 0.91, indicating that the questions were reliable. Nine out of 10 owners reported that the clinical signs of low back pain had disappeared at 6 and 12 weeks after treatment (90%), while one owner reported recurrence after an asymptomatic 6-week period (1/9 = 11%). Three owners reported recurrence of clinical signs after three months (3/9 = 33%). The owners of the four dogs that had a follow-up visit at 24 weeks after treatment, remained positive on the outcome and reported no change in behaviour or pain score, i.e. the dogs remained asymptomatic. Two owners reported the use of rescue analgesia during the 12-week follow-up period. Dog 2 received NSAIDs during three days of the first week after intradiscal injection. Dog 4 received NSAIDs on a daily basis during the first week after treatment and in the 4 weeks thereafter 2-3 times a week.

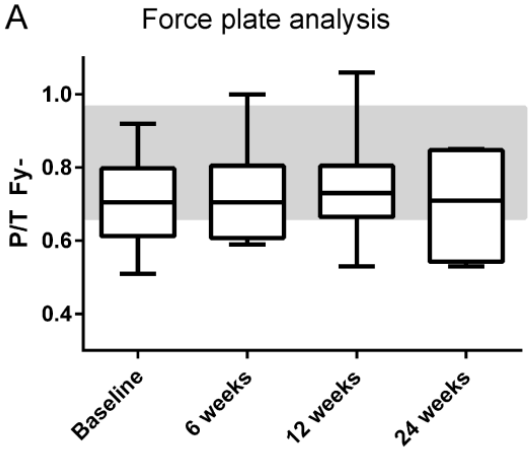

Figure 6. Mean pelvic / thoracic (P/T) Fy- values before, and after intradiscal injection with the celecoxib-loaded hydrogel at 6, 12 and 24 weeks: in grey the range of P/T Fy- values in healthy dogs is given.

Histological and biochemical evaluation of IVD tissue samples collected after intradiscal injection

Two dogs with recurrence of low back pain underwent standard of veterinary care surgical treatment, i.e. dorsal laminectomy and partial discectomy. Histological evaluation of the lumbosacral IVD tissue became available at respectively 15 (dog 1) and 19 (dog 2) weeks after intradiscal injection with a Pfirrmann grade of 3 and 2, respectively. The surgically obtained AF and NP tissues showed extensive degeneration at histological level. In the dorsal AF of dog 2, a focal granulomatous inflammation was present. In dog 4, the treated IVD with Pfirrmann grade 2 was collected in one piece *post mortem* at 12 weeks after intradiscal injection. This lumbosacral IVD showed severe degeneration of the NP and AF, with tears in the AF and dorsal herniation of NP material. In the dorsal ligament and the dorsal AF, a mild granulomatous focus was present, with fibroblasts and slight proliferation of vascular structures. No remnant hydrogel was observed in the 3 IVD tissue samples. COX-

2 staining was negative in the NP tissue of dog 1 and 4. In dog 2, 2% of the cells in the NP stained positive for COX-2. No COX-2 positive cells were found in the AF tissues of these 3 dogs which was markedly lower than the COX-2 expression that was found in surgically obtained samples of dogs undergoing routine decompressive surgery (figure 4B).

Table 4. Responses to owners' questionnaires of dogs before, and at 6, 12 and 24 weeks after intradiscal injection. *: Significant differences from baseline (p<0.05).

Question	Before treatment	After 6 weeks (n=10)	After 12 weeks (n=10)	After 24 weeks (n=4)
Pelvic limb lameness	3 (2-10)	10 (6-10) *	9 (2-10) *	10 (10-10)
Pelvic limb weakness	6 (-2-10)	10 (3-10) *	9.5 (3-10) *	9.5 (9-10)
Caudal lumbar pain	2.5 (2-9)	9 (5-10) *	9 (2-10) *	8.5 (8-10)
Difficulty rising up	3.5 (2-9)	9 (7-10) *	9 (2-10) *	9.5 (9-10)
Difficulty lying down	7 (2-10)	10 (8-10) *	10 (2-10) *	10 (9-10)
Muscle volume	7.5 (3-10)	8 (5-10)	9 (5-10) *	9 (9-9)
Position of the tail	6 (1-10)	10 (3-10)	9 (2-10)	9 (9-10)
Tail movement	8.5 (2-10)	10 (5-10)	9.5 (5-10)	9 (9-10)
Urinary and faecal continence	9.5 (4-10)	10 (6-10) *	10 (5-10)	10 (10-10)
Hypersensitivity of the lower back	5 (1-10)	10 (4-10) *	9.5 (4-10) *	9 (9-10)

Discussion

The present study demonstrated safety and effectivity of a locally applied controlled release system loaded with celecoxib, a COX-2 inhibitor. In naturally occurring mildly degenerated canine IVDs, PGE_2 levels did not decrease after intradiscal injection of the celecoxib-loaded hydrogel in this and a previous study employing a different platform [26]. Given that PGE_2 levels and COX-2 protein expression are much higher in symptomatic degenerated and herniated IVDs than in asymptomatically mildly degenerated tissues [15, 37], the clinical effect of the celecoxib-loaded hydrogel was further investigated in canine patients with chronic low back pain associated with IVD degeneration. Local delivery of the celecoxib-loaded hydrogel was related with improved quality of life in the majority of the canine patients without adverse effects.

The PCLA-PEG-PCLA thermogel was biocompatible both subcutaneously and intradiscally

Subcutaneous implantation of the propionyl-capped PCLA-PEG-PCLA thermogel in mice resulted in a slight to moderate foreign body reaction, mainly characterized by macrophage infiltration, which is in line with previous findings [38]. Intra-articular application of an acyl-

capped PCLA-PEG-PCLA unloaded and celecoxib-loaded hydrogel in talocrural joints of healthy horses [25] resulted in a transient subclinical inflammatory response indicated by an increase in the white blood cell count. The latter is commonly encountered also after standard of care hyaluronic acid injection. Nonetheless, there was no evidence of cartilage damage on histology neither in healthy horses, nor in healthy rats [38] after intra-articular injection of this hydrogel. Notably, a foreign body reaction was absent for both the unloaded and celecoxib-loaded (0.016 mg celecoxib/mL) hydrogel after intradiscal application in experimental Beagles, a model of mild IVD degeneration. The latter may well be explained by the absence of innate immune cells within the avascular and immune-privileged environment of the IVD [8].

Intradiscal injection of the PCLA-PEG-PCLA hydrogel, either unloaded or loaded, does not lead to acceleration of the degenerative process

In the present study intradiscal application did not affect Pfirrmann grading on the short term in experimental Beagle dogs, as well as on the long term follow up in canine patients with chronic low back pain. This is line with previous reports where safety of intradiscal injections was confirmed with other biomaterials [26, 39]. The significant increase in T2 relaxation times observed in the cohort of canine patients directly after injection can be explained by the contribution of the hydrogel, containing primarily 80% aqueous buffer, to the MRI signal. This type of hydrogel depot erodes / degrades fast, within 6-8 weeks after subcutaneous implantation. It remains to be determined whether similar degradation rates also apply to the IVD. Nonetheless, it seems that the hydrogel does not lead to acceleration of the degenerative process in patients and does not interfere with MRI follow up on the long term.

Intradiscal application of celecoxib-loaded hydrogel improved the quality of life of 9/10 canine patients studied with chronic low back pain

In the clinical study, neither clinical nor radiological adverse effects nor complications were noted during the 3 to 6 months follow-up. To assess locomotion in an objective manner, GRFs were measured by FPA [34]. Propulsive forces of the hind limbs did not significantly increase after 6 and 12 weeks after treatment. In dogs suffering from chronic low back pain, a decrease in propulsive forces of the hind limbs was previously reported, with a significant improvement six months after decompressive surgery [34]. However, in our study population, the pre-treatment propulsive values of the hind limbs (P/T Fy- values) were higher than the P/T Fy- values in the dogs of the former study [34]. The canine patients included in the present study mainly showed difficulty in performing certain complex movements (e.g. jumping, standing up, laying down) prior to treatment which can only be observed from owner's history taking or responses to questionnaires, and not by FPA. As such, the present study is underpowered to detect subtle changes in the P/T Fy-. Notably, owners perceived a clear and significant improvement of quality of life of their dog.

Clinical improvement is not accompanied by a regenerative effect based on quantitative MR imaging

Pfirrmann score and DHI did not significantly differ before and after injection, or at 12 weeks follow up. Since the DHI prior to treatment was not decreased, an increase in disc space was not expected. Given the limitation of the Pfirrmann grading system, this study employed quantitative T2 mapping MRI, a sequence that uses the T2 relaxation time for quantification of IVD degeneration by quantitative measurement of water and proteoglycan content [40]. Three months after treatment no regenerative effect at the MRI level was observed; T2 relaxation times were not different from pre-treatment values. It remains to be determined whether intradiscal application of controlled release systems of COX-2 inhibitors only acts anti-inflammatory and provide thereby clinical improvement by effective pain management, or that they have regenerative capacities that are only visible on the long term.

Future perspectives

The present clinical study is limited by the small group size and the absence of a placebo group, thereby allowing for owner's bias towards the results. Before randomized placebo-controlled clinical studies, additional studies need to be performed to fine tune the loading dose, the release profile in order to have proper anti-inflammatory and regenerative effects. The safe use of local delivery that we have demonstrated is an important step in reducing the side-effects of current systemic pharmaceutical treatment, and in reducing or postponing the need for major surgery for advanced stages of IVD disease. Such minimally invasive treatment strategies have important implications in reducing the total cost of care and the burden of the disease to patients and ageing populations in general.

Conclusions

This present study showed the safety and feasibility of intradiscal delivery of the COX-2 inhibitor celecoxib loaded on a thermoresponsive hydrogel loaded *in vivo* in an experimental and clinical setting with canine patients suffering from chronic low back pain. In the majority of the treated canine patients, quality of life improved without evident regenerative effects on MRI at 3 months follow up. As such, fine tuning of the delivery biomaterial platforms and strategies based on COX-2 inhibitors may not only harness pain but also exert regenerative effects on the long term.

Acknowledgements

We would like to acknowledge the help of Koen Santifort and Anouk Verbeek in the *in vitro* analyses, the assistance of Anke Wassink and Joris de Brouwer in adapting and carrying out MRI protocols and fluoroscopy and Arie Doornenbal for helping with the force plate analyses. We would like to thank Erik Wouters and Thijs How for referring canine patients with low back pain to participate in the clinical study.

References

1. Alleva J, Hudgins T, Belous J, Kristin Origenes A. Chronic low back pain. Dis.Mon. 2016;62:330-3.
2. Bergknut N, Egenvall A, Hagman R, Gustas P, Hazewinkel HA, Meij BP*, et al*. Incidence of intervertebral disk degeneration-related diseases and associated mortality rates in dogs. J.Am.Vet.Med.Assoc. 2012;240:1300-9.
3. de Schepper EI, Damen J, van Meurs JB, Ginai AZ, Popham M, Hofman A*, et al*. The association between lumbar disc degeneration and low back pain: the influence of age, gender, and individual radiographic features. Spine (Phila Pa.1976) 2010;35:531-6.
4. Hoy D, March L, Brooks P, Blyth F, Woolf A, Bain C*, et al*. The global burden of low back pain: estimates from the Global Burden of Disease 2010 study. Ann.Rheum.Dis. 2014;73:968-74.
5. Bach FC, Willems N, Penning LC, Ito K, Meij BP, Tryfonidou MA. Potential regenerative treatment strategies for intervertebral disc degeneration in dogs. BMC Vet.Res. 2014;10:3,6148-10-3.
6. Bergknut N, Rutges JP, Kranenburg HJ, Smolders LA, Hagman R, Smidt HJ*, et al*. The dog as an animal model for intervertebral disc degeneration? Spine (Phila Pa.1976) 2012;37:351-8.
7. Phillips KL, Cullen K, Chiverton N, Michael AL, Cole AA, Breakwell LM*, et al*. Potential roles of cytokines and chemokines in human intervertebral disc degeneration: interleukin-1 is a master regulator of catabolic processes. Osteoarthritis Cartilage 2015;23:1165-77.
8. Risbud MV and Shapiro IM. Role of cytokines in intervertebral disc degeneration: pain and disc content. Nat.Rev.Rheumatol. 2014;10:44-56.
9. Walter BA, Purmessur D, Likhitpanichkul M, Weinberg A, Cho SK, Qureshi SA*, et al*. Inflammatory Kinetics and Efficacy of Anti-inflammatory Treatments on Human Nucleus Pulposus Cells. Spine (Phila Pa.1976) 2015;40:955-963.
10. Le Maitre CL, Hoyland JA, Freemont AJ. Catabolic cytokine expression in degenerate and herniated human intervertebral discs: IL-1beta and TNFalpha expression profile. Arthritis Res.Ther. 2007;9:R77.
11. Binch A, Cole AA, Breakwell LM, Michael A, Chiverton N, Cross AK*, et al*. Expression and regulation of neurotrophic and angiogenic factors during human intervertebral disc degeneration. Arthritis Res.Ther. 2014;16:416.
12. Purmessur D, Walter BA, Roughley PJ, Laudier DM, Hecht AC, Iatridis J. A role for TNFalpha in intervertebral disc degeneration: a non-recoverable catabolic shift. Biochem.Biophys.Res.Commun. 2013;433:151-6.
13. Miyamoto H, Doita M, Nishida K, Yamamoto T, Sumi M, Kurosaka M. Effects of cyclic mechanical stress on the production of inflammatory agents by nucleus pulposus and anulus fibrosus derived cells in vitro. Spine (Phila Pa.1976) 2006;31:4-9.
14. Miyamoto H, Saura R, Harada T, Doita M, Mizuno K. The role of cyclooxygenase-2 and inflammatory cytokines in pain induction of herniated lumbar intervertebral disc. Kobe J.Med.Sci. 2000;46:13-28.
15. Willems N, Tellegen AR, Bergknut N, Creemers LB, Wolfswinkel J, Freudigmann C*, et al*. Inflammatory profiles in canine intervertebral disc degeneration. BMC Vet.Res. 2016;12:.
16. Samad TA, Moore KA, Sapirstein A, Billet S, Allchorne A, Poole S*, et al*. Interleukin-1beta-mediated induction of Cox-2 in the CNS contributes to inflammatory pain hypersensitivity. Nature 2001;410:471-5.
17. Sekiguchi M, Otoshi K, Kikuchi S, Konno S. Analgesic effects of prostaglandin E2 receptor subtype EP1 receptor antagonist: experimental study of application of nucleus pulposus. Spine (Phila Pa.1976) 2011;36:1829-34.
18. Sakai D and Grad S. Advancing the cellular and molecular therapy for intervertebral disc disease. Adv.Drug Deliv.Rev. 2015;84:159-71.
19. McCormack PL. Celecoxib: a review of its use for symptomatic relief in the treatment of osteoarthritis, rheumatoid arthritis and ankylosing spondylitis. Drugs 2011;71:2457-89.
20. Meij BP and Bergknut N. Degenerative lumbosacral stenosis in dogs. Vet.Clin.North Am.Small Anim.Pract. 2010;40:983-1009.
21. Monteiro-Steagall BP, Steagall PV, Lascelles BD. Systematic review of nonsteroidal anti-inflammatory drug-induced adverse effects in dogs. J.Vet.Intern.Med. 2013;27:1011-9.
22. Richette P, Latourte A, Frazier A. Safety and efficacy of paracetamol and NSAIDs in osteoarthritis: which drug to recommend? Expert Opin.Drug Saf. 2015;14:1259-68.
23. Motaghinasab S, Shirazi-Adl A, Parnianpour M, Urban JP. Disc size markedly influences concentration profiles of intravenously administered solutes in the intervertebral disc: a computational study on glucosamine as a model solute. Eur.Spine J. 2014;23:715-23.
24. Zhang L, Wang JC, Feng XM, Cai WH, Yang JD, Zhang N. Antibiotic penetration into rabbit nucleus pulposus with discitis. Eur.J.Orthop.Surg.Traumatol. 2014;24:453-8.

25. Petit A, Redout EM, van de Lest CH, de Grauw JC, Muller B, Meyboom R*, et al*. Sustained intra-articular release of celecoxib from in situ forming gels made of acetyl-capped PCLA-PEG-PCLA triblock copolymers in horses. Biomaterials 2015;53:426-36.
26. Willems N, Yang HY, Langelaan ML, Tellegen AR, Grinwis GC, Kranenburg HJ*, et al*. Biocompatibility and intradiscal application of a thermoreversible celecoxib-loaded poly-N-isopropylacrylamide MgFe-layered double hydroxide hydrogel in a canine model. Arthritis Res.Ther. 2015;17:214,015-0727-x.
27. Bikram M and West JL. Thermo-responsive systems for controlled drug delivery. Expert Opin.Drug Deliv. 2008;5:1077-91.
28. Petit A, Sandker M, Muller B, Meyboom R, van Midwoud P, Bruin P*, et al*. Release behavior and intra-articular biocompatibility of celecoxib-loaded acetyl-capped PCLA-PEG-PCLA thermogels. Biomaterials 2014;35:7919-28.
29. Petit A, Muller B, Meijboom R, Bruin P, van de Manakker F, Versluijs-Helder M*, et al*. Effect of polymer composition on rheological and degradation properties of temperature-responsive gelling systems composed of acyl-capped PCLA-PEG-PCLA. Biomacromolecules 2013;14:3172-82.
30. Bergknut N, Auriemma E, Wijsman S, Voorhout G, Hagman R, Lagerstedt AS*, et al*. Evaluation of intervertebral disk degeneration in chondrodystrophic and nonchondrodystrophic dogs by use of Pfirrmann grading of images obtained with low-field magnetic resonance imaging. Am.J.Vet.Res. 2011;72:893-8.
31. Willems N, Mihov G, Grinwis GC, van Dijk M, Schumann D, Bos C*, et al*. Safety of intradiscal injection and biocompatibility of polyester amide microspheres in a canine model predisposed to intervertebral disc degeneration. J.Biomed.Mater.Res.B.Appl.Biomater. 2015;105:707-714.
32. Willems N, Bach FC, Plomp SG, van Rijen MH, Wolfswinkel J, Grinwis GC*, et al*. Intradiscal application of rhBMP-7 does not induce regeneration in a canine model of spontaneous intervertebral disc degeneration. Arthritis Res.Ther. 2015;17:137-151.
33. Bergknut N, Grinwis G, Pickee E, Auriemma E, Lagerstedt AS, Hagman R*, et al*. Reliability of macroscopic grading of intervertebral disk degeneration in dogs by use of the Thompson system and comparison with low-field magnetic resonance imaging findings. Am.J.Vet.Res. 2011;72:899-904.
34. Suwankong N, Meij BP, Van Klaveren NJ, Van Wees AM, Meijer E, Van den Brom WE*, et al*. Assessment of decompressive surgery in dogs with degenerative lumbosacral stenosis using force plate analysis and questionnaires. Vet.Surg. 2007;36:423-31.
35. Tellegen AR, Willems N, Tryfonidou MA, Meij BP. Pedicle screw-rod fixation: a feasible treatment for dogs with severe degenerative lumbosacral stenosis. BMC Vet.Res. 2015;11:299.
36. An HS, Takegami K, Kamada H, Nguyen CM, Thonar EJ, Singh K*, et al*. Intradiscal administration of osteogenic protein-1 increases intervertebral disc height and proteoglycan content in the nucleus pulposus in normal adolescent rabbits. Spine (Phila Pa.1976) 2005;30:25-31.
37. Shimizu J, Mochida K, Kobayashi Y, Kitamura M, Tanaka H, Kishimoto M*, et al*. Inflammatory reaction in the herniated degenerative disc materials in miniature dachshunds. J.Vet.Med.Sci. 2010;72:81-4.
38. Sandker MJ, Petit A, Redout EM, Siebelt M, Muller B, Bruin P*, et al*. In situ forming acyl-capped PCLA-PEG-PCLA triblock copolymer based hydrogels. Biomaterials 2013;34:8002-11.
39. Mackenzie SD, Brisson BA, Gaitero L, Caswell JL, Liao P, Sinclair M*, et al*. Distribution and Short- and Long-Term Effects of Injected Gelified Ethanol into the Lumbosacral Intervertebral Disc in Healthy Dogs. Vet.Radiol.Ultrasound 2015;57:180,-190.
40. Takashima H, Takebayashi T, Yoshimoto M, Terashima Y, Tsuda H, Ida K*, et al*. Correlation between T2 relaxation time and intervertebral disk degeneration. Skeletal Radiol. 2012;41:163-7.

Supplementary file 1. Characterization of the propionyl-capped PCLA-PEG-PCLA hydrogel by ^{1}H NMR and GPC.

^{1}H NMR analysis

^{1}H NMR analysis of the polymer was performed using a Varian oxford, operating at 300 MHz. ^{1}H NMR spectra was referenced to the signal of chloroform at 7.26 ppm.

^{1}H NMR ($CDCl_3$, 300 MHz) δ: 5.20-5.00 (6H,-CO-C**H**(CH_3)-O-); 4.40-4.19 (4H,-PEG-O-CH_2-C**H$_2$**-O-CO-); 4.19-3.95 (36H, -CO-(CH_2)$_4$-C**H$_2$**-O-); 3.85-3.40 (132H, -O-C**H$_2$**-C**H$_2$**-O-); 2.50-2.30 (36H, -CO-C**H**$_2$-(CH_2)$_4$-O-) + (4H, -CO-C**H**$_2$-CH_3); 1.73-1.58 (72H, -CO-CH_2-C**H$_2$**-CH_2-C**H$_2$**-CH_2-O-); 1.58-1.30 (18H, -CO-CH(C**H$_3$**)-O-) + (36H, -CO-CH_2-CH_2-C**H$_2$**-CH_2-CH_2-O-); 1.25-1.10 (6H, -CO-CH_2-C**H**$_3$) (Figure S1).

Figure S1: ^{1}H NMR spectra of propionyl-capped PCLA-PEG-PCLA.

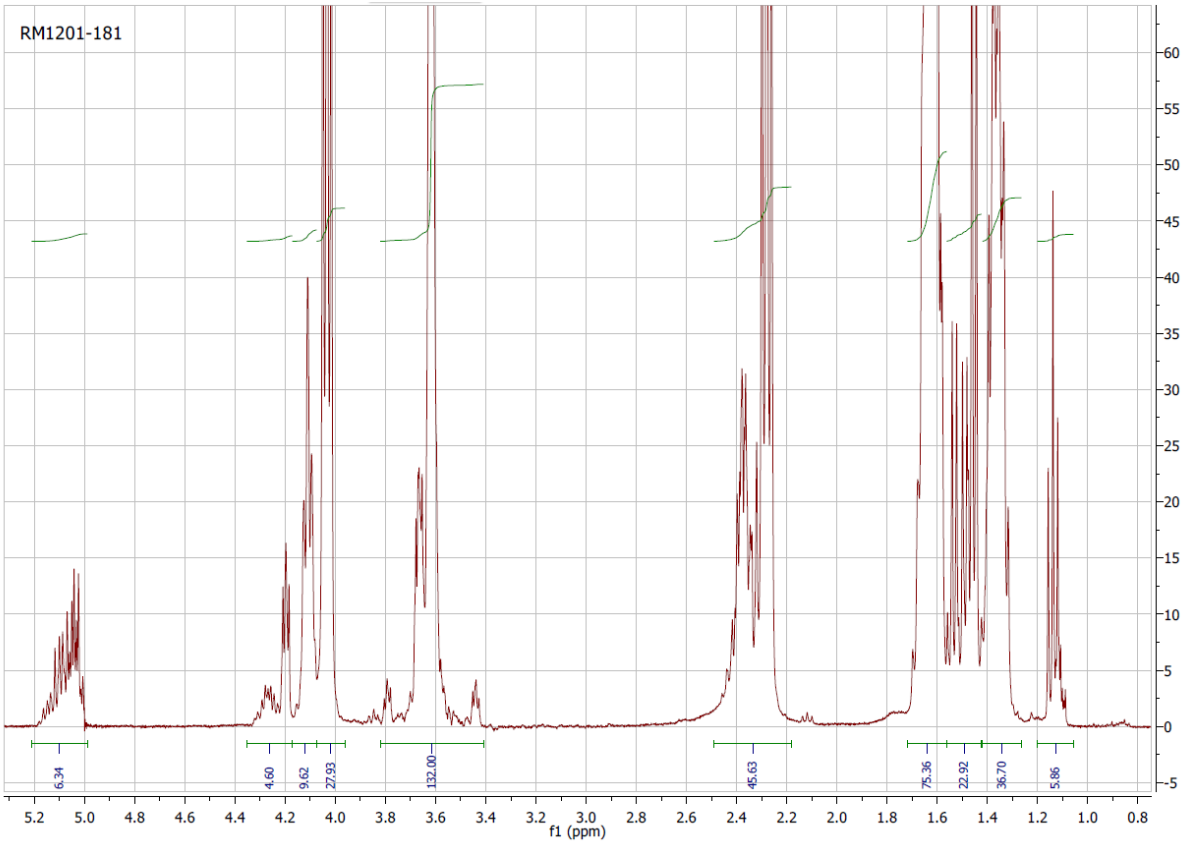

Gel permeation chromatography

The Mn and polydispersity index (PDI) of the polymer was determined by gel permeation chromatography (GPC) using an Agilent system Series 100 equipped with a guard column (PLgel 5 µm, 7.5 x 50 mm) and three Varian columns (PLgel, 5 µm, 500 Å, 300 x 7.5 mm). Detection was performed with a refractive index detector. The column temperature was set at 35 °C and THF was used as the mobile phase at a flow of 1 ml/min. The polymer was dissolved overnight in THF at a concentration of approx. 5 mg/ml and filtered through a 0.45 µm filter prior analysis. PEG standards of different molecular weights were used for reference and the injection volume was 50 µl (Table S1).

Table S1: Characteristics of propionyl-capped PCLA-PEG-PCLA as determined by GPC.

	Mn[a]	**PDI[b]**
Propionyl-capped PCLA-PEG-PCLA	4400 g/mol	1.35

[a] Mn (number-average molecular mass) is determined by GPC with THF as mobile phase and PEG standards were used for calibration; [b]PDI (polydispersity index).

Supplementary file 2. Histological evaluation of inflammatory responses after subcutaneous implantation in mice.

	Test sample						Control sample				
Animal number:	**1**	**2**	**3**	**4**	**5**	**6**	**1**	**2**	**3**	**5**	**6**
Inflammation											
Polymorphonuclear	0	1	1	0	1	1	1	1	1	1	1
Lymphocytes	0	0	0	0	0	0	0	0	0	0	0
Plasma cells	0	0	0	0	0	0	0	0	0	0	0
Macrophages	2	3	3	3	4	3	0	1	1	0	0
Giant cells	0	0	0	0	0	0	0	0	0	0	0
Necrosis	1	1	1	0	1	0	0	0	0	0	0
SUB-TOTAL (× 2)	**6**	**10**	**10**	**6**	**12**	**8**	**2**	**4**	**4**	**2**	**2**
Neovascularisation	0	0	0	0	1	1	1	0	0	1	1
Fibrosis	0	0	0	0	0	0	0	0	0	0	0
Fatty infiltrate	0	0	0	0	0	0	0	0	0	0	0
SUB-TOTAL	**0**	**0**	**0**	**0**	**1**	**1**	**1**	**0**	**0**	**1**	**1**
TOTAL	**6**	**10**	**10**	**6**	**13**	**9**	**3**	**4**	**4**	**3**	**3**

Implantation interval: 7 days.

	Test sample						Control sample				
Animal number:	**7**	**8**	**9**	**10**	**11**	**12**	**7**	**9**	**10**	**11**	**12**
Inflammation											
Polymorphonuclear	2	2	1	2	0	2	1	1	1	0	1
Lymphocytes	0	0	0	0	0	0	0	0	0	0	0
Plasma cells	0	0	0	0	0	0	0	0	0	0	0
Macrophages	3	3	4	3	2	3	2	1	1	1	0
Giant cells	0	0	0	0	1	0	0	0	0	0	0
Necrosis	1	1	0	1	0	1	0	0	0	0	0
SUB-TOTAL (× 2)	**12**	**12**	**10**	**12**	**6**	**12**	**6**	**4**	**4**	**2**	**2**
Neovascularisation	1	1	1	1	2	1	0	0	0	0	0
Fibrosis	0	0	0	0	0	0	0	0	0	0	0
Fatty infiltrate	0	0	0	0	0	0	0	0	0	0	0
SUB-TOTAL	**1**	**1**	**1**	**1**	**2**	**1**	**0**	**0**	**0**	**0**	**0**
TOTAL	**13**	**13**	**11**	**13**	**8**	**13**	**6**	**4**	**4**	**2**	**2**

Implantation interval: 28 days.

Based on the score of the test and control sites, the average difference between test and controls for each animal was calculated:

animal #	test	control	score
1	6	4	2
2	10	4	6
3	10	4	6
4	6	3	3
5	13	3	10
6	9	3	6
Mean 7d	**9,0**	**3,6**	**5,4**

animal #	test	control	score
7	13	2	11
8	13	2	11
9	11	4	7
10	13	4	9
11	8	2	6
12	13	2	11
Mean 28d	**11,8**	**3,0**	**9,2**

Based on ISO10993-6, 2007, Biological evaluation of Biomedical Devices – part 6, biocompatibility was rated at 5,4 at 7 days and 9,2 at 28 days, compatible with respectively slight and moderate reaction based on the following scheme:

0.0 - 2,9	no reaction
3,0 - 8,9	slight reaction
9.0 - 15	moderate reaction
> 15	severe reaction

Supplementary file 3. Primers used for quantitative RT-PCR

Table 1. Gene-specific primer sequences with associated amplification temperatures.

Gene	Primer sequence (5'-'3)	Amplicon size (bp)	Temp (°C)
Reference genes			
GAPDH	Fw TGTCCCCACCCCCAATGTATC	100	58
	Rv CTCCGATGCCTGCTTCACTACCTT		
HPRT	Fw AGCTTGCTGGTGAAAAGGAC	104	56-58
	Rv TTATAGTCAAGGGCATATCC		
RPS19	Fw CCTTCCTCAAAAAGTCTGGG	95	61-63
	Rv GTTCTCATCGTAGGGAGCAAG		
SDHA	Fw GCCTTGGATCTCTTGATGGA	92	61
	Rv TTCTTGGCTCTTATGCGATG		
Target genes			
ACAN	Fw GGACACTCCTTGCAATTTGAG	110	61-62
	Rv GTCATTCCACTCTCCCTTCTC		
ADAMTS5	Fw CTACTGCACAGGGAAGAG	148	61
	Rv GAACCCATTCCACAAATGTC		
AXIN2	Fw GGACAAATGCGTGGATACCT	128	60
	Rv TGCTTGGAGACAATGCTGTT		
BCL2	Fw GGATGACTGAGTACCTGAACC	80	61.5-63
	Rv CGTACAGTTCCACAAAGGC		
C-MYC	Fw GCCGGCGCCCAGCGAGGATA	108	61
	Rv GCGACTGCGACGTAGGAGGGCGAGC		
CASP3	Fw CGGACTTCTTGTATGCTTACTC	89	61
	Rv CACAAAGTGACTGGATGAACC		
CCND1	Fw ACTACCTGGACCGCT	151	60
	Rv CGGATGGAGTTGTCA		
COL1A1	Fw GTGTGTACAGAACGGCCTCA	109	61
	Rv TCGCAAATCACGTCATCG		
COL2A1	Fw GCAGCAAGAGCAAGGAC	150	60.5-65
	Rv TTCTGAGAGCCCTCGGT		
CTK8	Fw CCTTAGGCGGGTCTCTCGTA	149	63
	Rv GGGAAGCTGGTGTCTGAGTC		
CTK18	Fw GGACAGCTCTGACTCCAGGT	97	60
	Rv AGCTTGGAGAACAGCCTGAG		
FASL	Fw GGGGTCAGTCCTGCAACAACAA	93	54
	Rv ATCTTCCCTCCATCAGCATCAG		
IL1β	Fw: TGCTGCCAAGACCTGAACCAC	115	68
	Rv: TCCAAAGCTACAATGACTGACACG		
IL6	Fw: GAGCCCACCAGGAACGAAAGAGA	123	65
	Rv: CCGGGGTAGGGAAAGCAGTAGC		
IL10	Fw CCCGGGCTGAGAACCACGAC	91	63
	Rv AAATGCGCTCTTCACCTGCTCCAC		
MMP13	Fw CTGAGGAAGACTTCCAGCTT	250	65
	Rv TTGGACCACTTGAGAGTTCG		
TIMP1	Fw GGCGTTATGAGATCAAGATGAC	120	66
	Rv ACCTGTGCAAGTATCCGC		
TNFA	Fw CCCCGGGCTCCAGAAGGTG	83	65
	Rv GCAGCAGGCAGAAGAGTGTGGTG		

Continuation of table 1:

Primers used for qPCR analysis of target genes aggrecan (ACAN), a disintegrin and metalloproteinase with thrombospondin motifs 5 (ADAMTS5), axin 2 (AXIN2), B-Cell lymphoma 2 (BCL2), C-myc, Caspase 3 (CASP3), cyclin D1 (CCDN1), collagen type I α1 (COL1A1), collagen type II α1 (COL2A1), cytokeratin 8 (CK8), cytokeratin 18 (CK18), Fas Ligand (FasL), interleukin 1β (IL1 β), interleukin 6 (IL6), interleukin 10 (IL10), matrix metalloproteinase 13 (MMP13), Brachyury (T), tissue inhibitor of metalloproteinases 1 (TIMP1), tumor necrosis factor α (TNFα) and reference genes glyceraldehyde 3-phosphate dehydrogenase (GAPDH), hypoxanthine-guanine phosphoribosyltransferase (HPRT)), ribosomal protein S19 (RPS19) and succinate dehydrogenase complex, subunit A (SDHA).

Chapter 8

Intradiscal delivery of celecoxib-loaded microspheres restores disc homeostasis in a preclinical canine model

A. R Tellegen [1], I. Rudnik-Jansen [2], M. Beukers [1], A. Miranda-Bedate [1], F. C. Bach [1], W. de Jong [1], N. Woike [3], G. Mihov [3], J. Thies [3], B. P. Meij [1], L. B. Creemers [2], M. A. Tryfonidou [1]*

[1] Department of Clinical Sciences of Companion Animals, Faculty of Veterinary Medicine, Utrecht University, The Netherlands.

[2] Department of Orthopaedics, University Medical Centre Utrecht, The Netherlands.

[3] DSM Biomedical, The Netherlands.

Journal of Controlled Release (2018) 286: 439-450

Abstract

Low back pain, related to degeneration of the intervertebral disc (IVD), affects millions of people worldwide. Clinical studies using oral cyclooxygenase-2 (COX-2) inhibitors have shown beneficial effects, although side-effects were reported. Therefore, intradiscal delivery of nonsteroidal anti-inflammatory drugs can be an alternative treatment strategy to halt degeneration and address IVD-related pain. In the present study, the controlled release and biologic potency of celecoxib, a selective COX-2 inhibitor, from polyesteramide microspheres was investigated *in vitro*. In addition, safety and efficacy of injection of celecoxib-loaded microspheres were evaluated *in vivo* in a canine IVD degeneration model. *In vitro*, a sustained release of celecoxib was noted for over 28 days resulting in sustained inhibition of inflammation, as indicated by decreased prostaglandin E_2 (PGE_2) production, and anti-catabolic effects in nucleus pulposus (NP) cells from degenerated IVDs on qPCR. *In vivo*, there was no evidence of adverse effects on computed tomography and magnetic resonance imaging or macroscopic evaluation of IVDs. Local and sustained delivery of celecoxib prevented progression of IVD degeneration corroborated by MRI, histology, and measurement of NP proteoglycan content. Furthermore, it seemed to harness inflammation as indicated by decreased PGE_2 tissue levels and decreased neuronal growth factor immunopositivity, providing indirect evidence that local delivery of a COX-2 inhibitor could also address pain related to IVD degeneration. In conclusion, intradiscal controlled release of celecoxib from polyesteramide microspheres prevented progression of IVD degeneration both *in vitro* and *in vivo*. Follow-up studies are warranted to determine the clinical efficacy of celecoxib-loaded PEAMs in chronic back pain.

Introduction

Low back pain is the most common type of pain restricting daily activity and has a huge impact on quality of life and productivity [1, 2]. Due to the aging population and lifestyle changes, the burden on society will even continue to increase. Neck or back pain is associated with intervertebral disc (IVD) degeneration in a substantial part of the patients [3]. Genetic predisposition, mechanical overload, and unhealthy lifestyle can contribute to and aggravate degeneration of the IVD [4]. Increasing evidence points to a role for pro-inflammatory mediators in the degenerative process and to pain on a molecular level [5]. The latter occurs through several mechanisms. Pro-inflammatory mediators promote catabolic changes that lead to loss of proteoglycans in the core of the IVD, the nucleus pulposus (NP), resulting in a dehydrated disc with less shock-absorbing properties [6-8]. These biomechanical changes eventually lead to spinal instability and decreased disc height, with subsequent compression of nerves, exiting the intervertebral foramen. Tears and clefts appear in the degenerating annulus fibrosus (AF), the fibrous ring constraining the NP, and the disc can bulge into the spinal canal, leading to compression of neural tissues. Furthermore, in the degenerating IVD, blood vessels and nerve endings can penetrate the normally avascular and aneural IVD, via the production of neurotropic and angiogenic factors such as nerve growth factor (NGF) and vascular endothelial growth factor [5, 8-12]. This process is driven by pro-inflammatory mediators such as the cyclooxygenase-2 (COX-2) derived prostaglandin E_2 (PGE_2) and can, even in the absence of the aforementioned changes, contribute to discogenic pain [13]. Given that pain related to IVD degeneration may have multiple routes mediated by inflammation, oral anti-inflammatory drugs are being widely used in the clinic.

Current therapies for neck and back pain merely focus on pain management. To achieve biologic repair, novel treatment strategies also aim at inhibiting the degenerative process and restoring tissue integrity [14, 15]. They are challenged by the fact that tissue penetration of orally administered drugs into the avascular IVD is limited [16, 17]. To this end, local delivery of stem cells and/ or drugs seems to be a feasible strategy for the treatment of symptomatic IVD degeneration. Intradiscal transplantation of mesenchymal stromal cells (MSCs), although effective in treating pain, is challenged by high costs and the limited capacity of MSCs in enhancing IVD regeneration in clinical trials [18]. Drugs could provide a cost-effective alternative. Hereby, drug delivery systems enable drug loading at a higher dose and effectuate sustained drug release over prolonged period of time. Specifically for intradiscal application, such systems enable the development of minimally invasive treatment strategies keeping re-injections to a minimum; thereby supporting disc homeostasis while enabling biologic repair.

The evolution of resorbable degradable polymers from aliphatic polyesters to nitrogen bearing polymers such as polyurethanes, polyester amides and polyureas has been accompanied with better control over degradation and release properties. In addition, incorporation of amino acid-based building blocks provide one or more functional groups along the polymer chain that allow further modification of the polymer to tailor its

physicochemical properties and performance as drug eluting matrices [19, 20]. Microspheres based on biodegradable polyesteramide (PEA) polymers are a promising biomaterial platform for local drug delivery. These amino acid-based polymers provide good thermal and mechanical properties [21]. The polymer has been built of three di-amino monomers connected with di-acid linker in a polycondensation reaction. The monomer composition results in specific ester to amide bonds ratio which is essential for polymer biodegradation [19, 20]. An important advantage of these polymers is related to the fact that they predominantly degrade via an enzymatic mechanism and due to consequential surface erosion, drug release follows unique release kinetics [20], allowing for constant drug release in the degenerative IVD environment. PEA microspheres (PEAMs) can in this way serve as an autoregulatory drug delivery system [22]. In an inflammatory environment such as the osteoarthritic knee joint and degenerated IVD [23], proteases are abundantly present, leading to increased microsphere degradation and thus, faster drug release, harnessing inflammation. Recently, PEAMs have been shown to be safe for intradiscal application in a canine model predisposed to IVD degeneration, when employed with small needle sizes and limited injection volumes [24]. However, not much is known regarding optimal drug loading dose in a controlled release system for the degenerated IVD to achieve biologic repair.

The overall aim of the present study was to translate local controlled delivery of a COX-2 inhibitor for the purpose of biologic disc repair employing a clinically relevant animal model. Naturally occurring IVD degeneration in dogs resembles IVD degeneration in man with similar molecular, histological, radiological, and clinical characteristics. The dog is therefore a valuable translational large animal model for human and veterinary patients with chronic back pain [14, 25]. The biologic potency of controlled release of celecoxib on canine NP cells from degenerated IVDs, was first evaluated *in vitro*. Thereafter, safety and efficacy of a single intradiscal injection of PEAMs loaded with celecoxib in a dose range of 0.2 – 7 mg/mL corresponding to 10^{-4}M and 10^{-2}M total injected celecoxib, respectively, was evaluated *in vivo* employing a combination of diagnostic imaging, biochemical, and histological read out parameters.

Materials and methods

Synthesis and characterization of particle size, particle morphology, loading efficiency and release of celecoxib from polyesteramide microspheres

Synthesis and characterization of the polymer

The biomaterial in this study was a biodegradable poly(esteramide) based on α-amino acids, aliphatic dicarboxylic acids and aliphatic α-ω diols. The selected PEA comprises three types of building blocks randomly distributed along the polymer chain (Fig. 1A). The polymer was synthesized according to a procedure reported previously [26]. Briefly, the polymer was prepared via solution polycondensation of di-p-toluenesulfonic acid salts of bis-(α-amino acid) α,ω- diol diesters, lysine benzyl ester and di-N-hydroxysuccinimide sebacate in

anhydrous DMSO. The use of pre-activated acid in the reaction allows polymerization at low temperature (65 °C) affording side-product free polycondensates and predictable degradation products. The polymer was isolated from the reaction mixture in two precipitation steps. ^{1}H nuclear magnetic resonance (NMR) spectra were obtained on a Bruker Avance 500 MHz Ultrashield NMR; samples were recorded in DMSO d_6. Molecular weight and molecular weight distributions of PEA were determined by gel permeation chromatography equipped with refractive index detector. Samples were dissolved in tetrahydrofuran at a concentration of approximately 5 mg/mL and were run at a flow rate of 1 mL/min at 50 °C. The molecular weights were calibrated to a narrow polystyrene standard calibration curve, using Waters Empower software.

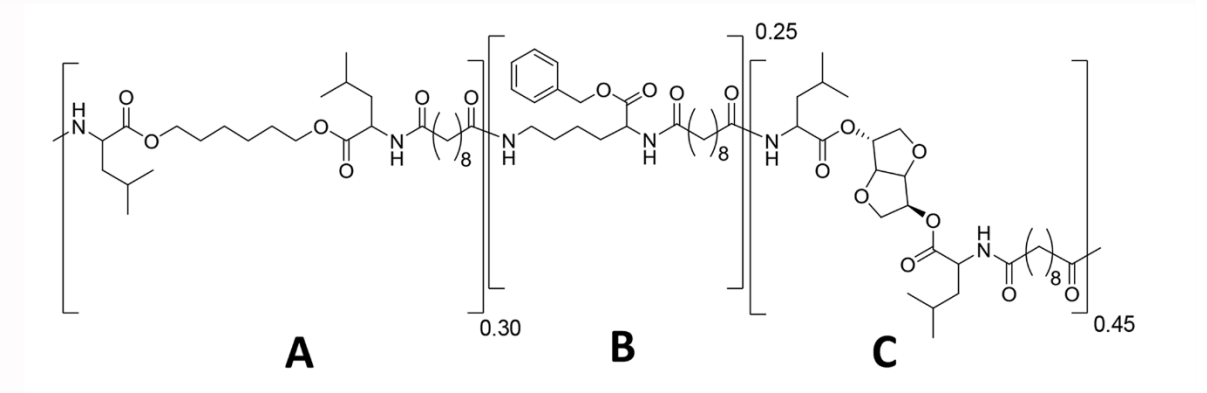

Figure 1. Structure of polyesteramide (PEA) III Ac Bz random copolymer consisting of building blocks A, B and C (Leu, Lys, Leu).

Microsphere preparation

Polyesteramide polymer was dissolved in dichloromethane (15wt/v%). To generate celecoxib (CXB) loaded PEAMs, the drug was added (Polymer: dichloromethane 5wt%). After homogenization, the solution was sonicated in a water bath for 3 minutes. The PEA-CXB solution was then emulsified in 20 mL of water phase (PVA 1wt%, NaCl 2.5wt%) by the use of an ultraturrax, stirring at 4000 rpm (8000 rpm for empty PEAMs) for 3 minutes. After emulsification, particles were hardened overnight under air flow. Before washing, particles were cooled with an ice-bath for 1 hour and washed with Tween 80. Excess of surfactant was removed by centrifugation. Before freeze-drying to remove residual solvent, particles were suspended in Tween 80 in order to reach the right concentration of particles per volume: 1.05 and 35 mg particles/mL for CXB-loaded PEAMs, with 20 wt% CXB in the loaded PEAMs. For the unloaded particles, a 35 mg/mL concentration was prepared. Once dried, the PEAMs were weighted in individual HPLC vials to the approximate amount of 1.05 or 35 mg PEAMs corresponding with 0.2 and 7 mg CXB, respectively, and γ-sterilized on dry ice (Table 1). The loading dose of the particles was chosen based on restrictions for the injectable volume to a degenerating disc and a previous study investigating the controlled release of 0.38–38 µg CXB per mL in a dose response fashion from a pNIPAAM hydrogel [27]. Provided

that only mild PGE_2 inhibition was observed in vivo in the latter study, a much higher CXB loading dose was chosen in the present in vivo study.

Release kinetics of celecoxib-loaded polyesteramide microspheres in PBS

Drug loading of CXB was determined by weighing ~15mg of microparticles and dissolving them in methanol:PBS (75:25 v/v). Samples were filtered over 0.45 µm Teflon filter and diluted towards an amount that fits within the middle range of calibration standards (0.1 µg/mL-20 µg/mL). Release of celecoxib from the PEAMs in PBS for 14 days was measured by HPLC as described previously [22]. Briefly, at least 15 mg of microspheres with 20% celecoxib loading were placed in centrifuge tubes and immersed in 40 mL phosphate buffered saline (PBS) at 37 °C under gentle shaking. After centrifugation, 36 mL buffer was removed and replaced with the same amount of fresh buffer at defined time-points such as 2 h, 5 h, day 1, day 2, 3, 4, 7, 8, 9, 11 and 14 days until completion of the release study. Release was stopped after 14 days release and mass balance was determined. After the last removal of buffer at 14 days, particles were washed with 10 mL of water to remove the remaining PBS buffer. Particles were centrifuged, and 15 mL of water was removed. This step was repeated three times. Particles were then dried in the oven under full vacuum and ambient condition for 48h. Particles were dissolved with methanol:PBS (75:25 v/v) mixture and measured with HPLC.

The effect of PEA based celecoxib-loaded microspheres on nucleus pulposus cells in vitro

Setup of in vitro experiment

The anti-inflammatory effects of the CXB-loaded PEA platform on canine NP cells, in the presence of the pro-inflammatory stimulus TNF-α (10 ng/mL), was tested in monolayer culture as a measure of the bioactivity of the released celecoxib (Fig. 2A). NP tissue was collected *post-mortem* from the (untreated) cervical spine of the dogs described in the *in vivo* experiment, in aseptic conditions. The cervical spine had received no treatment during the *in vivo* experiment. Thereafter, NPs were digested by 0.15% w/v pronase for 45 minutes (10165921001, Roche Diagnostics) and 0.15% w/v collagenase overnight (LS004177, Worthington). Cells were expanded in hgDMEM+Glutamax (31966, Gibco Life Technologies) containing 10% v/v FBS (16000-044, Gibco Life Technologies), 1% v/v penicillin/streptomycin (p/s, P11-010, PAA laboratories), 0.1 mM ascorbic acid 2-phosphate (Asap, A8960, Sigma-Aldrich), 10^{-9}M dexamethasone (D1756, Sigma-Aldrich), 1 ng/mL basic fibroblast growth factor (PHP105, AbD Serotec), and 0.05% v/v fungizone (15290-018, Invitrogen) at 37 °C, 21% O_2 and 5% CO_2. The culture medium was renewed every 3-4 days. At passage two, NP cells were cryopreserved in aliquots of 10^6 cells per vial in hgDMEM+Glutamax with 10% v/v DMSO (20-139, EMD Millipore Corporation) and 10% v/v FBS. Three days before the experiment, cells were thawed and seeded on a 24-wells plate (662160, Greiner bio-one) at a density of 60,000 cells per well under hypoxic conditions (5% O_2). Cells were cultured in chondrogenic medium (hgDMEM+Glutamax) containing 1% v/v p/s, 1% v/v ITS+ premix

(354352, Corning Life Sciences), 0.04 mg/mL L-proline (P5607, Sigma-Aldrich), 0.1 mM Asap and 1.25 mg/mL bovine serum albumin (A9418, Sigma-Aldrich).

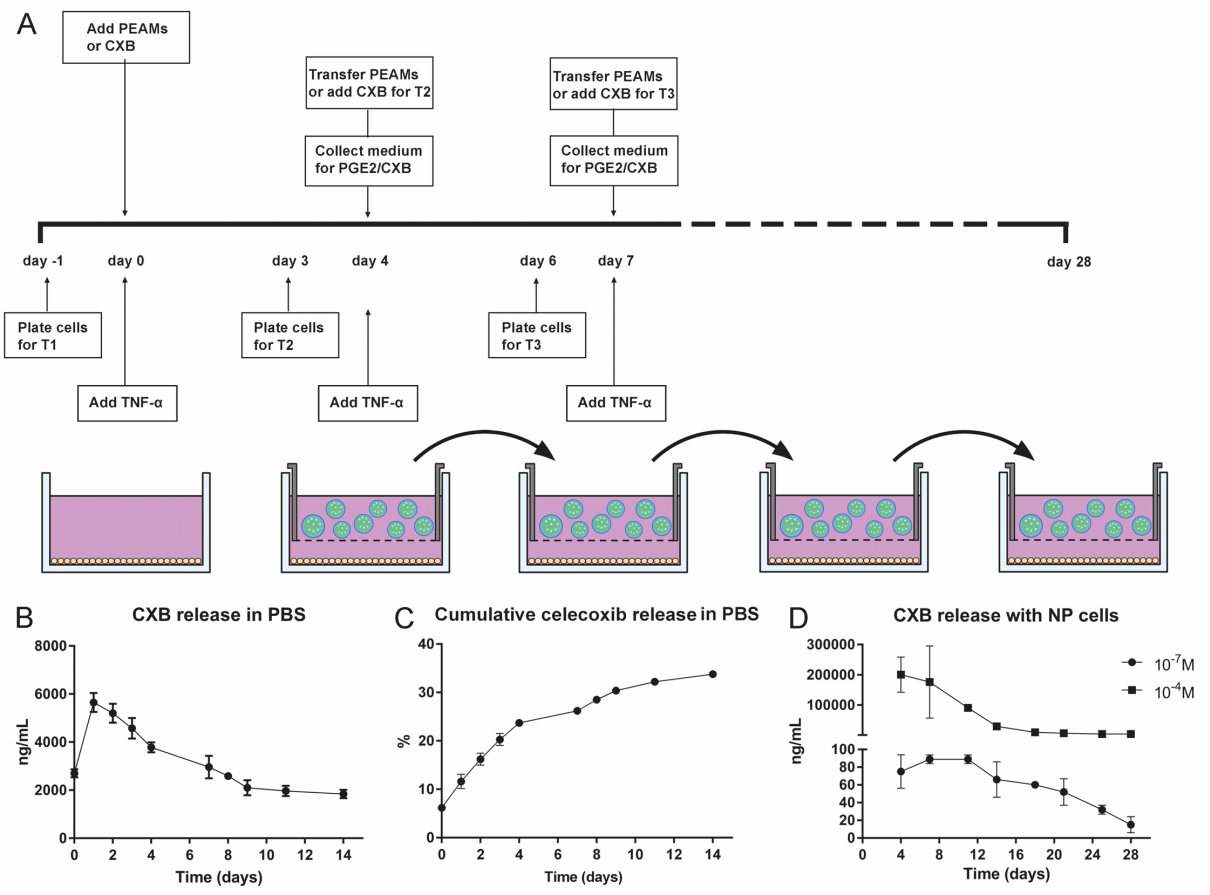

Figure 2. Controlled release of celecoxib *in vitro*. **A.** Schematic overview of *in vitro* celecoxib (CXB) release from polyesteramide microspheres (PEAMs) in the presence of nucleus pulposus (NP) cells from degenerated canine intervertebral discs (**A**). *n*=6 donors per condition per time point, in technical duplicates. Absolute (**B**) and (**C**) cumulative CXB release in PBS: after 14 days, approximately 30% was released. *n*=3 per time point. (**D**) Absolute CXB release from PEAMs containing CXB resulting into a final concentration of 10^{-7}M and 10^{-4}M CXB loaded on the PEAMs in the presence of NP cells: after 28 days, ~20% and 40% was released respectively, from the 10^{-7}M and 10^{-4}M loaded PEAMs. *n*=2 per time point.

On day 0, the medium was renewed and the unloaded or CXB-loaded PEAMs were dispersed in chondrogenic culture medium and placed in Transwell® baskets (pore size 0.4 µm, polycarbonate membrane, Costar Corning) (Fig. 2A). Two concentrations of CXB-loaded microspheres were utilized: 1.33 µg/mL and 1.33 mg/mL, corresponding with 10^{-7}M and 10^{-4}M celecoxib in order to achieve partial and complete inhibition of COX-2 activity within the culture system and thereby determine dose-dependent bioactivity. Cells and microspheres were co-incubated for 4 hours at 37°C, 5% CO_2 and 95% humidity. Subsequently, a pro-

inflammatory stimulus was provided by adding 10 ng/mL TNF-α (R&D Systems, Oxon, United Kingdom). Cells treated with a celecoxib bolus (equivalent to 10^{-6}M), were included as positive controls at each time interval. For determination of celecoxib bioactivity, NP cells and microspheres were co-incubated for 72 hours before the microspheres were transferred to a new 24-well culture plate containing cells seeded according to the procedure described above (*n*=6 donors, in duplicates). This procedure was repeated 8 times amounting to a release period of 28 days. Every 72 hours, medium was collected and stored at -80 °C.

In vitro read out parameters

In medium, PGE_2 levels were measured using the enzyme immunoassay PGE_2 EIA Kit (514010, Cayman Chemical), according to the respective manufacturer instructions. Celecoxib was measured using a competitive colometric ELISA (180719, Neogen Corp) following manufacturer's instructions. DNA content was measured using the Qubit® dsDNA High Sensitivity Assay Kit (Q32851, Invitrogen). RNA was isolated using the RNeasy® microkit (74004, Qiagen) according to the manufacturer's instructions, including a DNAse (RNAse-Free DNase Set, 79254, Qiagen) step. cDNA was synthesized using the iScript™ cDNA Synthesis Kit (170-8891, Bio-Rad) according to the manufacturer's instructions. Primer sequences were designed using PerlPrimer (Supplementary file 1). RT-qPCR was performed using the iQT™ SYBR Green Supermix Kit and the CFX384 Touch™ Real-Time PCR Detection System (both from Bio-Rad). For determination of relative gene expression, the Normfirst ($E^{\Delta\Delta Cq}$) method was used. For each target gene, the mean n-fold changes and standard deviations in gene expression were calculated. Four reference genes shown to be stable were chosen to normalize gene expression of target genes (Supplementary File 1).

In vivo experimental design

Animal experiments were approved and conducted in accordance with guidelines of the Animal Experiments Committee (project number AVD108002015282), as required by Dutch regulation. All animal experiments were conducted in compliance with the standards of animal care of the Faculty of Veterinary Medicine. Six healthy intact male dogs were purchased from Marshall BioResources (19 months of age, body weight 8-10 kg). In line with the reduction and refinement of experimental animal use, the dogs were employed for the study of two anti-inflammatory agents loaded on PEAMs, one of which was celecoxib, which is reported here. Three dogs were used in the current study. Controls, *i.e.* unloaded PEAMs, were shared between these two experiments, resulting in a total of *n*=6 IVDs per condition.

Intervertebral disc degeneration was induced at five alternating levels (T12-T13, L1-L2, L3-L4, L5-L6 and L7-S1; see below). Four weeks after induction of degeneration, magnetic resonance imaging (MRI) was performed to assess IVD degeneration at baseline. Thereafter, CXB-loaded and empty PEAMs were injected in a random fashion with *n*=6 IVDs per experimental group (*i.e.* non-induced IVDs, unloaded PEAMs (control, *n*=6 dogs), and low dose (LD) and high dose (HD) CXB-loaded PEAMs both as duplicates in *n*=3 dogs). Twelve weeks thereafter, MRI was performed, and the dogs were sacrificed with intravenous (IV)

administration of pentobarbital (200 mg/kg). *Post-mortem*, computed tomography (CT) of the lumbar spine was performed. Subsequently, the spinal column was harvested, and spinal units were collected as described previously [27] and further processed for macroscopic and histopathologic assessment and for biochemical analysis. Briefly, each spinal unit (½ vertebra – IVD – ½ vertebra) was mid-sagitally transected. One half of the IVD tissue containing (NP and AF) was snap frozen in liquid nitrogen and stored at -80 °C until further biochemical analyses. The other part was photographed for macroscopic evaluation (Thompson score) and fixed in 10% buffered formaldehyde.

Table 1. Details on polyesteramide microspheres used in the *in vivo* study. CXB, celecoxib; LD, low dose; HD, high dose.

Condition	**Size distribution D(0.5) (µm)**	**Span**	**Loading (wt%)**	**Particle concentration (mg/mL)**
Unloaded	31.9	1.168	0	35
LD-CXB	25.3	1.14	20	1.05
HD-CXB	25.3	1.14	20	35

Surgical induction of intervertebral disc degeneration

Degeneration of the IVD was achieved by the method described by Hiyama *et al*. (2008) [28]. Pre-operative analgesia was secured by IV administration of 4 mg/kg carprofen and 20 µg/kg buprenorphine. Premedication consisted of 10 µg/kg dexmedetomedine IV anesthesia was subsequently induced with 1-2 mg/kg propofol IV. The dogs received endotracheal tubes and general anesthesia was maintained by 1-1.5% v/v isoflurane gas, delivered in a 1:1 oxygen:air mixture. Peri-operative analgesia consisted of continuous rate infusion (CRI) of ketamine (10 µg/kg/min) and dexmedetomedine (2 µg/kg/hr). Throughout the complete procedure heart rate, respiration rate, body temperature, carbon dioxide and oxygen levels were monitored. The dogs were positioned in a right recumbent position and the surgical area was prepared aseptically to expose the left lateral AF of T12-T13 until the L5-L6 IVDs. The skin was incised and the IVDs were localized, an 18G needle was inserted superficially on the AF perimeter to check the location of the needle by intra-operative fluoroscopy. When correct needle placement was confirmed, the needle was inserted through the AF into the center of the NP and with a 10 mL syringe, the NP was aspirated. The L7-S1 IVD was approached dorsally in a percutaneous fashion, and correct needle placement on and through the dorsal AF was again confirmed by fluoroscopy. Postoperative analgesia consisted of subcutaneous administration of carprofen (4 mg/kg, q24h) and intramuscular (IM) administrations of buprenorphine (20 µg/kg q8h) for 3 days. Dogs were monitored daily in the first week postoperatively by a veterinarian (AT).

Intradiscal injection of PEAMs

Four weeks after induction of IVD degeneration, PEAMs were injected directly into the center of the IVD employing the same anesthesia protocol as was used for the induction of IVD degeneration. Pre- and postoperative analgesia consisted solely of buprenorphine, to exclude the possibility of carprofen interfering in the study after CXB-PEAM injections. Intradiscal injections were performed with 100 µL gastight Hamilton syringes (7656–01 Model 1710 RN, Hamilton Company USA) connected to 27 G needles (25mm, 12° beveled point; Hamilton Company USA). Per IVD, 40 µL was injected, a volume shown to be safe and not to induce further degeneration in this animal model [24, 29]. Approach of the IVDs was identical to the induction procedure, on the contralateral side. In each dog, unloaded PEAMs were injected in the T12-T13 disc. In the other IVDs, high (280 µg CXB/ 40 µL) and low (8.4 µg CXB/ 40 µL) doses of PEAMs loaded with CXB were injected in a random fashion, with *n*=2 per condition per dog.

Diagnostic imaging

MR images were obtained to assess the degree of degeneration, *i.e.* 4 weeks after induction of IVD degeneration, just prior to intradiscal injection of biomaterials, and repeated 12 weeks after treatment. The dogs received dexmedetomedine (10 µg/kg IV) and butorphanol (0.1 mg/kg) as premedication. General anesthesia was induced by IV administration of 1-2 mg/kg propofol. General anesthesia was maintained by CRI of propofol (5 mg/kg/hr IV) and dexmedetomedine (2 µg/kg/hr IV). An oxygen:air mixture was provided via an endotracheal tube. Throughout the complete procedure heart rate, respiration rate, CO2 and O2 levels were monitored. Dogs were positioned in dorsal recumbency. MR images were obtained using a high field 1.5T MRI unit (Ingenia, Philips, Best, The Netherlands). Sagittal T1-weighted Turbo Spin Echo (repetition time (TR) = 400 ms, echo time (TE) = 8 ms), and T2-weighted Turbo Spin Echo (TR = 3000, TE=110 ms) images were acquired using a field of view (FOV) of 75 x 220 mm and acquisition matrix of 124 x 313 and 124 x 261, respectively. Thirteen slices of 2 mm covered the spine from Th10 to the sacrum. For T2 mapping, a quantitative multiple spin-echo T2 mapping sequence was used with the following parameters: FOV = 75 x 219 mm, acquisition matrix = 96 x 273, slice thickness = 3 mm, TR = 2000. Eight echoes were acquired with TE = 13 to 104 ms with 13 ms echo spacing. Sagittal T1ρ-weighted imaging was performed using a spin-lock-prepared sequence with a three-dimensional multi-shot gradient echo (T1-TFE) readout with the following parameters: FOV = 76 x 220 mm, acquisition matrix = 76 x 220 slice thickness = 2 mm, TR/TE = 4.6s /2.3, TR = 5ms, TE = 2.5ms, TFE factor = 50, flip angle = 45°, shot interval = 3000 ms. To allow quantitative T1ρ mapping, data were acquired with different spin-lock times (TSL) of 0, 10, 20, 30 and 40 ms, with a spin-lock pulse amplitude set to 500 Hz. An oval region of interest (ROI) was manually segmented on the NP of all spinal segments in the mid-sagittal slice. T2 and T1ρ values were computed by voxelwise fitting and calculating the mean signal intensity (S) in each ROI, using the Levenberg-Marquardt nonlinear least-squares method as described before [27]. Twelve weeks after PEAM injection, the MRI was repeated and the dogs were subsequently euthanized. *Post-mortem* CT scans with dogs positioned in dorsal recumbency were made

with a 64-slice CT scanner (Siemens Somatom Definition AS, Siemens Healthcare) using the following parameters: 0.6 mm slice thickness, 120 kV, 350 mAs, 1000 ms tube rotation time, 0.35 spiral pitch factor, 512 x 512 pixel matrix and a fixed field of view of 93 mm. Reconstructions of 0.6 mm thick slices were made in a transverse and sagittal plane using soft tissue and bone reconstruction kernels. Images were reviewed in soft tissue (window width 300, window length 50) and bone (window width 3000, window length 600) settings. From T12 to S1, all IVDs were graded (AT, IR) according to the Pfirrmann score previously validated for use in dogs by Bergknut *et al* (2011) [30] on T2-weighted images. Presence and classification of sclerosis of the end plates and Modic changes were recorded by a board-certified radiologist (MB), and the Disc height index (DHI) of all IVDs in the study was calculated for all IVDs on T2-weighted MR images (AT, IR) [31].

Macroscopic grading, histopathological grading and collagen immunohistochemistry.
Digital images of the IVD segments were evaluated in random order by two blinded investigators (AT, IR) according to the Thompson grading scheme, validated for dogs previously by Bergknut *et al* (2011) [32]. Tissues were fixed at room temperature (RT) for 14 days and were subsequently decalcified in 0.5M ethylenediaminetetraacetic acid (EDTA) at RT for 9 weeks under continuous agitation. EDTA was refreshed weekly, and every two weeks, samples were placed in 10% buffered formaldehyde for 48 hours to maintain formalin tissue fixation. Sections (5 µm thick) were stained with hematoxylin and eosin and with Picrosirus red/ Alcian blue staining protocols [33] and evaluated in a blind and random order by two investigators (AT, IR) using the histological grading system validated for use in dogs [34] using an Olympus BX41 microscope. To detect changes in collagen deposition, immunohistochemistry for collagen type I, II and X was performed. To explore the disease modifying role of celecoxib, the immunopositivity of NGF, a well-known angiogenic and neurotrophic factor [8], was assessed by counting the percentage of immunopositively stained cells over total number of cells in the NP and ventral and dorsal AF. Specifications of the antigen retrieval and respective antibody concentrations are given in supplementary file 2. Briefly, deparaffinization was established through xylene (2x5 min) and graded ethanol (96, 80, 70, 60% v/v, 5 min each), followed by two rinses of TBS+0.1% v/v Tween (TBST0.1%, 2x5 min). Antigen retrieval was performed, followed by endogenous peroxidase inhibition for collagen I, II and X for 5 min and pre-incubation with blocking buffer for 30 min at RT. Thereafter, sections were incubated with primary antibody at 4°C overnight (Collagen I, II, and X) or 3h at RT for NGF. The EnVision-HRP detection system (Dako) was applied for 30 min at RT followed by incubation with streptavidin conjugated with horseradish peroxidase for 30 min at RT. All antibodies were visualized with the liquid DAB+ substrate chromogen (Dako). All stainings were accompanied by appropriate positive and negative (isotype) controls. Negative control did not show positive immunostaining.

GAG, DNA, collagen and PGE_2 content of the nucleus pulposus and annulus fibrosus
Transverse cryosections (60 µm thick) of the snap frozen IVDs were collected on glass slides. Immediately thereafter, the NP and AF were separated and collected in 400 µL and 750 µL

cOmplete lysis M EDTA-free buffer (Roche Diagnostics Nederland BV), respectively and stored at -80 °C until analysis. For biochemical analyses, the NP and AF were homogenized in cOmplete lysis M EDTA-free buffer in a TissueLyser II (Qiagen) for 2x30 seconds at 20 Hz. Inhibition of COX-2 activity was determined by measuring PGE_2 levels in the supernatants by ELISA as mentioned previously. The supernatant and pellet of each NP and AF sample was digested overnight in papain buffer (250 µg/mL papain (P3125, 100 mg, Sigma-Aldrich) and 1.57 mg/mL cysteine HCl (C7880, Sigma-Aldrich). The 1,9-dimethylmethylene blue (DMMB) assay was used to quantify glycosaminoglycan (GAG) content [35] of the pellets and supernatants. GAG concentrations were calculated by using chondroitin sulphate from shark cartilage (C4384, Sigma-Aldrich) as a standard and the absorbance was read at 540/595 nm. The Quant-iT™ dsDNA Broad-Range assay kit in combination with a Qubit™ fluorometer (Invitrogen) was used in accordance with the manufacturer's instructions to determine the DNA content of the papain-digested NP and AF pellets. Collagen content was quantified in the pellets of the NP and AF by using a hydroxyproline assay according to the method of Neuman and Logan [36]. Papain digested samples were freeze-dried overnight, hydrolysed at 108°C overnight in 4 M NaOH, centrifuged (15 seconds at 14,000 g) and stored at −20°C. Prior to measurements, samples were centrifuged (15 seconds at 14,000 g) once more, chloramine T reagent (2426, Merck, Schiphol-Rijk, The Netherlands) was added, and samples were allowed to shake for 20 minutes at 170 rpm. Freshly prepared dimethylaminobenzaldehyde (3058, Merck) was added, and samples were incubated for 20 minutes at 60 °C. The absorbance was read at 570 nm and collagen content was calculated from the hydroxyproline content by multiplying with a factor 7.5 [36]. DNA and collagen content in the supernatants were negligible and therefore not included in the calculations. Total GAG, collagen and PGE_2 content were normalized to DNA content of the sample.

Statistical analysis

Statistical analysis was conducted using SPSS software, version 22.0 and R studio software v3.3.1. Normality of the data was checked by assessing the Q-Q plots, histograms and Shapiro-Wilks tests. For non-parametric distributed data, Kruskall Wallis tests and subsequently Mann Whitney *U* tests were used. For normally distributed data, a general linear model was applied employing "dog" and "IVD level" as a random effect and "treatment" as fixed effect. The Benjamini & Hochberg test was used to correct for multiple testing. For categorical data, the *Monte-Carlo* re-sampling bootstrapping method was used. A two-sided Mann-Whitney Wilcoxon test was performed for an independence test of categorical data, using R studio software (*RStudio* v3.3.1). *P* values <0.05 were considered as statistically significant after correction for multiple testing.

Effect sizes (ES) were retrieved as *Hedge's g* for parametric data*:* medium, 0.5-0.8; large, 0.8-1.2; 1.2-2, very large and >2 huge [37]. Differences were considered as relevant when $p<0.05$ and/ or ES was medium or larger when *p*-value was <0.1. For non-parametric data, Cliff's delta was assessed: $0.28<ES<0.43$, medium; $0.43\leq ES<0.7$, large; $ES\geq 0.7$, extra-large [38].

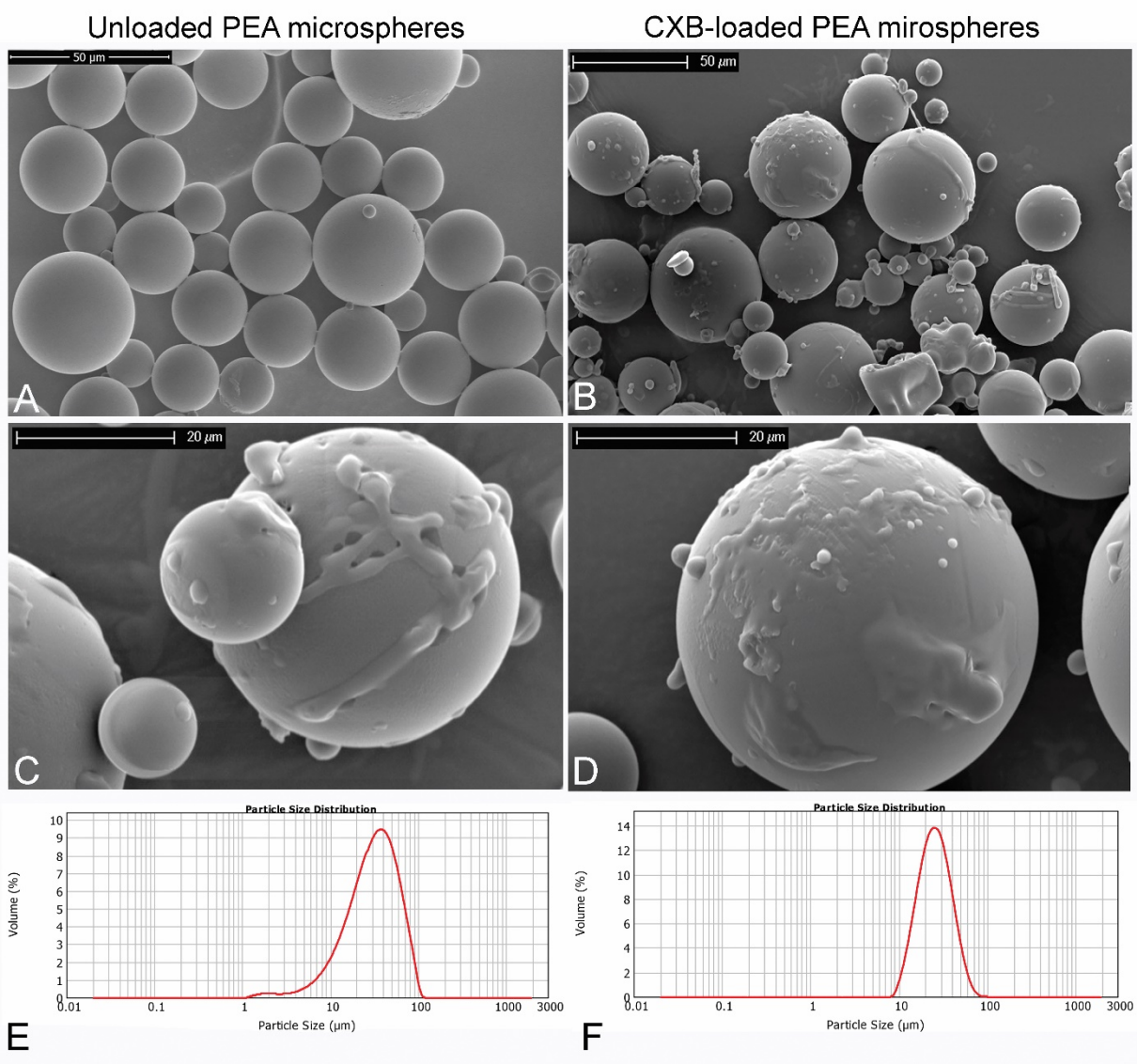

Figure 3. Polyesteramide (PEA) microspheres. Scanning electron microscopy pictures (SEM) of unloaded (**A, C**) and celecoxib-loaded (**B, D**) PEA microspheres, with concurrent particle size distributions (**E, F**).

Results

In vitro celecoxib release

Microsphere characterization

The obtained PEA polymer had an average molecular weight (Mn) of 70 kDa and a polydispersity index (PDI) of 1.70 (Fig. 1B). The average particle size of the unloaded microspheres was 31.9 µm, whereas the CXB-loaded particles had an average diameter of 25.3 µm (Table 1). This difference in size was mainly due to the different viscosity of the

used oil phase with respect to polymer:solvent ratio, since for the preparation of CXB-loaded PEAMs a 5% (wt/v) ratio was used compared to 15% (wt/v) for unloaded microspheres.

Table 2. Polymer characterization.

	Mn (kDa)	PDI	Tg	Relative monomer ratio
PEA III Ac Bz	69.5	1.70	54.3 °C	0.30:0.27:0.43

The relative ratio between the polymer building blocks was determined by Nuclear Magnetic Resonance (^{1}H NMR). Glass-liquid transition temperature (Tg) of the polymer was determined under dry conditions by differential scanning calorimetry (DSC). Mn, number of average molecular weight; PDI, polydispersity index.

Celecoxib was gradually released from polyesteramide microspheres for 28 days

Celecoxib release was determined in PBS for 14 days (Fig 2B,C) and in the presence of cultured NP cells provided with a pro-inflammatory stimulus for 28 days (Fig. 2D). In both experiments, there was a gradual release of CXB from the PEA microspheres (Fig. 2D). After 14 and 28 days, 30% and 40%, respectively, of the CXB was released from the PEA microspheres. The released CXB from the PEAMs, corresponding with 10^{-7}M, was close to the lower detection limit of the ELISA and was almost undetectable after 28 days of release. As such, the cumulative release of CXB from the low dose PEAM-condition was most probably underestimated and accounted for ~20%.

Polyesteramide based celecoxib-loaded microspheres exerted an anti-inflammatory and possibly anti-catabolic effect on canine nucleus pulposus cells from degenerated IVDs

The 10^{-6}M CXB-"bolus" and the 10^{-4}M CXB-PEAMs were both able to significantly suppress PGE_2 production in NP cells during the entire 28 days culture period (Fig. 4A, p=0.0001 and p=0.003, respectively). Even on day 28, PGE_2 production was inhibited by 80% and 78% (Fig. 4B) by CXB-bolus (p=0.003) and released from 10^{-4}M CXB-PEAMs (p<0.0001), respectively. The CXB released from the 10^{-7}M CXB-PEAMs was not able to effectively inhibit PGE_2 production demonstrating dose-dependent bioactivity of the released CXB. In line with this thought, CXB levels released by the 10^{-7}M CXB-PEAMs during the 1st day of culture were ~20 lower than those measured in the 10^{-6}M CXB-bolus group. There were no differences in total DNA content between conditions at any of the time points, indicating no effect of CXB-PEAMs on the cumulative result of proliferation and/ or cell death regardless of the loading dose.

On day 4, RT-qPCR analysis of NP cells from degenerated IVDs revealed a downregulation of *MMP13* mRNA expression in the 10^{-4}M CXB-PEAMs group compared to the control and CXB-bolus group (Fig. 4C, p=0.074, large ES; p=0.03 respectively). mRNA levels of *ADAMTS5* (Fig. 4D) and *TIMP1* (data not shown) were not influenced by CXB-loaded PEAMs. *COL2α1* mRNA

expression was increased in both CXB-PEAM groups compared to the control and CXB-bolus group (Fig. 4E, p=0.005, p=0.007, respectively). *ACAN* mRNA expression tended to be higher in the 10^{-7}M CXB-PEAMs vs. control group (p= 0.07; very large ES). Expression of *COL1α1* between conditions (Fig. 4G) was not affected. The mRNA expression of the pro-apoptotic gene *CASP3* was lowered by 10^{-4}M CXB-PEAMs (p=0.06, huge ES) vs. control, while the mRNA expression and ratio of pro-apoptotic (*BAX*) and anti-apoptotic (*BCL2*) markers were not affected by the culture conditions. The expression of proliferative markers *CCDN1* and *AXIN2* were not influenced by any of the culture conditions (data not shown), in line with the DNA measurements.

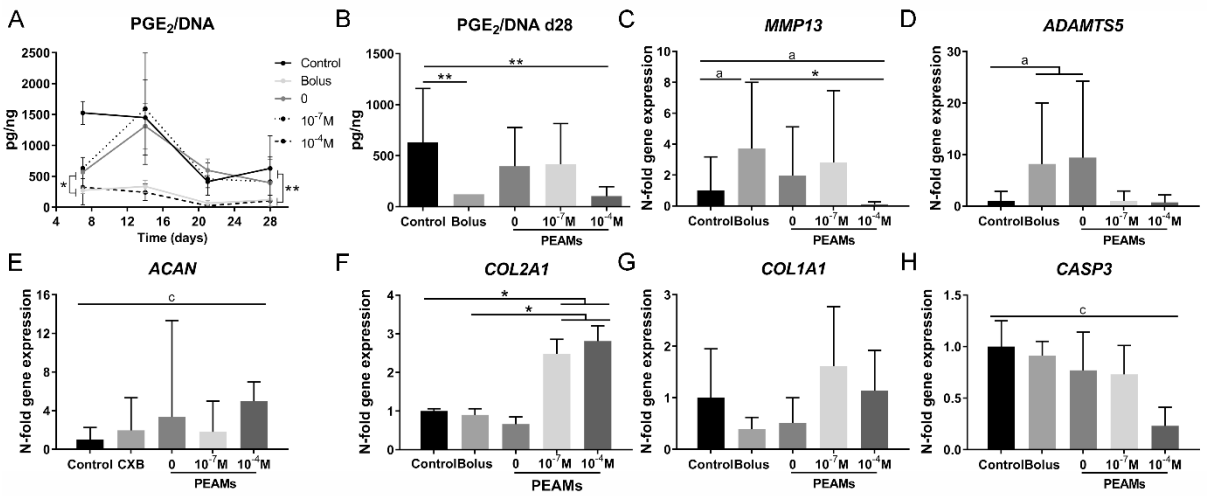

Figure 4. Controlled release of celecoxib (CXB) is able to inhibit prostaglandin E_2 (PGE_2) production over a prolonged period of time and exerts an anabolic and anti-catabolic effect. Nucleus pulposus cells isolated from early degenerated canine intervertebral discs were subjected to a pro-inflammatory stimulus (10 ng/mL TNFα) in the presence of unloaded polyesteramide microspheres (0 PEAMs), and microspheres loaded with 10^{-7}M CXB and 10^{-4}M CXB, or CXB bolus at 10^{-6}M. PGE_2/DNA during the entire culture period (A) and PGE_2/DNA at day 28 of culturing (B). Relative *MMP13* (C), *ADAMTS5,* (D), *COL2A1* (E), *ACAN* (F), *COL1A1* (G) and *CASP3* (H) expression at t=4 days. Control (chondrogenic medium with 10 ng/mL TNF-α) values were set at 1. * p<0.05; a, medium ES; c, very large ES. n=6 donors per condition and time point, in technical duplicates.

In vivo induced IVD degeneration

Magnetic resonance imaging revealed a protective effect of controlled release of celecoxib on T2 relaxation time and disc height index

All dogs showed uneventful recovery from induction surgery and were ambulant the next day. One dog appeared to have 8 lumbar vertebrae; therefore the total number of spinal units analysed was 43 instead of 42. One dog showed minor reductions in spinal reflexes of the left hind limb related to the surgical approach that recovered within 7 days. Four weeks after induction of IVD degeneration, there was a significant decrease (p<0.01) in T2 relaxation times, which remained low at 12 weeks follow-up with concurrent increase in the

Pfirrmann grade and decrease in T1ρ relaxation times (both $p<0.05$) (Fig. 5A-C). In line with these findings, the DHI was unchanged at 4 weeks after induction, but tended to be decreased at 12 weeks follow-up (Fig 5D; $p=0.06$; medium ES). The sustained release of CXB resulted in minor improvement of Pfirrmann grade (only for HD-CXB-PEAMs with $p=0.08$; large ES) and T2 relaxation times 12 weeks after injection, more pronounced in the HD-CXB-PEAM than in the LD-CXB-PEAM group ($p=0.03$, $p=0.07$; medium ES, respectively). While T1ρ relaxation times remained unchanged, intradiscal application of LD-PEAM and HD-PEAM CXB demonstrated minor improvement on DHI ($p=0.06$; $p= 0.07$; both medium ES respectively) 12 weeks after injection.

Computed tomography showed no adverse effects 12 weeks after treatment

Adverse effects after local delivery of CXB-loaded PEAMs were not detected on MRI and CT. In 2/6 degenerated control IVDs, sclerosis of both end plates was visible and in 1/6 levels, early spondylosis deformans was present at the caudal vertebral body. In the discs treated with the LD-CXB-PEAMs, there was early spondylosis formation present on the caudal vertebral body of 1 spinal unit (1/6), and subtle sclerosis of both end plates in another spinal unit (1/6). No abnormalities were noted in the discs treated with the HD-CXB-PEAMs or the other, non-induced levels. Sclerosis and spondylosis were mostly prominent on the left side where induction of disc degeneration was performed.

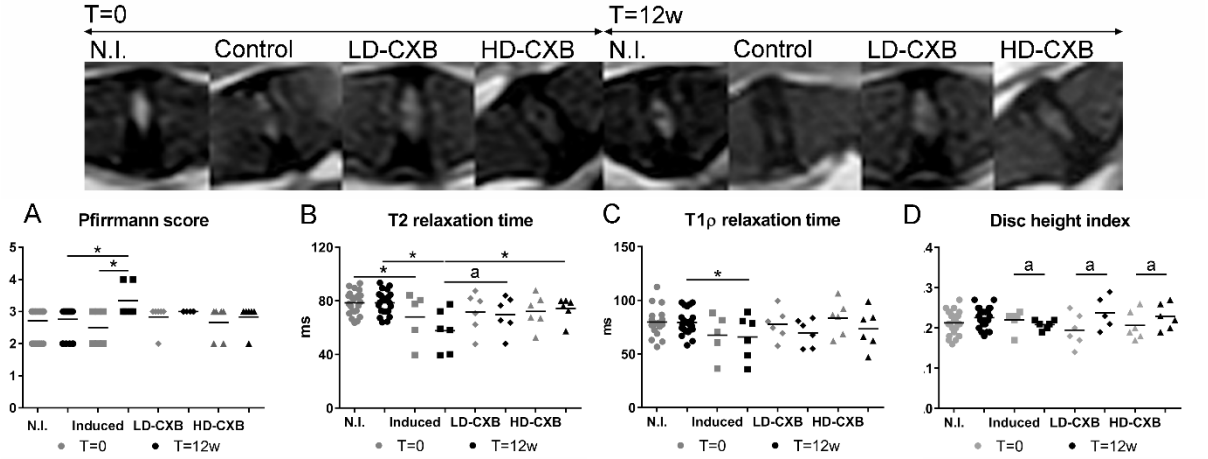

Figure 5. Effect of *in vivo* induction of intervertebral disc (IVD) degeneration and its treatment with celecoxib (CXB)-loaded polyesteramide microspheres (PEAMs) on magnetic resonance imaging parameters. T2 relaxation times (B) were significantly decreased four weeks after IVD degeneration induction surgery (grey markers, T=0). In degenerated IVDs that received unloaded PEAMs (control) compared to non-induced healthy IVDs (N.I.), Pfirrmann score (A) was increased, T2 relaxation times (B) and T1ρ relaxation times (C) were decreased at 12 weeks (black markers) and disc height index (DHI) tended to decrease with a medium ES. T2 relaxation times of IVDs treated with HD-CXB-PEAMs were significantly higher than control IVDs. The disc height index (D; DHI) was maintained (tended to improve with large ES) in the IVDs treated with either LD- or HD-CXB-PEAMs. $n=6$ IVDs per group ($n=24$ for the non-induced IVDs).* $p<0.05$; a, medium effect size. Horizontal bar indicates median (categorical data) or mean (continuous data).

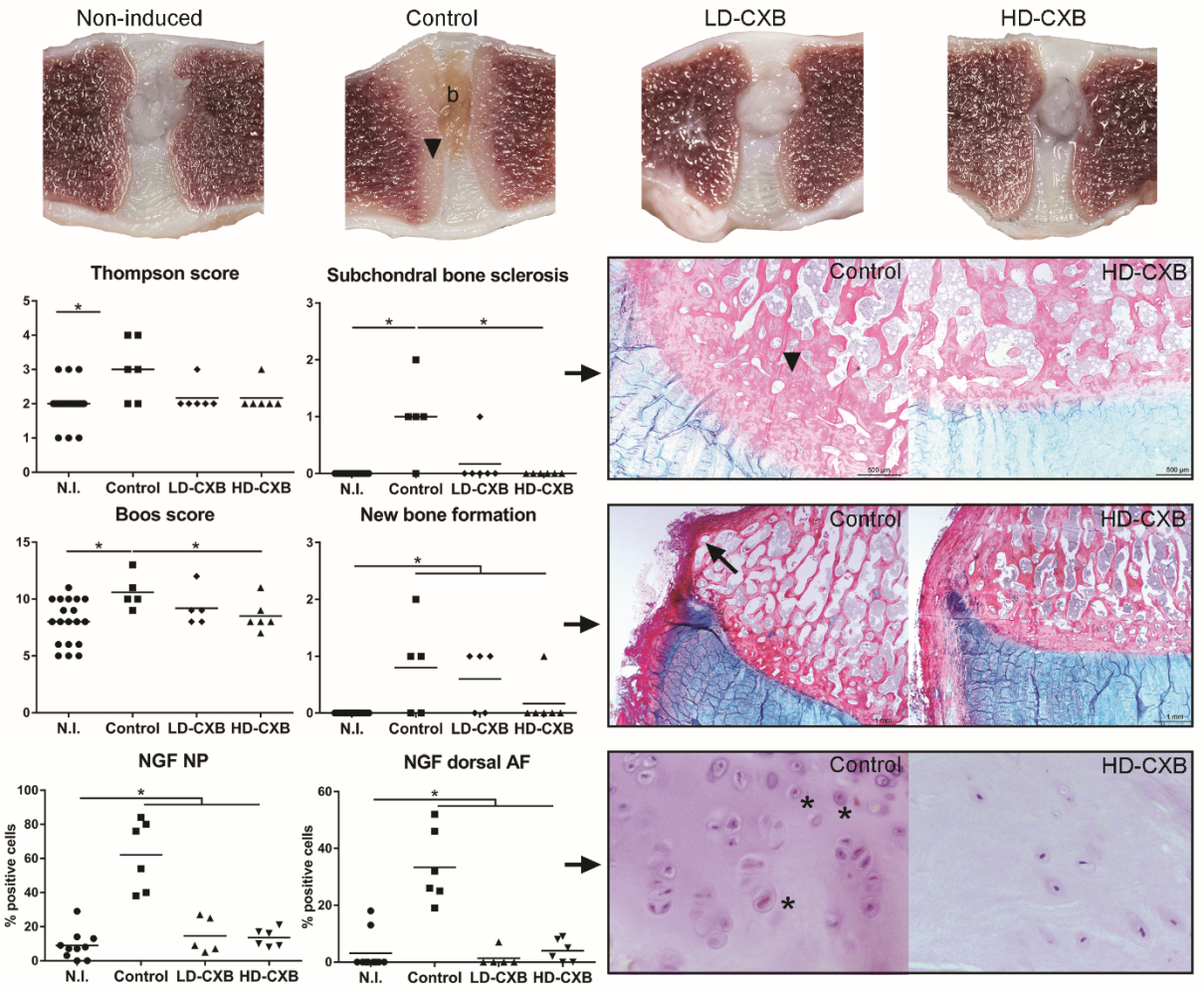

Figure 6. Controlled release of celecoxib (CXB) inhibited progression of intervertebral disc degeneration (IVDD), the development of subchondral bone sclerosis and osteophyte formation, and the immunopositivity of nerve growth factor (NGF). Representative macroscopic images of non-induced (N.I.), degenerated control, low dose (LD) CXB and high dose (HD) CXB IVDs, with the associated macroscopic (Thompson) degeneration score, showing less degeneration in discs treated with the CXB-loaded polyesteramide microspheres (PEAMs). Note the brown discoloration (b) in the induced IVDs which is absent on all CXB-treated IVDs. Controlled release of 280 µg/ 40 µL CXB-loaded PEAMs (HD-CXB-PEAM) resulted in less severe degeneration at the histologic level (overall Boos score). Detailed analysis of sub-scores of the Boos scores revealed less subchondral bone sclerosis and less new bone formation (black arrow). The arrowhead illustrates a typical example of subchondral bone sclerosis. Increased nerve growth factor (NGF) expression (* indicate immunopositive cell within the nucleus pulposus (NP)) was observed in degenerated control IVDs (both NP and annulus fibrosus (AF)), but not in IVDs treated with CXB-PEAMs. *p<0.05. n=6 IVDs per PEAM group; n=24 non-induced IVDs.

Macroscopic and microscopic evaluation of the IVDs showed a beneficial effect of celecoxib-PEAMs on macroscopic scoring of IVD degeneration

Post-mortem, macroscopic degeneration scores according to the Thompson scale were assigned to 55 IVDs (Fig. 6). The median Thompson score for the control degenerated discs was 3, which was significantly higher (p=0.017) than the score for the non-induced discs (median 2). The degenerated discs that were injected with CXB-loaded PEAMs did not statistically differ from the non-induced or the control degenerated discs.

Histological scores ranged from 3 to 13 (Fig. 6), corresponding with slight to moderate degeneration (as the histological score ranges from 0-29). The overall histological scores in the degenerated discs treated with the unloaded PEAMs where higher than the non-induced discs and discs treated with the LD- and HD-CXB-PEAM (p=0.004; p=0.04; p=0.02, respectively). Interestingly, the amount of subchondral sclerosis and new bone formation on the ventral aspect of the vertebrae was increased in induced (control) degenerated discs (p<0.01, Fig. 6), but not in IVDs treated with CXB-loaded PEAMs. There were no differences in collagen type I or collagen type II deposition between the treatment groups. Collagen type X was absent in all of the investigated IVDs, while its presence was confirmed in positive controls (*i.e.* hypertrophic zone of a canine growth plate). The induction of IVD degeneration led to the increased immunopositivity of NGF in the NP (Fig. 6, p<0.001), dorsal (Fig. 6, p<0.001) and ventral AF (p<0.001, data not shown), which was effectively decreased by both the low (p<0.001, p=0.026 and p=0.004 for the NP, ventral and dorsal AF, respectively) and the high dose (p<0.001, p=0.002 and p=0.003 for the NP, ventral and dorsal AF, respectively) CXB-loaded microspheres.

Controlled release of celecoxib resulted in decreased PGE_2 levels and prevented GAG loss

Induction of IVD degeneration led to increased total PGE_2 tissue levels in both the NP and AF (p=0.03, p=0.008, Fig. 7a). Celecoxib released from LD-CXB-PEAMs and HD-CXB-PEAMs reduced the PGE_2/DNA levels in the NP with 52% and 73% respectively (p=0.09 and p=0.068; ES 0.49 and 0.50). This resulted in a borderline significantly lower PGE_2/DNA (Fig. 7A; p=0.054; p=0.052; medium ES) compared to control degenerated tissues. In the AF, PGE_2/DNA (Fig. 6B) tended to be higher in the control degenerated IVDs compared to the non-induced discs (p=0.06; ES 1.0) and HD-CXB-PEAMs (p=0.089; large ES). Also in the AF, PGE_2 production was 63% and 76% suppressed by the LD- and HD-CXB-PEAMs respectively (p=0.007 and p=0.003). In the NP, the total GAG content and the GAG content corrected for DNA (Fig. 7C) were significantly lower in degenerated control IVDs compared to non-induced discs and both CXB-PEAM groups (p<0.05), while the latter two did not differ from the non-induced IVDs. In the AF, the GAG/DNA levels were not affected by the application of any treatment (Fig. 7D). There seemed to be a decrease in total collagen content in the NP as a result of IVDD induction (Fig. 7E; p=0.036). DNA content of the AF increased due to IVDD induction (Fig. 7H; p=0.051, very large ES), but DNA content remained unchanged in the NP (Fig. 7G).

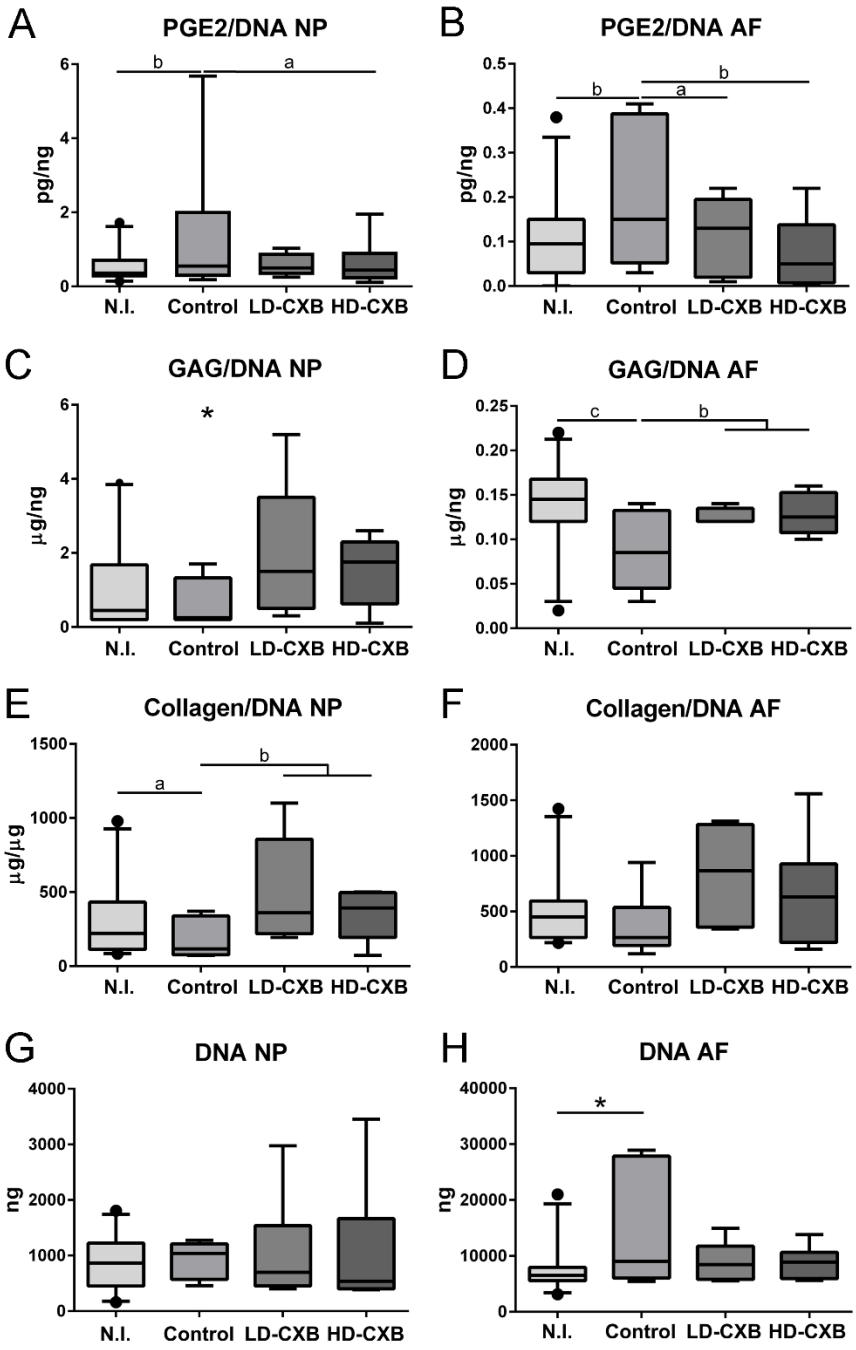

Figure 7. Celecoxib (CXB)-loaded microspheres inhibited prostaglandin E_2 (PGE_2) production and maintained glycosaminoglycan (GAG) content in comparison to control degenerated intervertebral discs (IVDs). PGE_2/DNA (A,B), GAG/DNA (C,D), Collagen/DNA (E,F) and total DNA (G,H) of the nucleus pulposus (NP) and annulus fibrosus (AF) with indicated mean values ± SD. * p<0.05; a, medium ES; b, large ES; c, very large ES (>1.2). n=6 IVDs per group, n=24 for the non-induced IVDs (N.I.) group. N.I., non-induced; control, degenerated discs receiving unloaded microspheres; LD, low dose (1.05 mg/mL) CXB-loaded microspheres; HD, high dose (35 mg/mL) CXB-loaded microspheres.

Discussion

This study demonstrated that sustained release of celecoxib from PEA microspheres was able to (1) suppress in a sustained manner PGE_2 production *in vitro* and *in vivo* and (2) counteract the detrimental effects of induced degeneration *in vivo* in a canine model of IVD degeneration. Intradiscal treatment with celecoxib-loaded PEA microspheres, resulting into an intradiscal dose of 280 µg, maintained T2 relaxation times on MRI and GAG content on biochemical level, improved the overall histological score of IVDs and inhibited early subchondral bone changes.

The polymer applied was based on α-amino acids, aliphatic dicarboxylic acids and aliphatic α-ω diols**.** The polymer has been built of three di-amino monomers connected with di-acid like in a polycondensation reaction. The monomers were chosen to balance mechanical and barrier properties of the biomaterial, controlling hard to soft segment ratio. Furthermore, these polymers showed remarkable shelf life time and could be easy processed to variety of forms such as the injectable particles described in this paper. The synthesis of PEA yielded a random co-polymer of high molecular weight (typically above 70 kDa). This resulted in a very good consistency of the material barrier properties when derived from different batches.

Release of celecoxib from PEAMs was shown for at least 28 days *in vitro* and suppressed PGE_2 production in TNF-α-stimulated NP cells from degenerated canine IVDs during the entire culture period, without affecting DNA content. Moreover, the mRNA expression of matrix degrading enzymes (*MMP13* and *ADAMTS5*) was inhibited and *COL2aI* and *ACAN* were enhanced. Controlled release of celecoxib with corresponding PGE_2 inhibition was previously shown for celecoxib released from PLGA microspheres in human chondrocytes from degenerated cartilage: sustained celecoxib release was confirmed for over 100 days and PGE_2 inhibition for 21 days [39]. PLGA microspheres disintegration resulted in acidic end products, which could induce toxic local pH levels [40, 41]. The more novel PEA platform does not result in toxic degradation products [26]. Extended release of celecoxib from PEA microspheres has been demonstrated in PBS*;* after 80 days, almost 50% was released into the medium. In the same study, the release of small molecules from PEA microspheres has shown to be accelerated through serine proteases from neutrophil cell lysate [22], indicating a possible a discrepancy between *in vitro* and *in vivo* release. However, the *in vitro* release of celecoxib in the present study seemed not to be overtly influenced by the presence of NP cells stimulated with TNF-α. Considering that *in vivo*, even chronically degenerated IVDs do not contain an abundance of (inflammatory) cells and inflammation is usually low-grade [42], when compared to neutrophil like cell lysate, celecoxib release from PEAMs might also be more gradual in the degenerated disc environment.

The applicability of celecoxib delivery in harnessing tissue inflammation and pain-parameters was also confirmed *in vivo* in a large animal model with experimentally induced IVD degeneration. In this study, PGE_2 production associated with the induction of IVD degeneration was inhibited up to 53% and 73% on average by a loading dose of 8.4 µg and

280 µg celecoxib, respectively. In a previous study, sustained local delivery of 10^{-5}M celecoxib in a pNIPAAM-based hydrogel in a canine model with spontaneous early IVD degeneration resulted in a maximal PGE_2 decrease of 35% [27]. This indicates that with increasing celecoxib loading dosages, there is more PGE_2 suppression. However, both in the spontaneous as in the induced degeneration canine models, the degeneration score was mild to moderate, but without overt clinical signs. Although enhanced PGE_2 production is known to increase with advancing degeneration, the most dramatic increase takes place when extrusion or protrusion of the IVD is present [42]. Because in both animal models, degeneration of the IVDs was not accompanied by protrusion or extrusion of IVD tissue, nor clinical signs indicating symptomatic IVD disease, PGE_2 levels were probably lower than in symptomatic IVDs as suggested earlier by retrospective analysis of symptomatic vs asymptomatic degenerated NP tissues [42]. A larger effect on PGE_2 levels could therefore be expected in symptomatic IVDs. In line with this thought, in canine patients suffering from spontaneous IVDD with low back pain, local injection of a controlled-release platform loaded with celecoxib corresponding with 10^{-5}M at the NP level resulted in a decrease of clinical signs for up to two months [43]. In addition to a decrease in PGE_2 levels, in the present study the controlled release of celecoxib also resulted in a decrease in NGF expression. NGF not only stimulates development of sensory nerve endings in degenerating IVDs, it can also generate pain by directly influence nerve fibers to produce nociceptive neuropeptides and express receptors that are associated with inflammatory pain, and has been known to induce matrix degrading enzymes [8]. Altogether, reduction of local PGE_2 levels and NFG immunopositivity were effectuated after local delivery of the celecoxib-loaded PEAMs indicating promising disease-modifying effects of this platform for chronic back pain related to IVD degeneration.

Interestingly, intradiscal application of celecoxib-loaded PEAMs prevented GAG loss in the degenerating NP indicative of structural repair. On MRI, induction of degeneration resulted in a decrease in signal intensity and T2 values indicating loss of proteoglycans and water, and thus advancing degeneration, which was confirmed by histology and biochemistry. Local application of HD-CXB-PEAMs reversed the degenerative process within the NP, where higher T2 values were detected, indicating preserved water content and integrity of collagen fibers. Accordingly, on biochemical level, there also appeared to be an improved GAG/DNA content and less overall collagen loss in the HD-CXB-PEAM treated IVDs. In line with these findings, in patients suffering from osteoarthritis, proteoglycan synthesis rate and retention of newly formed proteoglycans were significantly increased after oral celecoxib treatment compared to controls [44, 45], suggesting celecoxib as a disease-modifying drug. The mechanism of action of locally delivered celecoxib-loaded PEAMs could be dual: by harnessing inflammation and thereby limiting the amount of pain mediators and/or by inhibiting proteoglycan degradation. Both are mechanisms that inhibit ingrowth of neural and vascular tissue [8, 46].

Another source of back pain could be the subchondral endplate. Subchondral vertebral bone changes are common in chronic IVDD [3] and are referred to as Modic changes (MC) on MRI [47]. All types of MC are associated with chronic low back pain and worse disease outcome [48]. They are interconvertible and most probably reflect different disease stages [49]. The present study demonstrated a low frequency of MC, most probably related to the relatively short term follow up (*i.e.* 12 weeks after induction), which was only present in degenerated untreated discs allowing for no concrete conclusions. However, histological analysis revealed that the controlled release of celecoxib was able to prevent early subchondral bone changes, *i.e.* subchondral vertebral sclerosis and early new bone formation on the ventral vertebral margins. Interestingly, subchondral bone pathology in IVD degeneration shows striking similarities to subchondral bone remodeling in osteoarthritis and its relation to joint pain [50, 51]. In OA, the effect of celecoxib on subchondral bone has been studied in more detail [52], as subchondral bone sclerosis and osteophytes are hallmarks of degenerative joint disease [53, 54]. A daily oral dose of CXB significantly reduced osteophyte formation in a rat model of osteoarthritis [45], which was also seen after intra-articular injection of CXB in PEA microspheres in a preclinical OA rat model [55]. As such, it is tempting to hypothesize that local sustained delivery of a COX-2 inhibitor not only improves structural integrity of the NP itself, it also has the potency to improve subchondral bone health benefiting thereby the affected spinal segment.

Conclusions

To conclude, the *in vitro* and *in vivo* results indicate that controlled release platforms based on PEA microspheres seem very promising for therapeutic application for chronic back pain related to IVD degeneration. Celecoxib incorporated in PEAMs was safely administered intradiscally in experimental dogs, and exerted anti-inflammatory and anti-degenerative effects. These findings imply that local sustained presence of celecoxib may have the ability to harness inflammation and by reducing pain mediators, such as PGE_2 and NGF, may also result into less pain in a clinical setting. Follow-up studies focusing on pain and on a better understanding of how particle degradation and inherent drug release kinetics are influenced by the disease-state of the tissue are warranted to determine the efficacy of celecoxib-loaded PEAMs in inhibiting low back pain.

Acknowledgements

The authors would also like to thank Harry van Engelen, Saskia Plomp and Simone Kamphuijs for their assistance with data acquisition the *in vivo* experiment.

References

1. Hoy D, March L, Brooks P, Blyth F, Woolf A, Bain C*, et al*. The global burden of low back pain: estimates from the Global Burden of Disease 2010 study. Ann.Rheum.Dis. 2014;73:968-74.
2. Kaplan W, Wirtz V, Mantel-Teeuwisse A, Stolk P, Duthey B, Laing R. Priority diseases and reasons for inclusion. 2013;165-168.
3. de Schepper EI, Damen J, van Meurs JB, Ginai AZ, Popham M, Hofman A*, et al*. The association between lumbar disc degeneration and low back pain: the influence of age, gender, and individual radiographic features. Spine (Phila Pa.1976) 2010;35:531-6.
4. Battie MC, Videman T, Kaprio J, Gibbons LE, Gill K, Manninen H*, et al*. The Twin Spine Study: contributions to a changing view of disc degeneration. Spine J. 2009;9:47-59.
5. Risbud MV and Shapiro IM. Role of cytokines in intervertebral disc degeneration: pain and disc content. Nat.Rev.Rheumatol. 2014;10:44-56.
6. Adams MA and Roughley PJ. What is intervertebral disc degeneration, and what causes it? Spine (Phila Pa.1976) 2006;31:2151-61.
7. Freemont AJ. The cellular pathobiology of the degenerate intervertebral disc and discogenic back pain. Rheumatology (Oxford) 2009;48:5-10.
8. Navone SE, Marfia G, Giannoni A, Beretta M, Guarnaccia L, Gualtierotti R*, et al*. Inflammatory mediators and signalling pathways controlling intervertebral disc degeneration. Histol.Histopathol. 2017;32:523-42.
9. Walter BA, Purmessur D, Likhitpanichkul M, Weinberg A, Cho SK, Qureshi SA*, et al*. Inflammatory Kinetics and Efficacy of Anti-inflammatory Treatments on Human Nucleus Pulposus Cells. Spine (Phila Pa.1976) 2015;40:955-963.
10. Miyamoto H, Doita M, Nishida K, Yamamoto T, Sumi M, Kurosaka M. Effects of cyclic mechanical stress on the production of inflammatory agents by nucleus pulposus and anulus fibrosus derived cells in vitro. Spine (Phila Pa.1976) 2006;31:4-9.
11. Samad TA, Moore KA, Sapirstein A, Billet S, Allchorne A, Poole S*, et al*. Interleukin-1beta-mediated induction of Cox-2 in the CNS contributes to inflammatory pain hypersensitivity. Nature 2001;410:471-5.
12. Sekiguchi M, Otoshi K, Kikuchi S, Konno S. Analgesic effects of prostaglandin E2 receptor subtype EP1 receptor antagonist: experimental study of application of nucleus pulposus. Spine (Phila Pa.1976) 2011;36:1829-34.
13. Simon J, McAuliffe M, Shamim F, Vuong N, Tahaei A. Discogenic low back pain. Phys.Med.Rehabil.Clin.N.Am. 2014;25:305-17.
14. Bach FC, Willems N, Penning LC, Ito K, Meij BP, Tryfonidou MA. Potential regenerative treatment strategies for intervertebral disc degeneration in dogs. BMC Vet.Res. 2014;10:3,6148-10-3.
15. Sakai D and Grad S. Advancing the cellular and molecular therapy for intervertebral disc disease. Adv.Drug Deliv.Rev. 2015;84:159-71.
16. Motaghinasab S, Shirazi-Adl A, Parnianpour M, Urban JP. Disc size markedly influences concentration profiles of intravenously administered solutes in the intervertebral disc: a computational study on glucosamine as a model solute. Eur.Spine J. 2014;23:715-23.
17. Zhang L, Wang JC, Feng XM, Cai WH, Yang JD, Zhang N. Antibiotic penetration into rabbit nucleus pulposus with discitis. Eur.J.Orthop.Surg.Traumatol. 2014;24:453-8.
18. Richardson SM, Kalamegam G, Pushparaj PN, Matta C, Memic A, Khademhosseini A*, et al*. Mesenchymal stem cells in regenerative medicine: Focus on articular cartilage and intervertebral disc regeneration. Methods 2016;99:69-80.
19. Rodriguez-Galan A, Franco L, Puiggali J. Degradable Poly(ester amide)s for Biomedical Applications. 2011;3:65-99.
20. Sun H, Meng F, Dias AA, Hendriks M, Feijen J, Zhong Z. alpha-Amino acid containing degradable polymers as functional biomaterials: rational design, synthetic pathway, and biomedical applications. Biomacromolecules 2011;12:1937-55.
21. Andres-Guerrero V, Zong M, Ramsay E, Rojas B, Sarkhel S, Gallego B*, et al*. Novel biodegradable polyesteramide microspheres for controlled drug delivery in Ophthalmology. J.Control.Release 2015;211:105-17.
22. Janssen M, Timur UT, Woike N, Welting TJ, Draaisma G, Gijbels M*, et al*. Celecoxib-loaded PEA microspheres as an auto regulatory drug-delivery system after intra-articular injection. J.Control.Release 2016;244:30-40.
23. Le Maitre CL, Pockert A, Buttle DJ, Freemont AJ, Hoyland JA. Matrix synthesis and degradation in human intervertebral disc degeneration. Biochem.Soc.Trans. 2007;35:652-5.

24. Willems N, Mihov G, Grinwis GC, van Dijk M, Schumann D, Bos C*, et al*. Safety of intradiscal injection and biocompatibility of polyester amide microspheres in a canine model predisposed to intervertebral disc degeneration. J.Biomed.Mater.Res.B.Appl.Biomater. 2015;105:707-714.
25. Bergknut N, Rutges JP, Kranenburg HJ, Smolders LA, Hagman R, Smidt HJ*, et al*. The dog as an animal model for intervertebral disc degeneration? Spine (Phila Pa.1976) 2012;37:351-8.
26. Katsarava R, Beridze Z, Arabuli N, Kharadze D, Chu CC, Won CY. Amino acid- based bioanalogous polymers. Synthesis, and study of regular poly(ester amide)s based on bis(α-amino acid) α, ω-alkylene diesters, and aliphatic dicarboxylic acids. 1999;37:391-407.
27. Willems N, Yang HY, Langelaan ML, Tellegen AR, Grinwis GC, Kranenburg HJ*, et al*. Biocompatibility and intradiscal application of a thermoreversible celecoxib-loaded poly-N-isopropylacrylamide MgFe-layered double hydroxide hydrogel in a canine model. Arthritis Res.Ther. 2015;17:214,015-0727-x.
28. Hiyama A, Mochida J, Iwashina T, Omi H, Watanabe T, Serigano K*, et al*. Transplantation of mesenchymal stem cells in a canine disc degeneration model. J.Orthop.Res. 2008;26:589-600.
29. Willems N, Bach FC, Plomp SG, van Rijen MH, Wolfswinkel J, Grinwis GC*, et al*. Intradiscal application of rhBMP-7 does not induce regeneration in a canine model of spontaneous intervertebral disc degeneration. Arthritis Res.Ther. 2015;17:137-151.
30. Bergknut N, Auriemma E, Wijsman S, Voorhout G, Hagman R, Lagerstedt AS*, et al*. Evaluation of intervertebral disk degeneration in chondrodystrophic and nonchondrodystrophic dogs by use of Pfirrmann grading of images obtained with low-field magnetic resonance imaging. Am.J.Vet.Res. 2011;72:893-8.
31. An HS, Takegami K, Kamada H, Nguyen CM, Thonar EJ, Singh K*, et al*. Intradiscal administration of osteogenic protein-1 increases intervertebral disc height and proteoglycan content in the nucleus pulposus in normal adolescent rabbits. Spine (Phila Pa.1976) 2005;30:25-31.
32. Bergknut N, Grinwis G, Pickee E, Auriemma E, Lagerstedt AS, Hagman R*, et al*. Reliability of macroscopic grading of intervertebral disk degeneration in dogs by use of the Thompson system and comparison with low-field magnetic resonance imaging findings. Am.J.Vet.Res. 2011;72:899-904.
33. Gruber HE, Ingram J, Hanley EN,Jr. An improved staining method for intervertebral disc tissue. Biotech.Histochem. 2002;77:81-3.
34. Bergknut N, Meij BP, Hagman R, de Nies KS, Rutges JP, Smolders LA*, et al*. Intervertebral disc disease in dogs - Part 1: A new histological grading scheme for classification of intervertebral disc degeneration in dogs. Vet.J. 2013;195:156-63.
35. Farndale RW, Sayers CA, Barrett AJ. A direct spectrophotometric microassay for sulfated glycosaminoglycans in cartilage cultures. Connect.Tissue Res. 1982;9:247-8.
36. Neuman RE and Logan MA. The determination of hydroxyproline. J.Biol.Chem. 1950;184:299-306.
37. Sawilowsky SS. New effect size rules of thumb. J. Mod. Appl. Stat. Meth. 2009;8:597-599.
38. Cliff N. Dominance statistics: Ordinal analyses to answer ordinal questions. 1993;114:494-509.
39. Yang HY, van Dijk M, Licht R, Beekhuizen M, van Rijen M, Janstal MK*, et al*. Applicability of a newly developed bioassay for determining bioactivity of anti-inflammatory compounds in release studies--celecoxib and triamcinolone acetonide released from novel PLGA-based microspheres. Pharm.Res. 2015;32:680-90.
40. Kavanaugh TE, Werfel TA, Cho H, Hasty KA, Duvall CL. Particle-based technologies for osteoarthritis detection and therapy. Drug Deliv.Transl.Res. 2016;6:132-47.
41. Parumasivam T, Leung SS, Quan DH, Triccas JA, Britton WJ, Chan HK. Rifapentine-loaded PLGA microparticles for tuberculosis inhaled therapy: Preparation and in vitro aerosol characterization. Eur.J.Pharm.Sci. 2016;88:1-11.
42. Willems N, Tellegen AR, Bergknut N, Creemers LB, Wolfswinkel J, Freudigmann C*, et al*. Inflammatory profiles in canine intervertebral disc degeneration. BMC Vet.Res. 2016;12:.
43. Tellegen AR, Willems N, Beukers M, Grinwis GCM, Plomp SGM, Bos C*, et al*. Intradiscal application of a PCLA-PEG-PCLA hydrogel loaded with celecoxib for the treatment of back pain in canines: What's in it for humans? J.Tissue Eng.Regen.Med. 2018;12:642-652.
44. de Boer TN, Huisman AM, Polak AA, Niehoff AG, van Rinsum AC, Saris D*, et al*. The chondroprotective effect of selective COX-2 inhibition in osteoarthritis: ex vivo evaluation of human cartilage tissue after in vivo treatment. Osteoarthritis Cartilage 2009;17:482-8.
45. Panahifar A, Jaremko JL, Tessier AG, Lambert RG, Maksymowych WP, Fallone BG*, et al*. Development and reliability of a multi-modality scoring system for evaluation of disease progression in pre-clinical models of osteoarthritis: celecoxib may possess disease-modifying properties. Osteoarthritis Cartilage 2014;22:1639-50.
46. Purmessur D, Cornejo MC, Cho SK, Roughley PJ, Linhardt RJ, Hecht AC*, et al*. Intact glycosaminoglycans from intervertebral disc-derived notochordal cell-conditioned media inhibit neurite growth while maintaining neuronal cell viability. Spine J. 2015;15:1060-9.

47. Modic MT and Ross JS. Lumbar degenerative disk disease. Radiology 2007;245:43-61.
48. Dudli S, Fields AJ, Samartzis D, Karppinen J, Lotz JC. Pathobiology of Modic changes. Eur.Spine J. 2016;25:3723-34.
49. Perilli E, Parkinson IH, Truong LH, Chong KC, Fazzalari NL, Osti OL. Modic (endplate) changes in the lumbar spine: bone micro-architecture and remodelling. Eur.Spine J. 2015;24:1926-34.
50. Rutges JP, Jagt van der OP, Oner FC, Verbout AJ, Castelein RJ, Kummer JA*, et al*. Micro-CT quantification of subchondral endplate changes in intervertebral disc degeneration. Osteoarthritis Cartilage 2011;19:89-95.
51. Neogi T. Structural correlates of pain in osteoarthritis. Clin.Exp.Rheumatol. 2017;35 Suppl 107:75-8.
52. Zweers MC, de Boer TN, van Roon J, Bijlsma JW, Lafeber FP, Mastbergen SC. Celecoxib: considerations regarding its potential disease-modifying properties in osteoarthritis. Arthritis Res.Ther. 2011;13:239-250.
53. Bolbos RI, Zuo J, Banerjee S, Link TM, Ma CB, Li X*, et al*. Relationship between trabecular bone structure and articular cartilage morphology and relaxation times in early OA of the knee joint using parallel MRI at 3 T. Osteoarthritis Cartilage 2008;16:1150-9.
54. Glyn-Jones S, Palmer AJ, Agricola R, Price AJ, Vincent TL, Weinans H*, et al*. Osteoarthritis. Lancet 2015;386:376-87.
55. Tellegen AR, Jansen I, Thomas R, de Visser H, Kik M, Grinwis G*, et al*. Controlled release of celecoxib inhibits inflammation, bone cysts and osteophyte formation in a preclinical model of osteoarthritis. 2018;25:1438-47.

Supplementary file 1. Primers used for quantitative rt-qPCR

Protein	Forward sequence 5' → 3'	Exon	Reverse sequence 5' → 3'	Exon	Amplicon size (BP)	Annealing temp (°C)	Accession no.
Reference genes							
GAPDH	TGTCCCCACCCCCAATGTATC	2	CTCCGATGCCTGCTTCACTACCTT	2	100	58	NM_001003142
HPRT	AGCTTGCTGGTGAAAAGGAC	5/6	TTATAGTCAAGGGCATATCC	7	104	56-58	NM_001003357
RPS19	CCTTCCTCAAAAAGTCTGGG	2/3	GTTCTCATCGTAGGGAGCAAG	3	95	61-63	XM_005616513
SDHA	GCCTTGGATCTCTTGATGGA	6	TTCTTGGCTCTTATGCGATG	6	92	61	XM_535807
Target genes							
ACAN	GGACACTCCTTGCAATTTGAG	13/14	GTCATTCCACTCTCCCTTCTC	14	110	61-62	NM_001113455
ADAMTS5	CTACTGCACAGGGAAGAG	5	GAACCCATTCCACAAATGTC	6	148	61	XM_846025
BCL2	GGATGACTGAGTACCTGAACC	2	CGTACAGTTCCACAAAGGC	2	80	61.5-63	NM_001002949
CASP3	CGGACTTCTTGTATGCTTACTC	8	CACAAAGTGACTGGATGAACC	9	89	61	NM_001003042
COL1A1	GTGTGTACAGAACGGCCTCA	2	TCGCAAATCACGTCATCG	2	109	61	NM_001003090
COL2A1	GCAGCAAGAGCAAGGAC	52	TTCTGAGAGCCCTCGGT	53	150	60.5-65	NM_001006951
IL1B	TGCTGCCAAGACCTGAACCAC	4	TCCAAAGCTACAATGACTGACACG	4	115	68	NM_001037971
IL6	GAGCCCACCAGGAACGAAAGAGA	1	CCGGGGTAGGGAAAGCAGTAGC	2	123	65	NM_001003301
IL10	CCCGGGCTGAGAACCACGAC	3	AAATGCGCTCTTCACCTGCTCCAC	4	91	63	NM_001003077
MMP13	CTGAGGAAGACTTCCAGCTT	5	TTGGACCACTTGAGAGTTCG	5	250	65	XM_536598
PTGES1	CCAGTATTGCCGGAGTGACCAG	2	AAACGAAGCCCAGGAACAGGA	3	97	68	NM_001122854
T	AGACAGCCAGCAATCTG	5	TGGAGGGAAGTGAGAGG	6	115	53	NM_001003092.1
TIMP1	GGCGTTATGAGATCAAGATGAC	2	ACCTGTGCAAGTATCCGC	3	120	66	NM_001003182

Primers used for qPCR analysis of target genes aggrecan (ACAN), a disintegrin and metalloproteinase with thrombospondin motifs 5 (ADAMTS5), B-Cell lymphoma 2 (BCL2), Brachyury (T), Caspase 3 (CASP3), collagen type II α1 (COL2A1), collagen type I α1 (COL1A1), interleukin 1β (IL1B), interleukin 6 (IL6), interleukin 10 (IL10), matrix metalloproteinase 13 (MMP13), prostaglandin E synthase 1 (PTGES1), tissue inhibitor of metalloproteinases 1 (TIMP1) and reference genes glyceraldehyde 3-phosphate dehydrogenase (GAPDH), hypoxanthine-guanine phosphoribosyltransferase (HPRT)), ribosomal protein S19 (RPS19) and succinate dehydrogenase complex, subunit A (SDHA).

Supplementary file 2. Details of the primary antibodies and the immunohistochemistry protocols employed

Name	Manufacturer	Origin	Antibody Ig fraction	Antigen retrieval	Block	Dilution first antibody	Dilution secondary antibody
Collagen I	Abcam, Ab-6308	Human recombinant	Mouse Mab IgG1	Pronase 1 mg/ml, 30 min @37°C and hyaluronidase 10mg/mL, 30 min @37°C	PBS/BSA 5%	1:1500	EnVision K4001, Dako
Collagen II	DSHB, II-II6B3	Human recombinant	Mouse Mab IgG1	Pronase 1 mg/ml, 30 min @37°C and hyaluronidase 10mg/mL, 30 min @37°C	PBS/BSA 5%	1:2000	EnVision K4001, Dako
Collagen X	Quartett, 2031501005	Human recombinant	Mouse Mab IgG1	0.1% Pepsin, 20 min @37°C and hyaluronidase 10mg/mL, 30 min @37°C	1:10 goat serum / PBST	1:50	EnVision K4001, Dako
Neuronal growth factor	Abcam, Ab-6198	Human recombinant	Rabbit Pab IgG1	0.01M Citrate buffer, 20 min @80°C		1:800	EnVision K4002, Dako

Mab: monoclonal antibody; Pab: polyclonal antibody; Hyaluronidase: bovine hyaluronidase 4 450 IU/mg, adjusted to pH 5 with 0.1M HCl.; PBST: Phosphate buffered saline 0.1% Tween-20.

Chapter 9

Intradiscal application of controlled release of celecoxib from microparticles in canine patients suffering from low back pain

A. R. Tellegen [1], T. Wiersema [1], M. Beukers [1], N. Woike [3], G. Mihov [3], J. Thies [3], L. B. Creemers [2], M. A. Tryfonidou [1], B. P. Meij [1]

[1] Department of Clinical Sciences of Companion Animals, Faculty of Veterinary Medicine, Utrecht University, The Netherlands.
[2] Department of Orthopaedics, University Medical Centre Utrecht, The Netherlands
[3] DSM Biomedical, The Netherlands

Manuscript in preparation

Abstract

Low back pain associated with intervertebral disc degeneration is a common clinical entity in both dogs and humans. Oral non-steroidal anti-inflammatory drugs are effective in alleviating pain but can be accompanied by side effects. Novel treatments for degenerative disc disease focus on local application of sustained released drug formulations. The aim of this prospective, randomized controlled study was to determine safety and efficacy of locally delivered celecoxib in polyesteramide microspheres. Thirty dogs with clinical and radiological OA will be included: 20 patients received celecoxib-loaded microspheres, 10 received unloaded microspheres (placebo). Force plate analysis is used to objectively assess weight bearing. Pain-related behaviour is be scored by the owner. Magnetic resonance imaging is used to assess local tissue effects through qualitative (Pfirrmann scoring) and quantitative measurements (T2 mapping, disc height index). In this setup, the dog can be used as a model for the development of novel treatment modalities in both canine and human patients with chronic low back pain.

Introduction

Degeneration of the lumbosacral intervertebral disc (IVD) is strongly associated with low back pain (LBP) and in advanced stages causes neurologic deficits, leading to decreased quality of life in affected individuals [1, 2]. Oral analgesics such as non-steroidal anti-inflammatory drugs (NSAIDs) are often deployed to treat symptoms, but their (long term) use can be associated with adverse effects and insufficient pain relief [3]. Orally administered drugs might not be as effective as locally applied drugs. Local delivery not only ensures optimal drug exposure to the target tissue, it also avoids drug binding to plasma components and drug modifications that can influence efficacy [4]. Local administration of bioactive substances gain increasing attention for the treatment of degenerative joint diseases, both in human and veterinary medicine [5-9]. Biomaterials can facilitate local drug delivery and extend treatment duration by prolonging the presence of drugs in the IVD [10, 11]. Natural α-amino acid based polyesteramide microspheres (PEAMs) have been safely administered to the IVD with small diameter needles [12]. Translation of local controlled drug delivery to the veterinary and human patient with chronic back pain is scarce. Celecoxib was the first selective NSAID to be approved for use against musculoskeletal pain and its effectiveness upon oral administration against osteoarthritis- and low back pain has been demonstrated [13, 14]. In addition, preclinical studies employing celecoxib found beneficial effects on tissue level [8, 15, 16], even postulating it as a disease-modifying drug [17]. Indeed, PEAMs loaded with the COX-2 inhibitor celecoxib in a preclinical canine IVD degeneration model attenuated inflammatory mediators in the IVD and slowed down degenerative changes in the nucleus pulposus (NP) and adjacent subchondral bone of treated IVDs [18]. These anti-degenerative effects seem very promising but results on clinical efficacy remain to be determined. Local celecoxib delivery in a PCLA-PEG-PCLA platform was considered safe via percutaneous administration and reduction in clinical signs was perceived by the owner in a preliminary study with veterinary patients with LBP due to degenerative lumbosacral stenosis (DLSS) [8]. However, structural regenerative effects at the disc level were not demonstrated. This was most probably due to a combination of differential release profile between the two biomaterial platforms and the xx-fold lower loading dose of the PCLA-PEG-PCLA hydrogel. To this end, the aim of the present study was to evaluate the clinical efficacy of local delivery of celecoxib-loaded PEAMs compared to unloaded PEAMs (‘Placebo’) in canines suffering from low back pain due to DLSS.

Material and methods

Preparation of PEA microparticles

PEA microparticles were synthesized according to previously reported protocols [12, 18]. Suspensions of 35 PEAMs /mL for 20 wt% celecoxib-loaded (8 mg/mL celecoxib) and unloaded PEAMs were prepared. Directly prior to IA injection, PEAMs were re-suspended in 3 mL 0.9% sterile saline.

Study design

This study was conducted with the approval of the Ethical Committee of the Department of Clinical Sciences of Companion Animals, Utrecht University (trial number AVR 18-10, approval date 29-12-2017). It was conducted as a prospective, randomized, double-blinded, placebo-controlled clinical trial. All dogs were client-owned and written consent of the owner was obtained before study enrolment. A random number table was created for 30 dogs (Excel 2016, Microsoft). A power analysis was performed on historical data from our institution *a priori*, to calculate minimal required group size with an α of 0.05, power of 0.9 and an effect size of 1.32. Twenty dogs were allocated to the treatment group (35 mg/mL PEAMs with 20wt% celecoxib) and ten dogs were allocated to the control group (35 mg/mL PEAMs). Dogs were divided in weight groups to determine injection volume: 15-30; 30-45; >45 kg 75 µL, 100 µL, 125 µL. The owners and assessing veterinarians were unaware of group allocation. Seven days prior to the inclusion in the study and baseline measurements, the administration of all pain medications was discontinued. Follow-up visits were planned 6, 12 and 24 weeks after intradiscal injection (Figure 1).

Inclusion criteria

Client-owned dogs that were presented at the Utrecht University Small Animal Clinic and met the inclusion criteria (table 1), were included. Prior to admission of the study, all dogs underwent a full clinical examination by a board-certified orthopaedic surgeon (BM), consisting of a general physical, orthopaedic and neurologic examination. To confirm the diagnosis of IVD degeneration, magnetic resonance images (MRI) were obtained. Written consent was obtained from all dog owners before study enrolment.

Table 1. Inclusion- and exclusion criteria for participation in the prospective clinical study.

Inclusion criteria	Exclusion criteria
History of low back pain for at least 6 weeks	Previously performed surgery on IVD of interest
Refractory to oral pain medication for at least 4 weeks	Active discospondylitis or active infection on surgical site (i.e. pyoderma)
Side effects of oral pain medication	Lumbosacral fracture
Pfirrmann grade II-IV on T2-weighted MRI	Spinal neoplasia
Body weight > 15 kg	Chondrodystrophic breed

IVD, intervertebral disc.

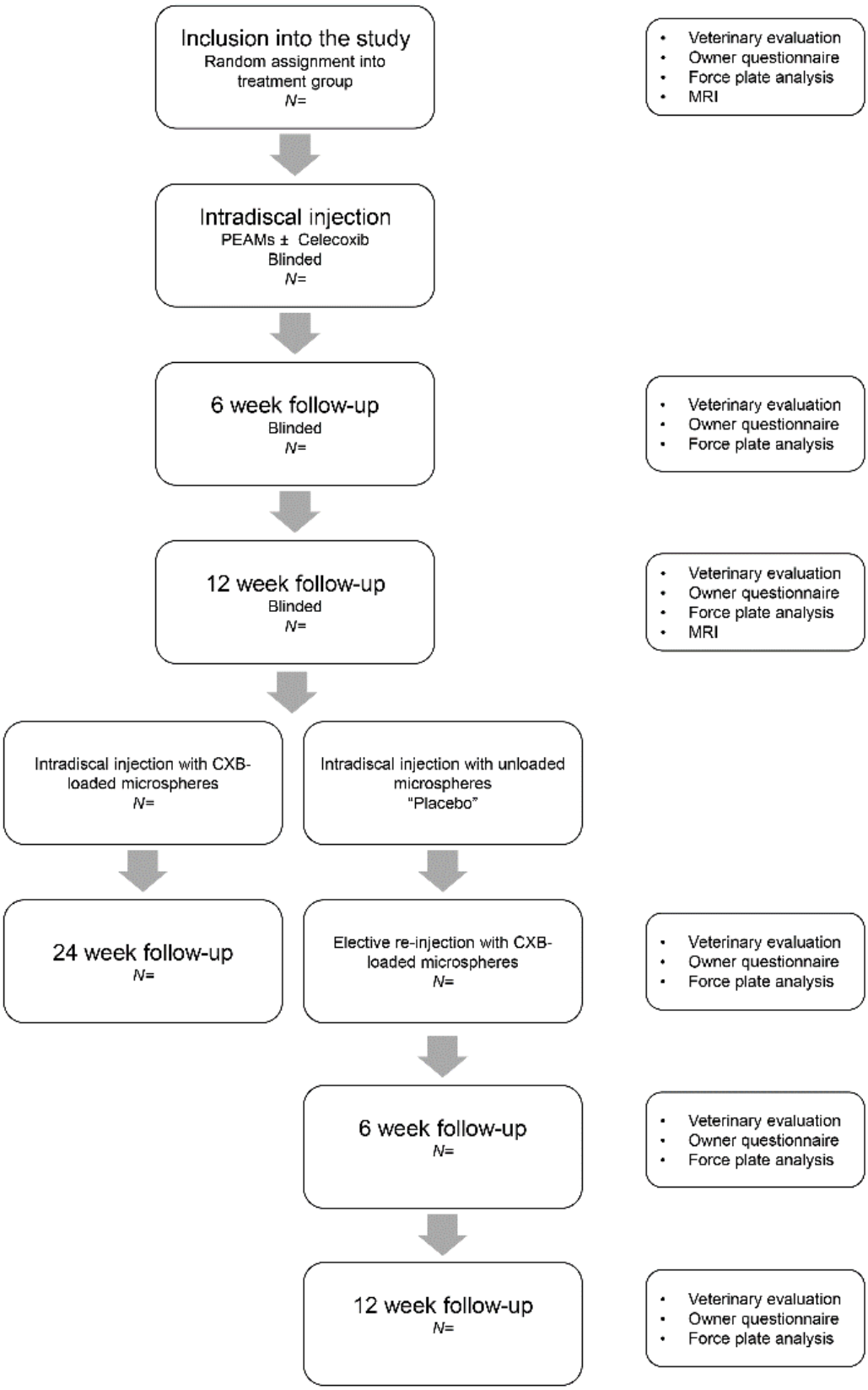

Figure 1. Flow chart of the prospective, randomized controlled study evaluating the clinical efficacy of intradiscal injection of celecoxib-loaded or unloaded polyesteramide microspheres. The study is ongoing, 21 patients have been included so far.

Intradiscal injection

The intradiscal injection was performed under CT guidance. The entire procedure was carried out under general anaesthesia. Premedication consisted of intravenous (I.V.) administration of butorphanol (0.2 mg/kg) and dexmedetomedine (5 µg/kg), followed by induction of anaesthesia with I.V. administration of propofol (1 mg/kg). All dogs received an endotracheal tube, maintenance of anaesthesia was achieved by administration of isoflurane (2%). The dog was placed in sternal recumbency with flexion of the lumbosacral joint and extension of the hind limbs. The surgical site was clipped and prepared aseptically. The lumbosacral space was located through palpation of the iliac crests, the tuber coxae and the spinous process of L7 and sacrum. A 20G epidural needle (4509757-13, Braun) was inserted through the skin until bone or ligamentum flavum was encountered. The depth and placement of the needle was checked by CT Siemens Somatom Definition AS, Siemens Healthcare) and adjusted when necessary. The needle was then advanced through the ligamentum flavum until the dorsal annulus fibrosus (AF) was reached. When correct placement was again confirmed by CT, the stylet was removed and a 12 cm long, 27G needle (7803-01, Hamilton) was inserted in the epidural needle that acted as a guide to position the tip of the 27G needle on top of the AF. The 27G needle was subsequently advanced through the dorsal AF into the centre of the NP and the correct depth of the 27G needle was confirmed with CT. Finally, a 100 µL gastight syringe (7656-01, Hamilton) was connected to the 27G needle and the PEAM suspension was slowly injected. After the syringe was emptied, and prior to removal, CT was repeated to verify the correct position of the needle tip in the centre of the NP. The needle was then slowly retracted through the AF, allowing for the collagen fibres to close behind the needle to prevent leakage of hydrogel outside the NP compartment. Physical activity was limited to short leash walks on the first week after treatment. Thereafter, owners could gradually take up activity as before the start of the study, if the dog tolerated this.

Magnetic resonance imaging

Prior to and three months after intradiscal injection, high-field MRI were obtained using a Philips Ingenia 1.5T MRI (Philips, Eindhoven, The Netherlands). During the MRI procedures, dogs were fully anesthetized using standard protocols. The dogs were positioned in dorsal recumbency with the pelvic limbs extending caudally. At all three time points, a T2 weighted Turbo Spin Echo, a T1 weighted Spectral Pre-Saturation with Inversion Recovery and T2 mapping sequences were obtained. All images were assessed by a board-certified veterinary radiologist (MB). The L6-L7 IVD and the L7-S1 disc were graded according to the Pfirrmann grading system [19] on T2 weighted images obtained prior to injection. The amount of disc protrusion into the spinal canal was categorized as mild (<25% of spinal canal), moderate (25-50%) or severe (>50%) protrusion. Mean T2 relaxation times were determined in an oval region of interest (ROI) in the lumbosacral IVDs on midsagittal T2-mapping images. ROIs were also drawn in fat and muscle tissue to serve as an internal control. The disc height index (DHI) was measured on the MR images on all time points using the method of Masuda et al (TW) [20].

Kinetic gait analysis

Prior to the intradiscal injection, and 6, 12 and 24 weeks after the intradiscal injection, ground reaction forces (GRF) were measured with a quartz crystal piezoelectric force plate (Kistler type 9261, Kistler Instrumente) together with the Kistler 9865E charge amplifiers as has been described previously [21, 22]. Measurements were obtained with a frequency of 100 Hz. The signals corresponded with the GRFs in the mediolateral (Fx), craniocaudal (Fy) and vertical (Fz) direction. The Fz was calibrated with a standard weight before each recording session. The velocity with which the dog walked on the runway was measured, using two photoelectric detectors. FPA recordings were automatically started and stopped by these photoelectric switches. Measurements in which both a thoracic limb and the ipsilateral pelvic limb had contact with the plate were included. A minimum of ten recordings of these recordings were used for data processing. All forces were normalized for body weight. Ratios between pelvic (P) and thoracic (T) limbs were calculated: P/T Fy-, P/T Fy+ and P/T Fz+. The obtained values were compared to values obtained from a cohort of orthopedically sound dogs [22].

Owner assessment of pain related behaviour

Questionnaires to owners regarding behaviour and function of the dog, assessed the outcome of treatment for low back pain in canine patients, previously validated and used in comparable studies [8, 21, 22] were supplied before treatment and at every follow-up visit (supplementary file 1). If owners perceived lameness that was of similar (or worse) severity compared to pre-treatment which lasted for at least 1-2 days, they were allowed to administer pain medication that the dog received prior to inclusion. The owner contacted the study coordinator (AT) for guidance by phone or email, and if necessary, could book an extra in-house check-up. The owners were asked to assess their dog at least twice a day and note down the severity of lameness and the administration of analgesic drugs in the log diary.

Statistical analysis

Inclusion of the patients is still ongoing and therefore the present data set has not yet been subjected to statistically analysis. Statistical software (IBM SPSS Statistics 24) was used for all comparisons. Normality of the data will be checked by assessing the Q-Q plots, histograms and Shapiro-Wilks tests. If normally distributed, a repeated-measures ANOVAs will be used to test for differences within the questionnaire and force plate analysis data, within group (CXB-PEAMs and unloaded PEAMs), between time points, and between groups within time points. In the case of non-parametric data, Friedman's test, followed by Wilcoxon's signed rank tests for each time point will be conducted. For the parameters 'age', 'weight', 'DHI' and T2 mapping values, a one-way ANOVA or Kruskal-Wallis tests followed by Mann-Whitney U-tests will be applied. To compare the proportions of dogs that received additional pain relief medication between treatment- and placebo group, a Fisher's exact test will be performed. *P* values <0.05 will be considered significant.

References

1. Bergknut N, Egenvall A, Hagman R, Gustas P, Hazewinkel HA, Meij BP*, et al*. Incidence of intervertebral disk degeneration-related diseases and associated mortality rates in dogs. J.Am.Vet.Med.Assoc. 2012;240:1300-9.
2. Meij BP and Bergknut N. Degenerative lumbosacral stenosis in dogs. Vet.Clin.North Am.Small Anim.Pract. 2010;40:983-1009.
3. KuKanich B, Bidgood T, Knesl O. Clinical pharmacology of nonsteroidal anti-inflammatory drugs in dogs. Vet.Anaesth.Analg. 2012;39:69-90.
4. Evans CH, Kraus VB, Setton LA. Progress in intra-articular therapy. Nat.Rev.Rheumatol. 2014;10:11-22.
5. Kallewaard JW, Geurts JW, Kessels A, Willems P, van Santbrink H, van Kleef M. Efficacy, Safety, and Predictors of Intradiscal Methylene Blue Injection for Discogenic Low Back Pain: Results of a Multicenter Prospective Clinical Series. Pain Pract. 2016;16:405-12.
6. Levi D, Horn S, Tyszko S, Levin J, Hecht-Leavitt C, Walko E. Intradiscal Platelet-Rich Plasma Injection for Chronic Discogenic Low Back Pain: Preliminary Results from a Prospective Trial. Pain Med. 2016;17:1010-22.
7. Muto M, Ambrosanio G, Guarnieri G, Capobianco E, Piccolo G, Annunziata G*, et al*. Low back pain and sciatica: treatment with intradiscal-intraforaminal O(2)-O (3) injection. Our experience. Radiol.Med. 2008;113:695-706.
8. Tellegen AR, Willems N, Beukers M, Grinwis GCM, Plomp SGM, Bos C*, et al*. Intradiscal application of a PCLA-PEG-PCLA hydrogel loaded with celecoxib for the treatment of back pain in canines: What's in it for humans? J.Tissue Eng.Regen.Med. 2018;12:642-652.
9. Willems N, Yang HY, Langelaan ML, Tellegen AR, Grinwis GC, Kranenburg HJ*, et al*. Biocompatibility and intradiscal application of a thermoreversible celecoxib-loaded poly-N-isopropylacrylamide MgFe-layered double hydroxide hydrogel in a canine model. Arthritis Res.Ther. 2015;17:214,015-0727-x.
10. Chuah YJ, Peck Y, Lau JE, Hee HT, Wang DA. Hydrogel based cartilaginous tissue regeneration: recent insights and technologies. Biomater.Sci. 2017;5:613-31.
11. Henry N, Clouet J, Le Bideau J, Le Visage C, Guicheux J. Innovative strategies for intervertebral disc regenerative medicine: From cell therapies to multiscale delivery systems. Biotechnol.Adv. 2018;36:281-94.
12. Willems N, Mihov G, Grinwis GC, van Dijk M, Schumann D, Bos C*, et al*. Safety of intradiscal injection and biocompatibility of polyester amide microspheres in a canine model predisposed to intervertebral disc degeneration. J.Biomed.Mater.Res.B.Appl.Biomater. 2015;105:707-714.
13. O'Donnell JB, Ekman EF, Spalding WM, Bhadra P, McCabe D, Berger MF. The effectiveness of a weak opioid medication versus a cyclo-oxygenase-2 (COX-2) selective non-steroidal anti-inflammatory drug in treating flare-up of chronic low-back pain: results from two randomized, double-blind, 6-week studies. J.Int.Med.Res. 2009;37:1789-802.
14. McCormack PL. Celecoxib: a review of its use for symptomatic relief in the treatment of osteoarthritis, rheumatoid arthritis and ankylosing spondylitis. Drugs 2011;71:2457-89.
15. Tellegen AR, Jansen I, Thomas R, de Visser H, Kik M, Grinwis G*, et al*. Controlled release of celecoxib inhibits inflammation, bone cysts and osteophyte formation in a preclinical model of osteoarthritis. 2018;25:1438-47.
16. Dong J, Jiang D, Wang Z, Wu G, Miao L, Huang L. Intra-articular delivery of liposomal celecoxib-hyaluronate combination for the treatment of osteoarthritis in rabbit model. Int.J.Pharm. 2013;441:285-90.
17. Nakata K, Hanai T, Take Y, Osada T, Tsuchiya T, Shima D*, et al*. Disease-modifying effects of COX-2 selective inhibitors and non-selective NSAIDs in osteoarthritis: a systematic review. Osteoarthritis Cartilage 2018;10.1016/j.joca.2018.05.021:.
18. Tellegen AR, Rudnik-Jansen I, Beukers M, Miranda-Bedate A, Bach FC, de Jong W*, et al*. Intradiscal delivery of celecoxib-loaded microspheres restores intervertebral disc integrity in a preclinical canine model. J.Control.Release 2018;286:439-50.
19. Bergknut N, Auriemma E, Wijsman S, Voorhout G, Hagman R, Lagerstedt AS*, et al*. Evaluation of intervertebral disk degeneration in chondrodystrophic and nonchondrodystrophic dogs by use of Pfirrmann grading of images obtained with low-field magnetic resonance imaging. Am.J.Vet.Res. 2011;72:893-8.
20. An HS, Takegami K, Kamada H, Nguyen CM, Thonar EJ, Singh K*, et al*. Intradiscal administration of osteogenic protein-1 increases intervertebral disc height and proteoglycan content in the nucleus pulposus in normal adolescent rabbits. Spine (Phila Pa.1976) 2005;30:25-31.
21. Tellegen AR, Willems N, Tryfonidou MA, Meij BP. Pedicle screw-rod fixation: a feasible treatment for dogs with severe degenerative lumbosacral stenosis. BMC Vet.Res. 2015;11:299.
22. Suwankong N, Meij BP, Van Klaveren NJ, Van Wees AM, Meijer E, Van den Brom WE*, et al*. Assessment of decompressive surgery in dogs with degenerative lumbosacral stenosis using force plate analysis and questionnaires. Vet.Surg. 2007;36:423-31.

Supplementary file 1. Questionnaire to the owners of dogs before, at 6 weeks, 12 weeks and 24 weeks after intradiscal application of polyesteramide microparticles with celecoxib.

Types	Questions
YES or NO questions	Did the symptoms disappear after surgery?
	Did the symptoms recur after surgery (after an initial improvement)?
Open questions	How is your dog after surgery?
	Does your dog refuse certain movements?
	Did your dog receive further treatment after surgery?
Questions with a 10-point scale	Does your dog have pain in the pelvic limbs and shows lameness?
	Does your dog show weakness in the pelvic limbs?
	Does your dog have low back pain?
	Does your dog have difficulty rising up?
	Does your dog have difficulty lying down?
	How would you rate muscle volume in the pelvic limbs of your dog?
	How is your dog holding its tail?
	Is your dog able to wag its tail?
	Does your dog show loss of control of urination and defecation?
	Does your dog show pain when you touch the lower back?

Supplementary file 2. Signalment and history of the dogs included in the study to date.

Dog	Group	Breed	Sex	Age (years)	Body weight (kg)
1	P	Rhodesian Ridgeback	FC	4	52
2	P	Labrador retriever	M	1	31
3	C	Old English bulldog	FC	1	33
4	P	Beagle	MC	6	15
5	C	Labrador retriever	M	10	39
6	P	Border Collie	M	3	19
7	C	Labrador retriever	FC	3	28
8	P	Labrador retriever	MC	3	25
9	C	Labrador retriever	MC	3	28
10	C	Labradoodle	FC	6	23
11	C	Labradoodle	MC	1	21
12	C	German Shepherd cross	FC	6	28
13	C	Crossbreed	FC	2	13
14	P	Golden retriever cross	F	7	27
15	C	Weimaraner	FC	5	27
16	C	Rottweiler	FC	1	40
17	P	Labrador retriever cross	MC	1	33
18	C	Flatcoated retriever	FC	7	26
19	C	German Shepherd dog	MC	6	34
20	C	Golden retriever x German Shepherd	MC	2	32
21	C	Perro de Agua Español	MC	9	25

P, placebo; C, celecoxib; FC, female castrated; M, male; MC, male castrated; F, female.

Chapter 10

Pedicle screw-rod fixation: a feasible treatment for dogs with low back pain

A. R. Tellegen [1], N. Willems [1], M. A. Tryfonidou [1], B. P. Meij [1]

[1] Department of Clinical Sciences of Companion Animals, Faculty of Veterinary Medicine, Utrecht University, The Netherlands.

Published in BMC Veterinary Research (2015): 11:299

Abstract

Degenerative lumbosacral stenosis is a common problem in large breed dogs. For severe degenerative lumbosacral stenosis, conservative treatment is often not effective and surgical intervention remains as the last treatment option. The objective of this retrospective study was to assess the middle to long term outcome of treatment of severe degenerative lumbosacral stenosis with or without evidence of radiological discospondylitis. Twelve client-owned dogs with severe degenerative lumbosacral stenosis underwent pedicle screw-rod fixation of the lumbosacral junction. During long term follow-up, dogs were monitored by clinical evaluation, diagnostic imaging, force plate analysis, and by using questionnaires to owners. Clinical evaluation, force plate data, and responses to questionnaires completed by the owners showed resolution (*n*=8) or improvement (*n*=4) of clinical signs after pedicle screw-rod fixation in 12 dogs. There were no implant failures, however, no interbody vertebral bone fusion of the lumbosacral junction was observed in the follow-up period. Four dogs developed mild recurrent low back pain that could easily be controlled by pain medication and an altered exercise regime. Pedicle screw-rod fixation offers a surgical treatment option for large breed dogs with severe degenerative lumbosacral stenosis with or without evidence of radiological discospondylitis in which no other treatment is available. Pedicle screw-rod fixation alone does not result in interbody vertebral bone fusion between L7 and S1.

Introduction

Low back pain in dogs is a common problem and can be the result of different pathologies [1]. Degenerative lumbosacral stenosis (DLSS) is the most common cause of caudal lumbar back pain in middle to large breed dogs [2]. DLSS is characterized by bony and soft tissue changes leading to stenosis of the spinal canal and moderate to severe compression of the cauda equina. The intervertebral disc (IVD) is often degenerated and this results in a shift of load bearing from the IVD to surrounding structures. This may lead to spinal instability [2]. Low back pain can also be caused by other conditions, such as discospondylitis [3], trauma (fracture and/or luxation), or neoplasia [3, 4]. Discospondylitis is a bacterial infection of the IVD and adjacent intervertebral end plates and commonly originates from a primary urogenital infection via hematogenous spread [3]. Discospondylitis can result in severe proliferation of fibrous tissue and bone, vertebral instability, subchondral bone resorption and secondary DLSS [5]. Computed tomography (CT) and magnetic resonance imaging (MRI) are the most informative modalities to investigate the LS area [6, 7].

Treatment of DLSS can be conservative or surgical. Low back pain in DLSS can be treated with non-steroidal anti-inflammatory drugs and/or opioids, body weight reduction, and an adjusted exercise pattern or physiotherapy. Epidural infiltration with methylprednisolone acetate has been reported as medical treatment for DLSS provided that the dog do not show urinary or fecal incontinence and proprioceptive deficits, and does not suffer from concurrent discospondylitis [8]. In case of discospondylitis long term antibiotic drugs are the primary treatment. Surgical treatment of DLSS is accomplished by dorsal laminectomy or foraminotomy, and if indicated, partial discectomy and uni- or bilateral facetectomy. In the short-term, surgical intervention leads to improvement of clinical signs in 78-93% of cases [9, 10] but in the long-term clinical signs recurred in 17-38% of cases [9, 10], which is also known as failed back syndrome [11, 12]. Moreover, force plate analyses (FPAs) showed that the propulsive force of the pelvic limbs is not fully restored after decompressive surgery for DLSS [13]. It has been postulated that decompressive surgery, and especially facetectomy, can worsen LS instability in some patients, resulting in further overall degeneration and recurrence or worsening of clinical symptoms [9, 14].

Therefore, we previously investigated the feasibility of pedicle screw-rod fixation (PSRF) in a cadaver study [14, 15] and in an *in vivo* pilot study [14] in large breed dogs. Screw entry points and guideline values for safe insertion of pedicle screws into the canine L7 and S1 vertebrae have been determined in other studies [14, 16, 17]. The purpose of spinal fixation and interbody fusion is to restore and maintain disc space height and to increase the stability of the operated segment [18], thereby making further ongoing degenerative changes clinically irrelevant. The aim of the present study is to report the long-term results of PSRF in 12 client-owned dogs with severe DLSS and also to assess whether PSRF leads to spinal fusion of the LS junction.

Materials and methods

Dogs

Twelve dogs with DLLS treated by PSRF were included in this retrospective study. The medical records of the dogs were systematically reviewed and the signalment, clinical history, findings on clinical examination, force plate data, radiographic, and CT- and/or MR imaging were retrieved (table 1). Due to the retrospective nature of the current study, no ethical approval was required. The owners consented to the use and disclosure of patient- and questionnaire data for the current study.

Clinical examination

All dogs underwent a full clinical examination, consisting of a general physical, orthopedic and neurological examination by a board-certified veterinary surgeon (BPM). Neurological deficits were graded based on the scale used by Griffith (modified by Sharp and Wheeler 2005): grade 0 (normal), grade 1 (spinal pain only), grade 2 (ambulatory paraparesis), grade 3 (non-ambulatory paraparesis), grade 4 (paralysis posterior with deep pain perception), and grade 5 (paralysis posterior without deep pain perception).

Diagnostic imaging

Ventrodorsal and lateral radiographic views were obtained with the LS spine in neutral position. CT- and MRI-scans were obtained under general anesthesia and dogs were positioned in sternal recumbency with the pelvic limbs extended caudally. CT-scans were obtained with a third-generation CT-scanner[a]. Contiguous 2-mm-thick slices were acquired. MRI was performed with a 0.2 Tesla open magnet[b]. Contiguous 3-mm-thick sagittal T1- and T2-weighted images and transverse T1-weighted MR images were obtained. Pre-operatively, CT-scans and / or MRI scans were performed. The acquired diagnostic images were evaluated by a board-certified radiologist, a board-certified orthopedic surgeon (BPM), and a PhD student / DVM (ART). During surgery, correct position of the screws and the amount of distraction was verified by fluoroscopy. Post-operatively, the position of the pedicle screws, the amount of bony fusion and the development of adjacent segment pathology (ASP) were recorded by radiography or computed tomography on several occasions. In four dogs manual distraction was applied, and the amount of distraction was calculated by comparing the disc height indices prior to treatment with the PSRF device in place. The disc height index was calculated on the radiographs and midsagittal CT reconstructions by using the method described by Hoogendoorn et al [19]. Imaging performed during follow up visits is summarized in Table 1.

Force plate analysis (FPA)

Ground reaction forces (GRFs) were measured using a quartz crystal piezoelectric force plate[c] together with the Kistler 9865E charge amplifiers. The force plate itself was 60 cm wide and 40 cm long, and was mounted flush with the surface in the center of an 11 m long walkway. The middle 5 m of the runway was bordered by a 50-cm high fence to guide the dogs over the force plate. GRFs were measured by force transducers, which were located in

every corner of the plate. The amplifiers were connected to an analog-digital converter, interfaced with a computer that stored the signals. The sampling rate was 100 Hz. The signals corresponded with the GRFs in the mediolateral (Fx), craniocaudal (Fy) and vertical (Fz) direction. The Fz was calibrated with a standard weight before each recording session. Forward velocity of the dog was measured during FPA, using two photoelectric switches spaced 3 m apart and centered on the force plate and computer timing. FPA recordings were automatically started and stopped by these photoelectric switches. All dogs were guided over the force plate on a leash at a walking gait with an average speed of 1.08 m/s (standard deviation 0.08 m/s). Data recorded from measurements in which a thoracic limb and, after a short interval, the ipsilateral pelvic limb contacted the plate were considered valid. A minimum of eight recordings were used for data processing. All forces were normalized for body weight. Ratios between pelvic (P) and thoracic (T) limbs were calculated: P/T Fy-, P/T Fy+ and P/T Fz+. +. Obtained results were compared to previous FP results in normal dogs and dogs with low back pain [20].

Surgical procedure and postoperative care

All dogs were operated by the same ECVS board-certified surgeon (BPM). All dogs underwent a dorsal laminectomy [2] and several additional procedures before PSRF depending on the imaging and surgical findings. Discectomy yielded nucleus pulposus (NP) material that was cultured for bacteria in 10/12 dogs. The spinous processes of L7 and S1 and the lamina of L7 were preserved to serve as autologous bone transplant in ten dogs. In one dog (case 4) a cancellous bone transplant was obtained from the iliac crest. The bone chips and cancellous bone were packed into the intervertebral disc space up to 5 mm beneath the floor of the vertebral canal. An autologous fat transplant, harvested from free subcutaneous tissue, was placed ventral to the cauda equina, and a larger piece was deposited dorsally in the laminectomy site with the aim of preventing dural adhesions and new bone formation [2]. In one dog the compression was severely lateralized necessitating a unilateral facetectomy (dog 5), in two other dogs bilateral facetectomy was necessary (dog 8 and 10). In dog 5 the left S1 nerve had an abnormal appearance and was completely resected and sent for histology.

Thereafter, PSRF was performed as described by Smolders et al [14]. Briefly, the entry points of L7 and S1 were identified and the corridors in the cancellous bone within the pedicle were prepared using a bone awl and probe[d]. Once the ventral cortex was reached, the pedicle probe was removed from the screw corridor. To facilitate screw anchorage in the ventral vertebral cortex, predrilling of the ventral cortex was performed with a K-pin (1.2 mm). Four 25 mm long, 4 mm wide titanium pedicle screws[d] were inserted into the pedicle and vertebral body. Two 5 cm long, 6 mm wide titanium rods were used to connect the L7 pedicle screw with the ipsilateral S1 pedicle screw. The rod was slightly adjusted with a rod bender to acquire a proper fit on both screw heads. Once a tight fit was obtained, the sleeves and nuts were applied and tightened.

Table 1. Overview of read out parameters in 12 dogs with lumbosacral degenerative stenosis (DLSS) treated with pedicle screw-rod fixation.

Dog no	Pre-op	Intra-op	Post-op	Follow up period (months)		
				< 3 mo	< 6 mo	> 6 mo
1	CT, MRI	BC, HP	RX	CT		CT, RX (12 mo); CT, RX, FPA (46 mo)
2	RX, CT	BC, HP	RX	RX		CT, FPA (40 mo)
3	RX, CT	BC, HP	RX	RX		RX, FPA (35 mo)
4	CT, MRI	BC, HP	RX, CT	RX		
5	CT, MRI	BC, HP	RX			
6	RX, CT	BC	RX		RX	
7	CT, MRI		RX			CT, FPA (10 mo)
8	CT	BC	RX	CT, RX, FPA	CT, RX, FPA	CT, FPA (7.5 mo)
9	CT	BC, HP	RX	RX		
10	CT, MRI	BC, HP	RX	RX, FPA	CT, FPA	
11	CT, RX, MRI		RX	RX	RX, CT	
12	CT	BC, HP	RX	RX	RX, FPA	CR (14 mo)

Abbreviations: Pre-op, pre-operative; intra-op, intra-operative; post-op, postoperative; mo, months; CT, computed tomography; MRI, magnetic resonance imaging; BC, bacteriologic culture; HP, histopathologic evaluation; RX, plain radiography; FPA, force plate analysis.

Optimal screw anchorage was achieved by involving both the medial and lateral pedicle cortex. "Cortical encroachment" was identified when the pedicle cortex could not be visualized or as "frank penetration" when the screw was outside the pedicular boundaries [21-23]. Screw placement was considered optimal when screws involved the cortical bone and not fully penetrated the ventral vertebral cortex. Intraoperative fluoroscopy was used to verify correct placement of the screws. Four dogs underwent manual distraction as well because of intervertebral foraminal stenosis evident on pre-operative imaging. Manual distraction was applied to the base of the pedicle screws using a Gelpi retractor followed by tightening the screw heads to the rods. The amount of distraction was estimated based on the mobility of the LS segment and did not exceed 5 mm. Postoperative care consisted of leash restraint and exercise restriction for a period of six weeks and after that, the dogs were allowed to gradually return to their normal exercise regime within three months after surgery.

Follow-up and questionnaires to owners

Follow-up data were collected from the medical records, by using questionnaires [6, 13, 20] to owners, by interviewing the owners and by reexamination of the dogs. Questionnaires for follow-up evaluation (Table 2) were sent to all owners of dogs that had undergone PSRF within the last four years. Two dogs were lost in follow-up due to unrelated mortalities. The

questionnaires included questions regarding the history, clinical signs before surgery and the owner's satisfaction with the outcome at three months and one year after surgery.

Table 2. Questionnaire to the owners of dogs before, at three months and more than one year after pedicle screw-rod fixation for degenerative lumbosacral stenosis.

Types	Questions
YES or NO questions	Did the symptoms disappear after surgery?
	Did the symptoms recur after surgery (after an initial improvement)?
Open questions	How is your dog after surgery?
	Does your dog refuse certain movements?
	Did your dog receive further treatment after surgery?
Questions with a 10-point scale	Does your dog have pain in the pelvic limbs and shows lameness?
	Does your dog show weakness in the pelvic limbs?
	Does your dog have low back pain?
	Does your dog have difficulty rising up?
	Does your dog have difficulty lying down?
	How would you rate muscle volume in the pelvic limbs of your dog?
	How is your dog holding its tail?
	Is your dog able to wag its tail?
	Does your dog show loss of control of urination and defecation?
	Does your dog show pain when you touch the lower back?

Statistical analysis

Statistical analysis was performed using software (SPSS 22 for Windows; SPSS Inc., Chicago, IL). Normal distribution of the data was checked by performing the Shapiro Wilks test. The reliability of the responses to the questionnaires was tested by calculation of Cronbach's α where a value of >0.70 was considered reliable [24]. Comparison of the mean scores of the questionnaires before surgery, at 6 months, and >1 year after surgery was conducted using the Friedman's test. If there was a significant difference ($P<0.05$), post hoc tests were performed for each time point. The pre-operative Griffith score for neurological (dys)function was compared to the Griffith score appointed at the last follow up visit using the Wilcoxon signed rank test. Significance was set at $P<0.05$.

Results

Dogs

Seven male (3 intact, 4 neutered) and five female (2 intact, 3 neutered) dogs with a median age of 8 years (1-12 years) and a median body weight of 32 kg (22- 55 kg) were included in the study (Table 3). All dogs were kept as companion animals. Four dogs had undergone previous decompressive surgery once but developed failed back syndrome.

Table 3. Overview of signalment, history and radiological diagnosis in 12 dogs with lumbosacral degenerative stenosis (DLSS) and / or discospondylitis that were treated with pedicle screw-rod fixation.

Dog	Breed	Sex	Age (yrs)	History	Radiological diagnosis
1	Labrador retriever	FC	5	LS pain, paraparesis	DLSS & DS
2	Rottweiler	M	8	LS pain	DLSS & DS
3	GSD	FC	8	LS pain, paraparesis	DLSS & DS
4	GSD	MC	11	LS pain, paraparesis; DL 6 yrs earlier	DLSS & DS
5	Rhodesian Ridgeback	F	10	LS pain, left paraparesis, urinary incontinence; DL 6 months earlier	DLSS & DS
6	GSD	M	12	LS pain, paraparesis	DLSS & DS
7	Cane Corso	MC	7	LS pain	DLSS
8	American Bulldog	M	5	LS pain	DLSS & DS
9	Border Collie	MC	9	LS pain	DLSS & DS
10	Rhodesian Ridgeback	FC	7	LS pain, paraparesis; DL 4 yrs earlier	DLSS
11	Vizsla	MC	12	LS pain	DLSS
12	Am Staff terrier	F	5	LS pain, left paraparesis; DL 3 yrs earlier	DLSS

Abbreviations: LS, lumbosacral; GSD, German Shepherd Dog; F, female; FC, female castrated; M, male, MC, male castrated; DS, discospondylitis; DL, dorsal laminectomy; yrs, years.

Clinical examination

All dogs presented with pelvic limb lameness and caudal lumbar pain; seven dogs also showed paraparesis. In all dogs pain was evoked upon pressure and extension of the LS spine and tail extension. One dog suffered from urinary incontinence. The neurological Griffith score before surgery was grade 1 (5 dogs), 2 (4 dogs) and 3 (3 dogs) (Table 3,4).

Diagnostic imaging

Imaging was performed pre-operatively using plain radiography (4 dogs), CT (12 dogs), and MRI (5 dogs) (Table 1). In all 12 dogs the final radiological diagnosis was DLSS with presumptive radiologic evidence of concurrent discospondylitis in eight dogs (Table 3). Pre-operative radiologic and CT findings included spinal stenosis of the lumbosacral junction (Fig. 1A) in 10 dogs, end plate sclerosis of both lumbosacral end plates (Fig. 2) in 11 cases, end plate osteolysis (Fig. 2C) in 7 cases, vacuum phenomenon in the IVD (Fig. 2a) in 3 cases, elongation of the sacral lamina up to or under the caudal end of the lamina of L7 as described by Suwankong et al [6] (Fig. 3A) in 4 cases and LS step formation (ventral subluxation of S1 with respect to L7) (Fig. 3A) in 4 cases. A narrowed IVD space was visible in two dogs. Non-bridging spondylosis deformans (Fig. 2A) was recorded pre-operatively in

nine dogs, bridging spondylosis in two dogs. Protrusion of the IVD was seen in all dogs; severe protrusion (>50% reduction of spinal canal width) (Fig. 2A) in ten dogs, a moderate compression (25-50% reduction of spinal canal width) in one dog and mild protrusion (<25% reduction of spinal canal width) in one dog. Dorsal displacement of the dural sac, combined with a decrease in the epidural fat signal dorsal to the dural sac at the level of L7-S1 was recorded in nine dogs on CT or MRI (Fig. 1,2). Thickening of spinal nerves was detected in four dogs. The signal intensity of the L7-S1 IVD on T2-weighted images was severely decreased in all five dogs which underwent MRI (Fig. 2B). Dog 4 had undergone dorsal laminectomy 6 years earlier (Table 1) and on MR a bulging LS disc was noted in combination with dorsal displacement of nerve tissue at the level of L7-S1. Calcifications in the IVD space were recorded as well. On the CT images there was marked ventral spondylosis deformans, IVD calcifications and vacuum phenomenon. Moreover, there was still severe central and right lateral disc protrusion present, leading to the right lateral nerve compression near the right facet joint. Dog 5 had undergone decompressive surgery 6 months earlier (Table 4). CT showed that the cauda equina was displaced dorsally as a consequence of bulging disc material. Both the L7 and S1 end plates were irregular and sclerotic. There was pronounced new bone formation around the lumbosacral junction, in the intervertebral foramina and around the sacroiliac joints. The left exiting spinal nerve was markedly enlarged, indicative for a peripheral nerve sheath tumor. There was severe muscle atrophy present in the left quadriceps and gluteus muscles.

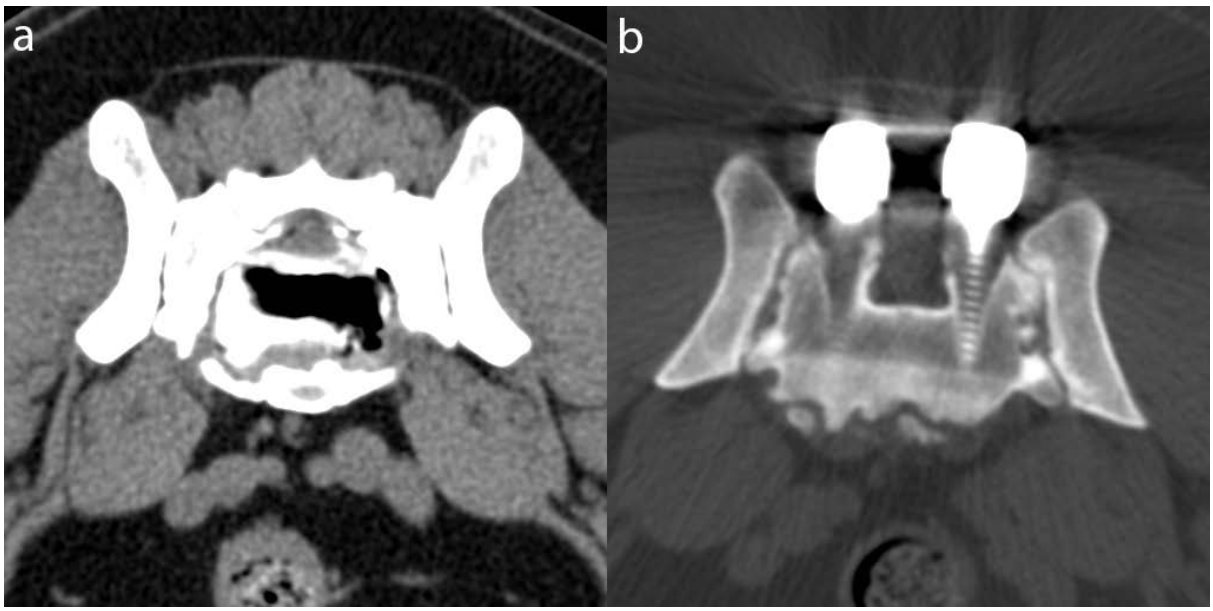

Figure 1A. Transverse CT image of the lumbosacral (LS) junction of a 9-year-old Border collie (dog 9) with degenerative lumbosacral stenosis and discospondylitis. Spinal stenosis and severe intervertebral disc (IVD) bulging are visible and there is gas accumulation (vacuum phenomenon) present in the center of the L7-S1 IVD. **B.** Transverse CT image at level of S1 of a dog (dog 1) with pedicle screw-rod fixation, four years after implantation. No bony fusion between the L7 and S1 vertebrae was visible.

Table 4. Overview of surgery details and clinical outcome in 12 dogs with lumbosacral degenerative stenosis (DLSS) that were treated with pedicle screw-rod fixation.

Dog	Surgery	Bone graft	Clinical outcome (follow-up (FU) period)	Griffith score pre-op	Griffith score last FU
1	L7-S1: DL, PD, PSRF	Bone L7+S1	Excellent (4 yrs)	3	0
2	L7-S1: DL, PD, PSRF	Bone L7+S1	Excellent (4 yrs)	1	0
3	L7-S1: DL, PD, PSRF	Bone L7+S1	Excellent (3 yrs)	2	0
4	L7-S1: rDL, PD, PSRF & Distraction	Bone iliac crest. Osteostixis EPs	Improved (euth. 6 mo heart disease)	2	2
5	L7-S1: rDL, PD, L Facetectomy, L Foraminotomy, Excision L7 nerve, PSRF	Bone L7+S1	Improved (euth. 15 mo, neoplasia)	3	3
6	L6-S1: DL, L7-S1: DL, PSRF	Bone L7+S1	Improved (1.5 years, euth. hemangiosarcoma)	2	0
7	L7-S1: DL, PD, L&R Facetectomy, PSRF & Distraction	Bone L7+S1	Excellent (1 yr)	1	0
8	L7-S1: DL, PD, PSRF	Bone L7+S1 Burring Eps	Improved (euth. 8 mo)	3	1
9	L6-S1: DL, L7-S1: PD; L&R Facetectomy, PSRF & Distraction	Bone L7+S1	Excellent (6 mo)	1	0
10	L7-S1: rDL, PD, PSRF	Bone L7+S1	Excellent (6 mo)	2	0
11	L6-S1: DL, L7-S1: PD PSRF & Distraction	Bone L7+S1	Excellent (11 mo)	1	0
12	rDL, Partial L Facetectomy, L Foraminotomy, PSRF	None	Excellent (6 mo)	1	0

Excellent: resolution of clinical signs. Improved: decrease of clinical signs. Abbreviations: DL, dorsal laminectomy; rDL, revision DL; PD, partial discectomy; PSRF, pedicle-screw rod fixation; L, left; R, right; EPs, end plates; yrs, years; mo, months; euth., euthanized

Surgical findings

Following dorsal laminectomy and partial discectomy (Table 4), pedicle screws were inserted and were used to distract, realign and stabilize the LS segment. In ten dogs, the protrusion of the IVD was considered severe, in one dog, there was moderate protrusion. The amount of epidural fat was decreased in ten dogs and absent in one dog. In six dogs, inflammation of the epidural fat was noticed by the surgeon. In 11 dogs thickening of neural tissue, especially

the S1 nerve roots, was visible. Two of ten disc tissue samples returned with a positive bacterial culture. *Bacillus spp* (dog 5) and *Staphylococcus aureus* (dog 8) were identified in two dogs. Histopathological examination of tissue samples collected during surgery showed degeneration of the annulus fibrosus and nucleus pulposus in all cases. Histopathological examination of the excised nerve (dog 5) showed an undifferentiated neurofibrosarcoma of the nerve root, characterized by round- and spindle shaped neoplastic cells.

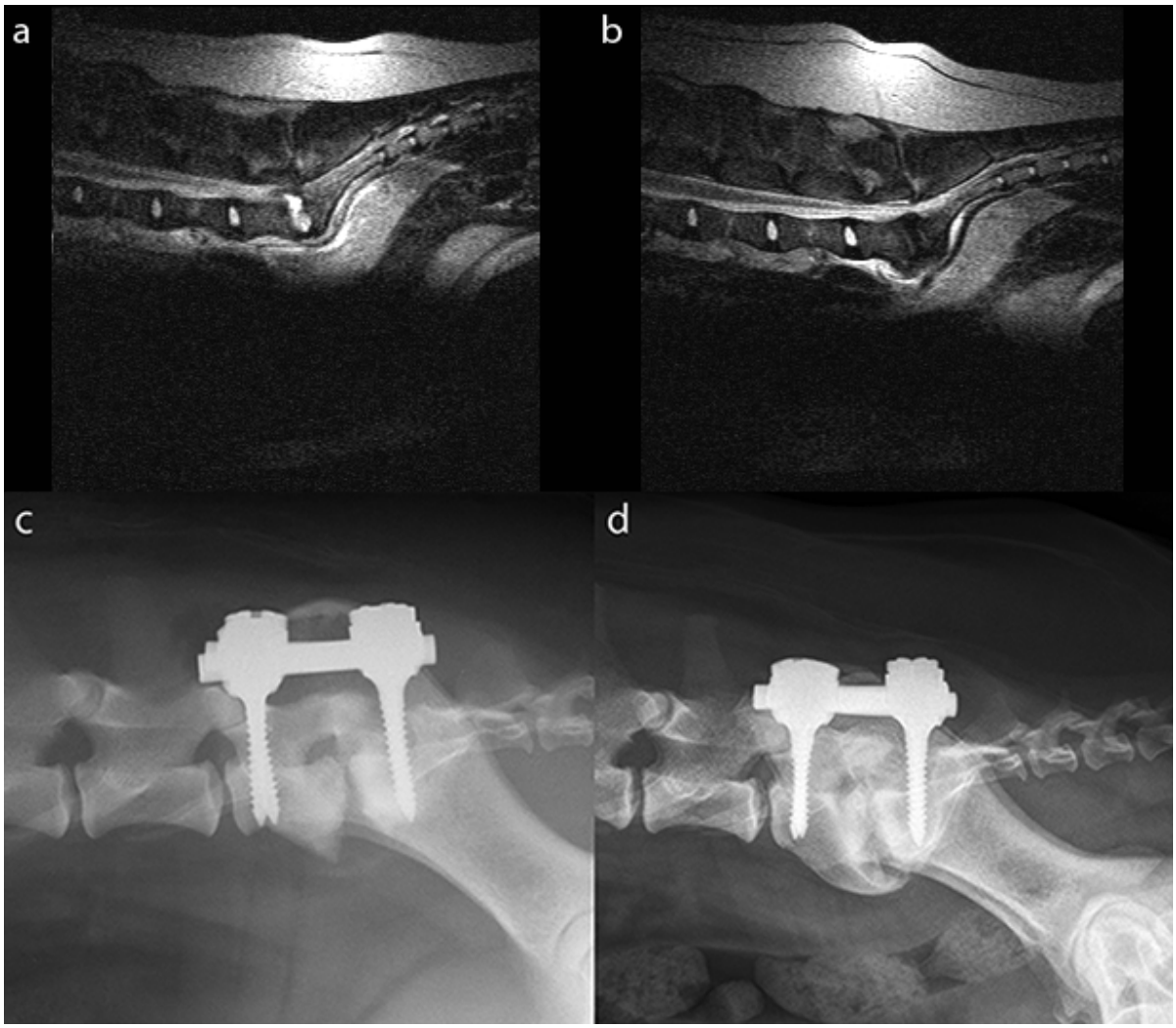

Figure 2A. Sagittal T2-weighted MR image of a 5-year-old Labrador retriever (dog 1) with degenerative lumbosacral stenosis and acute onset of discospondylitis. There is a hyperintense signal (exudate) visible in the intervertebral disc space. **B.** Sagittal T2-weighted MR image of dog 1 after three months of treatment with oral antibiotics. The inflammatory exudate has disappeared. **C**. Immediate postoperative radiograph of dog 1 after pedicle screw-rod fixation (PSRF) showing osteolysis of the L7 and S1 endplates. **D.** Radiograph of dog 1 at four years after PSRF. Spondylosis deformans has formed ventral to the LS junction.

Follow-up (imaging and clinical signs)

Radiography or CT was performed to evaluate the position of the screws and the amount of interbody vertebral bone fusion. In the follow-up period after surgery imaging was performed at 4-6 weeks (radiography or CT, 7 dogs), at three months (radiography or CT, 4 dogs), at six months (CT, 3 dogs), at one year (CT, 2 dogs), at three years (radiography or CT, 2 dogs), and at four years (CT, 1 dog) (Table 1). Placement of the screws was considered to be correct [14] in 11 out of 12 dogs (92%) based on radiographic evaluation. In six dogs, CT was performed postoperatively (Fig.1b). Optimal screw anchorage was achieved by involving both the medial and lateral pedicle cortex. Cortical encroachment of the lateral pedicle wall was noticed on CT with the right L7 screw in two dogs. Penetration of the ventral cortex was recorded on CT in three dogs, involving four screws. No implant failures were seen. In eight dogs, there was complete resolution of clinical signs after surgery, in two dogs the severity of the clinical signs decreased. These two dogs (dog 4 and 5) had already undergone prior decompressive surgery by dorsal laminectomy. In two dogs (dog 6 and 8), the clinical signs recurred after initial remission. Plain radiographs and CT scans were obtained. No adverse advents as a result of the pedicle screw implantation surgery were noted. Neurologic dysfunction in dog 6 did not improve markedly after surgery and dragging with the left hind limb persisted. Dog 8 was euthanized at eight months after surgery at request of the owner, since low back pain recurred every time antibiotic treatment was ceased. After surgery, the Griffith neurological grading score was 0 (9 dogs), 1 (1 dog), 2 (1 dog) and 3 (1 dog) (Table 4). The median pre-operative Griffith score was 2 (with a range from 1-3), whereas the Griffith score obtained at the last follow up visit was 0 (with a range from 0 to 3). The Wilcoxon signed rank test revealed a significant improvement in Griffith scores before surgery and at the last follow up visit ($p=0.004$). The development of adjacent segment pathology was noticed in one dog after three years on plain radiographs (Fig. 3B), but the dog did not display signs of low back pain. At any time point after PSRF, in none of the other dogs ASP was noticed on diagnostic imaging nor clinically. In the four dogs that underwent manual distraction of the LS junction, the IVD space height increased by 67% (dog 4), 11% (dog 7), 114% (dog 9), and 9% (dog 11) compared with the IVD height prior to surgery. Six months after surgery, distraction of the LS junction was still present in three dogs. In one dog (dog 11) there was loss of distraction as evidenced by sudden low back pain at one week postoperatively, and radiographic evidence of collapse of the L7-S1 IVD space without implant failure. The pain was controlled with oral analgesics for two weeks.

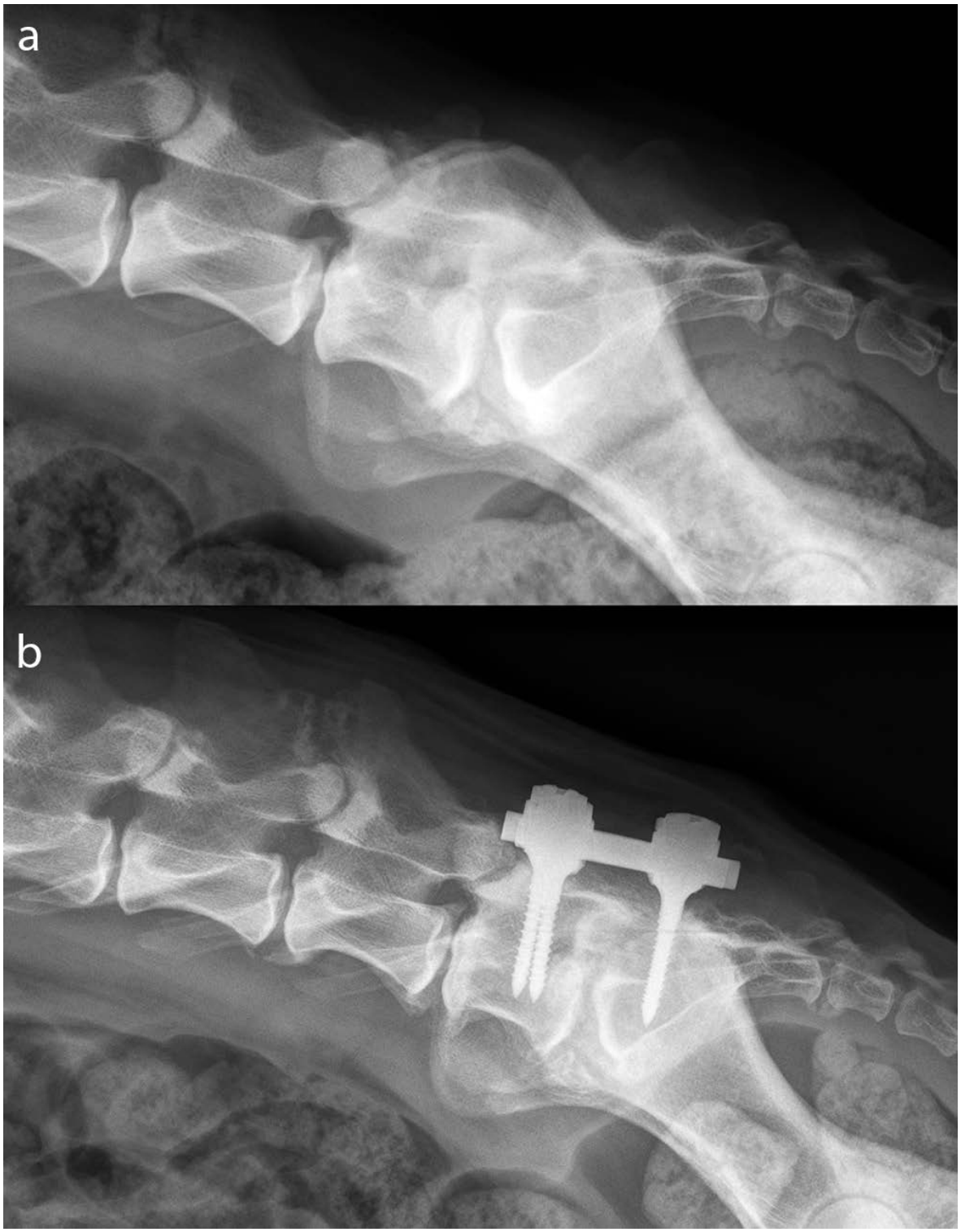

Figure 3A. Pre-operative radiograph of an eight years old German shepherd dog (dog 3) diagnosed with degenerative lumbosacral stenosis. There is non-bridging spondylosis deformans, end plate sclerosis, lumbosacral step formation and elongation of the sacral lamina underneath L7**. B.** Radiograph showing dog 3 three years after pedicle screw-rod fixation with implants in correct position. At the level of L5-L6 and L6-L7, there is radiological evidence for adjacent segment pathology, seen by narrowing of the intervertebral foramen. No interbody fusion was present between L7 and S1.

Force plate analysis

Pre-operative force plate analysis was performed in three dogs (dogs 8, 10 and 12) (Fig. 4). In two dogs (dogs 8 and 10), the P/T Fy- and P/T Fz+ ratios were lower than reference ranges described in a previous study [20]. In dog 10, FPA was performed six months after surgery and values were still below reference ranges, this dog was lost for further follow up. Dog 7 showed normal P/T Fy- values after 10 months. FPA performed in three dogs (dog 1, 2 and 3) more than three years after surgery showed P/T Fy- ratios comparable to normal dogs [20].

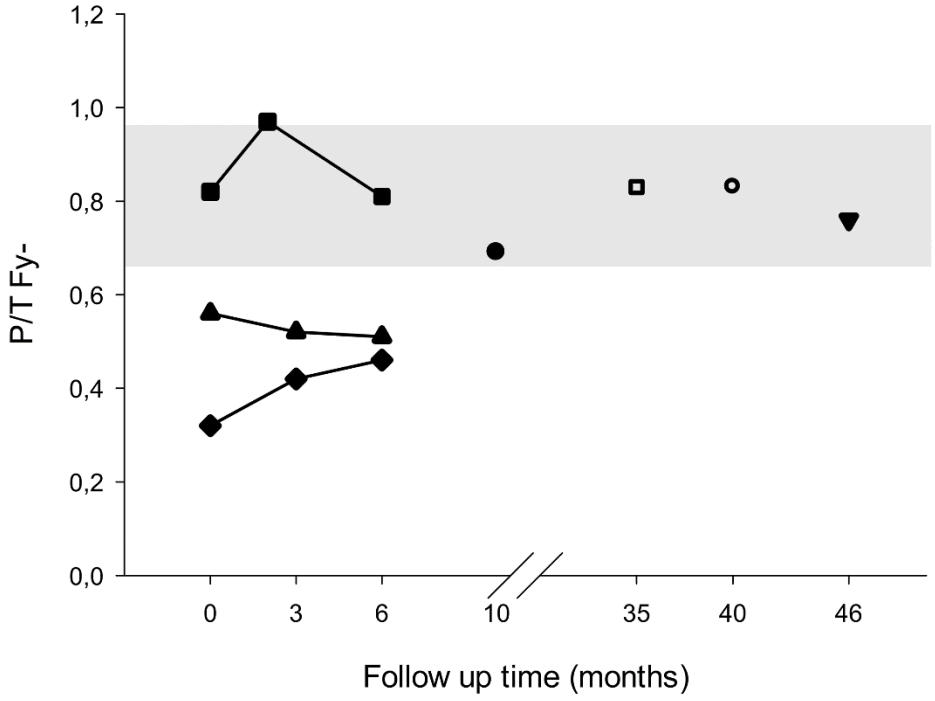

Figure 4. P/T Fy- values of seven dogs (■=dog 12; ▲=dog 10; ♦ =dog 8; ●=dog 7; □=dog 3; ○=dog 2; ▼=dog 1). The grey area marks reference values for the average P/T Fy- value ±1 SD previously determined for healthy dogs [20].

Owner questionnaires

Eight out of twelve (67%) owners responded to the questionnaire. The follow-up period ranged from five months to more than four years. Prior to surgery, owners mentioned low back pain, hind limb lameness, and reluctance to perform certain movements as the most striking clinical signs. All owners reported that the clinical signs of their dog had disappeared after surgery. However, in four dogs the clinical signs recurred. In three dogs these signs were mild and could be treated effectively with NSAIDs. In the fourth dog, discospondylitis persisted despite aggressive long term (6 months) antibiotic therapy, for which the dog was eventually euthanized at eight months after PSRF. Six owners did not report any recurrences during the follow-up period; the long-term outcome of three dogs is unknown since they

were euthanized due to unrelated illnesses (i.e. heart failure, hemangiosarcoma). Three dogs showed concurrent orthopedic problems such as hip dysplasia (*n*=1) and osteoarthritis of the stifle joint (*n*=2) in the follow up period. Five dogs continued to receive intermittent pain medication, with four dogs receiving non-steroidal anti-inflammatory drugs (NSAIDs), one dog tramadol and one dog a combination of NSAIDs and neuromodulatory drugs (gabapentin).

Table 5. Results (median and range) of responses to the questionnaires of dogs treated with PSRF before surgery, after 6 months and more than 1 year after surgery. * $p<0.05$, Friedman test, compared with value before surgery. † Group comparisons were borderline significant ($p=0.061$), individual comparisons of time points did show significant difference ($p<0.05$).

Questions	Before surgery	After 6 months	After more than 1 year
Complaints of pelvic limbs	3 (1-4)	8 (4-10) *	7 (5-9) *
Pelvic limb weakness	4 (1-10)	8 (6-10) †	7 (6-10) †
Caudal lumbar pain	1 (1-4)	7 (4-10) *	7 (5-9) *
Difficulty rising up	4 (1-6)	8 (7-10) *	7 (5-10) *
Difficulty lying down	8 (1-6)	10 (8-10)	10 (5-10)
Muscle volume of the pelvic limbs	4 (1-7)	7 (5-9) *	7 (6-7) *
Position of the tail	3 (1-10)	9 (1-10)	9 (1-10)
Movement of the tail	5 (2-10)	10 (3-10)	9 (3-10)
Control of urination and defecation	10 (3-10)	10 (10-10)	10 (10-10)
Hypersensitivity of the caudal spine	3 (1-10)	9 (3-10) †	10 (9-10)

Before evaluating the answers of the owners to the questionnaire, the reliability of the answers was tested by calculating the Cronbach's alpha value. The Cronbach's alpha value of the responses to the questionnaire was 0.88, indicating that the answers were reliable. The data were normally distributed. All eight owners that had filled in the questionnaire reported that the clinical signs of low back pain had disappeared after surgery (100%). Three owners reported that the clinical signs of low back pain had recurred after an asymptomatic period of time (3/8 = 38%). Table 5 shows the results to the questionnaire before, six months, and more than one year after surgery. All data are expressed as the median and the range. The level of significance was set at $P<0.05$. There was a significant and sustained decrease in caudal limb lameness, caudal lumbar pain and difficulty in rising up more than six months after surgery. Moreover, muscle volume had significantly increased six months after surgery, compared to the pre-operative situation. There was a trend of decrease in pelvic hind limb lameness and hypersensitivity of the caudal spine ($P=0.061$) after six months.

Discussion

The pilot study of Smolders *et al* (2012) [14] suggested that PSRF of the canine LS junction can be used as an addition to surgical decompression for dogs with LS disease and presumed instability of the LS joint. The results showed stability of the implants and improvement of hind limb function in Greyhounds with mild LS disease. The current study presented the follow-up of 12 client-owned dogs with severe DLSS treated with PSRF. With data retrieved from diagnostic imaging, FPAs and clinical examinations together with owner questionnaires, we conclude that PSRF can be a feasible treatment option for dogs with DLSS in which previous decompressive surgery failed and/or medical treatment is ineffective to control low back pain. The authors are aware of the limitations of this retrospective study. The study group is relatively small and due to the retrospective nature of the study, the follow up of the patients was not standardized. Not all owners were willing to attend control visits with their dog or had financial constraints. All cases were referred as severe and complicated cases, where conservative treatment or previous surgery had failed, or for which no other treatment was available. Even more, in several cases euthanasia was advised by the referring veterinarian, but the owner persisted for third opinion referral.

Propulsive forces in the hind limb are decreased in dogs with DLSS as compared to healthy dogs [20]. In the present study, the collected FPA data showed an initial worsening after surgery, but after six months overall results were improving, with values at six months after surgery higher than before surgery. Notably, ground reaction forces were comparable to normal dogs [20]. These findings are in agreement with results from previous studies on FPA before and after decompressive surgery [20] and the in vivo pilot study on PSRF from the same group [14]. Given that FPA is used to objectively measure ground reaction forces in both humans and dogs [20, 25-27], these findings indicate an overall clinical improvement in the long term.

The percentages of dogs with clinical remission and recurrence found in our study were similar to those for dorsal laminectomy alone [20], although the dogs in the current study suffered from more severe LS disease than the average population undergoing decompressive surgery. Decompressive surgery has proven to be insufficient in a small percentage of cases, i.e., due to the development or worsening of LS instability after surgery [9, 10, 14]. In four dogs in this study a previous decompressive surgery was already performed with inadequate effect. In humans with low back pain due to end stage degenerative disc disease, spinal fusion using cages with or without pedicle screw fixation is currently the state-of-the-art [28-30], rather than decompressive surgery alone. Moreover, spinal fusion is often performed during revision surgery for failed back syndrome [12, 31, 32].

Placement of the screws was considered to be correct [14] in 48/52 screws (92%) and no implant failures were seen. In three cases, cortical encroachment of the medial pedicle wall by four screws was detected but this did not result in clinical signs. Optimal screw anchorage is achieved by involving the cis- and trans-cortex, as well as the medial and lateral pedicle

wall. Full penetration of the ventral cortex was seen with seven screws in five dogs. Although full penetration carries the risk of damaging vascular structures, there was no indication that this happened. Full penetration is most likely the result of the fixed length of the screws. The pedicle screw rod fixation device that was used in this study was produced for paediatric human spinal fixation which apparently was still too large for some of the dogs, e.g. dog number 11 (Border collie). This underscores the need for the development and production of pedicle screws for the canine species.

The aim of PSRF is to stabilize the LS junction. This is achieved in the short term by the inserted instrumentation and in the long term by fusion of the spinal segments. However, in this study no interbody vertebral bone fusion was achieved. Several authors have reported on surgical stabilization in the veterinary field as well. Mckee et al [33] have performed distraction-stabilization in dogs with discospondylitis by the method described by Slocum et al [34] and Auger et al [35] have performed articular facet joint distraction with an external fixator. More recently, Golini et al published a study about transarticular fixation as treatment for DLSS in dogs [36]. In all abovementioned studies, a considerable number of implant failures was seen which in some cases required additional surgery. In the current study, there was no implant failure. The dogs recovered very well but there was no evidence for spinal fusion in the long-term follow-up. To achieve interbody fusion, additional methods are necessary. In the current study, we used autologous bone grafts in 11 cases but without success as far as bony fusion is concerned. Fitzpatrick and colleagues developed a dorsal fixation system, which uses a screw-rod construct in combination with a wedge-shaped screw. This screw is positioned in between the L7 and S1 vertebrae [37, 38]. With this device, bone ingrowth was visible. In human medicine, interbody spinal fusion is promoted by several techniques. In addition to iliac crest autograft, metal and composite interbody cages, allograft bone dowels and bone grafts infused with recombinant bone morphogenetic proteins (BMPs) or bone marrow derived stem cells are readily available for human patients and show promising effects [18, 39]. Moreover, in dogs the subchondral bone is relatively thicker than in humans whereas the canine end plates are thinner [40, 41]. This may counteract bony fusion between the two vertebrae in canines. Therefore, more aggressive burring of the end plates to penetrate the subchondral bone would be appropriate in canines to achieve spinal fusion. Although bony fusion of the last lumbar vertebra and the sacrum is desired, there was no significant difference in outcome in human [32] and canine [35] patients that did show spinal fusion compared to patients that failed to develop interbody fusion after spinal fusion surgery [32, 35].

Recurrence of clinical signs after PSRF stabilization could be related to ASP. ASP can be defined as degeneration or other pathologic processes occurring cranial or caudal to a region of vertebral column fusion, the most common pathology being IVD degeneration [42]. In the current study, only two vertebrae were fixated. One of the dogs (dog 3) in this study showed signs of ASP on radiography at three years after surgery. This dog was not painful on the lumbar region during clinical examination and also the force plate data showed no signs of

lumbar pain. ASP has been found in humans after spinal fusion surgery [43] and also in dogs after cervical fusion [44, 45]. Lumbar spinal fusion in humans resulted in radiologic evidence of ASP in 10-80% after 10 years. Loss of motion in the fused segment leads to increased workload and altered biomechanics in adjacent segments [46]. However, at this moment it is unclear if ASP is a natural degenerative process or if ASP is the result of fusion surgery [47]. Clinically relevant ASP was only noted in 6-26.1% of the human patients, with radiologic confirmed ASP, after ten years [46]. ASP does not seem a frequent clinical problem in dogs, most likely since they may not live long enough to develop adjacent segment pathology. In humans, the increasing number of fused vertebrae is associated with an increased risk of developing ASP. Additionally, dorsal laminectomy adjacent performed to the fused segment, pre-existent IVD degeneration and pre-existent facet degeneration in the adjacent segment are also risk factors associated with the development of clinical ASP [46, 48].

Only two of the ten bacterial cultures showed a positive result, even though in eight dogs, there was radiological evidence for discospondylitis. It remains also unclear whether in these eight dogs discospondylitis was the primary etiology or whether it was superimposed on pre-existent DLSS since the end stage of severe lumbosacral discospondylitis is usually DLSS. Making the definitive diagnosis of discospondylitis is also challenging, for the detection of bacteria in the IVD can be rather difficult. Extensive degenerative changes in the IVD could also resemble discospondylitis. Urine and blood cultures only give positive results in 29 to 78% of the cases [49, 50] and due to antibiotic treatment prior to culture, bacterial cultures often remain negative [50, 51]. This could also be the case in our study, as five dogs were treated for discospondylitis conservatively with antibiotics prior to the collection of disc material for bacterial culture. Interestingly, the topic of bacteria in IVDs causing low back pain has received considerable attention in recent years in the field of spine research in humans and has since been the subject of heated debate [52-54]. This debate was initiated by reports by Albert *et al* (2008) [55] on findings of bacteria in IVD material harvested during spinal surgery [56] and publication of a randomized clinical trial showing successful treatment of humans with chronic low back pain using long term oral antibiotics [57]. In the light of these findings in humans, the positive bacterial cultures in our canine patients with low back pain which has been reported by our group previously [6] are not surprising. It may even be questioned whether the environment of the degenerated IVD in dogs with DLSS is more prone to settling of bacteria originating from low grade urogenital infections or that bacteria indeed play a much more important role as the initiating factor in the process of IVD degeneration in dogs.

Distraction of the IVD space results in widening of the foramina and thereby results in indirect decompression of the exiting L7 spinal nerves, it will limit motion and permit fusion [18]. Moreover, distraction can normalize disc height and pressure [58]. A combination of spinal fixation through PSRF and distraction without concurrent discectomy could potentially show a beneficial effect on stability and IVD physiology in dogs, as is seen in human patients suffering from end stage knee osteoarthritis. After two months of applied distraction of the

knee joint, clinical improvement and the formation of cartilage-like tissue in the distracted knee were evident for at least two years [59]. In the current study, PSRF in combination with discectomy and distraction was performed in four dogs. Postoperative radiography showed successful distraction in all four cases. In three dogs the LS joint remained distracted for at least six months postoperatively. The fourth dog became very painful three days after surgery and radiography showed collapse of the L7-S1 IVD space. The dog was treated with pain medication and clinical signs resolved. This case demonstrates that distraction alone with PSRF in dogs with severe DLSS exerts strain on the interface between bone and pedicle screws and this may be solved by the use of an vertebral interbody cage. In dogs with caudal cervical spondylomyelopathy, a combination of vertebral stabilization and intervertebral implants tend to be more effective in gaining bony fusion and can also maintain distraction [44]. In spinal surgery in human patients with low back pain, intervertebral cages are also frequently used (with or without vertebral stabilization) [60-62]. Aggressive abrasion of the end plates together with a spinal cage may also promote spinal fusion. The use of a cage as a stand-alone-device or in combination with PSRF (and the effect on spinal fusion) needs to be investigated in future studies.

PSRF can be an effective therapy option for dogs with severe DLSS disease with or without radiological evidence of discospondylitis, in which no other treatment is available. PSRF alone does not result in interbody vertebral bone fusion between L7 and S1.

Acknowledgements

We would like to thank Arie Doornenbal and Elise Petersen for their technical assistance.

References

1. Bergknut N, Egenvall A, Hagman R, Gustas P, Hazewinkel HA, Meij BP*, et al*. Incidence of intervertebral disk degeneration-related diseases and associated mortality rates in dogs. J.Am.Vet.Med.Assoc. 2012;240:1300-9.
2. Meij BP and Bergknut N. Degenerative lumbosacral stenosis in dogs. Vet.Clin.North Am.Small Anim.Pract. 2010;40:983-1009.
3. Webb AA. Potential sources of neck and back pain in clinical conditions of dogs and cats: a review. Vet.J. 2003;165:193-213.
4. Bagley RS. Spinal neoplasms in small animals. Vet.Clin.North Am.Small Anim.Pract. 2010;40:915-27.
5. LeCouteur R and Grandy J. Diseases of the spinal cord. In: Textbook of veterinary internal medicine. Feldman SJ, Ed. Saunders WB, Philadelphia, 2005, pp: 859-60.
6. Suwankong N, Meij BP, Voorhout G, de Boer AH, Hazewinkel HA. Review and retrospective analysis of degenerative lumbosacral stenosis in 156 dogs treated by dorsal laminectomy. Vet.Comp.Orthop.Traumatol. 2008;21:285-93.
7. Suwankong N, Voorhout G, Hazewinkel HA, Meij BP. Agreement between computed tomography, magnetic resonance imaging, and surgical findings in dogs with degenerative lumbosacral stenosis. J.Am.Vet.Med.Assoc. 2006;229:1924-9.
8. Janssens L, Beosier Y, Daems R. Lumbosacral degenerative stenosis in the dog. The results of epidural infiltration with methylprednisolone acetate: a retrospective study. Vet.Comp.Orthop.Traumatol. 2009;22:486-91.
9. De Risio L, Sharp NJ, Olby NJ, Munana KR, Thomas WB. Predictors of outcome after dorsal decompressive laminectomy for degenerative lumbosacral stenosis in dogs: 69 cases (1987-1997). J.Am.Vet.Med.Assoc. 2001;219:624-8.
10. Danielsson F and Sjostrom L. Surgical treatment of degenerative lumbosacral stenosis in dogs. Vet.Surg. 1999;28:91-8.
11. Chrobok J, Vrba I, Stetkarova I. Selection of surgical procedures for treatment of failed back surgery syndrome (FBSS). Chir.Narzadow Ruchu Ortop.Pol. 2005;70:147-53.
12. Omidi-Kashani F, Hasankhani EG, Ashjazadeh A. Lumbar spinal stenosis: who should be fused? An updated review. Asian Spine J. 2014;8:521-30.
13. van Klaveren NJ, Suwankong N, De Boer S, van den Brom WE, Voorhout G, Hazewinkel HA*, et al*. Force plate analysis before and after dorsal decompression for treatment of degenerative lumbosacral stenosis in dogs. Vet.Surg. 2005;34:450-6.
14. Smolders LA, Voorhout G, van de Ven R, Bergknut N, Grinwis GC, Hazewinkel HA*, et al*. Pedicle screw-rod fixation of the canine lumbosacral junction. Vet.Surg. 2012;41:720-32.
15. Meij BP, Suwankong N, Van der Veen AJ, Hazewinkel HA. Biomechanical flexion-extension forces in normal canine lumbosacral cadaver specimens before and after dorsal laminectomy-discectomy and pedicle screw-rod fixation. Vet.Surg. 2007;36:742-51.
16. Watine S, Cabassu JP, Catheland S, Brochier L, Ivanoff S. Computed tomography study of implantation corridors in canine vertebrae. J.Small Anim.Pract. 2006;47:651-7.
17. Carson WL, Duffield RC, Arendt M, Ridgely BJ, Gaines RW,Jr. Internal forces and moments in transpedicular spine instrumentation. The effect of pedicle screw angle and transfixation--the 4R-4bar linkage concept. Spine (Phila Pa.1976) 1990;15:893-901.
18. Williams AL, Gornet MF, Burkus JK. CT evaluation of lumbar interbody fusion: current concepts. AJNR Am.J.Neuroradiol. 2005;26:2057-66.
19. Hoogendoorn RJ, Wuisman PI, Smit TH, Everts VE, Helder MN. Experimental intervertebral disc degeneration induced by chondroitinase ABC in the goat. Spine (Phila Pa.1976) 2007;32:1816-25.
20. Suwankong N, Meij BP, Van Klaveren NJ, Van Wees AM, Meijer E, Van den Brom WE*, et al*. Assessment of decompressive surgery in dogs with degenerative lumbosacral stenosis using force plate analysis and questionnaires. Vet.Surg. 2007;36:423-31.
21. Wiesner L, Kothe R, Schulitz KP, Ruther W. Clinical evaluation and computed tomography scan analysis of screw tracts after percutaneous insertion of pedicle screws in the lumbar spine. Spine (Phila Pa.1976) 2000;25:615-21.
22. Schizas C, Michel J, Kosmopoulos V, Theumann N. Computer tomography assessment of pedicle screw insertion in percutaneous posterior transpedicular stabilization. Eur.Spine J. 2007;16:613-7.
23. Amato V, Giannachi L, Irace C, Corona C. Accuracy of pedicle screw placement in the lumbosacral spine using conventional technique: computed tomography postoperative assessment in 102 consecutive patients. J.Neurosurg.Spine 2010;12:306-13.

24. Field A. Exploratory factor analysis. In: Discovering Statistics using SPSS. Anonymous 2005, pp: 619-680.
25. Hazewinkel HA, van den Brom WE, Theijse LF, Pollmeier M, Hanson PD. Reduced dosage of ketoprofen for the short-term and long-term treatment of joint pain in dogs. Vet.Rec. 2003;152:11-4.
26. Simmonds MJ, Lee CE, Etnyre BR, Morris GS. The influence of pain distribution on walking velocity and horizontal ground reaction forces in patients with low back pain. Pain Res.Treat. 2012;2012:214980.
27. McLaughlin RM. Kinetic and kinematic gait analysis in dogs. Vet.Clin.North Am.Small Anim.Pract. 2001;31:193-201.
28. Spruit M, van Jonbergen JP, de Kleuver M. A concise follow-up of a previous report: posterior reduction and anterior lumbar interbody fusion in symptomatic low-grade adult isthmic spondylolisthesis. Eur.Spine J. 2005;14:828-32.
29. Sears W. Posterior lumbar interbody fusion for degenerative spondylolisthesis: restoration of sagittal balance using insert-and-rotate interbody spacers. Spine J. 2005;5:170-9.
30. Dai LY, Chen WH, Jiang LS. Anterior instrumentation for the treatment of pyogenic vertebral osteomyelitis of thoracic and lumbar spine. Eur.Spine J. 2008;17:1027-34.
31. Onesti ST. Failed back syndrome. Neurologist 2004;10:259-64.
32. Masferrer R, Gomez CH, Karahalios DG, Sonntag VK. Efficacy of pedicle screw fixation in the treatment of spinal instability and failed back surgery: a 5-year review. J.Neurosurg. 1998;89:371-7.
33. McKee WM, Mitten R, Labuc R. Surgical treatment of lumbosacral discospondylitis by a distraction-fusion technique. 1990;31:15,-20.
34. Slocum B and Devine T. L7-S1 fixation-fusion for treatment of cauda equina compression in the dog. J.Am.Vet.Med.Assoc. 1986;188:31-5.
35. Auger J, Dupuis J, Quesnel A, Beauregard G. Surgical treatment of lumbosacral instability caused by discospondylitis in four dogs. Vet.Surg. 2000;29:70-80.
36. Golini L, Kircher PR, Lewis FI, Steffen F. Transarticular fixation with cortical screws combined with dorsal laminectomy and partial discectomy as surgical treatment of degenerative lumbosacral stenosis in 17 dogs: clinical and computed tomography follow-up. Vet.Surg. 2014;43:405-13.
37. Kovach K, Fitzpatrick N, Farrell M. Pedicle screw-rod construct with multi-directional clamps for stabilisation of vertebral instability in discospondylitis
. BSAVA Congress 2012: Scientific proceedings: Veterinary programme 2012;576-7.
38. Fitzpatrick N and Danielski A. Lumbosacral distraction-fusion using a novel intervertebral distraction spacer and dorsally applied screw-rod fixation system for treatment of degenerative lumbosacral stenosis in 12 dogs. 21st Annual scientific meeting. Proceedings - small animals. 2012;243.
39. Hart R, Komzak M, Okal F, Nahlik D, Jajtner P, Puskeiler M. Allograft alone versus allograft with bone marrow concentrate for the healing of the instrumented posterolateral lumbar fusion. Spine J. 2014;14:1318,-1324.
40. Zhang Y, Lenart BA, Lee JK, Chen D, Shi P, Ren J*, et al*. Histological features of endplates of the mammalian spine: from mice to men. Spine (Phila Pa.1976) 2014;39:E312-7.
41. Bergknut N, Rutges JP, Kranenburg HJ, Smolders LA, Hagman R, Smidt HJ*, et al*. The dog as an animal model for intervertebral disc degeneration? Spine (Phila Pa.1976) 2012;37:351-8.
42. Ortega M, Goncalves R, Haley A, Wessmann A, Penderis J. Spondylosis deformans and diffuse idiopathic skeletal hyperostosis (dish) resulting in adjacent segment disease. Vet.Radiol.Ultrasound 2012;53:128-34.
43. Wang JC, Arnold PM, Hermsmeyer JT, Norvell DC. Do lumbar motion preserving devices reduce the risk of adjacent segment pathology compared with fusion surgery? A systematic review. Spine (Phila Pa.1976) 2012;37:S133-43.
44. Steffen F, Voss K, Morgan JP. Distraction-fusion for caudal cervical spondylomyelopathy using an intervertebral cage and locking plates in 14 dogs. Vet.Surg. 2011;40:743-52.
45. Trotter EJ. Cervical spine locking plate fixation for treatment of cervical spondylotic myelopathy in large breed dogs. Vet.Surg. 2009;38:705-18.
46. Lawrence BD, Wang J, Arnold PM, Hermsmeyer J, Norvell DC, Brodke DS. Predicting the risk of adjacent segment pathology after lumbar fusion: a systematic review. Spine (Phila Pa.1976) 2012;37:S123-32.
47. Riew KD, Norvell DC, Chapman JR, Skelly AC, Dettori JR. Introduction/Summary statement: adjacent segment pathology. Spine (Phila Pa.1976) 2012;37:S1-7.
48. Chow DH, Luk KD, Evans JH, Leong JC. Effects of short anterior lumbar interbody fusion on biomechanics of neighboring unfused segments. Spine (Phila Pa.1976) 1996;21:549-55.
49. Burkert BA, Kerwin SC, Hosgood GL, Pechman RD, Fontenelle JP. Signalment and clinical features of diskospondylitis in dogs: 513 cases (1980-2001). J.Am.Vet.Med.Assoc. 2005;227:268-75.

50. Fischer A, Mahaffey MB, Oliver JE. Fluoroscopically guided percutaneous disk aspiration in 10 dogs with diskospondylitis. J.Vet.Intern.Med. 1997;11:284-7.
51. Lucio E, Adesokan A, Hadjipavlou AG, Crow WN, Adegboyega PA. Pyogenic spondylodiskitis: a radiologic/pathologic and culture correlation study. Arch.Pathol.Lab.Med. 2000;124:712-6.
52. Ahmad Z, Rai A, Donell S, Crawford R. Letter to the editor concerning: "Antibiotic treatment in patients with chronic low back pain and vertebral bone edema (Modic type 1 changes): a double-blind randomized controlled trial of efficacy" by Albert HB et al. Eur Spine J (2013) 22:697-707. Eur.Spine J. 2013;22:2344-5.
53. Sotto A and Dupeyron A. Letter to the editor concerning: "Antibiotic treatment in patients with chronic low back pain and vertebral bone edema (Modic type 1 changes): a double-blind randomized controlled trial of efficacy" by Albert HB et al. Eur Spine J (2013) 22:697-707. Eur.Spine J. 2013;22:1704-5.
54. Birkenmaier C. Should we start treating chronic low back pain with antibiotics rather than with pain medications? Korean J.Pain 2013;26:327-35.
55. Albert HB, Kjaer P, Jensen TS, Sorensen JS, Bendix T, Manniche C. Modic changes, possible causes and relation to low back pain. Med.Hypotheses 2008;70:361-8.
56. Albert HB, Lambert P, Rollason J, Sorensen JS, Worthington T, Pedersen MB*, et al*. Does nuclear tissue infected with bacteria following disc herniations lead to Modic changes in the adjacent vertebrae? Eur.Spine J. 2013;22:690-6.
57. Albert HB, Sorensen JS, Christensen BS, Manniche C. Antibiotic treatment in patients with chronic low back pain and vertebral bone edema (Modic type 1 changes): a double-blind randomized clinical controlled trial of efficacy. Eur.Spine J. 2013;22:697-707.
58. Kroeber M, Unglaub F, Guehring T, Nerlich A, Hadi T, Lotz J*, et al*. Effects of controlled dynamic disc distraction on degenerated intervertebral discs: an in vivo study on the rabbit lumbar spine model. Spine (Phila Pa.1976) 2005;30:181-7.
59. Wiegant K, van Roermund PM, Intema F, Cotofana S, Eckstein F, Mastbergen SC*, et al*. Sustained clinical and structural benefit after joint distraction in the treatment of severe knee osteoarthritis. Osteoarthritis Cartilage 2013;21:1660-7.
60. Ito Z, Imagama S, Kanemura T, Satake K, Ando K, Kobayashi K*, et al*. Volumetric change in interbody bone graft after posterior lumbar interbody fusion (PLIF): a prospective study. Eur.Spine J. 2014;23:2144-9.
61. Liebensteiner MC, Jesacher G, Thaler M, Gstoettner M, Liebensteiner MV, Bach CM. Restoration and preservation of disc height and segmental lordosis with circumferential lumbar fusion: a retrospective analysis of cage versus bone graft. J.Spinal.Disord.Tech. 2011;24:44-9.
62. Nemoto O, Asazuma T, Yato Y, Imabayashi H, Yasuoka H, Fujikawa A. Comparison of fusion rates following transforaminal lumbar interbody fusion using polyetheretherketone cages or titanium cages with transpedicular instrumentation. Eur.Spine J. 2014;23:2150-5.

Chapter 11
General discussion

Background

Osteoarthritis (OA) and low back pain (LBP) due to intervertebral disc (IVD) degeneration are the most common musculoskeletal conditions and pose a large socioeconomic burden on society. With ageing of the population, sedentary and unhealthy lifestyles, the incidences are expected to rise further [1, 2]. Also in companion animals such as dogs, cats and horses, degenerative joint diseases are a major health problem, and there are striking similarities in etiologies and disease presentations among species [3-5]. Regardless of the species, current treatments are mostly aimed at reducing symptoms. They broadly consist of conservative management with oral analgesics and lifestyle/ exercise modifications, or surgical intervention whereby diseased tissue is removed or replaced. Research within the field of regenerative medicine focuses on the development of innovative therapies that do not only provide pain relief and improvement in function, but also restore the properties of the affected tissues. Therefore, it would be favourable to start diagnostic and therapeutic intervention at an early stage, to prevent disease progression. As current therapies do not alter the course of degenerative joint disease, salvage strategies need to be optimised as well.

In light of the 'One Medicine' principle, in which human and veterinary medicine can benefit from each other, outcomes of research in this field can ideally be applied to both man and companion animals. Considering that the progressive nature of these diseases requires long-term treatment, the development of drugs suitable for prolonged treatment with minimal side effects is desirable. In this respect, biomaterial carriers could function as a local delivery vehicle, and drug release can thereby be tapered. Previous research has appointed low-grade inflammation as one of the driving factors in both OA as IVDD [6-9]. Therefore, in this thesis the application of locally administered anti-inflammatory drugs, embedded in biomaterials that provide gradual drug release, were investigated, aimed at improvement of clinical signs and regeneration of diseased joint and IVD tissues. For terminal stages of degenerative joint diseases, an extensive pallet of salvage procedures has been developed for human patients, but have not yet been extensively applied in canine patients. Within this context, in this thesis long-term follow-up of canine patients suffering from severe and chronic LBP were treated with salvage procedures inspired from the human fields. Results and future/ clinical perspectives of these two treatment strategies, i.e. regeneration and salvage, for early and terminal stages of degenerative joint diseases are discussed below.

Differences between dog breeds with regard to joint homeostasis

The dog is frequently used as a large animal model to study the numerous aspects of degenerative joint diseases, from molecular facets of disease origination to the evaluation of novel treatments [10-13]. However, within the canine species there is a large variety in body conformation. The short-legged, chondrodysplastic statures of Dachshunds, Basset hounds and Welsh Corgis, among others, is caused by a retrogene insertion of the FGF4 gene on

CFA18, causing overactivation of FGFR3 receptor signalling [14], which leads to disorganization and premature closure of the growth plates of long bones. These chondrodystrophic (CD) dogs have different clinical presentations of IVD disease [15]. In the NP of CD dogs, the notochordal cells disappear at an early age, which is accompanied by early degenerative changes [16]. In these dogs acute disc disease can occur at several levels (mainly located in the cranial cervical or thoracolumbar region) at a relatively young age. Recently, a second FGF4 retrogene insertion on CFA12 was associated with skeletal dysplasia and IVD disease across dog breeds [17]. In non-chondrodystrophic (NCD) dogs, the notochordal cells remain the dominant cell type throughout the majority of life, maintaining disc health. In these dogs, disc disease mainly occurs in a single level as a result of anatomical abnormalities or physical overload. They often present with chronic progressive clinical signs, mainly located at the lower back or caudocervical spine.

Differences in several signalling pathways between CD and NCD IVDs including the canonical Wnt pathway have been associated with advancing IVD degeneration [18]. These observations sprouted the hypothesis that articular cartilage might also differ between CD and NCD dogs. It is widely accepted that OA mostly occurs in large- and giant breed dogs [4]. To our knowledge, not much is known regarding differences in OA susceptibility between CD and NCD dogs. Therefore, in **chapter 2**, we aimed to identify possible differences in joint homeostasis and OA susceptibility with a focus on the canonical Wnt pathway, since it was previously found that Wnt and FGF signalling cooperate in the suppression of chondrocyte differentiation [19]. With the aid of *ex vivo* explant cultures and the retrospective evaluation of histological and biochemical samples from experimentally induced OA joints, we discovered that CD cartilage is better capable of retaining GAGs than NCD derived cartilage. Moreover, and surprisingly, in healthy NCD-derived cartilage and synovial tissues, there was a higher degeneration and inflammation grade compared to healthy CD tissues, although the average age of CD donors was twice as high. With the induction of experimental OA, these differences in cartilage damage and synovial inflammation were aggravated. No clear differences in Wnt signalling could be detected between healthy cartilage tissue and primary chondrocytes derived from healthy cartilage. These findings indicate that CD dogs might be protected against OA development, but Wnt signalling may not be the main driver herein. Interestingly, anecdotal clinical evidence for this was provided in a study where it was found that the Welsh Corgi, a typical CD dog breed, despite having features of hip dysplasia, had a low frequency of conventional OA [20]. Moreover, humans affected by chondrodysplasia due to aberrant FGFR3 signalling, also exhibit a low incidence of OA, despite having bone and joint abnormalities [21]. Hence, although the exact molecular mechanisms remain to be discovered, there is a difference in joint homeostasis caused by chondrodystrophy in dogs. To have a better understanding of the underlying OA-protective mechanisms of chondrodystrophy, further assessment of molecular pathways in CD and NCD-derived tissues from osteoarthritic joints is indicated. The Wnt signalling is known to be altered with OA [22-24] and the current findings do not yet exclude Wnt signalling as one of the players in the observed differential OA susceptibility. In addition to interacting with the FGF pathway, Wnt

is also associated with other pathways in chondrocytes, such as BMP/TGF-β and PTHrP signalling [25-27].

Related to this, the assay that was used to determine canonical Wnt activation highlighted differences between primary chondrocytes from female and male donors. It has previously been shown that both the Wnt signalling pathway and sex hormones play an important role in the development of bone and joint tissue [27]. During the development of OA sex hormones might also play a part [28-30], as females are more frequently affected by OA than men [31, 32]. As early as 1952 it was recognised that post-menopausal women have a higher risk of developing OA, suggesting hormonal influence on the progression of the disease. Later research confirmed this, as in a young female population hand OA was more common in those after menopause, even after correction for age [33]. Osteoporosis is another common musculoskeletal disorder in elderly women, caused by declining oestrogen levels after menopause. There seems to be an inverse relationship between the occurrence of OA and osteoporosis and studies have confirmed roles for Wnt-associated molecules in both OA and osteoporosis [34, 35]. Knock-out of the Wnt antagonist Frizzled related protein (FRZB) was associated with increased OA severity after experimental OA induction, and also with an increased bone mass, suggesting increased susceptibility to OA with higher Wnt levels [36]. Most of these findings were described in humans or mice. In dogs, similar effects on bone parameters were found after ovariectomy in bitches, although this seldom leads to clinical problems in canines [37-39]. Of interest is that both females and bitches have cranial cruciate ligament injury and OA more frequently than men and male dogs [40, 41]. Moreover, in both species, OA development and progression are aggravated with declining hormonal influence (i.e. menopause in females, ovariectomy in bitches) [40, 42-45] . Overall, there are indications that sex hormones can influence both Wnt signalling and OA development also in the canine species and this remains a fascinating area for future research. In clinical veterinary practice, these differences should also be considered, as should body weight and activity level. The prognosis for OA in CD dogs might be different, and also diagnostic findings should be interpreted with caution, as also the macroscopic joint conformation can be different from NCD dogs [20, 33, 46].

Development of novel treatment strategies for OA

It has become increasingly clear that OA is not just characterized by “wear-and-tear” driven cartilage degeneration, but that surrounding tissues such as the synovial lining and the subchondral bone all play an important role [6, 47, 48]. The recognition of OA as a disease involving the whole joint offers new opportunities to identify novel disease-modifying drugs (DMOADs) that can target specific joint tissues. In line with this, differentiating OA phenotypes has gained increasing attention as different phenotypes might benefit from selected treatments. A ‘personalized medicine’ approach, in which a distinction is made between OA phenotypes might improve patient stratification, increase the success rate of

DMOADs and eventually be cost-effective [49, 50]. A similar approach could be beneficial for veterinary patients, as the response to treatment and the course of OA may differ between genders and CD and NCD dogs as discussed above.

To achieve this objective, researchers can use several animal models that aid researchers in studying specific aspects of OA. In **chapter 3**, **4** and **5** a novel treatment strategy was explored with the use of both a preclinical model of surgically induced OA and canine patients suffering from spontaneous OA. The applicability and disease-modifying actions on tissue level of an intra-articular (IA) injection of a drug delivery platform was described in **chapter 3**, while clinical efficacy in canine OA patients was demonstrated in **chapters 4** and **5**, in which two different anti-inflammatory drugs were loaded into the drug delivery platform.

In **chapter 3** the disease-modifying properties of the COX-2 inhibitor celecoxib were investigated, gradually released from polyesteramide microspheres (PEAMs). In line with previous studies [51], protective effects of the prolonged celecoxib release were not detected on cartilage histology. The absence of protective effects of celecoxib on cartilage may in part be explained by the type of OA model used. In fact, surgical procedures themselves may introduce confounding factors that affect downstream bone remodelling [52]. ACL transection with partial medial meniscectomy (ACLT+pMMx) is a commonly used method of OA induction in the rat which gives rise to uniform and predictable changes within 4-12 weeks [53, 54]. Although within several weeks post-operatively, the knee joint partly regains stability and weight bearing of the operated limb is no longer affected, quick irreversible changes on tissue level occur [10]. It has been argued that the rapid onset of lesions after surgery may make surgical models less responsive to interventions [10]. In line with this, ACLT+pMMx induced a significant decrease in weight bearing of the operated limbs of the rats in chapter 3 of this thesis. However, three weeks after surgery, static weight bearing normalized. Hereby, we were unable to determine the analgesic effects of the PEAMs loaded with celecoxib. Little *et al* (2012) proposed that the molecular mechanisms of both structural damage and pain may be distinct in different animal models and therefore, depending on the research question, different or multiple animal models should be used [54]. In the study of Ferland *et al* (2011), the ACLT+pMMx model did not induce significant changes in gait parameters and pain-related behaviour, measured by the CatWalk and von Frey tests [55]. On the contrary, the more severe monoiodoacetate (MIA) model did result in clear changes, and orally administered celecoxib did have an effect on gait parameters in the beginning of the study and an alleviating effect on mechanical allodynia throughout the study. Altogether, this could indicate that the ACLT model in our study did not cause substantive chronic changes in hind paw weight distribution, that could be counteracted by IA celecoxib.

Another reason for the lack of differences with the static weight bearing method could be that the method was not sensitive enough to capture subtle differences in weight bearing, even though it has been reported to produce reproducible results [56]. Static weight bearing

on each limb is measured when the rats are standing on their hind legs in the experimental setup. Weight bearing in a more natural position (i.e. on four legs) could lead to less variation and more sensitive measurements. A dynamic weight bearing system could provide more accurate weight bearing assessment. In a mice arthritis model, dynamic weight bearing could detect an increase in weight bearing when the mice were treated with oral celecoxib, as compared to untreated controls [57]. Additionally, movement and exercise cannot be restricted in rats. Celecoxib-loaded PEAMs may have provided adequate analgesia, which resulted in restored use of the OA joint. Lastly, rodents are prey animals. Because of that, they have the tendency to disguise any gait deficiencies, as that could attract the attention of predators in the wild [56], which could explain the lack of differences.

To truly assess analgesic effects of prolonged celecoxib release in a clinically relevant animal model, we moved forward to client-owned dogs with naturally occurring OA, as a model for their own species and human OA patients. **Chapter 4** and **5** provided clinical evidence that locally applied prolonged celecoxib or triamcinolone acetonide release improved pain-related behaviour and quality of life in dogs with clinically relevant OA. Clinical trials in (veterinary) patients are challenged by the fact that patient variability is relatively large and environmental factors are more difficult to control than in experimental animals. At the same time, this is also an advantage, as humans and pets are exposed to similar environments, which can aid in translation to the general population. *Post hoc* analyses can be performed to investigate whether certain subpopulations respond different to the investigated treatment. In the described studies, however, this was not possible due to the small patient numbers used typical for a phase I/II clinical study. From our own observations, it seemed that patients with severe OA accompanied by extremely large osteophytes responded less obvious to the treatment. In these subjects, the range of motion was restricted by the peri-articular new bone formed in the natural course of OA. Unfortunately, the force plate analysis and the owner can often not distinguish mechanical lameness from pain in these patients. For example, some owners did report their dog to behave more ‘cheerful’ and active after IA injection of PEAMs loaded with one of the two anti-inflammatory drugs, suggestive for a decrease in pain, but did not observe much difference in lameness after any treatment (IA PEAM injection or oral analgesics). Moreover, in some dogs, lameness shifted to the contralateral leg on account of bilateral OA and owners found it hard to appreciate the difference. These examples illustrate the importance of owner questionnaires and ‘subjective’ assessment by the attending veterinarian. Furthermore, it would be helpful to educate owners in assessing the mobility of their pet. A clinical design including (veterinary) patients limits the possibilities of several outcome measurements, such as (frequent) sampling of tissues or bodily fluids, or the possibility of acquiring tissue samples by more invasive techniques. In line with this, sufficient synovial fluid was not acquired in all dogs at all time-points, thereby limiting the power of the subsequent synovial fluid analyses.

Upregulation of pro-inflammatory mediators in canine IVDD

The involvement of low-grade inflammation in OA is well described in literature and scientific attention for inflammatory mediators in the process of IVD degeneration is increasing. As most reports focus on human subjects, we investigated the inflammatory status of healthy and diseased canine IVDs. These results could serve as a basis for the dog as a translational model for anti-inflammatory therapies for both canine and human IVD disease.

In **Chapter 6**, cytokine and chemokine profiles of the degenerating IVD were described. It appeared that PGE_2 and CCL2 were upregulated in the NPs of degenerated and herniated IVDs, compared to non-degenerated or non-herniated IVDs. Moreover, COX-2 expression in both the NP and annulus fibrosus (AF) increased with advancing degeneration. Enhanced COX-2 expression was also found in surgically obtained NP tissues from dogs with symptomatic IVD disease, as was demonstrated in **chapter 7**. These findings indicate that in canine IVD disease, similar to the situation in man, there is a low-grade inflammation, which drives degenerative changes inside the NP and IVD. They also justify anti-inflammatory drugs as a treatment for clinical IVD disease, for they are capable of inhibiting inflammatory pain. This was already demonstrated in clinical trials in man, wherein subjects with LBP show (short-term) pain relief from intradiscal injections with IL-6 or TNF-α antagonists [58, 59]. Clinical results of targeting specific cytokines have been mixed, which might in part be explained by the complexity of the cytokine signalling pathways involved in IVDD. Targeting COX-2 might have the benefit of directly decreasing downstream PGE_2 levels, thereby directly influencing nociceptive pathways and LBP and indirectly influencing other inflammatory signalling pathways [60]. If properly balanced and properly timed, the inflammatory response may also contribute to tissue repair [7]. This balance between inflammation and regeneration has been illustrated in mice lacking IL-1β and TNF-α that show decreased M1 macrophage recruitment and impaired axonal regeneration after sciatic nerve injury [61]. Moreover, biomaterials based on the pro-inflammatory fibrinogen showed enhanced MSC recruitment and stimulation of growth factor production, while downregulating inflammatory cytokines for bone regeneration *in vitro* [62, 63]. These findings suggest that regeneration goes parallel with (a low level of) inflammation. Notwithstanding, pro-inflammatory mediators play a pivotal part in the development of post-traumatic OA, that develops after acute injury to the joint. For post-traumatic OA, anti-inflammatory therapy seems to attenuate progression of DJD [64, 65]. Similar conclusions can be drawn from *ex vivo* models of post-traumatic IVDD [66, 67]. Timing, duration and type of disease could also make a difference, as the role of pro-inflammatory mediators are helpful to repair acute tissue damage after injury, but feed the vicious cycle in a chronic degenerative state.

Development of novel treatment strategies for low back pain

Since IVDD is driven by catabolic and anti-anabolic actions of pro-inflammatory mediators, a sensible regenerative approach would be the local delivery of anabolic or anti-inflammatory factors [68]. However, systemically administered drugs often fail to reach sufficient drug concentrations in the poorly vascularised NP, and effects are often short-lived [69, 70]. Even locally delivered drugs, growth factors or MSCs are only short-acting, thereby limiting their regenerative effects [68]. Drug delivery platforms based on biodegradable polymers can facilitate safe and prolonged local delivery of bioactive substances into the degenerated IVD [71-73]. Our group has previously demonstrated *in vivo* biocompatibility of a pNIPAAM-based hydrogel, a PCLA-PEG-PCLA hydrogel and a polyesteramide microsphere platform as part of the BioMedical Materials (BMM) program IDiDAS (Fig. 1) [74-76].

Historically, several strategies have been explored using biomaterials to regain a functional spinal unit. Earlier research focused on metallic or non-metallic devices that mimicked biomechanical properties of the disc [77, 78]. However, the use of these prosthetic discs requires surgery and has been associated with implant migration and the lack of sustained stresses [72]. More recent studies have focused on polymer-based biomaterials, to either substitute the NP in late stages of degeneration or to function as a carrier/ scaffold for biomolecules and cells in early disease, without necessarily immediately reconstituting the biomechanical properties of the treated disc [71, 79]. In the latter, minimally invasive procedures are preferred, and degradation of polymers should result in non-toxic products.

In this thesis, the intradiscal application of the previously studied biomaterials was explored further. The PCLA-PEG-PCLA hydrogel described in **chapter 7** is liquid at room temperature but becomes viscous at body temperature, thereby facilitating local injection through a long (epidural) small diameter needle. In addition, it reduces the risk of leakage from the disc into the epidural space, considering the fact that in IVDD also the AF, that constrains the NP, is degenerated and loses its biomechanical properties. In this study, small quantities of hydrogel were injected acting as a drug carrier, without increasing intradiscal pressure, facilitating the local and extended delivery of celecoxib.

As the goal was to restore the functional disc tissue in an early to moderately degenerated IVD (in addition to pain relief), care was taken not to inflict iatrogenic damage with local injections. In a clinical setting, reinjections should be kept to a minimum and injections should be performed with small Gauge needles and small injection volumes [80]. Minimally invasive percutaneous intradiscal injections are already being performed on a regular basis in patients with low back pain. For example, ablation with oxygen-ozone (O2-O3) to aid in retropulsion and digestion of disc tissue was described in a large group of patients with lumbar disc herniation [81]. Moreover, methylene blue has been applied intradiscally in LBP patients on account of its neurolytic properties [82]. Although clinical outcomes were favourable for both therapies, they are not aimed to restore disc homeostasis. In contrast, the aim of prolonged local exposure to celecoxib was to exert an anti-inflammatory and

ideally also regenerative effect on tissue level. The intradiscal application of celecoxib-loaded PCLA-PEG-PCLA hydrogel resulted in long-term reduction of LBP in the majority of the treated dogs, although no regenerative effects were perceived on MRI at the relatively short term follow up period of 3 months. We cannot exclude that next to finding the optimal loading dose of the anti-inflammatory drug in order to achieve the optimal balance in the interplay of inflammation and regeneration, considerably longer term follow up may be needed to observe structural regenerative effects at the disc level.

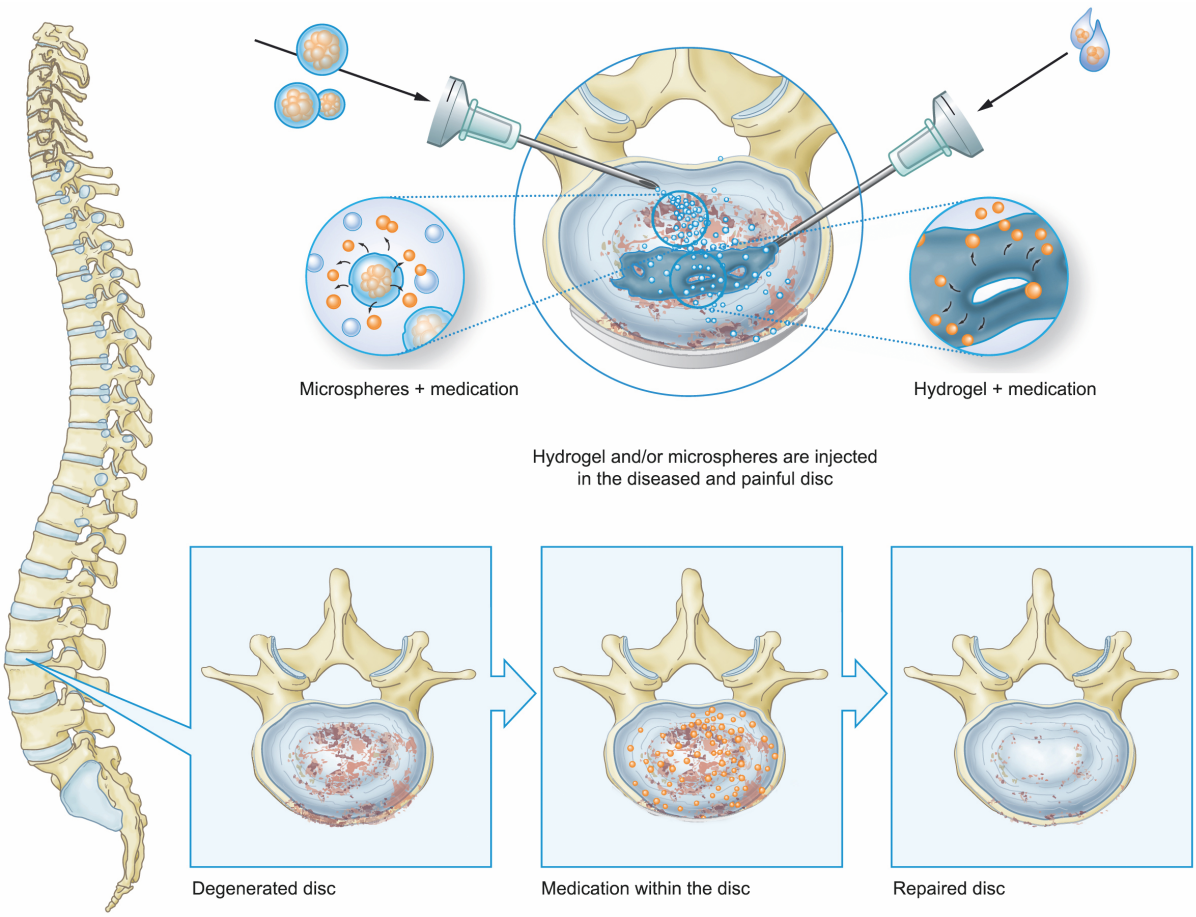

Figure 1. Intradiscal delivery of anti-inflammatory medication incorporated in microspheres (left) or hydrogels (right) that provide sustained release, could enhance repair of the degenerated intervertebral disc. Adapted from ©BMM / Rogier Trompert Medical Art.

In order to further optimise the intradiscal delivery of celecoxib, higher loading dosages were investigated in a preclinical canine IVD model in **chapter 8**. In addition to a reduction of inflammation, a single injection of celecoxib-loaded microspheres resulted in significantly higher signal intensity on qualitative and quantitative MRI, and preservation of disc height, as compared to treatment with unloaded PEAMs. In line with this, less degenerative changes were present on histological and biochemical analysis, indicative of an inhibitory effect of

celecoxib on the degenerative process. A decrease in two pain mediators, PGE_2 and neuronal growth factor (NGF) were found, but no assessments on pain could be performed in this study, due to the fact that multiple levels per dog were injected. Therefore, in **chapter 9** the setup of an ongoing prospective study is described in which the clinical effect of an intradiscal injection with celecoxib-PEAMs in client-owned dogs with degenerative lumbosacral (DLSS) is being assessed taking into consideration also the placebo effect.

Local application of anti-inflammatory drugs is only suitable for therapeutic intervention in early to moderate stage IVD disease. When severe degenerative changes have occurred in the lumbosacral region, surgery is often the only option. Dorsal laminectomy, the preferred procedure in canine patients, includes partial removal of the laminar bone of L7 and S1, followed by the removal of degenerated disc material (nuclectomy). Facetectomy and foraminotomy can achieve further decompression of neural tissue, although it can lead to increased lumbosacral instability [83]. In the short-term, surgical intervention leads to clinical improvement in 78-93% of patients, but in the long term, clinical signs recurred in 17-38% [84, 85]. **Chapter 10** reported on the use of pedicle screw-rod fixation (PSRF) of the lumbosacral junction in 12 dogs with severe DLSS, as an adjunctive treatment to dorsal laminectomy, or in case of revision surgery. Screw placement was considered correct in 93% of the screws. The implants used were the smallest PSRF implant set available for paediatric human procedures, which fitted in medium- to large sized dogs. However, penetration of the ventral cortex was reported for four screws, three of them in the two smallest dogs. In the future, customized veterinary implants or 3D printed implants could optimise implant size for each patient, if necessary. Another strategy to further improve screw placement could consist of 3D-printed virtual drill guides, based on the pre-operatively performed CT scan, as described for the placement of cervical transpedicular screws in dogs. These drill guides could reduce surgical time and optimise screw placement, although the percentage correct screw placement was not higher than in our study [86].

The described salvage procedure of PSRF can be further improved considering the clinical representation and related biomechanics. In 4/12 dogs treated with PSRF, distraction of the LS junction was performed to increase the neuroforaminal apertures of L7-S1, hypothetically leading to more decompression of exiting spinal nerves. Distraction of the lumbosacral IVD space was maintained in 3 out of 4 dogs, while in 1 dog, there was radiographic evidence of IVD space collapse 1 week post-operatively (resulting in aggravated low back pain). To prevent collapse of the disc space, an intervertebral cage can be added to the PSRF construct, or used as a stand-alone device to increase spinal stability and restore disc height, in combination with dorsal laminectomy [87]. A larger decrease in range of motion was seen when PSRF and a cage were combined, as compared to a cage alone. Whether this difference is clinically relevant remains to be explored in canine patients with long-term follow-up. From studies on lumbar spinal fusion in man, it has become clear that although there is a significant increase in radiographic adjacent segment pathology (ASP), the incidence of clinical signs related to ASP is substantially lower and does not correlate well

with radiographic findings [88]. One systematic review found an increase of ASP after lumbar fusion compared to (motion sparing) total disc replacement, with an increased risk attributed to fusion of 5.8% [89]. Another meta-analysis compared lumbar fusion with lumbar pedicular dynamic stabilisation and concluded that both techniques did not differ in terms of functional recovery and motion preservation, although they did find higher complication rates and ASP development in the patients treated with fusion [90]. It should be noted that ASP rates are low and therefore, the overall statistical 'strength' is low to moderate. Moreover, several confounding factors such as fusion length, age, obesity and pre-existing degenerative changes feed the existing controversy regarding the true aetiology of ASP [88, 91]. In canines, evidence of ASP is limited to one report on outcome after transarticular fixation in dogs with DLSS, in which no ASP was radiographically observed after a median follow-up time of 12 months [92]. Whether ASP is also clinically relevant in canines with DLSS needs to be evaluated, as dogs have shorter lifespan than their human counterparts, and they load their (lumbosacral) spine in a different way.

Considerations and future perspectives

Several therapeutic strategies are being investigated in order to regenerate the diseased joint or IVD [71, 79]. Most studies focus on tissue regeneration via gene therapy, stem cells or the application of growth factors, with a subset targeting inflammation in order to reduce clinical signs and halt degeneration [93-96]. A less invasive, more economic and more uniform approach could be the local delivery of well-known anti-inflammatory drugs [97]. Corticosteroids have shown to provide short-term pain relief in patients with OA and LBP, but are also associated with reduced tissue healing and negative effects at tissue level [98-100]. Selective NSAIDs are also effective in inhibiting pain and inflammation, and have favourable safety profiles. However, to date their application remains oral or topical, no formulations for local NSAID injection are available, yet. When combined with suitable biomaterials, dosage and release of small-molecule anti-inflammatory drugs can be tailored to the specific needs of the target tissues, thereby providing long-term pain relief even after a single injection. Re-injections could be provided, if necessary. Therefore, the biomaterials should be biodegradable and result in non-toxic degradation products. Moreover, in inflammatory diseases, drug delivery platforms can be designed to behave autoregulatory, as the levels of proteases that breakdown the biomaterial are correlated with the presence of inflammation [51]. If there is a low level of inflammatory mediators present, release will be more gradual than in tissues with a higher inflammatory profile. In the latter, higher local drug concentrations can be required.

The ultimate goal is tissue regeneration in an early disease state, to postpone or even replace more invasive therapies. In this extent, is it imperative to assess the joint or the IVD as an organ [101], and consider not only cartilage or NP, but also take into account adjacent bone and connective tissues. By targeting synovial inflammation or delay progressive bony

changes, overall disease progression can be decelerated [6, 58, 102-105]. When bringing this closer to the patient, imaging modalities that help form guidelines on staging and phenotyping the patient will help instruct and design appropriate therapeutic treatment strategies. Those may for example entail, dependent on the stage of the disease, at an early stage the sustained release of anti-inflammatory drugs, while at intermediate stages of the disease a combination thereof with cell- and/or growth factor-based strategies.

Studies in this thesis have shown that local delivery of celecoxib has both analgesic, anti-inflammatory at the joint and disc level and even regenerative effects at the disc level. Clinical improvement of OA patients was also perceived after local extended delivery of triamcinolone acetonide. Future research should focus on which treatment is suitable for which patient, and in which stage. Local injections can be used in young individuals to postpone invasive surgery if there is no acute surgical indication but can also be applied in (veterinary) patients with end stage disease that are refractory to surgical treatment or suffer from comorbidities that make surgical intervention undesirable. In case of DLSS, however, some patients might benefit more from surgery, for example if there are indications of neuroforaminal stenosis or severe compression of the cauda equina. Similar considerations should be made regarding spinal fusion, since it is known that certain dogs have recurrence of clinical signs after standard decompressive surgery. The optimisation of more advanced diagnostic modalities (i.e. dynamic MRI) could provide additional information to the surgeon to decide on the surgical approach.

With the advancement of biomedical knowledge and (veterinary) health care, the emphasis will shift to personalized medicine. By performing an extended diagnostic workup and subsequently applying the most optimal treatment for each individual patient, treatment efficacy and eventually costs will improve.

Key points of this thesis

Development of novel treatment strategies for OA

- In healthy cartilage there are differences between dog breed types, presumably caused by chondrodystrophy. NCD-derived cartilage seemed to be more sensitive to pro-inflammatory stimuli than cartilage from CD dogs, possibly predisposing NCD dogs to the development of OA.
- Local sustained release of celecoxib from polyesteramide microspheres (PEAMs) in a preclinical OA rat model demonstrated inhibition of synovial inflammation and subchondral bone changes.
- Sustained celecoxib release from PEAMs in the presence of canine primary chondrocytes was confirmed for 28 days and suppressed PGE_2 during the entire culture period, without negatively influencing cellular homeostasis.
- A randomized controlled trial confirmed clinical efficacy of local application of celecoxib-loaded PEAMs in client-owned dogs with OA: there was improvement in lameness and pain-related behaviour, accompanied by decreased PGE_2 levels in the synovial fluid.
- Sustained intra-articular release of triamcinolone acetonide from PEAMs resulted in less lameness and pain-related behaviour in 12 client-owned dogs suffering from OA.

Development of novel treatment strategies for low back pain

- Levels of pro-inflammatory mediators PGE_2 and CCL2 in degenerated and herniated IVDs were significantly higher compared with non-degenerated and non-herniated canine IVDs. COX-2 expression in the NP and AF, and reactive changes in the AF increased with advancing degeneration stages.
- The safety and feasibility of intradiscal delivery of the COX-2 inhibitor celecoxib loaded on a thermoresponsive hydrogel were demonstrated *in vivo,* in both experimental Beagles with naturally occurring IVDD and in a clinical setting with canine patients suffering from chronic low back pain.
- *In vitro*, celecoxib release from PEAMs was shown for over 28 days resulting in prolonged inhibition of PGE_2 production, and anti-catabolic effects in NP cells from degenerated IVDs on gene expression level.
- Celecoxib incorporated in PEAMs was safely administered intradiscally in experimental dogs, exerted anti-inflammatory and anti-degenerative effects, and reduced expression of inflammatory- and pain mediators PGE_2 and NGF.
- PSRF offered a surgical treatment option for large breed dogs with severe in which no other treatment was available.

References

1. Hoy D, March L, Brooks P, Blyth F, Woolf A, Bain C*, et al*. The global burden of low back pain: estimates from the Global Burden of Disease 2010 study. Ann.Rheum.Dis. 2014;73:968-74.
2. Kaplan W, Wirtz V, Mantel-Teeuwisse A, Stolk P, Duthey B, Laing R. Priority diseases and reasons for inclusion. 2013;165-168.
3. Bergknut N, Egenvall A, Hagman R, Gustas P, Hazewinkel HA, Meij BP*, et al*. Incidence of intervertebral disk degeneration-related diseases and associated mortality rates in dogs. J.Am.Vet.Med.Assoc. 2012;240:1300-9.
4. Johnston SA. Osteoarthritis. Joint anatomy, physiology, and pathobiology. Vet.Clin.North Am.Small Anim.Pract. 1997;27:699-723.
5. van Weeren PR and Back W. Musculoskeletal Disease in Aged Horses and Its Management. Vet.Clin.North Am.Equine Pract. 2016;32:229-47.
6. Hugle T and Geurts J. What drives osteoarthritis?-synovial versus subchondral bone pathology. Rheumatology (Oxford) 2017;56:1461-71.
7. Molinos M, Almeida CR, Caldeira J, Cunha C, Goncalves RM, Barbosa MA. Inflammation in intervertebral disc degeneration and regeneration. J.R.Soc.Interface 2015;12:20150429.
8. Phillips KL, Cullen K, Chiverton N, Michael AL, Cole AA, Breakwell LM*, et al*. Potential roles of cytokines and chemokines in human intervertebral disc degeneration: interleukin-1 is a master regulator of catabolic processes. Osteoarthritis Cartilage 2015;23:1165-77.
9. Rahmati M, Mobasheri A, Mozafari M. Inflammatory mediators in osteoarthritis: A critical review of the state-of-the-art, current prospects, and future challenges. Bone 2016;85:81-90.
10. Bendele AM. Animal models of osteoarthritis. J.Musculoskelet.Neuronal Interact. 2001;1:363-76.
11. McCoy AM. Animal models of osteoarthritis: comparisons and key considerations. Vet.Pathol. 2015;52:803-18.
12. Gregory MH, Capito N, Kuroki K, Stoker AM, Cook JL, Sherman SL. A review of translational animal models for knee osteoarthritis. Arthritis 2012;2012:764621.
13. Lampropoulou-Adamidou K, Lelovas P, Karadimas EV, Liakou C, Triantafillopoulos IK, Dontas I*, et al*. Useful animal models for the research of osteoarthritis. Eur.J.Orthop.Surg.Traumatol. 2014;24:263-71.
14. Parker HG, VonHoldt BM, Quignon P, Margulies EH, Shao S, Mosher DS*, et al*. An expressed fgf4 retrogene is associated with breed-defining chondrodysplasia in domestic dogs. Science 2009;325:995-8.
15. Smolders LA, Bergknut N, Grinwis GC, Hagman R, Lagerstedt AS, Hazewinkel HA*, et al*. Intervertebral disc degeneration in the dog. Part 2: chondrodystrophic and non-chondrodystrophic breeds. Vet.J. 2013;195:292-9.
16. Bach FC, Willems N, Penning LC, Ito K, Meij BP, Tryfonidou MA. Potential regenerative treatment strategies for intervertebral disc degeneration in dogs. BMC Vet.Res. 2014;10:3,6148-10-3.
17. Brown EA, Dickinson PJ, Mansour T, Sturges BK, Aguilar M, Young AE*, et al*. FGF4 retrogene on CFA12 is responsible for chondrodystrophy and intervertebral disc disease in dogs. PNAS 2017;114:11476–11481.
18. Smolders LA, Meij BP, Riemers FM, Licht R, Wubbolts R, Heuvel D*, et al*. Canonical Wnt signaling in the notochordal cell is upregulated in early intervertebral disk degeneration. J.Orthop.Res. 2012;30:950-7.
19. Buchtova M, Oralova V, Aklian A, Masek J, Vesela I, Ouyang Z*, et al*. Fibroblast growth factor and canonical WNT/beta-catenin signaling cooperate in suppression of chondrocyte differentiation in experimental models of FGFR signaling in cartilage. Biochim.Biophys.Acta 2015;1852:839-50.
20. Karbe GT, Biery DN, Gregor TP, Giger U, Smith GK. Radiographic hip joint phenotype of the Pembroke Welsh Corgi. Vet.Surg. 2012;41:34-41.
21. Klag KA and Horton WA. Advances in treatment of achondroplasia and osteoarthritis. Hum.Mol.Genet. 2016;25:R2-8.
22. Garcia-Ibarbia C, Perez-Castrillon JL, Ortiz F, Velasco J, Zarrabeitia MT, Sumillera M*, et al*. Wnt-related genes and large-joint osteoarthritis: association study and replication. Rheumatol.Int. 2013;33:2875-80.
23. June RK, Liu-Bryan R, Long F, Griffin TM. Emerging role of metabolic signaling in synovial joint remodeling and osteoarthritis. J.Orthop.Res. 2016;34:2048-58.
24. Kumarasinghe DD, Perilli E, Tsangari H, Truong L, Kuliwaba JS, Hopwood B*, et al*. Critical molecular regulators, histomorphometric indices and their correlations in the trabecular bone in primary hip osteoarthritis. Osteoarthritis Cartilage 2010;18:1337-44.
25. Levi D, Horn S, Tyszko S, Levin J, Hecht-Leavitt C, Walko E. Intradiscal Platelet-Rich Plasma Injection for Chronic Discogenic Low Back Pain: Preliminary Results from a Prospective Trial. Pain Med. 2016;17:1010-22.
26. Kirchner F and Anitua E. Intradiscal and intra-articular facet infiltrations with plasma rich in growth factors reduce pain in patients with chronic low back pain. J.Craniovertebr Junction Spine 2016;7:250-6.

27. Usami Y, Gunawardena AT, Iwamoto M, Enomoto-Iwamoto M. Wnt signaling in cartilage development and diseases: lessons from animal studies. Lab.Invest. 2016;96:186-96.
28. Linn S, Murtaugh B, Casey E. Role of sex hormones in the development of osteoarthritis. PM R. 2012;4:S169-73.
29. Pan Q, O'Connor MI, Coutts RD, Hyzy SL, Olivares-Navarrete R, Schwartz Z*, et al*. Characterization of osteoarthritic human knees indicates potential sex differences. Biol.Sex.Differ. 2016;7:27.
30. Tanamas SK, Wijethilake P, Wluka AE, Davies-Tuck ML, Urquhart DM, Wang Y*, et al*. Sex hormones and structural changes in osteoarthritis: a systematic review. Maturitas 2011;69:141-56.
31. Srikanth VK, Fryer JL, Zhai G, Winzenberg TM, Hosmer D, Jones G. A meta-analysis of sex differences prevalence, incidence and severity of osteoarthritis. Osteoarthritis Cartilage 2005;13:769-81.
32. Valdes AM, Loughlin J, Oene MV, Chapman K, Surdulescu GL, Doherty M*, et al*. Sex and ethnic differences in the association of ASPN, CALM1, COL2A1, COMP, and FRZB with genetic susceptibility to osteoarthritis of the knee. Arthritis Rheum. 2007;56:137-46.
33. Smith EJ, Marcellin-Little DJ, Harrysson OL, Griffith EH. Influence of chondrodystrophy and brachycephaly on geometry of the humerus in dogs. Vet.Comp.Orthop.Traumatol. 2016;29:220-6.
34. Geusens PP and van den Bergh JP. Osteoporosis and osteoarthritis: shared mechanisms and epidemiology. Curr.Opin.Rheumatol. 2016;28:97-103.
35. Lodewyckx L and Lories RJ. WNT Signaling in osteoarthritis and osteoporosis: what is the biological significance for the clinician? Curr.Rheumatol.Rep. 2009;11:23-30.
36. Lories RJ, Peeters J, Bakker A, Tylzanowski P, Derese I, Schrooten J*, et al*. Articular cartilage and biomechanical properties of the long bones in Frzb-knockout mice. Arthritis Rheum. 2007;56:4095-103.
37. Dannucci GA, Martin RB, Patterson-Buckendahl P. Ovariectomy and trabecular bone remodeling in the dog. Calcif.Tissue Int. 1987;40:194-9.
38. Martin RB, Butcher RL, Sherwood LL, Buckendahl P, Boyd RD, Farris D*, et al*. Effects of ovariectomy in beagle dogs. Bone 1987;8:23-31.
39. Wilson AK, Bhattacharyya MH, Miller S, Mani A, Sacco-Gibson N. Ovariectomy-induced changes in aged beagles: histomorphometry of rib cortical bone. Calcif.Tissue Int. 1998;62:237-43.
40. Adams P, Bolus R, Middleton S, Moores AP, Grierson J. Influence of signalment on developing cranial cruciate rupture in dogs in the UK. J.Small Anim.Pract. 2011;52:347-52.
41. Sutton KM and Bullock JM. Anterior cruciate ligament rupture: differences between males and females. J.Am.Acad.Orthop.Surg. 2013;21:41-50.
42. Hart BL, Hart LA, Thigpen AP, Willits NH. Long-term health effects of neutering dogs: comparison of Labrador Retrievers with Golden Retrievers. PLoS One 2014;9:.
43. Hart BL, Hart LA, Thigpen AP, Willits NH. Neutering of German Shepherd Dogs: associated joint disorders, cancers and urinary incontinence. Vet.Med.Sci. 2016;2:191-9.
44. Martin-Millan M and Castaneda S. Estrogens, osteoarthritis and inflammation. Joint Bone Spine 2013;80:368-73.
45. Watt FE. Hand osteoarthritis, menopause and menopausal hormone therapy. Maturitas 2016;83:13-8.
46. Lerer A, Nykamp SG, Harriss AB, Gibson TW, Koch TG, Brown SH. MRI-based relationships between spine pathology, intervertebral disc degeneration, and muscle fatty infiltration in chondrodystrophic and non-chondrodystrophic dogs. Spine J. 2015;15:2433-9.
47. Zhuo Q, Yang W, Chen J, Wang Y. Metabolic syndrome meets osteoarthritis. Nat.Rev.Rheumatol. 2012;8:729-37.
48. Glyn-Jones S, Palmer AJ, Agricola R, Price AJ, Vincent TL, Weinans H*, et al*. Osteoarthritis. Lancet 2015;386:376-87.
49. Roubille C, Pelletier JP, Martel-Pelletier J. New and emerging treatments for osteoarthritis management: will the dream come true with personalized medicine? Expert Opin.Pharmacother. 2013;14:2059-77.
50. Tonge DP, Pearson MJ, Jones SW. The hallmarks of osteoarthritis and the potential to develop personalised disease-modifying pharmacological therapeutics. Osteoarthritis Cartilage 2014;22:609-21.
51. Janssen M, Timur UT, Woike N, Welting TJ, Draaisma G, Gijbels M*, et al*. Celecoxib-loaded PEA microspheres as an auto regulatory drug-delivery system after intra-articular injection. J.Control.Release 2016;244:30-40.
52. Maerz T, Newton MD, Kurdziel MD, Altman P, Anderson K, Matthew HW*, et al*. Articular cartilage degeneration following anterior cruciate ligament injury: a comparison of surgical transection and noninvasive rupture as preclinical models of post-traumatic osteoarthritis. Osteoarthritis Cartilage 2016;24:1918-27.
53. Gerwin N, Bendele AM, Glasson S, Carlson CS. The OARSI histopathology initiative - recommendations for histological assessments of osteoarthritis in the rat. Osteoarthritis Cartilage 2010;18 Suppl 3:S24-34.

54. Little CB and Zaki S. What constitutes an "animal model of osteoarthritis"--the need for consensus? Osteoarthritis Cartilage 2012;20:261-7.
55. Ferland CE, Laverty S, Beaudry F, Vachon P. Gait analysis and pain response of two rodent models of osteoarthritis. Pharmacol.Biochem.Behav. 2011;97:603-10.
56. Malfait AM, Little CB, McDougall JJ. A commentary on modelling osteoarthritis pain in small animals. Osteoarthritis Cartilage 2013;21:1316-26.
57. Robinson I, Sargent B, Hatcher JP. Use of dynamic weight bearing as a novel end-point for the assessment of Freund's Complete Adjuvant induced hypersensitivity in mice. Neurosci.Lett. 2012;524:107-10.
58. Risbud MV and Shapiro IM. Role of cytokines in intervertebral disc degeneration: pain and disc content. Nat.Rev.Rheumatol. 2014;10:44-56.
59. Sainoh T, Orita S, Miyagi M, Inoue G, Yamauchi K, Suzuki M*, et al*. Single intradiscal injection of the interleukin-6 receptor antibody tocilizumab provides short-term relief of discogenic low back pain; prospective comparative cohort study. J.Orthop.Sci. 2016;21:2-6.
60. Kawabata A. Prostaglandin E2 and pain--an update. Biol.Pharm.Bull. 2011;34:1170-3.
61. Nadeau S, Filali M, Zhang J, Kerr BJ, Rivest S, Soulet D*, et al*. Functional recovery after peripheral nerve injury is dependent on the pro-inflammatory cytokines IL-1beta and TNF: implications for neuropathic pain. J.Neurosci. 2011;31:12533-42.
62. Almeida CR, Vasconcelos DP, Goncalves RM, Barbosa MA. Enhanced mesenchymal stromal cell recruitment via natural killer cells by incorporation of inflammatory signals in biomaterials. J.R.Soc.Interface 2012;9:261-71.
63. Maciel J, Oliveira MI, Colton E, McNally AK, Oliveira C, Anderson JM*, et al*. Adsorbed fibrinogen enhances production of bone- and angiogenic-related factors by monocytes/macrophages. Tissue Eng.Part A. 2014;20:250-63.
64. Olson SA, Horne P, Furman B, Huebner J, Al-Rashid M, Kraus VB*, et al*. The role of cytokines in posttraumatic arthritis. J.Am.Acad.Orthop.Surg. 2014;22:29-37.
65. Punzi L, Galozzi P, Luisetto R, Favero M, Ramonda R, Oliviero F*, et al*. Post-traumatic arthritis: overview on pathogenic mechanisms and role of inflammation. RMD Open 2016;2:.
66. Dudli S, Ferguson SJ, Haschtmann D. Severity and pattern of post-traumatic intervertebral disc degeneration depend on the type of injury. Spine J. 2014;14:1256-64.
67. Dudli S, Boffa DB, Ferguson SJ, Haschtmann D. Leukocytes Enhance Inflammatory and Catabolic Degenerative Changes in the Intervertebral Disc After Endplate Fracture In Vitro Without Infiltrating the Disc. Spine (Phila Pa.1976) 2015;40:1799-806.
68. Fontana G, See E, Pandit A. Current trends in biologics delivery to restore intervertebral disc anabolism. Adv.Drug Deliv.Rev. 2015;84:146-58.
69. Motaghinasab S, Shirazi-Adl A, Parnianpour M, Urban JP. Disc size markedly influences concentration profiles of intravenously administered solutes in the intervertebral disc: a computational study on glucosamine as a model solute. Eur.Spine J. 2014;23:715-23.
70. Zhang L, Wang JC, Feng XM, Cai WH, Yang JD, Zhang N. Antibiotic penetration into rabbit nucleus pulposus with discitis. Eur.J.Orthop.Surg.Traumatol. 2014;24:453-8.
71. Chuah YJ, Peck Y, Lau JE, Hee HT, Wang DA. Hydrogel based cartilaginous tissue regeneration: recent insights and technologies. Biomater.Sci. 2017;5:613-31.
72. Pereira DR, Silva-Correia J, Oliveira JM, Reis RL. Hydrogels in acellular and cellular strategies for intervertebral disc regeneration. J.Tissue Eng.Regen.Med. 2013;7:85-98.
73. Rai MF and Pham CT. Intra-articular drug delivery systems for joint diseases. Curr.Opin.Pharmacol. 2018;40:67-73.
74. Tellegen AR, Willems N, Beukers M, Grinwis GCM, Plomp SGM, Bos C*, et al*. Intradiscal application of a PCLA-PEG-PCLA hydrogel loaded with celecoxib for the treatment of back pain in canines: What's in it for humans? J.Tissue Eng.Regen.Med. 2018;12:642-652.
75. Willems N, Mihov G, Grinwis GC, van Dijk M, Schumann D, Bos C*, et al*. Safety of intradiscal injection and biocompatibility of polyester amide microspheres in a canine model predisposed to intervertebral disc degeneration. J.Biomed.Mater.Res.B.Appl.Biomater. 2015;105:707-714.
76. Willems N, Yang HY, Langelaan ML, Tellegen AR, Grinwis GC, Kranenburg HJ*, et al*. Biocompatibility and intradiscal application of a thermoreversible celecoxib-loaded poly-N-isopropylacrylamide MgFe-layered double hydroxide hydrogel in a canine model. Arthritis Res.Ther. 2015;17:214,015-0727-x.
77. D'Este M, Eglin D, Alini M. Lessons to be learned and future directions for intervertebral disc biomaterials. Acta Biomater. 2018;.
78. Vital JM and Boissiere L. Total disc replacement. Orthop.Traumatol.Surg.Res. 2014;100:S1-14.

79. Henry N, Clouet J, Le Bideau J, Le Visage C, Guicheux J. Innovative strategies for intervertebral disc regenerative medicine: From cell therapies to multiscale delivery systems. Biotechnol.Adv. 2018;36:281-94.
80. Willems N, Bach FC, Plomp SG, van Rijen MH, Wolfswinkel J, Grinwis GC*, et al*. Intradiscal application of rhBMP-7 does not induce regeneration in a canine model of spontaneous intervertebral disc degeneration. Arthritis Res.Ther. 2015;17:137-151.
81. Muto M, Ambrosanio G, Guarnieri G, Capobianco E, Piccolo G, Annunziata G*, et al*. Low back pain and sciatica: treatment with intradiscal-intraforaminal O(2)-O (3) injection. Our experience. Radiol.Med. 2008;113:695-706.
82. Kallewaard JW, Geurts JW, Kessels A, Willems P, van Santbrink H, van Kleef M. Efficacy, Safety, and Predictors of Intradiscal Methylene Blue Injection for Discogenic Low Back Pain: Results of a Multicenter Prospective Clinical Series. Pain Pract. 2016;16:405-12.
83. Meij BP and Bergknut N. Degenerative lumbosacral stenosis in dogs. Vet.Clin.North Am.Small Anim.Pract. 2010;40:983-1009.
84. Chrobok J, Vrba I, Stetkarova I. Selection of surgical procedures for treatment of failed back surgery syndrome (FBSS). Chir.Narzadow Ruchu Ortop.Pol. 2005;70:147-53.
85. De Risio L, Sharp NJ, Olby NJ, Munana KR, Thomas WB. Predictors of outcome after dorsal decompressive laminectomy for degenerative lumbosacral stenosis in dogs: 69 cases (1987-1997). J.Am.Vet.Med.Assoc. 2001;219:624-8.
86. Hamilton-Bennett SE, Oxley B, Behr S. Accuracy of a patient-specific 3D printed drill guide for placement of cervical transpedicular screws. Vet.Surg. 2018;47:236-42.
87. Teunissen M, van der Veen AJ, Smit TH, Tryfonidou MA, Meij BP. Effect of a titanium cage as a stand-alone device on biomechanical stability in the lumbosacral spine of canine cadavers. Vet.J. 2017;220:17-23.
88. Park P, Garton HJ, Gala VC, Hoff JT, McGillicuddy JE. Adjacent segment disease after lumbar or lumbosacral fusion: review of the literature. 2004;29:1938-44.
89. Wang JC, Arnold PM, Hermsmeyer JT, Norvell DC. Do lumbar motion preserving devices reduce the risk of adjacent segment pathology compared with fusion surgery? A systematic review. Spine (Phila Pa.1976) 2012;37:S133-43.
90. Huang YJ, Zhao SJ, Zhang Q, Nong LM, Xu NW. Comparison of lumbar pedicular dynamic stabilisation systems versus fusion for the treatment of lumbar degenerative disc disease: A meta-analysis. Acta Orthop.Belg. 2017;83:180-93.
91. Ou CY, Lee TC, Lee TH, Huang YH. Impact of body mass index on adjacent segment disease after lumbar fusion for degenerative spine disease. Neurosurgery 2015;76:396,401; discussion 401-2; quiz 402.
92. Golini L, Kircher PR, Lewis FI, Steffen F. Transarticular fixation with cortical screws combined with dorsal laminectomy and partial discectomy as surgical treatment of degenerative lumbosacral stenosis in 17 dogs: clinical and computed tomography follow-up. Vet.Surg. 2014;43:405-13.
93. Fotouhi A, Maleki A, Dolati S, Aghebati-Maleki A, Aghebati-Maleki L. Platelet rich plasma, stromal vascular fraction and autologous conditioned serum in treatment of knee osteoarthritis. Biomed.Pharmacother. 2018;104:652-60.
94. Grol MW and Lee BH. Gene therapy for repair and regeneration of bone and cartilage. Curr.Opin.Pharmacol. 2018;40:59-66.
95. De Bari C and Roelofs AJ. Stem cell-based therapeutic strategies for cartilage defects and osteoarthritis. Curr.Opin.Pharmacol. 2018;40:74-80.
96. Richardson SM, Kalamegam G, Pushparaj PN, Matta C, Memic A, Khademhosseini A*, et al*. Mesenchymal stem cells in regenerative medicine: Focus on articular cartilage and intervertebral disc regeneration. Methods 2016;99:69-80.
97. Rudnik-Jansen I, Colen S, Berard J, Plomp S, Que I, van Rijen M*, et al*. Prolonged inhibition of inflammation in osteoarthritis by triamcinolone acetonide released from a polyester amide microsphere platform. J.Control.Release 2017;253:64-72.
98. Minamide A, Tamaki T, Hashizume H, Yoshida M, Kawakami M, Hayashi N. Effects of steroid and lipopolysaccharide on spontaneous resorption of herniated intervertebral discs. An experimental study in the rabbit. Spine (Phila Pa.1976) 1998;23:870-6.
99. Vandeweerd JM, Zhao Y, Nisolle JF, Zhang W, Zhihong L, Clegg P*, et al*. Effect of corticosteroids on articular cartilage: have animal studies said everything? Fundam.Clin.Pharmacol. 2015;29:427-38.
100. Wernecke C, Braun HJ, Dragoo JL. The effect of intra-articular corticosteroids on articular cartilage: a systematic review. Orthop.J.Sports Med. 2015;3:2325967115581163.
101. Loeser RF, Goldring SR, Scanzello CR, Goldring MB. Osteoarthritis: a disease of the joint as an organ. Arthritis Rheum. 2012;64:1697-707.

102. Barr AJ, Campbell TM, Hopkinson D, Kingsbury SR, Bowes MA, Conaghan PG. A systematic review of the relationship between subchondral bone features, pain and structural pathology in peripheral joint osteoarthritis. Arthritis Res.Ther. 2015;17:228.
103. Dudli S, Fields AJ, Samartzis D, Karppinen J, Lotz JC. Pathobiology of Modic changes. Eur.Spine J. 2016;25:3723-34.
104. Sellam J and Berenbaum F. The role of synovitis in pathophysiology and clinical symptoms of osteoarthritis. Nat.Rev.Rheumatol. 2010;6:625-35.
105. Yu D, Xu J, Liu F, Wang X, Mao Y, Zhu Z. Subchondral bone changes and the impacts on joint pain and articular cartilage degeneration in osteoarthritis. Clin.Exp.Rheumatol. 2016;34:929-34.

Addendum

Summary

The main aim of the research reported in this thesis was to develop novel treatment strategies for osteoarthritis (OA) and intervertebral disc (IVD) disease, in order to prevent or delay disease progression. To this end, anti-inflammatory drugs loaded in controlled release platforms were delivered via intra-articular (IA) or intradiscal injection directly into the degenerated joint or IVD tissue, in preclinical models as well as in phase I/II studies in veterinary patients. In addition, for cases of severe disc degeneration, when both conservative and standard-of-care surgical treatment fail, the feasibility and efficacy of instrumented fusion of the affected spinal unit were explored in veterinary patients.

Background

Degenerative joint diseases, such as OA and IVD degeneration are clinical entities in both human beings and companion animals. The joint and IVD share many similarities regarding extracellular matrix organization and the cascade of degenerative events. Both healthy articular cartilage and the nucleus pulposus, which resides in the core of the IVD, are avascular and aneural tissues, but with advancing degeneration, there is invasion of inflammatory cells, blood vessels and nociceptive nerve endings. Pro-inflammatory mediators produced by both resident and invading cells promote catabolic tissue changes and sensitization to pain. Underlying bone interacts on a molecular level and gives rise to osteophytes, bone cysts and eventually becomes sclerotic. All these changes can cause clinical symptoms such as pain and reduced mobility.

Current therapies for OA and IVD degeneration can be divided into conservative and surgical modalities. Conservative disease management broadly consists of oral (non-steroidal) anti-inflammatory drugs, optimal body weight maintenance, altered exercise regime and physical therapy, which can be supplemented by oral analgesics such as opioids and GABA-agonists, and nutraceuticals. There is a variety of surgical techniques available, depending on the involved joint and severity of degenerative changes. They can involve removal of abnormal tissue, altering biomechanics, joint-stabilizing techniques or joint replacement. However, these therapies do not restore biomechanical function or homeostasis of the extracellular matrix and resident cells and hence can still lead to progression of degenerative joint disease. IA or intradiscal injections are a safe and elegant way to directly deliver drugs into the diseased tissue. Biomaterials play an important role in local drug applications. Biomaterial characteristics can be tapered to guarantee safe delivery and sustained and controlled release of the encapsulated drug. In view of the inflammatory character of joint and disc degeneration, studies on minimally invasive local application of anti-inflammatory drugs were undertaken for early disease stages. Prolonged exposure of anti-inflammatory drugs was hypothesized to provide analgesia and to slow down the progression of degeneration on tissue level. Safety and efficacy of biomaterials releasing anti-inflammatory drugs were first evaluated *in vitro* and *in vivo* in preclinical studies. The optimised medication was further translated in the veterinary clinic utilizing the canine OA and low

back pain patient as a research model for translation of treatments for veterinary and human patients. For end stage IVD disease, long-term follow-up of surgical stabilization of the lumbosacral junction in canine patients inspired from ongoing surgical procedures employed in human patients was described.

Part I: Development of novel treatment strategies for OA

Dog breeds vary greatly in size and body conformation and one-size-fits-all might not apply. Differences in pathophysiology and clinical presentation of IVD disease confirm that this is indeed the case. For that reason, **Chapter 2** explored whether there are intrinsic differences in cartilage and synovial tissues derived from chondrodystrophic (CD) and non-chondrodystrophic (NCD) dogs, and if so, whether they could account for a differential susceptibility to OA development. It appeared that in macroscopic healthy joints of young adult NCD dogs, unlike in those of CD dogs, there were already early signs of cartilage degeneration and synovial inflammation. Meta-analysis of retrospective data from standardized experimental canine OA models revealed that NCD dogs responded with more severe osteoarthritic changes and synovial inflammation than CD dogs. On a biochemical level, CD dogs were also better capable of retaining GAGs inside the cartilage. No differences were found regarding canonical Wnt signalling in healthy cartilage. These findings have implications for future fundamental and translational research, since the type of dog used in preclinical research might influence study outcomes. Empirical evidence indicates that clinical OA is more prevalent in NCD dogs. If epidemiological studies confirm these differences, different diagnostic and therapeutic protocols could be developed for different dog breeds (i.e., personalised veterinary medicine).

To cater to the increasing need for minimally invasive treatments for OA in both people and companion animals, the research has focused on local controlled delivery systems for novel or well-known medications. COX-2 inhibitors such as celecoxib are known to be effective against OA pain and are postulated to possess disease-modifying properties. The long-term use of oral NSAIDs, which is inevitable in certain patient populations due to the chronic progressive nature of OA, can lead to undesirable side effects. Intra-articular delivery of a drug platform that provides prolonged celecoxib release is a promising strategy for OA patients: it reduces systemic drug exposure and can enhance treatment efficacy. Modern drug delivery systems are mostly based on biodegradable polymer carriers, for example as injectable hydrogels or microparticles that provide constant gradual drug release. The study reported in **Chapter 3** shows promising preclinical findings of celecoxib-loaded polyesteramide microspheres in a surgical OA rat model. Although no protective effects on cartilage pathology could be assessed, the prolonged IA presence of celecoxib did effectively reduce important OA hallmarks, i.e., synovial inflammation, subchondral bone changes (i.e. subchondral sclerosis, bone cysts) and osteophyte formation.

For that reason, the step from bench to the veterinary bedside was made in **Chapter 4**. A prospective, randomized controlled clinical study confirmed safety and clinical efficacy of

locally injected celecoxib-loaded microspheres in companion dogs with clinical OA. Only in the group that received celecoxib-loaded microspheres was a reduction of clinical signs perceived. In line with the findings reported in Chapter 3, attenuation of synovial inflammation was seen with celecoxib-loaded microspheres; no effects on radiological read out parameters were found during the two-month follow up period. In **Chapter 5**, preliminary safety of IA administration of microspheres loaded with triamcinolone acetonide was investigated in a patient population with moderate to severe OA. Objective kinetic gait analysis and owner questionnaires show that in the majority of client-owned dogs prolonged IA triamcinolone acetonide release led to improvement. Unloaded microspheres and microspheres loaded with celecoxib or triamcinolone acetonide were applied without substantial adverse clinical or radiological effects. These results are promising for the translation of local drug delivery platforms in both human and veterinary medicines.

Part II: Development of novel treatment strategies for low back pain

The second part of the research reported in this thesis focused on innovative therapies for chronic low back pain. Studies on human tissue show that in IVD degeneration, as in OA, pro-inflammatory cytokines drive the degenerative cascade. Whether these pro-inflammatory mediators are also associated with canine IVD degeneration, and in which stage of the disease, was not previously investigated in detail. For that reason, inflammatory profiles in canine IVD degeneration were assessed in **Chapter 6**. Levels of pro-inflammatory cytokines prostaglandin E_2 and CLL2 were higher in degenerated and herniated IVDs, compared to non-degenerated IVDs *in situ*. COX-2 protein expression, the enzyme that mediates prostaglandin E_2 production, in the NP and AF and reactive changes in the AF increased with advancing degeneration stages. These findings indicate first that similar inflammatory factors are involved in IVD in canine and human discs, justifying the use of canines as a suitable pre-clinical or clinical model to investigate novel therapies. Second, by targeting inflammation in an early disease stage, the degenerative process could be halted or even reversed after local delivery of anti-inflammatory drugs, in both people and dogs.

For that reason, local application of celecoxib, delivered in a thermoresponsive PCLA-PEG-PCLA hydrogel (**Chapter 7**), and α-amino-acid based biodegradable polyesteramide microspheres (**Chapter 8**) were studied. Both controlled release platforms were based on biodegradable polymers with non-toxic degradation products and favourable sustained drug release profiles in previously published *in vitro* or *in vivo* studies. Both drug delivery systems showed good biocompatibility and did not influence tissue homeostasis upon intradiscal injection in an experimental canine IVD degeneration model. Percutaneous intradiscal administration of the celecoxib-loaded PCLA-PEG-PCLA hydrogel showed favourable clinical results in a preliminary safety study in companion dogs suffering from degenerative lumbosacral stenosis. C**hapter 9** describes the setup of a prospective, randomized, controlled clinical study to provide clinical evidence of applicability of percutaneous intradiscal injection of celecoxib-loaded microspheres. The study is ongoing.

Low back pain resulting from degenerative lumbosacral stenosis (DLSS) frequently occurs in large breed dogs and is associated with degeneration and protrusion of the IVD and spinal instability. When conservative management is insufficient, surgical decompression is indicated. Although short-term outcome is high, recurrence of clinical signs is reported in up to 38% of cases, presumably caused by worsening of LS instability. **Chapter 10** concludes this thesis with promising medium to long-term follow-up of 12 client-owned dogs with severe low back pain. When DLSS has progressed and conservative and surgical methods have proven insufficient, PSRF with or without spinal distraction should be considered as a suitable treatment strategy. With PSRF alone, no interbody fusion of L7 and S1 was achieved. To achieve bony fusion of the lumbosacral junction, extensive burring of both end plates, the application of an (autologous) bone graft and/ or the application of growth factors should be further investigated.

Dutch summary / Nederlandse samenvatting

Het overkoepelende doel van de studies beschreven in dit proefschrift is het ontwikkelen van behandelingen voor gewrichtsslijtage (artrose) en slijtage (degeneratie) van de tussenwervelschijf (TWS) in een vroeg stadium van de aandoening, om pijn te bestrijden en het ziekteverloop te vertragen, bij zowel mens als hond. Hierdoor kunnen meer belastende medicamenteuze of chirurgische behandelingen uitgesteld of zelfs voorkomen worden. In het kader hiervan zijn studies uitgevoerd waarin de werkzaamheid onderzocht werd van een lokale injectie in het aangedane gewricht of de aangedane tussenwervelschijf, met biocompatibele en biologisch afbreekbare gecontroleerde afgiftesystemen, die geleidelijk ontstekingsremmende medicatie aan het omringende weefsel afgeven. Voor honden met ernstige lage rugpijn door TWS slijtage, waarbij de gangbare therapieën onvoldoende effect hebben, is de effectiviteit van chirurgische fusie van de lage rug met implantaten onderzocht.

Achtergrond

Degeneratieve gewrichtsziekten zoals artrose en lage rugpijn als gevolg van TWS degeneratie zijn veelvoorkomende klinische problemen bij zowel mensen als gezelschapsdieren. Het gewricht en de TWS vertonen veel overeenkomsten op weefsel- en celniveau, en ook wat betreft de pathologische veranderingen van het weefsel. Zowel gewrichtskraakbeen als de kern van de TWS, de nucleus pulposus, bevatten in een gezond stadium geen bloedvaten of zenuwuiteinden. Met het proces van degeneratie dringen vaten en zenuwen wel het weefsel binnen, samen met ontstekingscellen. De ontstekingsmediatoren geproduceerd door zowel de natieve cellen als de inkomende ontstekingscellen stimuleren afbraak van het omringende weefsel, en zorgen voor het genereren van pijnsignalen. Het onderliggende bot doet ook mee aan dit degeneratieproces, en uiteindelijk ontstaan er botveranderingen zoals osteofyten (benige uitsteeksels). Al deze veranderingen kunnen resulteren in pijn en verminderde mobiliteit. De huidige therapie-opties voor artrose en TWS degeneratie kunnen verdeeld worden in conservatieve en chirurgische modaliteiten. Conservatieve therapie bestaat globaal uit orale (non-steroïdale) ontstekingsremmers, gewichtsmanagement, een aangepast bewegingsregime en fysiotherapie, eventueel aangevuld met opioïd-achtige pijnstillers en/ of voedingssupplementen zoals omega-3 vetzuren. Er zijn veel verschillende chirurgische behandelmethoden beschikbaar, afhankelijk van onder andere de lokalisatie, de ernst en de aard van de aandoening. Zo kan men chirurgisch afwijkend weefsel verwijderen, bijvoorbeeld bij een hernia, of in een vergevorderd geval het gewricht of de rug met implantaten stabiliseren, of het gewricht vervangen door een prothese. Deze therapieën herstellen echter niet de homeostase van het weefsel en de cellen, en kunnen daarom progressie van degeneratie niet voorkomen.

Intra-articulaire of intradiscale injecties zijn een veilige en elegante manier om medicijnen direct in het aangetaste weefsel toe te dienen. Biomaterialen kunnen zo gemaakt worden dat ze injecteerbaar zijn door een dunne naald, en ze geleidelijke afgifte van

geïncorporeerde bio-actieve stoffen kunnen faciliteren. Vanwege het inflammatoire karakter van artrose en TWS degeneratie zijn er studies uitgevoerd om een minimaal-invasieve lokale toediening van anti-inflammatoire medicatie te optimaliseren. De hypothese was dat langdurige lokale blootstelling aan anti-inflammatoire medicatie zorgt voor analgesie (pijnstilling) en ook het ziekteproces op weefselniveau afremt. De veiligheid en effectiviteit van de gecontroleerde afgifte van anti-inflammatoire medicijnen uit biomaterialen werden eerst geëvalueerd in preklinische studies, zowel *in vitro* als *in vivo*. De geoptimaliseerde medicatie werd verder vertaald naar de veterinaire kliniek, waarbij cliëntgebonden honden met artrose en lage rugpijn als gevolg van TWS degeneratie behandeld werden. In dit geval diende de hond zowel als model voor zijn eigen species, alsook als model voor de mens. Voor honden met vergevorderde TWS degeneratie, refractair op zowel conservatieve als chirurgische interventie, is chirurgische stabilisatie van de lumbosacrale overgang verder onderzocht.

Deel I: de ontwikkeling van nieuwe behandelstrategieën voor artrose

Hondenrassen variëren aanzienlijk in grootte en lichaamsbouw, en one-size-fits-all gaat hier niet altijd op. Een mooi voorbeeld hiervan is TWS degeneratie en daaruit voortvloeiend de hernia nuclei pulposi. De pathofysiologie en klinische presentatie van deze aandoening zijn beduidend anders in kortpotige chondrodystrofe (CD) en normaal geproportioneerde niet-chondrodystrofe (NCD) honden. Omdat de korte poten bij CD honden veroorzaakt worden door een verstoring van de enchondrale verkalking (de transitie van kraakbeen naar bot), werd in **hoofdstuk 2** onderzocht of er intrinsieke verschillen zijn in het kraakbeen en synovium van CD en NCD honden, en of dit verschil invloed heeft op de gevoeligheid voor het ontwikkelen van artrose. Meta-analyse van retrospectieve data van gestandaardiseerde artrose-inductie in honden in experimentele setting toonde een hogere mate van artrotische veranderingen en synoviale inflammatie in NCD kraakbeen dan in kraakbeen van CD honden. Op biochemisch niveau was het CD kraakbeen beter in staat om glycosaminoglycanen in het kraakbeen te behouden tijdens een kweekperiode van 21 dagen. Er werden geen verschillen in Wnt signalering gevonden in gezond kraakbeen van CD en NCD honden. Desalniettemin hebben bovenstaande bevindingen implicaties voor toekomstig onderzoek, omdat het type hond dat gebruikt wordt in preklinisch onderzoek de studieresultaten kan beïnvloeden. Empirisch bewijs indiceert ook dat in de veterinaire praktijk artrose vaker voorkomt in NCD honden, al is hier nooit gericht onderzoek naar verricht. Epidemiologische studies hiernaar zouden kunnen leiden tot andere diagnostische en therapeutische protocollen voor de verschillende hondenrassen (een soort gepersonaliseerde diergeneeskunde).

Om aan de toenemende vraag naar minimaal invasieve behandelingen voor degeneratieve gewrichtsziekten bij mens en hond te voldoen, is steeds meer onderzoek gericht op lokaal injecteerbare afgifte systemen voor nieuwe of al geregistreerde medicijnen. Bestaande COX-2 remmers zoals celecoxib zijn effectief in de bestrijding van gewrichts- en lage rugpijn, en hebben wellicht ook gunstige effecten op het ziekteverloop van artrose en TWS degeneratie.

Langdurig oraal gebruik van NSAIDs kan echter leiden tot ongewenste systemische bijwerkingen. Lokale toediening van een platform dat gedurende langere tijd celecoxib afgeeft aan het omringende weefsel zou bijwerkingen kunnen omzeilen en de lokale effectiviteit verhogen. Innovatieve afgiftesystemen zijn gebaseerd op biologisch afbreekbare polymeren, bijvoorbeeld in de vorm van injecteerbare hydrogelen of micropartikels, die een constante afgifte van medicijnen garanderen gedurende langere tijd (weken tot maanden). De gecontroleerde afgifte van celecoxib uit micropartikels is onderzocht in een artrose model in **hoofdstuk 3**. Hoewel er geen beschermend effect op kraakbeen niveau zichtbaar was, werden er wel minder botveranderingen en synoviale ontsteking gezien. In **hoofdstuk 4** is daarom de stap gemaakt naar de toepassing in veterinaire patiënten. Een prospectieve, gerandomiseerde placebogecontroleerde studie bevestigde de klinische effectiviteit van een intra-articulaire injectie met celecoxib-geladen microsferen in cliëntgebonden honden met artrose. In overeenstemming met hoofdstuk 3 was er een reductie van synoviale ontsteking. In **hoofdstuk 5** zijn de resultaten beschreven van een preliminaire studie naar de intra-articulaire toepassing van microsferen geladen met het corticosteroïd triamcinolone acetonide in cliëntgebonden honden met ernstige artrose. De behandeling leidde in de meerderheid van de patiënten tot klinische verbetering, afgelezen aan objectieve gangen analyse en vragenlijsten aan de eigenaar. Zowel de ongeladen microsferen als de microsferen geladen met celecoxib of triamcinolone acetonide leidden niet tot ongewenste bijeffecten. Deze resultaten zijn veelbelovend in de vertaling van lokale afgiftesystemen met ontstekingsremmende medicatie naar de humane en veterinaire kliniek.

Deel II: de ontwikkeling van nieuwe behandelstrategieën voor lage rugpijn

Het tweede deel van deze dissertatie is gericht op innovatieve behandelmethoden voor lage rugpijn. Uit studies met humane patiënten is naar voren gekomen dat bij TWS degeneratie er een belangrijke rol is weggelegd voor pro-inflammatoire mediatoren. Of dit ook het geval is in honden, was nog niet eerder in detail onderzocht op weefselniveau. In **hoofdstuk 6** zijn dan ook de pro-inflammatoire profielen van de verschillende stadia en uitingsvormen van TWS degeneratie in kaart gebracht. De concentraties van het pro-inflammatoire prostaglandine GE_2 en het chemokine CCL2 waren hoger in gedegenereerde en gehernieerde TWS dan in niet-gedegenereerde en niet gehernieerde tussenwervelschijven. De eiwitexpressie van COX-2 en de reactieve veranderingen van het weefsel waren hoger naarmate de degeneratie toenam. Deze bevindingen wijzen erop dat er overeenkomstige pro-inflammatoire factoren aanwezig zijn in TWS degeneratie bij de hond. Hiermee wordt het gebruik van de hond in een experimentele setting gerechtvaardigd in de ontwikkeling van nieuwe therapieën voor chronische rugpijn. Tevens is het streven om ook voor honden dergelijke therapieën aan te bieden.

Op basis van bovengenoemde resultaten is de lokale toediening van celecoxib, geïncorporeerd in een thermoresponsieve PCLA-PEG-PCLA hydrogel (**hoofdstuk 7**) en polyesteramide microsferen (**hoofdstuk 8**) onderzocht. Beide gecontroleerde

afgiftesystemen zijn biologisch afbreekbare polymeren met een gunstig afgifteprofiel en zonder toxische afvalproducten, zoals beschreven in eerdere *in vitro* als *in vivo* studies. Beide gecontroleerde afgiftesystemen lieten een goede biocompatibiliteit zien na intradiscale injectie bij Beagles met experimenteel opgewekte TWS degeneratie. Zowel het biomateriaal alleen als het biomateriaal met celecoxib beïnvloedden de weefselhomeostase niet. Percutane intradiscale toediening van de PCLA-PEG-PCLA hydrogel met celecoxib resulteerde in gunstige klinische resultaten in honden met lage rugpijn door degeneratieve lumbosacrale stenose (**hoofdstuk 7**). In **hoofdstuk 9** is de opzet van een prospectieve, gerandomiseerde placebogecontroleerde studie beschreven waarmee het klinische effect van een percutane intradiscale injectie met microsferen met celecoxib wordt geëvalueerd.

Lage rugpijn komt vaak voor bij honden van grote rassen en is geassocieerd met degeneratie en protrusie van de TWS en met spinale instabiliteit. Voor honden die niet voldoende (meer) reageren op de conservatieve therapie, is chirurgische decompressie geïndiceerd. Hoewel het grootste gedeelte van de honden significante klinische verbetering vertoont na de operatie, wordt recidive van de klachten gezien in ruim een derde van de behandelde honden. Wellicht is het verergeren van de spinale instabiliteit een gevolg van de chirurgische ingreep een belangrijke oorzaak van deze recidiverende klachten. Bij honden die al dan niet geopereerd zijn, waarbij lumbosacrale instabiliteit een belangrijke rol in het klinische klachtenpatroon lijkt te spelen, zou chirurgische stabilisatie van de lumbosacrale overgang een geschikte therapeutische strategie kunnen zijn. In **hoofdstuk 10** werd daarom een cohort van 12 cliëntgebonden honden met ernstige degeneratieve lumbosacrale stenose beschreven die zijn behandeld met pedikelschroeffixatie en voor langere tijd zijn gevolgd. Uit de resultaten van deze retrospectieve studie kon worden geconcludeerd dat pedikelschroeffixatie, met of zonder spinale distractie, een veilige en effectieve behandeling is voor honden waarbij eerder conservatief en chirurgisch ingrijpen niet afdoende was. Alleen fixatie met het pedikelschroeven systeem gaf in dit cohort honden geen direct benige fusie tussen L7 en S1.

List of abbreviations

ACAN	Aggrecan
AC	Articular cartilage cell
ACL	Anterior cruciate ligament
ACLT	Anterior cruciate ligament transection
ACS	Autologous conditioned serum
ADAMTS5	A disintegrin and metalloproteinase with thrombospondin motifs 5
AF	Annulus fibrosus
AIC	Akaike Information Criterion
Asap	Ascorbic acid 2-phosphate
ASC	Adipose-derived stem cell
ASI	Asymmetry index
ASP	Adjacent segment pathology
AXIN-2	Axin-related protein
BAX	B-cell lymphoma-2 associated X
BCL2	B-cell lymphoma-2
BCS	Body condition score
bFGF	Basic fibroblast growth factor
BML	Bone marrow lesion
BMP	Bone morphogenetic protein
Bp	Base pairs
BSA	Bovine serum albumin
BW	Body weight
CASP3	Caspase 3
Cav-1	Caveolin-1
CCL2	Chemokine (C-C) motif ligand 2
CCND1	Cyclin D1
CD	Chondrodystrophic
CD68	Cluster of differentiation 68
CI	Confidence interval
CK	Cytokeratin
CLC	Chondrocyte-like cell
COL1A1	Collagen type 1 alpha 1
COL2A1	Collagen type 2 alpha 1
COL10	Collagen type X
COX	Cyclooxygenase
CRI	Constant rate infusion
CS	Corticosteroid
Ct	Cycle threshold
CT	Computed tomography
CXB	Celecoxib
CXC-1	C-X-C Motif Chemokine Ligand 1

DEC	Dier experimenten commissie
DH	Disc height
DHI	Disc height index
DJD	Degenerative joint disease
DL	Dorsal laminectomy
DLSS	Degenerative lumbosacral stenosis
DMEM	Dulbecco's modified Eagle's medium
DMMB	Dimethylmethylene blue
DMOAD	Disease-modifying osteoarthritis drug
DNA	Deoxyribonucleic acid
ECM	Extracellular matrix
ED	Elbow dysplasia
EDTA	Ethylenediaminetatraacetic acid
ELISA	Enzyme Linked Immunosorbent Assay
EP	End plate
EP4	Prostaglandin E_2 receptor 4
ES	Effect size
FasL	Fas ligand
FBS	Foetal bovine serum
FCP	Fragmented coronoid process
FGF4	Fibroblast growth factor 4
FGFR3	Fibroblast growth factor receptor 3
FOV	Field of view
FPA	Force plate analysis
FR-β	Folate receptor beta
FRZB	Frizzled related protein
Fy-	Peak propulsive force
Fy+	Peak braking force
Fz+	Peak vertical force
GABA	Gamma-aminobutyric acid
GAG	Glycosaminoglycan
GAPDH	Glyceraldehyde 3-phosphate dehydrogenase
GDP	Gross domestic product
GM-CSF	Granulocyte-macrophage colony-stimulating factor
GRF	Ground reaction force
HD	Hip dysplasia
Hg-DMEM	High glucose Dulbecco's modified Eagle's medium
HPRT	hypoxanthine-guanine phosphoribosyl-transferase
HRP	Horseradish peroxidase
HYP	Hydroxyproline
IA	Intra-articular

IHC	Immunohistochemistry
IL-1ß	Interleukin 1 beta
IL-10	Interleukin 10
IM	Intramuscular
iNOS	Inducible nitric oxide synthase
IP-10	Interferon-inducible protein 10
ITS	Insulin-transferrin-selenium
IV	Intravenous
IVD	Intervertebral disc
IVDD	Intervertebral disc degeneration
LBP	Low back pain
LS	Lumbosacral
µ-CT	micro-computed tomography
Mab	Monoclonal antibody
MC	Modic changes
MCD	Medial coronoid disease
MCP-1	Monocyte chemoattractant protein 1
MIA	Monosodium Iodoacetate
MMP13	Matrix metalloproteinase 13
MRI	Magnetic resonance imaging
mRNA	Messenger ribonucleic acid
MSC	Mesenchymal stromal cell
N/A	Not available
NBF	Neutral buffered formalin
NC	Notochordal cell
NCD	Non-chondrodystrophic
NCCM	Notochordal cell-conditioned medium
NGF	Nerve growth factor
NF-κβ	Nuclear factor kappa-light-chain-enhancer of activated B cells
NMR	Nuclear magnetic resonance
NO	Nitric oxide
NP	Nucleus pulposus
NPC	Nucleus pulposus cell
N.S.	Not significant
NSAID	Non-steroidal anti-inflammatory drug
OA	Osteoarthritis
OARSI	Osteoarthritis Research Society International
P1	Passage 1
Pab	Polyclonal antibody
PBS	Phosphate buffered saline
PD	Partial discectomy

PDI	Polydispersity Index
PEG-PCLA-PEG	poly(ε‐caprolactone‐co‐lactide)‐b‐poly(ethylene glycol)‐bpoly(ε‐caprolactone‐colactide)
PEA	Polyesteramide
PEAM	Polyesteramide microsphere
PGE_2	Prostaglandin E_2
PLGA	Poly lactic-*co*-glycolic acid
PMMx	Partial medial meniscectomy
pNIPAAM	Poly-N-isopropylacrylamide
PO	Per os
PML	Polymorphonuclear
PPF	Peak propulsive force
PRP	Platelet rich plasma
p/s	Penicillin/streptomycin
PSRF	Pedicle screw-rod fixation
P/T	Pelvic/thoracic
PTHrP	Parathyroid hormone related peptide
PVF	Peak vertical force
ROI	Region of interest
RPS19	40S ribosomal protein S19
RT	Room temperature
RT-qPCR	Reverse transcriptase quantitative polymerase chain reaction
SD	Standard deviation
SDHA	Succinate dehydrogenase complex subunit A
SEM	Scanning electron microscopy
SF	Synovial fluid
T	Brachyury
T1rho	Application of T1 in rotating frame
T2W	T2-weighted
TA	Triamcinolone acetonide
TBP	TATA-Box binding protein
TBS	Tris buffered saline
TCF	T-cell factor
Tg	Glass transition temperature
TGF-β	Transforming growth factor beta
TIMP1	Tissue inhibitor of metalloproteinases
TNF-α	Tumour necrosis factor alpha
TPO	Triple pelvic osteotomy
TSE	Turbo spin echo
TWS	Tussenwervelschijf
VI	Vertical force

Acknowledgements / Dankwoord

Dit proefschrift was niet tot stand gekomen zonder de hulp van velen. Ik zou iedereen die hieraan heeft bij gedragen willen bedanken, waaronder een aantal mensen in het bijzonder.

Geachte Prof. Dr. Meij, beste Björn, ik kan je niet genoeg bedanken voor al het vertrouwen dat je in mij gesteld hebt de afgelopen jaren. Niet alleen heb je me aan het onderzoek van Nicole Willems gekoppeld en daarna de mogelijkheid gegeven om een PhD traject onder jouw supervisie te starten, ook heb ik meerdere malen het fort in Bilthoven-Noord mogen bewaken. Ik heb altijd erg veel gehad aan jouw rustige en overzichtelijke blik en je enorme wetenschappelijke en klinische kennis en vaardigheden.

Geachte Prof. Dr. Tryfonidou, beste Marianna, jouw onuitputtelijke optimisme en passie voor het biomedische onderzoek binnen de Faculteit Diergeneeskunde (en inmiddels ook daarbuiten) zijn voor velen, en ook voor mij, een inspiratiebron. Onder jouw leiding heb ik de onderzoekslijn Regeneratieve Orthopedie enorm zien groeien. Je bent altijd bereikbaar voor advies, overleg of een peptalk om het onderzoek in goede banen te leiden, waarvoor hulde!

Geachte Dr. Creemers, beste Laura, onwijs bedankt voor de verfrissende blik op het biomedische onderzoeksveld en ons onderzoek in het bijzonder. Jouw creativiteit met tegelijkertijd objectiviteit zijn ontzettend waardevol. Dank voor alle kritische feedback op manuscripten en het razendsnelle emailverkeer. Daarnaast waren congressen en andere uitjes altijd een feestje met jou!

Dear Dr. Thies, dear Jens, you are the most enthusiastic person I know, and I could use motivational TED talks from you more often! I really enjoyed working with you during my PhD.

Lieve Frances, het was me een waar genoegen om gedurende het PhD traject een kamer met jou te delen. We hebben in de loop der jaren heel wat lief, leed, frustraties, roddels en lekkers gedeeld. Ik kon altijd bij je terecht met labtechnische vragen en ook vragen omtrent het proefschrift en de promotieplechtigheid heb je altijd geduldig beantwoord. Ik mis ons dagelijks contact en jouw droge en nuchtere humor, maar ik hoop dat we contact blijven houden na deze intensieve jaren.

Lieve Michelle, we go way back! Sinds jouw HP jaar en mijn onderzoekstage hebben we periodes wel en niet samen op het lab gezeten en ook heel wat lief en leed en frustraties gedeeld, naast de nodige discussies over vrouwenquota.. Ik bewonder je vasthoudendheid en je toewijding en ik wil je ontzettend bedanken voor de fijne tijd de afgelopen jaren. Ik hoop dat we nog veel wijn samen zullen proeven ;-)!

Imke Jansen, onze verschillende opleidingsachtergronden maakten ons een sterk team in het ArIADNE consortium. Het was een intensieve periode, en ik ben blij dat we het samen hebben kunnen doen. Bedankt voor de gezelligheid en goede samenwerking de afgelopen jaren, met als hoogtepunt onze reis naar Amerika!

Dear Nina, I think I almost drove you insane several times with deadlines and last-minute requests.. I really enjoyed working with you, as you are very knowledgeable regarding the microspheres we've extensively employed in this dissertation, and you were always very involved. George Mihov, thank you for the calm but critical notes during our meetings and email contact. Julien Berard and Monika Jobard, thank you for your scientific input. Mike de Leeuw en Maarten van Dijk, ontzettend veel dank voor de prettige samenwerking omtrent alle studies met de gelen van InGell en ook de input voor het manuscript.

Prof. Dr. Hazewinkel, uw bijdrage aan de veterinaire orthopedie is van onschatbare waarde geweest voor het hedendaagse onderzoek. Hartelijk dank voor het delen van uw kennis.

Prof. Dr. René van Weeren, bedankt voor de input op papers en de bemoedigende woorden tijdens het jaarlijkse PhD voortgangsgesprek, en de gezelligheid op de OARSI in Liverpool.

Prof. Dr. Erik Teske, hartelijk dank voor uw bijdrage aan de klinische studies met artrose patiënten op de UKG, en uw gastvrijheid in de cytologieruimte van het UVDL.

Dr. Penning, beste Louis, jouw brede kennis is van grote waarde tijdens de wekelijke overleggen in het JDV gebouw. Daarnaast ben je ook altijd in voor een borrel, een geintje of een praatje.

Dr. Willems, lieve Nicole, ik ben nog steeds ontzettend blij dat ik mijn onderzoekstage bij jou heb kunnen doen en daarna je collega-onderzoekster ben geworden. Jouw nooit aflatende enthousiasme en precisie zijn enorm bewonderingswaardig en ik heb het werken met jou altijd als heel inspirerend ervaren.

Dr. Guy Grinwis, hartelijk dank voor de waardevolle inbreng in veel van de studies van dit proefschrift.

Dr. Robert Favier, hartelijk dank voor de regelmatige 'mentor-sessies' gedurende het eerste deel van mijn promotie-traject.

Dr. Paul Mandigers, Drs. Quirine Stassen en Drs. Montse Diaz-Espineira, dank voor de input voor de patiëntenstudies op de UKG.

Alberto Miranda Bedate, thank you so much for your statistical knowledge and your inventive (and edible) input during all our discussions and meetings.

Martijn Beukers, onwijs bedankt voor alle hulp met de beeldvorming, samples en manuscripten, en natuurlijk de leuke samenwerking.

Arie Doornenbal, bedankt voor de fijne samenwerking en de hulp met alle honden (en ratjes) en force plate (en pressure plate) analyses. Jammer dat we niet zo vaak meer even kunnen kletsen!

Saskia Plomp, wat was ik blij dat je na je tijd in het UMCU de onderzoeksgroep van René van Weeren kwam ondersteunen. Zo konden we af en toe toch nog profiteren van je expertise, je bakkunsten en natuurlijk je vrolijke karakter! Laten we af en toe nog eens samen gaan paardrijden of tapas eten..

Frank Riemers, ik ben je zeer dankbaar voor alle technische input tijdens onze wekelijkse overleggen en heel lang geleden toen je me in het lab begeleidde als student. Het over en weer uiten van slechte grappen en frustraties in de tijd dat we kamergenoten waren heeft me door het laatste deel van m'n promotie-traject geloodst ☺.

Jeannette Wolfswinkel, vele malen dank voor je expertise in het lab. Je bent echt onmisbaar in het JDV lab.

Willem De Jong, onwijs bedankt voor alle hulp met het begeleiden van studenten en het uitvoeren van labwerk! Karin Sanders, Loes Oosterhoff, Kerstin Schneeberger en Manon Bouwmeester, ik ga jullie missen! En niet vergeten om af en toe even te lummelen ;-). Ook de rest van mijn JDV collega's, waaronder Frank van Steenbeek, Jan Mol, Peter Leegwater, Manon Vos, Monique van Wolferen, Elpetra Timmermans, Adri Slob en Yaobi Ceelen wil ik bedanken voor de leuke discussies en lekkere hapjes gedurende de gezamenlijke lablunches.

Ben Gorissen en Ellen Meijer, dank voor alle input voor alle gangenanalyses en alles daaromheen.

Collega's van de afdeling Diagnostische Beeldvorming Joris de Brouwer, Anke Wassink, Elise Petersen, en alle anderen, super bedankt voor jullie flexibiliteit en hulp voor alle beeldvormende kwesties.

Collega's van de afdeling anesthesie en sterilisatie: Carolien Kolijn, Ies Akkerdaas, Ron van Wandelen, Max Verver, Marieke de Vries, Jiske L'Ami, Zwanie Angevaare, Loes van Gennip, Marjolein Eshuis, Isabel Janssen, Iris Veen, Stefanie Horst, Abraham Calero Rodriguez, Wesley Mossel, ik vond het een waar genoegen om met jullie samen te werken!

Krista Post, Lucinda van Stee, Anneleen Spillebeen, Sarah Van Rijn, Sara Janssens, Tjarda Reints Bok, Judith Visser, Rick Beishuizen, Femke Verseijden, Annika Haagsman en Floor Driessen, ik waardeer het enorm dat jullie patiënten voor mijn studies hebben gerekruteerd, en dat ik mee mocht doen aan de wekelijkse Journal- en Book clubs. Tijn Wiersema, je hebt de klinische studie met veel enthousiasme en precisie overgenomen, super bedankt!

Harry van Engelen, bedankt dat je altijd voor ons klaarstond en bereid was met ons mee te denken. Het was erg fijn om jou in ons team te hebben.

Zonder studenten had dit proefschrift nooit het daglicht gezien. Aileen Dessing, wat heb jij een werk verzet! Ondanks tegenvallende resultaten hebben we uiteindelijk een mooie paper kunnen maken met al jouw *in vitro* werk als basis. Kaat Houben, ook jij hebt heel wat pilots moeten draaien en heel wat samples moeten verwerken, maar het resultaat mag er zijn.

Koen Santifort, Anouk Verbeek, Joyce Bestebroer, Anne Marie van der Hoeven, Erin de Gendt, Sofie Boegschoten, Robbert-Jan Ramaekers, Simone Kamphuijs, Sabine Brunschot, Mandy van de Vooren, Inge Danen, Femke Meijer, hartelijk dank voor jullie hulp en enthousiasme. Ferdi van Heel, Lisanne Laagland, Joshka Wolfs, Kim de Rooij, Maxine Lourenburg, Norah Ahrens en Danielle Maris, hartelijk dank voor de gezelligheid en de fijne samenwerking in het lab!

Koen Vaessen, Helma Avezaat, Anja van der Sar, Ivonne van Dreumel, Jeroen van Ark, Nico Attevelt, Hester de Bruin, Suzan Postma en Fred Poelma, ik ben jullie zeer erkentelijk voor de professionele doch liefdevolle zorg en hulp met de honden en de ratjes.

Nicoline Korthagen, dank voor alle waardevolle input tijdens onze wekelijkse overleggen en daarbuiten. Luciënne Vonk, Mattie van Rijen, Behdad Pouran, Joao Marques Garcia, Koen Willemsen, bedankt voor de prettige samenwerking in het UMCU. Pieter Emans, Ufuk Tan Timur en Maarten Jansen vanuit het MUMC, hartelijk dank voor het delen van jullie expertise.

Lisanne van der Voort en Bas Niemans, hartelijk dank voor het prachtige beeldmateriaal. Lisanne, super bedankt voor het omtoveren van mijn idee in een heel mooi cover-ontwerp!

Roelof Maarschalkerweerd, Dick van Zuilen, Nicolien van Klaveren, ik ben echt super blij dat ik na m'n onderzoek meteen bij jullie aan de slag kon! Het is niet alleen een ontzettend uitdagende en leerzame omgeving, maar ook nog eens heel gezellig en collegiaal. Kiona de Nies, Joris Vink, Bas Wetzels, Liz Moerbeek, Monique Beerepoot, Tess van der Lubbe, Rick Otten, Saskia van Stralen, Eline van der Kraan, Rebecca Smart, Janiek Muller, Evelien van der Ploeg, Wendy Beggel, Anne Berghout, Lonnet Kunst, Anouk Kok, Marita Hoefnagel, Timo Friemann, Lia de Hilster, Suzanne Wyling, Debby van Breukelen en Wendy de Ruijter, jullie zijn super fijne collega's! Uiteraard gaat mijn dank ook uit naar alle dierenartsen en paraveterinairen van de spoedkliniek voor hun collegialiteit in de afgelopen periode.

Hans Terwee, ontzettend bedankt voor alle praktische veterinaire kennis, levenslessen en natuurlijk het vertrouwen dat je in mij gesteld hebt al die jaren op het Groote Plein. Anna Weller, ook jou wil ik ontzettend bedanken voor de leuke en leerzame tijd tijdens het extern onderwijs en als collega's en vriendinnen daarna. José Dieker, Annika Schekkerman, Annemaria Vermeer, Marieke Kikkert en Eline Kapteyn, hartelijk dank voor alle ondersteuning én gezelligheid gedurende mijn tijd in Weesp.

Zowel de K.N.G.F. en de Stichting Hulphond Nederland hebben een aantal honden laten deelnemen aan één van de klinische studies. Ik ben hen daarvoor zeer erkentelijk.

Ik ben de eigenaren van de honden die mee hebben gedaan aan één (of meerdere!) patiëntenstudies enorm dankbaar voor hun vertrouwen voor, tijdens en na het onderzoek.

Ik ben een groot aantal dierenartsen zeer erkentelijk voor het verwijzen van patiënten(eigenaren) naar de UKG voor deelname aan de klinische studies. In het bijzonder wil ik graag Erik Wouters, Thijs How, Daan Kranendonk, Wouter Molenbroek en Wendy Nooijen noemen.

Lieve Marlique, een ochtend of avond op de Molshoop is altijd een fijn intermezzo en ik ben je dan ook zeer dankbaar voor alle mogelijkheden die je me hebt gegeven. Ik hoop nog vele jaren bij jou en Ger te kunnen rijden!

Lieve vriend(in)en, bedankt voor het meeleven en de afleiding gedurende mijn PhD. Karen, Ivana en Carley, zonder jullie was mijn studietijd niet zo legendarisch verlopen.. Super om te zien hoe jullie je ontwikkeld hebben als mens en dierenarts, en leuk om (veterinaire) ervaringen uit te blijven wisselen. Eyleen, leuk om al die tijd met jou te hebben gebootcampt en paard te rijden, ik hoop dat we dit nog even kunnen voortzetten. Adeline, wat hebben wij al een hoop samen gelachen, gegeten, gedronken, gefeest, gereisd en geklaagd. Ik hoop dat we dit nog lang blijven doen.

Lieve Rob, Thecla, Janneke, Peter, Anneloes, Marieke, Stefan, Saskia en Pieter, Lucas en Tessa, lief hoe snel jullie me hebben opgenomen in de familie. Ik bof enorm met jullie!

Lieve Luus, ik kan me geen liever en leuker zusje wensen. We zijn heel verschillende richtingen opgegaan, maar ik ben super trots op wat jij allemaal al bereikt hebt en wat je allemaal nog in je mars hebt. Ik hoop dat je hier binnenkort ook wat meer van kan gaan genieten.

Lieve pap en mam, ik kan jullie niet genoeg bedanken voor alle hulp en steun die jullie mij en Lucia altijd gegeven hebben, zodat we de mogelijkheid hadden ons breed te kunnen ontwikkelen. Uiteindelijk ben ik door jullie dierenarts én onderzoeker geworden, zij het uiteindelijk zonder verstand van vee.

Allerliefste Onno, “alles komt goed, ook als het niet goedkomt”: dit heb je inmiddels zo vaak tegen me gezegd dat ik er zo langzamerhand een beetje in begin te geloven. Bedankt dat je er altijd voor me bent, of dat in Utrecht, India of ergens anders is. Ik heb zin in de toekomst met jou samen, en ik ben blij dat je weer hier bent.

List of peer-reviewed publications

A. R. Tellegen, N. Willems, M. A. Tryfonidou, B. P. Meij. Pedicle screw-rod fixation: a feasible treatment for dogs with severe degenerative lumbosacral stenosis. *BMC Veterinary Research* 2015, 11:299.

N. Willems, H. Yang, M. L. P. Langelaan, **A. R. Tellegen,** G. C. M. Grinwis, H. C. Kranenburg, F. M. Riemers, S. G. M. Plomp, E. G. M. Craenmehr, W. J. A. Dhert, N. E. Papen-Botterhuis, B. P. Meij, L. B. Creemers, M. A. Tryfonidou. Biocompatibility and intradiscal application of a thermoreversible celecoxib-loaded poly-N-isopropylacrylamide MgFe-layered double hydroxide hydrogel in a canine model. *Arthritis Research & Therapy* 2015, 17:214.

N. Willems, **A. R. Tellegen**, N. Bergknut, L. B. Creemers, J. Wolfswinkel, C. Freudigmann, K. Benz, G. C. M. Grinwis, M. A. Tryfonidou, B. P. Meij. Inflammatory profiles in canine intervertebral disc degeneration. *BMC Veterinary Research* 2016, 12:10.

A. R. Tellegen, N. Willems, M. Beukers, G. C.M. Grinwis, S. G.M. Plomp, C. Bos, M. van Dijk, M. de Leeuw, L. B. Creemers, M. A. Tryfonidou, B. P. Meij. Intradiscal application of a PCLA–PEG–PCLA hydrogel loaded with celecoxib for the treatment of back pain in canines: What's in it for humans? *Journal of Tissue Engineering and Regenerative Medicine* 2018, 12:3.

F. C. Bach, **A. R. Tellegen**, M. Beukers, A. Miranda-Bedate, M. Teunissen, W. de Jong, S. de Vries, L. B. Creemers, K. Benz, B. P. Meij, K. Ito, M. A. Tryfonidou. Biologic canine and human intervertebral disc repair by notochordal cell-derived matrix: from bench towards bedside. *Oncotarget* 2018, 9:26507-26526.

A. R. Tellegen, I. Rudnik-Jansen, B. Pouran, H. de Visser, R. E. Thomas, M. J. L. Kik, G. C. M. Grinwis, J. C. Thies, N. Woike, G. Mihov, P. J. Emans, B. P. Meij, L. B. Creemers, M. A. Tryfonidou. Controlled release of celecoxib inhibits inflammation and subchondral bone changes in a preclinical model of osteoarthritis. *Drug Delivery* 2018, 25:1.

A. R. Tellegen, I. Jansen, M. Beukers, A. Miranda-Bedate, W. de Jong, N. Woike, G. Mihov , J. C. Thies, B. P. Meij, L. B. Creemers, M. A. Tryfonidou. Intradiscal delivery of celecoxib-loaded microspheres restores disc homeostasis in a preclinical canine model. *Journal of Controlled Release* 2018, 286:439-450.

A. R. Tellegen, M. Beukers, N. van Klaveren, K.L. How, N. Woike, G. Mihov, J. Thies, E. Teske, L. B. Creemers, M. A. Tryfonidou, B. P. Meij. A novel intra-articular slow-release formulation of triamcinolone acetonide effectively reduces symptoms in dogs with osteoarthritis. Submitted to *Acta Veterinaria Scandinavica* (2018).

A. R. Tellegen, K. Houben, A. J. Dessing, F. R. Riemers, B. P. Meij, A. Miranda-Bedate, M. A. Tryfonidou. The dog as a model for osteoarthritis: chondrodystrophy does matter. Submitted to *Journal of Orthopaedic Research* (2018).

A. R. Tellegen, M. Beukers, R. Maarschalkerweerd, D. van Zuilen, N. J. van Klaveren, K. Houben, E. Teske, R. van Weeren, N. Woike, G. Mihov, J. Thies, L. B. Creemers, B. P. Meij, M.

A. Tryfonidou. Sustained release of locally delivered celecoxib provides pain relief for osteoarthritis in dogs: a prospective, randomized controlled clinical trial. In review at *The Veterinary Journal* (2018).

I. Rudnik-Jansen, **A. R. Tellegen**, B. Pouran, K. Schrijver, B. P. Meij, P. J. Emans, E. de Gendt, R. E. Thomas, M. J.L. Kik, H. M. de Visser, H. Weinans, A. Egas, E. van Maarseveen, N. Woike, G. Mihov, J. C. Thies, M. A. Tryfonidou, L. B. Creemers. Prolonged corticosteroid exposure aggravates surgically induced osteoarthritis by inhibited healing. Submitted to *The Spine Journal* (2018).

I. Rudnik-Jansen, **A. R. Tellegen,** M. Beukers, N. Woike, G. Mihov, J. C. Thies, B.P. Meij, M.A. Tryfonidou, L. B. Creemers. Safe intradiscal delivery of triamcinolone acetonide in degenerated intervertebral discs by a poly(esteramide) microsphere platform. Submitted to *The Spine Journal* (2018).

I. Rudnik-Jansen, K. Schrijver, N. Woike, **A. R. Tellegen,** S. Versteeg, G. Mihov, J.C. Thies, N. Eijkelkamp, M. A. Tryfonidou, L. B. Creemers. Intra-articular injection of triamcinolone acetonide releasing biomaterial microspheres inhibits pain and inflammation in an acute arthritis model. Submitted to *Drug Delivery* (2018).

Conference proceedings

2014

A. R. Tellegen, N. Willems, M. A. Tryfonidou, B. P. Meij. Pedicle screw-rod fixation: a promising treatment for dogs with severe lumbosacral disease. *European Veterinary Conference Voorjaarsdagen*, April 17-19 2014, Amsterdam, The Netherlands. (oral presentation)

A. R. Tellegen, N. Willems, M. A. Tryfonidou, B. P. Meij. Pedicle screw-rod fixation: a promising treatment for dogs with severe lumbosacral disease. *Veterinary Science Day*, November 20 2014, Amsterdam, The Netherlands. (poster presentation)

2015

A. R. Tellegen, M. Beukers, M. van Dijk, M. de Leeuw, G.C.M. Grinwis, A. Miranda-Bedate, M.A. Tryfonidou, B. P. Meij. Controlled release of celecoxib as a treatment for low back pain in dogs. *European Veterinary Conference Voorjaarsdagen*, April 9-11 2015, Amsterdam, The Netherlands. (oral presentation)

A. R. Tellegen, M. Beukers, M. van Dijk, M. de Leeuw, G.C.M. Grinwis, A. Miranda-Bedate, M.A. Tryfonidou, B. P. Meij. Controlled release of celecoxib as a treatment for low back pain in dogs. *NVMB Annual Meeting*, May 28-29 2015, Lunteren, The Netherlands. (oral presentation)

A. R. Tellegen, M. Beukers, M. van Dijk, M. de Leeuw, G.C.M. Grinwis, A. Miranda-Bedate, M.A. Tryfonidou, B. P. Meij. Controlled release of celecoxib as a treatment for low back pain in dogs. *Veterinary Science Day*, November 9 2015, Bunnik, The Netherlands. (oral presentation)

2016

A. R. Tellegen, M. Beukers, M. van Dijk, M. de Leeuw, G.C.M. Grinwis, A. Miranda-Bedate, M.A. Tryfonidou, B. P. Meij. Controlled release of celecoxib as a treatment for low back pain in dogs. *Global Spine Congress*, April 13-16 2016, Dubai, United Arab Emirates. (oral presentation)

A. R. Tellegen, M. Beukers, M. van Dijk, M. de Leeuw, G.C.M. Grinwis, A. Miranda-Bedate, M.A. Tryfonidou, B. P. Meij. Controlled release of celecoxib as a treatment for low back pain in dogs. *OARSI World Congress*, March 31st - April 3rd 2016, Amsterdam, The Netherlands. (poster presentation)

A. R. Tellegen, I. Jansen, R. E. Thomas, H. de Visser, M. J. L. Kik, G. C. M. Grinwis, N. Woike, G. Mihov, P. Emans, B. P. Meij, L. B. Creemers, M. A. Tryfonidou. Controlled release of celecoxib

from polyesteramide microparticles in a rat model of osteoarthritis. *NVMB Annual Meeting*, May 12-13 2016, Lunteren, The Netherlands. (oral presentation)

A. R. Tellegen, I. Jansen, R. E. Thomas, H. de Visser, M. J. L. Kik, G. C. M. Grinwis, N. Woike, G. Mihov, P. Emans, B. P. Meij, L. B. Creemers, M. A. Tryfonidou. Controlled release of celecoxib from polyesteramide microparticles in a rat model of osteoarthritis. *NBTE Annual meeting*, December 1st 2016, Lunteren, The Netherlands. (oral presentation)

2017

A. R. Tellegen, I. Jansen, R. E. Thomas, H. de Visser, M. J. L. Kik, G. C. M. Grinwis, N. Woike, G. Mihov, P. Emans, B. P. Meij, L. B. Creemers, M. A. Tryfonidou. Controlled release of celecoxib from polyesteramide microparticles in a rat model of osteoarthritis. *ORS Annual meeting*, March 19-22 2017, San Diego, USA. (poster presentation)

A. R. Tellegen, I. Jansen, R. E. Thomas, H. de Visser, M. J. L. Kik, G. C. M. Grinwis, N. Woike, G. Mihov, P. Emans, B. P. Meij, L. B. Creemers, M. A. Tryfonidou. Controlled release of celecoxib from polyesteramide microparticles in a rat model of osteoarthritis. *European Veterinary Conference Voorjaarsdagen*, April 19-21 2017, The Hague, The Netherlands. (poster presentation)

A. R. Tellegen , N. Willems , M. Beukers , G.C.M. Grinwis , S.G.M. Plomp, M. De Leeuw , M. Van Dijk, L.B. Creemers, M.A. Tryfonidou , B.P. Meij. Intradiscal application of a PCLA-PEG-PCLA hydrogel loaded with celecoxib for the treatment of back pain: a translational approach. *NVMB Annual Meeting*, May 11-12 2017, Lunteren, The Netherlands. (poster presentation)

A. R. Tellegen , N. Willems , M. Beukers , G.C.M. Grinwis , S.G.M. Plomp, M. De Leeuw , M. Van Dijk, L.B. Creemers, M.A. Tryfonidou , B.P. Meij. Intradiscal application of a PCLA-PEG-PCLA hydrogel loaded with celecoxib for the treatment of back pain: a translational approach. *ISSLS Annual Meeting*, May 29th - June 2nd 2017, Athens, Greece. (poster presentation)

A. R. Tellegen , M. Beukers , I. Jansen , G.C.M. Grinwis, N. Woike, G. Mihov, B.P. Meij , L.B. Creemers , M.A. Tryfonidou. Controlled release of celecoxib from polyesteramide microparticles in a canine pre-clinical intervertebral disc degeneration model. *ISSLS Annual Meeting*, May 29th - June 2nd 2017, Athens, Greece. (poster presentation)

A. R. Tellegen , N. Willems , M. Beukers , G.C.M. Grinwis , S.G.M. Plomp, M. De Leeuw , M. Van Dijk, L.B. Creemers, M.A. Tryfonidou , B.P. Meij. Intradiscal application of a PCLA-PEG-PCLA hydrogel loaded with celecoxib for the treatment of back pain: a translational approach. *TERMIS*, June 26-30 2017, Davos, Switzerland. (poster presentation)

A. R. Tellegen , M. Beukers , I. Jansen , G.C.M. Grinwis, N. Woike, G. Mihov, B.P. Meij , L.B. Creemers , M.A. Tryfonidou. Controlled release of celecoxib from polyesteramide microparticles in a canine pre-clinical intervertebral disc degeneration model. *TERMIS*, June 26-30 2017, Davos, Switzerland. (oral presentation - nominated for young investigator's award)

A. R. Tellegen, M. Beukers, I. Jansen, G.C.M. Grinwis, R.E. Thomas, M.J.L. Kik, N. Woike, J.C. Thies, G. Mihov, B.P. Meij, L. B. Creemers, M.A. Tryfonidou. Controlled release of celecoxib from polyesteramide microparticles in a pre-clinical osteoarthritis model and canine patients suffering from osteoarthritis. *Veterinary Science Day*, November 16 2017, Bunnik, The Netherlands. (oral presentation)

2018

A. R Tellegen, Beukers, N. Woike, G. Mihov, J. C. Thies, L. B. Creemers, N. van Klaveren, K. L. How, M. A. Tryfonidou, B. P. Meij. Sustained release of triamcinolone acetonide for the treatment of osteoarthritis: a case series of 12 client-owned dogs. *European Veterinary Conference Voorjaarsdagen*, April 11-13 2018, The Hague, The Netherlands. (oral presentation)

A. R. Tellegen, M. Beukers, I. Jansen, G. C. M. Grinwis, N. Woike, G. Mihov, B. P. Meij, L. B. Creemers, M. A. Tryfonidou. Intradiscal delivery of celecoxib-loaded microspheres restores disc homeostasis in a preclinical canine model. *OARSI World Congress*, April 26-29 2018, Liverpool, UK. (poster presentation)

A. R. Tellegen, I. Jansen, R. E. Thomas, H. de Visser, M. J. L. Kik, G. C. M. Grinwis, N. Woike, G. Mihov, P. Emans, B. P. Meij, L. B. Creemers, M. A. Tryfonidou. Controlled release of celecoxib inhibits inflammation and subchondral bone changes in a rat model of osteoarthritis. *OARSI World Congress*, April 26-29 2018, Liverpool, UK. (poster presentation)

Curriculum vitae

Anna Tellegen was born on the 8th of January 1988 in Utrecht, the Netherlands. After graduating from secondary school in 2006 (College Blaucapel, Utrecht), she obtained her propaedeutic diploma in Biomedical Sciences at Utrecht University (The Netherlands) in 2007. Thereafter she studied Veterinary Medicine, also at Utrecht University. In 2011-2012, she was secretary of 'Hygieia', the Dutch Student Association promoting knowledge and interdisciplinary collaborations concerning 'One Health'. After graduating from Veterinary Medicine in 2014, she worked as a veterinarian in ´Dierenkliniek het Groote Plein´ in Weesp and started her PhD under supervision of prof. dr. Björn Meij, prof. dr. Marianna Tryfonidou (Faculty of Veterinary Medicine, Utrecht University) and dr. Laura Creemers (University Medical Centre Utrecht). This PhD project focused on the controlled release of anti-Inflammatory agents for prolonged inhibition of inflammation, pain and degeneration in degenerative joint disease, as part of the ArIADNE consortium, a collaboration with DSM Biomedical and the Dutch Arthritis Foundation. She supervised several Bachelor- and Master students and participated in organising the elective course on regenerative medicine for Veterinary Medicine and Biomedical Sciences Bachelor students. She was a board member of the Veterinary PhD Council (2015-2017), the Veterinary Science Day Committee (2016-2017) and the 'UKG Nieuws & Avond' committee. Currently, she is employed at the Orthopaedics Department and the Emergency & Critical Care Department of the Medisch Centrum voor Dieren in Amsterdam.